Université du Québec à Chicoutimi

Thèse présentée comme exigence partielle du programme de Doctorat en Ingénierie

Par

Tammam BASBOUS

Hybridation pneumatique d'un moteur Diesel en vue de son utilisation dans un Système Hybride Éolien-Diesel avec Stockage d'Énergie sous forme d'Air Comprimé

Janvier 2013

RÉSUMÉ

Il y a plus de 200,000 canadiens qui vivent dans environ 300 communautés isolées, qui ne sont pas connectées aux réseaux électriques provinciaux ou territoriaux. La plupart de ces communautés sont alimentées en électricité via des groupes électrogènes Diesel et subissent ainsi les coûts de carburant qui ne cessent d'augmenter ainsi que les autres frais d'exploitation comme le transport du carburant, la maintenance de Diesel et la dégradation de la qualité de l'air. La perte annuelle d'Hydro-Québec dans les réseaux isolés, résultant de l'écart entre le coût de production de l'électricité et sa tarification, s'élève à 133 millions de dollars.

Les énergies renouvelables dont principalement l'énergie éolienne, constituent un potentiel important pour réduire la dépendance à l'égard des combustibles fossiles dans les réseaux électriques. Au cours des deux dernières décennies, il y a eu un taux accéléré des installations d'éoliennes de grande taille, sous forme de grands parcs connectés aux systèmes électriques provinciaux ou nationaux. Les coûts pour ces grandes éoliennes ont diminué jusqu'au point où ils commencent à être comparables aux technologies traditionnelles de génération d'électricité. Cependant, l'intermittence de l'énergie éolienne empêche les parcs éoliens de fonctionner d'une façon autonome dans les sites isolés qui sont paradoxalement très riches en cette ressource naturelle.

Les Systèmes Hybrides Éoliens-Diesel (SHED) s'imposent donc comme alternative presqu'unique aux génératrices Diesels. Le Taux de Pénétration en Puissance (TPP) éolienne est un facteur important pour la réduction de la consommation de carburant. Pour des questions de rentabilité, les SHED à haut TPP ne sont pas encore rentables, et ceci

principalement à cause de la dissipation de l'énergie éolienne durant les périodes où la puissance éolienne disponible est supérieure à la demande.

Le stockage d'énergie excédentaire est une des solutions pour augmenter la rentabilité des ces installations. Des recherches récentes ont conclu que la technique de stockage d'énergie sous forme d'air comprimé dans des cavernes souterraines est la plus adéquate pour les applications SHED compte tenu de ses différents points forts comme le coût, la densité énergétique, la densité de puissance, la durabilité et l'efficacité. Cette technique est très mature et présente déjà à Huntorf en Allemagne et Macintosh en Alabama aux États-Unis, mais combinée avec des turboréacteurs à gaz naturel connectés au réseau central de l'électricité.

Afin de permettre la transformation de l'excès de l'énergie éolienne en air comprimé et transformer l'air comprimé en électricité, il est nécessaire d'avoir un ou plusieurs convertisseurs. Proposer une série de compresseurs et de moteurs à air comprimé est une solution coûteuse qui ne peut probablement pas voir le jour à cause de son manque de rentabilité. Une solution économiquement viable serait une hybridation pneumatique du groupe électrogène Diesel, déjà existant sur place, le transformant en un Moteur Hybride Pneumatique-Diesel (MHPD) capable de jouer, en plus de son rôle initial, le rôle d'un moteur à air comprimé et celui d'un compresseur d'air, d'où l'idée d'un Système Hybride Eolien – Diesel – Air Comprimé (SHEDAC) proposée et étudiée dans le détail dans cette thèse.

Cette thèse présente une analyse détaillée des modifications à apporter au moteur Diesel afin de le transformer en un MHPD. Elle expose également une optimisation du concept ainsi qu'une évaluation de son apport en termes d'économie de carburant dans

un site cible et ceci pour différentes hypothèses de volume de stockage d'air et de TPP éolienne installée.

Dans le village isolé nord-Canadien Tuktoyaktuk, actuellement équipé d'une génératrice Diesel de 1 MW, la production d'électricité nécessite 1080 tonnes de carburant par an. Si un SHED à haute pénétration (TPP = 2) était mis en place dans ce village, la consommation de carburant serait seulement 561 tonnes par an, soit une baisse de 48%. En ajoutant un système de stockage d'air comprimé de 100,000 m^3 et en transformant le moteur Diesel en un MHPD, la consommation annuelle de carburant baisserait encore de 13%, pour atteindre 415 tonnes.

Afin d'obtenir ce gain significatif, il est nécessaire d'apporter plusieurs modification au moteur Diesel d'origine. Parmi ces modifications, on note principalement :

1. l'ajout de deux vannes trois voies, une installée dans le conduit d'admission, reliant celui-ci soit à la sortie du compresseur soit à la sortie du réservoir d'air comprimé ; et une installée dans le conduit d'échappement, connectant celui-ci soit à l'entrée de la turbine, soit à l'air libre ;
2. le remplacement du système de distribution par arbre à came par un système de distribution électromagnétique ou piézo-électrique permettant de prendre le contrôle, via un dispositif externe, sur les instants d'ouverture et de fermetures des soupapes d'admission et d'échappement du moteur ;
3. la prise sous contrôle du système d'injection via un dispositif extérieur, permettant d'actionner ou de couper l'injection du carburant, et d'en contrôler la quantité et la durée.

Le contenu de la thèse est présenté sous forme de cinq articles originaux publiés ou soumis à des journaux scientifiques avec comité de lecture, ainsi que trois articles publiés dans des congrès scientifiques avec comité de lecture. Chacun de ces articles fait, au moment de sa soumission, l'objet de l'état de l'avancement de l'étude, selon la méthodologie détaillée dans le chapitre I.

ABSTRACT

Canada has over 200,000 citizens living in remote communities, many of whom rely on diesel generators for their electricity supply. The economical cost of energy is therefore very high due to not only inherent cost of fuel but also to transportation and maintenance costs. The environmental cost of energy is also high as the use of fossil fuels for electricity generation is a significant source of greenhouse gas emissions.

Renewable energy for remote areas is being investigated to reduce the oil dependency. Among all renewable energies, the wind energy experiences the fastest growing rate, at more than 30% annually for the last 5 years in Canada, which led to significant reduction in installation cost. However, the intermittency of this free energy makes impossible replacing the Diesel generators by wind farms in remote areas. The use of hybrid Wind-Diesel Systems (WDS) is therefore the only reasonable alternative to Diesels. For a WDS, the fuel saving is higher for greater Wind Power Penetration Rate (WPPR), which is the ratio of the maximal wind generated power to the maximal load. Unfortunately, WDS with high WPPR are not cost - effective due to the high amount of wasted energy that occurs when the wind power is higher than the load. For this reason, adding an energy-storage element to the WDS is the only way to increase the WPPR and therefore the fuel savings.

Previous studies proved that Compressed Air Energy Storage (CAES) is very adequate for WDS due to its low cost, high power density, good efficiency and reliability. In order to store and restore energy, one or several pneumatic converters are needed. Knowing that the maximal power of the air motors existing in the market does

not exceed 5 kW, suggesting the addition of several air motors and compressors would not be cost effective. To solve this problem, this research suggests a pneumatic hybridization of the existing Diesel engine in order to transform it into a Hybrid Pneumatic-Diesel Engine (HPDE) able to operate as a conventional Diesel engine, an air compressor and air motor. The innovative idea of doing a multi-hybrid wind-Diesel-compressed air system is therefore born.

This thesis investigates in details all the modifications of the Diesel engine required to transform it into a HPDE. It presents an optimization of the concept and an evaluation of its potential of fuel-savings generated by a WDS-HPDE power generation compared to a Diesel-only power generation and a WDS power generation, depending on the WPPR and the storage capacity, in a certain area.

The North-Canadian remote village Tuktoyaktuk is presently equipped with a Diesel power supply system of 1MW capacity. The power production consumes 1080 tons of fuel every year. If a high penetration WDS (WPPR=2) were installed, the power production would consume only 561 tons of fuel, i.e. 48% less. By adding a CAES of 100,000 m^3 and turning the Diesel engine into an HPDE, the fuel consumption of the multi-hybrid system for generating the power in Tuktoyaktuk would be only 415 tons, i.e. 13% less.

To obtain this significant fuel economy, the following modifications of the Diesel engine's architecture are necessarily:

1. The addition of two 3-way valves: the first one, installed in the admission duct, connects the engine's intake either to the charger's outlet or to the CAES tank ; the

second one, installed in the exhaust duct, connects the engine's exhaust either to the turbine's inlet or to the atmosphere;

2. The replacement of the cam-driven valve system by an electromagnetic or a piezo-electric valve system. The timing and duration of opening and closing of intake and exhaust valves could therefore be controlled via an external device.
3. The control of the fuel injection system (duration and timing) via an external device.

This thesis is produced in the form of five original papers published or submitted to international journals and three papers published in international conferences with reviewing committee. Each of these journal-articles summarizes the results of one part of the methodology explained in the first chapter.

DEDICACE

Je dédie ce mémoire à Shaden, ma chère épouse qui m'a tant soutenu et supporté mon indisponibilité durant deux années de jeune mariée.

REMERCIEMENTS

Cette thèse a été effectuée au sein du Laboratoire International des Matériaux Antigivre (LIMA) de l'Université du Québec à Chicoutimi (UQAC) ainsi qu'au Laboratoire de Recherche en Energie Eolienne (LREE) de l'Université du Québec à Rimouski (UQAR).

Le travail n'aurait pas pu être réalisé sans le soutien de nombreuses personnes à qui je souhaiterais témoigner ma vive reconnaissance et que je souhaite remercier au travers de ces quelques lignes.

J'adresse d'abord mes vifs remerciements à mon directeur Jean PERRON, professeur à l'UQAC et directeur du LIMA, pour m'avoir accepté pour le doctorat, pour sa direction attentive et sa disponibilité durant les périodes de ma présence à Chicoutimi, malgré ses nombreuses occupations avec le déménagement du LIMA vers le nouveau bâtiment.

Je tiens à remercier également mon premier codirecteur Adrian ILINCA, professeur à l'UQAR et directeur du LREE, pour son encadrement et son aide précieuse à débloquer tous les problèmes d'ordre administratif que j'ai rencontrés.

Je réserve également un très grand remerciement à mon deuxième codirecteur Rafic YOUNES, doyen de la faculté de génie de l'Université Libanaise, pour sa forte implication dans les travaux techniques de modélisation et d'optimisation, ainsi que pour le temps qu'il m'a accordé durant nos rencontres au Canada, en France et au Liban.

Je réserve aussi un sincère remerciement aux remarquables techniciens du LIMA, Martin TRUCHON et Carol MERCIER ainsi qu'à l'étudiant Philippe BEAULAC qui ont pu réaliser les essais préliminaires pour la validation du concept et réfléchir aux modifications à apporter au banc moteur Diesel conventionnel pour le transformer en un moteur hybride pneumatique-Diesel.

Enfin, que toutes les personnes qui ont directement ou indirectement contribué à l'élaboration de ce projet, trouvent ici l'expression de ma profonde gratitude.

TABLE DES MATIERES

INDEX DES FIGURES (HORS ARTICLES)

INDEX DES TABLEAUX (HORS ARTICLES)

INDEX DES NOMENCLATURES ET ABREVIATIONS

GES :	Gaz à Effet de Serre
CAC :	Consommation Annuelle de Carburant
AEEE :	Association Européenne de l'Énergie Éolienne
SHED :	Système Hybride Éolien-Diesel
SHEDAC :	Système Hybride Éolien-Diesel avec stockage d'Air Comprimé
SHED-SI :	Système Hybride Éolien-Diesel avec Stockage Idéal
SHEDAC-MHPD :	Système Hybride Éolien-Diesel avec stockage d'Air Comprimé combiné avec le concept Moteur Hybride Pneumatique-Diesel
MHPD :	Moteur Hybride Pneumatique-Diesel
TPP :	Taux de Pénétration en Puissance
TPE :	Taux de Pénétration en Énergie
CAES :	Compressed Air Energy Storage
EFF :	Efficacité
CA :	Compresseur d'Air
MAC :	Moteur à Air Comprimé
APA :	Air Power Assited
ECS :	Etat de Charge du Stockage
PE :	Puissance Eolienne
CH :	Charge
TR :	Temps de Réponse
SDV :	Système de Distribution Variable
CPP :	Contribution de la Puissance Pneumatique
PMH :	Point Mort Haut
PMB :	Point Mort Bas
OSA :	Ouverture de la Soupape d'Admission

FSA :	Fermeture de la Soupape d'Admission
OSE :	Ouverture de la Soupape d'Echappement
FSE :	Fermeture de la Soupape d'Echappement
INJ :	Injection de Carburant
IC :	Injection de Carburant
NEDC:	New European Driving Cycle
ARTEMIS:	Assessment and Reliability of Transport Emission Models and Inventory System

CHAPITRE I

INTRODUCTION

I.1. Energie éolienne pour des sites isolés au Québec et Canada

I.1.1. Généralisation des génératrices Diesels et problématiques associées

Par définition, on appelle site isolé chaque région, communauté ou habitation permanente ou établie pour au moins 5 ans, qui compte au moins dix habitations et qui n'est pas ou ne peut pas être reliée au réseau public de distribution d'électricité ou de gaz naturel de longue distance ou au moyen de la génération conventionnelle [1]. Certaines régions dans le monde (îles, régions lointaines, agglomérations montagneuses, etc.) se retrouvent dans cette situation en général parce qu'il s'avère techniquement trop complexe d'amener le réseau électrique jusqu'à ces secteurs à cause du coût prohibitif des lignes de transmission et des pertes liées à la distribution de la puissance [2] ou parce que le coût d'une telle opération n'est pas justifié par rapport à d'autres solutions potentielles.

Au Canada, qui occupe un immense territoire et où la population est extrêmement éparse, un peu plus de 300 communautés comptant un total de 200,000 personnes répondent à ces conditions (Yukon, Nunavut, Îles, ...). La Figure I.1, indique la position de ces communautés et montre les réseaux de distribution d'électricité et de gaz. Il faut ajouter à ces communautés les postes des frontières, les nombreuses installations techniques (tours et relais de télécommunications, systèmes météo), touristiques (pourvoiries, chalets, etc.), agricoles et piscicoles qui ne sont pas connectées aux réseaux provinciaux ou nationaux de distribution et de transport d'électricité [3-9]. Le Tableau I.1 indique la répartition par région des communautés éloignées au Québec, leur population ainsi que la puissance électrique installée [10].

Plusieurs des communautés éloignées se caractérisent par une très forte dépendance envers les combustibles provenant de l'extérieur et par le coût élevé de l'énergie. Dans la plupart des endroits, des services publics d'électricité, Affaires indiennes et Nord-canadiennes et des communautés autochtones produisent de l'électricité à l'aide de génératrices autonomes fonctionnant au Diesel.

Tableau I. 1 : Territoires non reliés au réseau principal d'HQ en 2003 [10]

Territoire	Îles-de-la-Madeleine	Nunavik	Basse-Côte-Nord	Haute-Mauricie	Île d'Anticosti	Total
Nombre d'abonnés	6832	4097	2503	776	187	14395
Puissance installée (MW)	68	27	38	8	3	144

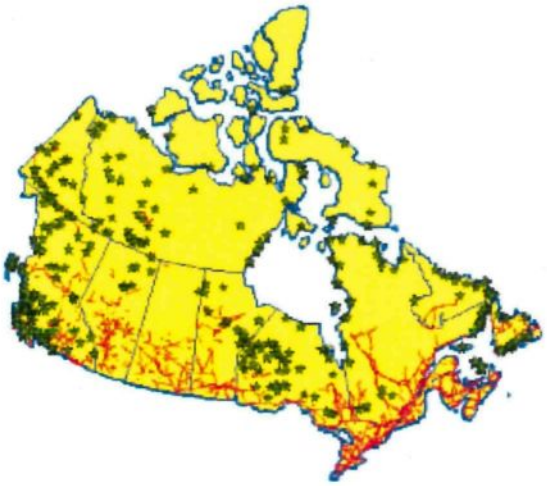

Figure I. 1 : Carte du Canada illustrant les communautés isolées et les réseaux de distribution d'énergie [11]

De plus, la demande en électricité est en hausse dans les réseaux autonomes, ce qui nécessite soit une augmentation des capacités existantes, soit le rajout d'autres sources d'électricité pour fournir de l'énergie supplémentaire. La capacité des réservoirs en carburants fossiles est ainsi une contrainte importante, étant donnés les coûts élevés qui accompagneraient leur expansion.

Les besoins en chaleur sont également pourvus par les produits pétroliers dans les réseaux autonomes. Trouver des alternatives basées sur la biomasse, les thermopompes, la cogénération ou le solaire thermique pourrait offrir des opportunités de réduire le coût annuel des services mais aussi les émissions de GES. Ces alternatives permettraient de poursuivre un chemin plus durable et de remédier à la hausse de la demande pour les carburants tout en évitant l'agrandissement des réservoirs existants [12].

De plus, les prix élevés, un désir de diminuer les dépenses énergétiques, de garder l'emploi à l'intérieur de ces communautés éloignées, la volonté de travailler vers la durabilité et l'indépendance énergétique tout en réduisant les impacts sur l'environnement, constituent l'ensemble des motivations pour minimiser l'utilisation du Diesel dans les communautés isolées canadiennes [13].

Les conditions énergétiques, économiques et environnementales de fonctionnement des génératrices Diesel approvisionnant les réseaux autonomes ne sont pas optimaux et devraient être améliorées.

1. Sur le plan énergétique : il est reconnu que l'utilisation de groupes électrogènes Diesel sous faibles facteurs d'utilisation (faible charge ou charge partielle) leur est très néfaste au niveau de l'usure et entraîne des consommations élevées de carburant [14-15]. Ceci est principalement dû à une viscosité inadéquate de l'huile de lubrification à cause d'un manque d'énergie thermique dégagée par la combustion du moteur. Ce manque de viscosité dégrade la qualité de la lubrification des paliers d'arbre à cames et du vilebrequin du moteur. La conséquence de cette usure se porte directement sur la consommation de carburant qui augmente lors du fonctionnement à charge nominale du moteur. L'objectif à ce niveau est donc de maintenir le facteur d'utilisation des groupes électrogènes supérieur à 30%.
2. Sur lé plan économique : le Diesel est importé de loin et ne crée à peu près aucun emploi dans les communautés. En outre, les groupes électrogènes Diesel, tout en étant relativement peu chers à l'achat, sont généralement chers à exploiter et maintenir, particulièrement au niveau de la charge partielle, en raison du prix élevé du carburant livré aux sites isolés [16]. Ainsi, puisque le prix du combustible Diesel est très dépendant du mode de transport employé, ce sont les difficultés de transport et les particularités de livraison qui font varier ce coût et augmenter davantage le coût d'exploitation des génératrices Diesels [14]. Par exemple, le coût du kWh produit dans les localités accessibles seulement par la voie des airs est généralement supérieur que celui produit dans celles accessibles par bateau ou par voie terrestre. Au Québec, les coûts moyens de production de l'électricité à partir du Diesel atteignaient en 2007 plus de 40¢/kWh dans les réseaux autonomes, alors que le prix moyen de vente de l'électricité s'établit, comme dans l'ensemble du Québec, à environ 6¢/kWh. Hydro-Québec estime

ainsi à environ 133 millions de dollars les pertes subies chaque année et qui reflètent l'écart entre les coûts élevés de production d'électricité à partir des Diesels dans ces régions et le prix uniforme de l'électricité [10]. Ceci fait en sorte que la rentabilité des énergies nouvelles y est beaucoup plus élevée qu'au sud du Québec.

3. Sur le plan environnemental : en plus d'être non-optimale et dispendieuse, l'exploitation des génératrices au Diesel dans les réseaux autonomes a des impacts significatifs sur le plan environnemental. Elle contamine l'air local et le sol (génératrices vieilles et rouillées) et contribue grandement à l'émission des gaz à effet de serre (GES). Au total, les émissions de GES résultant de l'utilisation de génératrices sont estimées à 140,000 tonnes par an pour les abonnés des réseaux autonomes Canadiens et Québécois. Cette quantité d'émissions équivaut à la quantité de GES émise par 35,000 automobiles durant une année [10]. La substitution du Diesel par des ressources renouvelables était déjà un objectif important chez les exploitants des réseaux autonomes même avant la hausse récente des prix des carburants fossiles. Dans la conjoncture actuelle, cet intérêt est devenu pressant.

I.1.2. Développement de l'énergie éolienne, en particulier dans les sites isolés nord-Canadiens

En principe, le coût élevé des carburants fossiles dans les réseaux autonomes devrait ouvrir la porte à des alternatives basées sur les énergies renouvelables qui sont moins compétitives dans les régions ayant accès au réseau principal. La plupart de ces communautés sont situées près de la côte et possèdent une bonne ressource éolienne. Une valorisation de la ressource éolienne dans ces réseaux autonomes pourrait donc réduire les déficits d'exploitation en privilégiant le vent, un carburant local, plutôt que le Diesel, un carburant importé.

L'énergie éolienne tient actuellement le rôle de vedette parmi toutes les énergies renouvelables contribuant à la production d'électricité. Elle est l'une des plus prometteuses, en termes environnementaux, de compétitivité, de champ d'application, de création d'emplois et de richesses. Le potentiel de production d'électricité éolienne dans le monde est énorme, même en excluant les régions sensibles en matière d'environnement, il représente plus ou moins cinq fois la consommation totale

actuelle d'électricité dans le monde. Il est estimé à $30x10^{15}$ kWh par an pour l'ensemble du globe et entre $5x10^{12}$ et $50x10^{12}$ kWh par an pour la part terrestre exploitable [17].

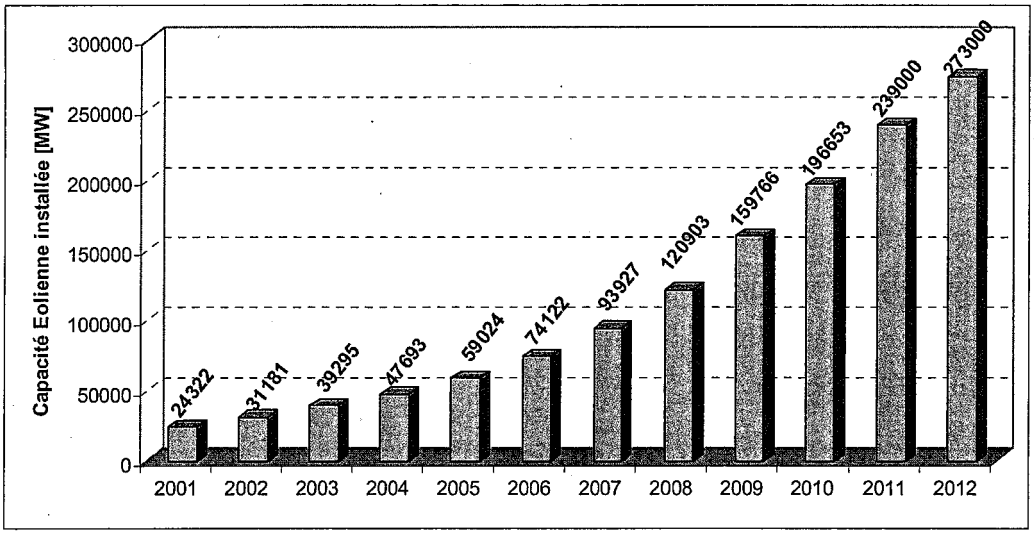

Figure I. 2 : Puissance éolienne installée dans le monde entre 2001 et 2012 [17]

La production de l'énergie éolienne est la source d'électricité renouvelable qui croît le plus rapidement dans le monde avec un taux de croissance moyen de 30% par an au cours des cinq dernières années. Entre 2001 et 2012, la capacité de production d'électricité d'origine éolienne dans le monde entier est passée de 24 GW à 273 GW comme le montre la Figure I.2 [17]. La capacité de production éolienne actuellement installée génère plus de 1% de la consommation mondiale en électricité. Les perspectives sont tout aussi spectaculaires. L'Association Européenne de l'Énergie Éolienne (AEEE) estime que 12% de l'électricité mondiale sera d'origine éolienne en 2020 et plus de 20% en 2040.

À la fin de l'année 2012, le Canada avait une capacité installée de production d'électricité d'origine éolienne d'environ 5903 MW alors qu'elle n'était que 198 MW en 2001, comme le montre la Figure I.3. D'un bout à l'autre du Canada (Figure I.4), l'électricité d'origine éolienne alimente déjà plus de 500,000 foyers et entreprises d'une manière propre, fiable et efficace. Si ce type d'électricité remplaçait l'électricité provenant de centrales au charbon, cela supprimerait l'émission d'environ 1 million de tonnes de dioxyde de carbone dans l'atmosphère chaque année [18]. Compte tenu de l'abondance inégalée des ressources éoliennes dont dispose le pays, il existe encore la

possibilité de faire davantage pour maximiser le développement économique et industriel ainsi que des avantages environnementaux liés à ce type d'énergie.

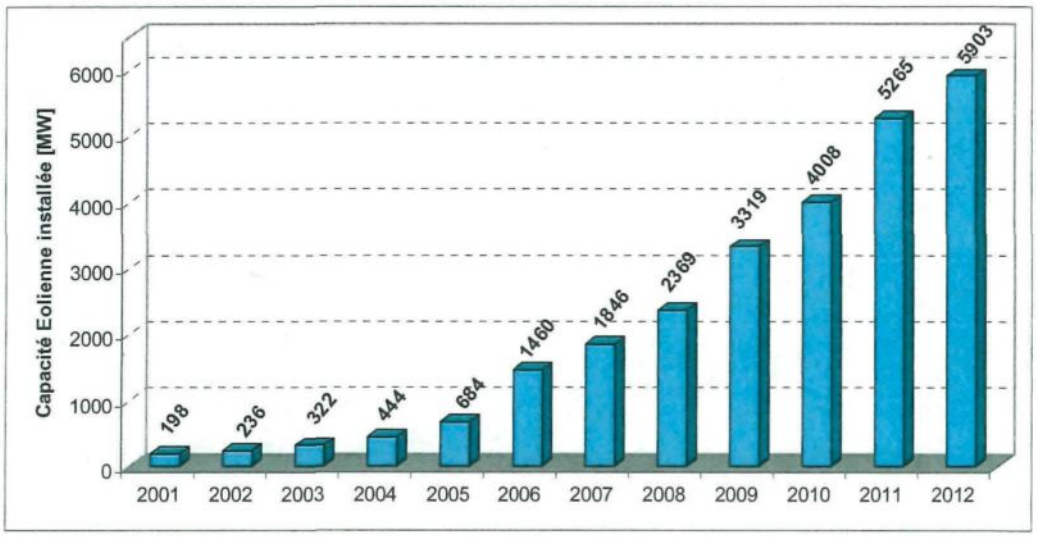

Figure I. 3 : Puissance éolienne installée au Canada entre 2001 et 2012 [18]

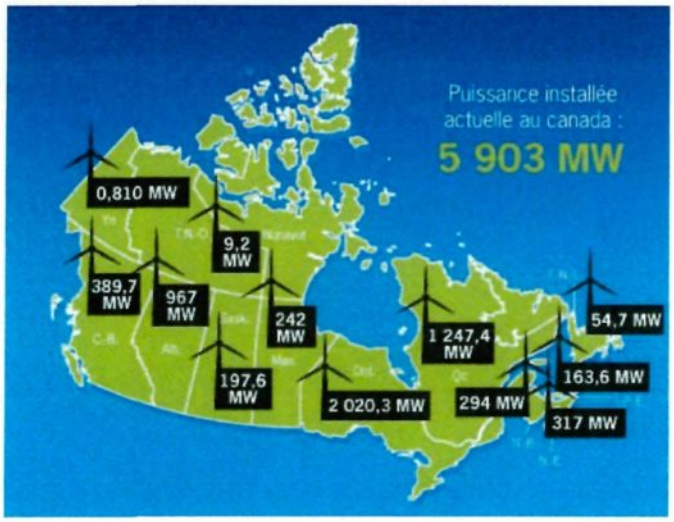

Figure I. 4 : Puissance éolienne installée au Canada jusqu'à la fin de 2012 [18]

Le potentiel éolien théorique du Québec est considérable compte tenu de l'immensité du territoire. Toutefois, une étude rendue publique en juin 2005 évaluait à 3 600 MW le potentiel intégrable au réseau électrique d'Hydro-Québec en tenant compte des technologies actuelles et des contraintes liées au transport de l'énergie sur de longues distances. Avec les mêmes technologies, ce potentiel atteindrait 4 000 MW en 2015 [19].

Le coût de l'énergie éolienne est en baisse constante depuis plusieurs années. Ce prix dépend de nombreux facteurs et par conséquent est différent d'un pays à l'autre, et même d'un site à l'autre, puisque la vitesse du vent est un des facteurs les plus importants (la puissance produite par une éolienne est proportionnelle au cube de la vitesse du vent). Malgré tout, on peut dire que le coût de cette énergie a été divisé par deux ces 10 dernières années [20]. Parmi les facteurs ayant provoqué cette baisse, on peut citer la baisse des prix des aérogénérateurs, l'augmentation de la rentabilité et de la disponibilité et la baisse des coûts de maintenance. Avec la tendance vers des turbines toujours plus grandes - la baisse des coûts d'infrastructure que cela entraîne et les réductions du coût des matériaux - le prix de l'énergie éolienne continue à diminuer régulièrement. Il faut de plus noter qu'en prenant en compte le coût associé à la pollution produite par les autres sources d'énergie, le coût de l'énergie éolienne devient encore plus compétitif.

I.1.3. Les obstacles au développement de l'énergie éolienne dans les sites isolés

Plusieurs défis sont à surmonter afin de permettre un développement systématique de l'énergie éolienne dans les sites isolés dans le nord su Canada :

1) la rigueur du climat avec des températures extrêmement basses et des phénomènes givrage qui limitent fortement la performance des éoliennes ;
2) la problématique de l'intermittence du vent et de la puissance éolienne produite. Cette intermittence est à haute fréquence et à basse fréquence :
   a. à haute fréquence, avec des oscillations de vitesse du vent à des amplitudes de allant jusqu'à plus ou moins quatre mètres par seconde (Figure I.5), qui génère inévitablement des problèmes de contrôle et de régulation de fréquence ;

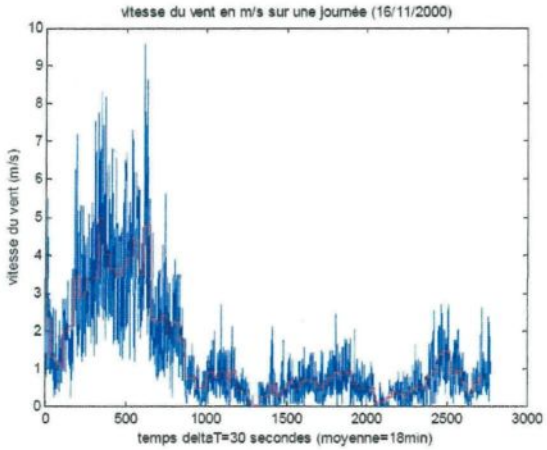

Figure I. 5 : Illustration de l'oscillation de la vitesse du vent [17]

b. À faible fréquence, avec des oscillations de vitesse moyennes entre jour et nuit, hiver et été, etc. Alors que les éoliennes conventionnelles atteignent leur puissance nominale à une vitesse du vent entre 15 m/s et 25 m/s, la vitesse du vent suit une distribution de Weibull avec une valeur moyenne rarement au dessus de 9 m/s, comme le montre la Figure I.6. De ce fait, un parc éolien génère une production annuelle qui est de l'ordre du tiers de sa production nominale qu'il aurait pu atteindre si la vitesse du vent était toujours entre 15m/s et 25m/s, comme illustré dans la Figure I.7.

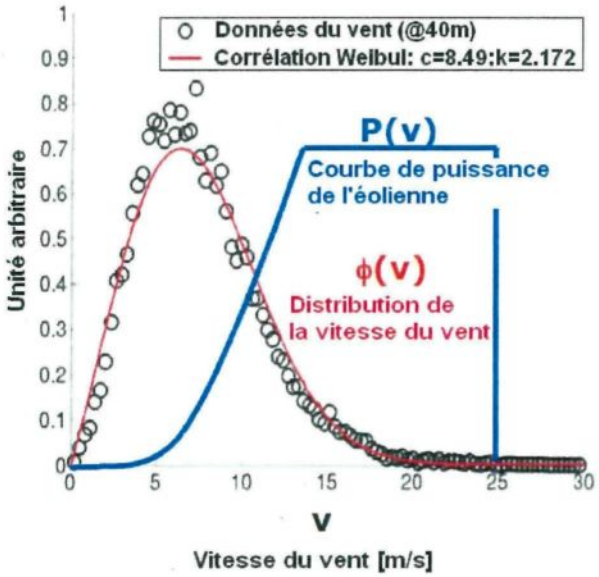

Figure I. 6 : Exemple de la distribution annuelle du vent et d'une courbe de puissance d'une éolienne

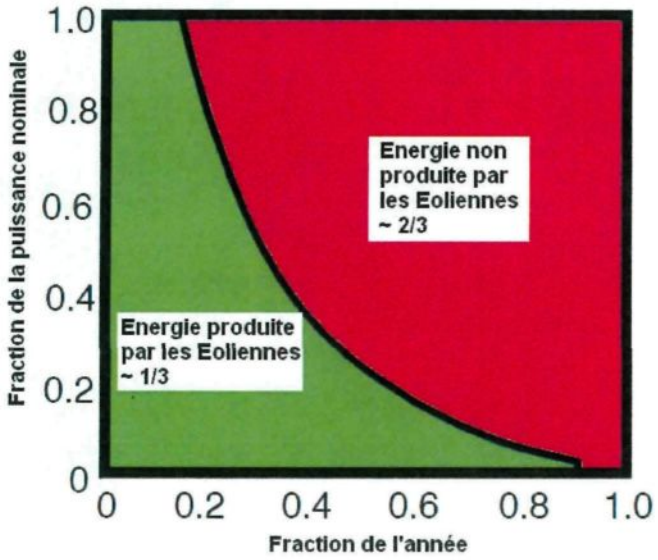

Figure I. 7 : Exemple du taux annuel d'exploitation d'un parc éolien

3) Le caractère aléatoire de la production éolienne : quand la puissance éolienne est disponible, il faut l'exploiter, sinon elle est perdue (« *take it or leave it* »). Or, il se trouve que la demande est, elle aussi, fluctuante et qu'il s'avère très fréquent que les périodes de consommation élevée ne soient malheureusement pas en phase avec les périodes de vent fort.

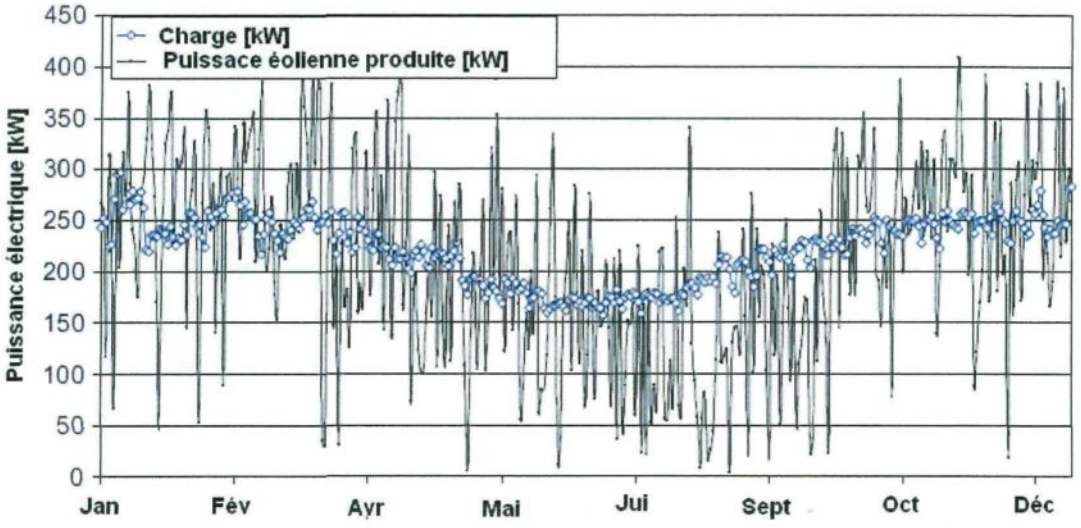

Figure I. 8 : Exemple illustrant la puissance éolienne produite par un parc éolien de puissance nominale 450 kW et la puissance appelée par un réseau dont la puissance maximale autorisée est aussi 450 kW

C'est en effet pour ces deux dernières raisons qu'un parc éolien ne peut pas fonctionner d'une façon autonome dans un site isolé. Pour un système éolien ayant une puissance nominale égale à la puissance maximale autorisée par le réseau, un manque d'alimentation aurait lieu très fréquemment comme illustré dans la Figure I.8.

I.2. Système Hybride Eolien-Diesel (SHED)

I.2.1. Description du système SHED

La nécessité de trouver une solution fiable et économique pour la génération d'électricité dans les sites isolés, alternative à la production par Diesel qui s'est avérée dispendieuse et polluante, ainsi que la disponibilité d'une technologie éolienne abordable ont alimenté l'intérêt grandissant pour les Systèmes Hybrides Éolien-Diesel (SHED). Les SHED assurent le compromis entre une énergie éolienne produite avec un combustible « gratuit » et la constance de la production assurée par le Diesel, tout en gardant un coût d'investissement limité. En général, la plupart des SHED actuellement en place ont été transformés à partir de centrales Diesels déjà existantes en leur ajoutant une centrale éolienne et un système de contrôle. En plus des éléments principaux qui sont les éoliennes et le Diesel, le SHED peut également incorporer un système de délestage comme un réservoir de stockage d'eau chaude qui alimente le système de chauffage des foyers, comme le montre la Figure I.9. Cette approche est utilisée actuellement dans des communautés nordiques au Yukon [16], Nunavut [21] au Canada et Alaska aux États-Unis [22] et dans la plupart des sites isolés (îles, zones montagneuses, ...) ailleurs dans le monde.

Les SHED des sites isolés peuvent être classifiés en fonction du degré de pénétration de l'énergie éolienne [23]. On défini le Taux de Pénétration de la Puissance (TPP) éolienne comme étant le ratio de la puissance maximale que peut produire le parc éolien $(P_{max\_}\text{éolienne})$, sur la puissance maximale de la charge $(P_{max\_}\text{charge})$.

$$\mathrm{TPP} = \frac{P_{max\_}\text{éolienne}}{P_{max\_}\text{charge}} \qquad \text{(I.1)}$$

On définit également le Taux de Pénétration de l'Énergie (TPE) éolienne comme étant le ratio de l'énergie éolienne annuellement produite ($E_{annuelle\_éolienne}$), sur l'énergie consommée annuellement par le réseau ($E_{annuelle\_charge}$).

$$TPE = \frac{E_{annuelle\_éolienne}}{E_{annuelle\_charge}} = \frac{\int_{t=1jour}^{365jours} P\_éolienne \cdot dt}{\int_{t=1jour}^{365jours} P\_charge \cdot dt} \qquad (I.2)$$

Pour un site donné, le TPP dépend du nombre et puissance unitaire des éoliennes installées alors que le TPE dépend du TPP ainsi que de la vitesse moyenne du vent sur le site.

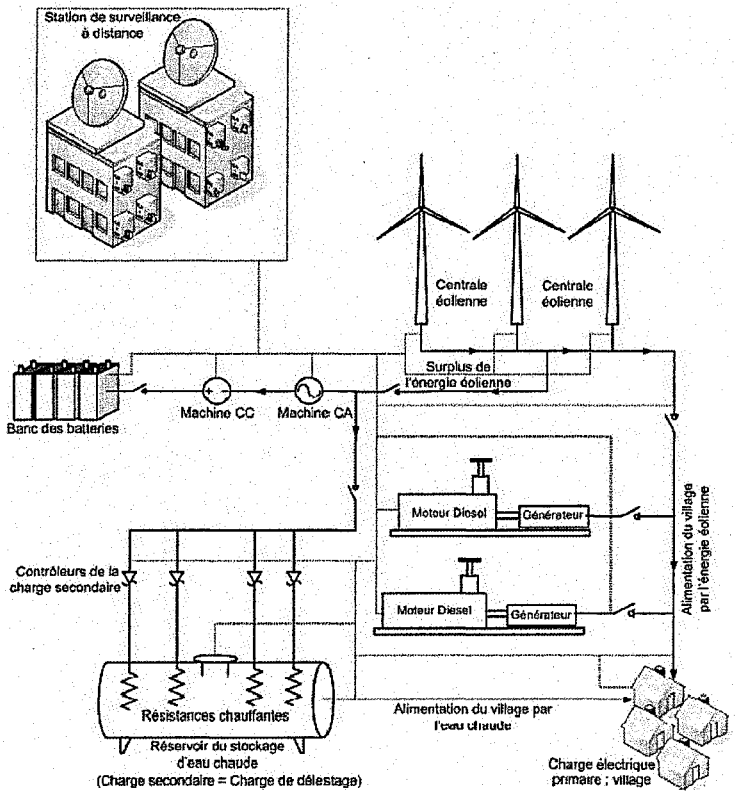

Figure I. 9 : Schéma de principe d'un SHED avec charge de délestage [24]

Une classification des grands systèmes éolien-Diesel sur trois niveaux à été proposée [23]. Cette classification sépare les systèmes en fonction du taux de pénétration de l'énergie éolienne et donne leurs caractéristiques de fonctionnement.

1) le SHED à faible pénétration de l'énergie éolienne : pour lequel le TPP est inférieur à 50% et le TPE est inférieur à 20%. Dans ce type de SHED, la production éolienne a pour simple objectif de réduire de quelques pourcents la sollicitation du moteur Diesel. Celui-ci reste donc toujours en marche. L'énergie éolienne alimente directement le réseau sans la nécessité d'un système de supervision ;

2) le SHED à moyenne pénétration de l'énergie éolienne : pour lequel le TPP est entre 50% et 100% et le TPE est entre 20% et 50%. Ce type de SHED est un peu plus ambitieux que le précédent pour ce qui concerne la réduction de la sollicitation du Diesel qui reste malgré cela tout le temps en marche. Mais le risque de la surproduction éolienne ainsi que la nécessité de maintenir le Diesel en marche avec une charge minimale de 30% de sa puissance nominale, imposent la mise en place d'un système de délestage ou de charges secondaires. Toutefois, la commande de ce système reste relativement simple ;

3) le SHED à forte pénétration de l'énergie éolienne : pour lequel le TPP est entre 100% et 400% et le TPE est entre 20% et 100%. Ce type de SHED est conçu afin de permettre l'arrêt complet des Diesels dans le cas où la production éolienne est suffisante. Une commande complexe ainsi qu'un système auxiliaire pour contrôler la tension et la fréquence sont nécessaire. Suivant l'intensité du vent, trois modes de fonctionnement peuvent être distingués pour les systèmes à haute pénétration, comme le montre la Figure I.10 :

   a. Vents faibles (vitesse inférieure à 3 m/s), Diesels seuls : Dans ce cas, le système de contrôle des éoliennes les met hors circuit. C'est le groupe électrogène (Diesel) qui assure la production de puissance et les asservissements de tension et de fréquence.

   b. Vents moyens (vitesse entre 3 et 10 m/s), Diesels et éoliennes en service : Par vents d'intensité moyenne, la puissance éolienne n'est généralement pas suffisante pour fournir à elle seule la totalité de la demande. Les éoliennes contribuent à fournir une partie de la puissance demandée par la charge et le groupe électrogène fournit alors la différence. Ceci permet de diminuer l'apport des Diesels et par conséquent de réaliser des économies. Dans ce

mode de fonctionnement, les régulations de tension et de fréquence sont réalisées par le groupe électrogène.

c. Vents forts (vitesse supérieure à 10 m/s), éoliennes seules : Par vents suffisamment forts pour que la production éolienne soit supérieure à la demande, il est alors possible d'éteindre complètement les Diesels. Une configuration connue, mais non unique, consiste à utiliser un embrayage unidirectionnel entre les Diesels et les génératrices synchrones afin de découpler ces dispositifs [25-26]. Les Diesels étant éteints et découplés des machines synchrones, ces dernières n'entraînent aucune charge. Elles sont utilisées uniquement comme compensateurs synchrones, ce qui permet au régulateur de tension du groupe électrogène de demeurer en service. Par contre, la régulation de fréquence ne peut plus être assurée par le groupe électrogène éteint. Pour cette raison, une charge de lissage (ou système de stockage) doit être mise en service et contrôlée par un régulateur de fréquence qui dicte la puissance à dissiper dans la charge de lissage. La fréquence demeure constante lorsque la loi de commande suivante est respectée : la puissance éolienne doit être égale à la puissance de la demande plus la puissance dissipée dans la charge de lissage.

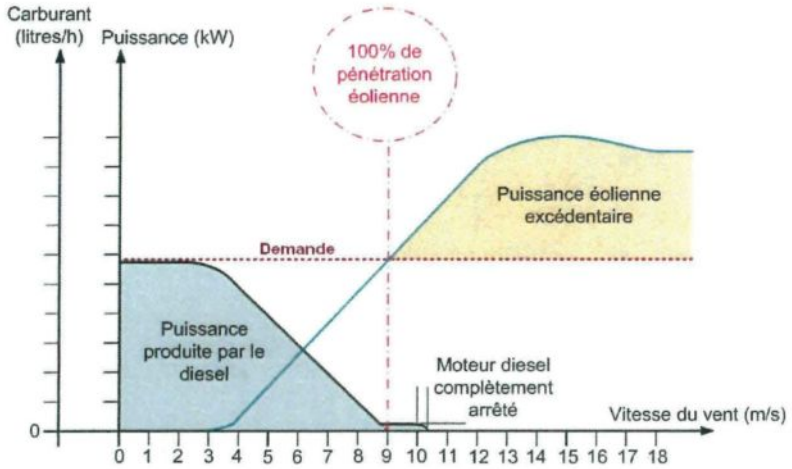

Figure I. 10 : Exemple de la variation de la répartition de la puissance entre le moteur Diesel et le parc éolien en fonction de la vitesse du vent, pour un SHED à haute pénétration [27]

I.2.2. Apport énergétique du SHED

L'économie du carburant obtenue en remplaçant une centrale Diesel par un SHED est fonction du Taux de Pénétration de l'Energie éolienne (TPE). Etant donné que le TPE dépend du TPP et de la vitesse moyenne du vent, nous avons illustré dans la Figure I.11, la consommation annuelle de carburant d'un SHED en fonction de ces deux paramètres, dans un site dont la valeur moyenne de la puissance est 500 kW (cas du village de Tuktoyaktuk). Le coût du carburant est donné à titre indicatif et calculé sur la base de 90¢ par litre.

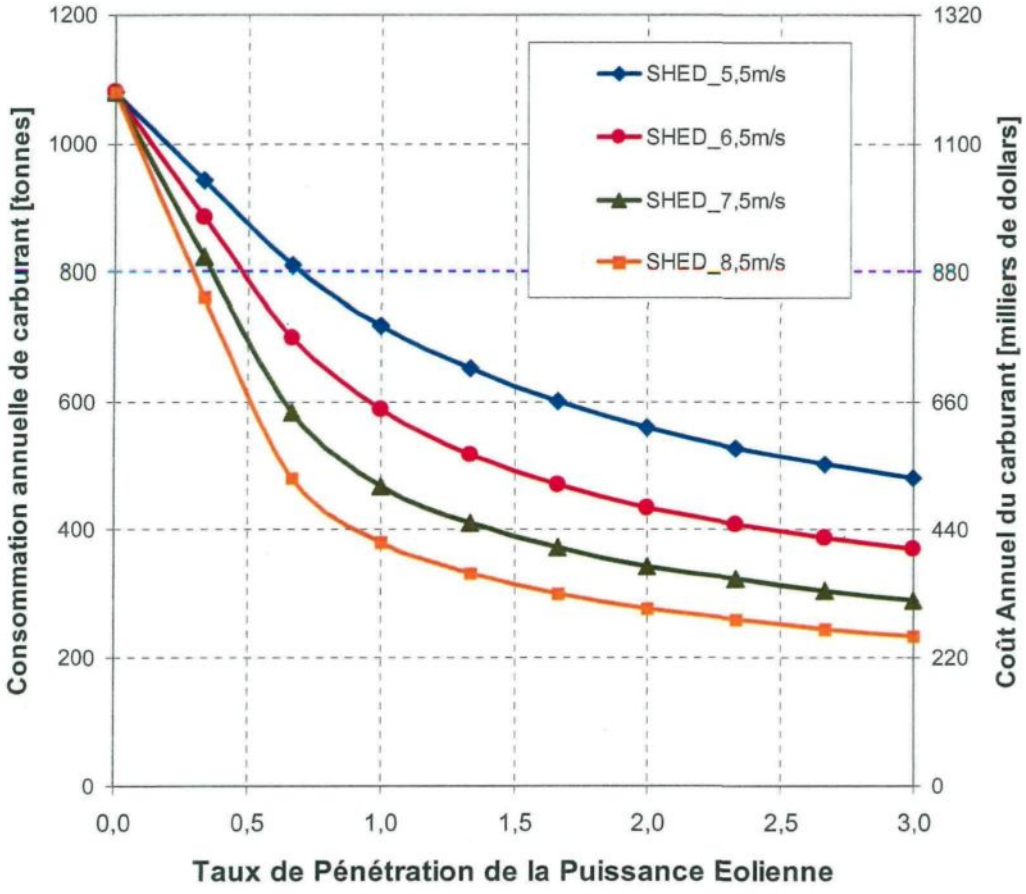

Figure I. 11 : Consommation annuelle d'un SHED en fonction du TPP éolien et de la vitesse moyenne du vent

Le point de départ des courbes (TPP=0) correspond à une génération par Diesel seul. La vitesse moyenne du vent a été obtenue en variant artificiellement les mesures de vitesses instantanées mesurées dans le village Tuktoyaktuk en 2007. Les données

d'origines correspondent à une vitesse moyenne de 5.5 m/s. Au regard des courbes de consommation de carburant présentés dans la Figure I.11, il est possible d'observer que l'économie de carburant obtenue grâce à un SHED est davantage importante que la vitesse du vent est élevée et / ou que le TPP est important. La pente de ces courbes nous renseigne sur la rentabilité du système SHED. Nous pouvons constater que la rentabilité du système SHED augmente plus rapidement pour les TPP inférieures à 1. La raison est simple : le taux de dissipation de l'énergie éolienne, qui représente l'énergie non exploitée lorsque la puissance éolienne est supérieure à la consommation, augmente avec l'augmentation du TPP, d'où l'aplatissement des courbes de consommation pour les forts TPP.

I.2.3. Stockage d'énergie pour l'amélioration de l'efficacité énergétique de la rentabilité des SHED à fortes pénétrations

Le stockage d'énergie a pour objectif de permettre l'exploitation de l'énergie éolienne initialement dissipée soit parce que la puissance de consommation instantanée est inférieure à la puissance éolienne disponible, soit parce que la puissance éolienne n'est pas assez forte pour permettre l'arrêt complet des Diesels qui continuent à fonctionner à 30% de leur charge nominale.

En stockant cette énergie excessive qui provient gratuitement, il est possible de la restituer plus tard et réduire la sollicitation ainsi que la consommation des génératrices Diesels. L'idée est donc de transférer l'énergie durant les périodes ou la demande est plus faible que la production éolienne aux périodes où la demande est plus élevée que cette production. En profitant ainsi du plein potentiel éolien, il est possible de maximiser l'économie de carburant ainsi que la rentabilité du système. La Figure I.12 est un complément de la Figure I.11, avec l'ajout des courbes de consommation de carburant d'un SHED supposé combiné avec un système de stockage idéal (SI) de l'énergie, c'est-à-dire un système ayant un rendement de 100%. Nous pouvons constater qu'une consommation « zéro-carburant » peut être idéalement obtenu pour un certain TPP, qui dépend de la vitesse moyenne sur le site. Pour une vitesse moyenne de 5,5 m/s (cas de Tuktoyaktuk), un SHED à très haute pénétration (TPP=2,5) pourrait solliciter très peu ou pas du tout son moteur Diesel si un système de stockage super-performant est mis en place. Plus le site est venteux,

plus ce seuil idéal de TPP assurant la « zéro consommation de carburant » est faible. Pour une vitesse moyenne de 8,5 m/s, ce seuil n'est que 1,1.

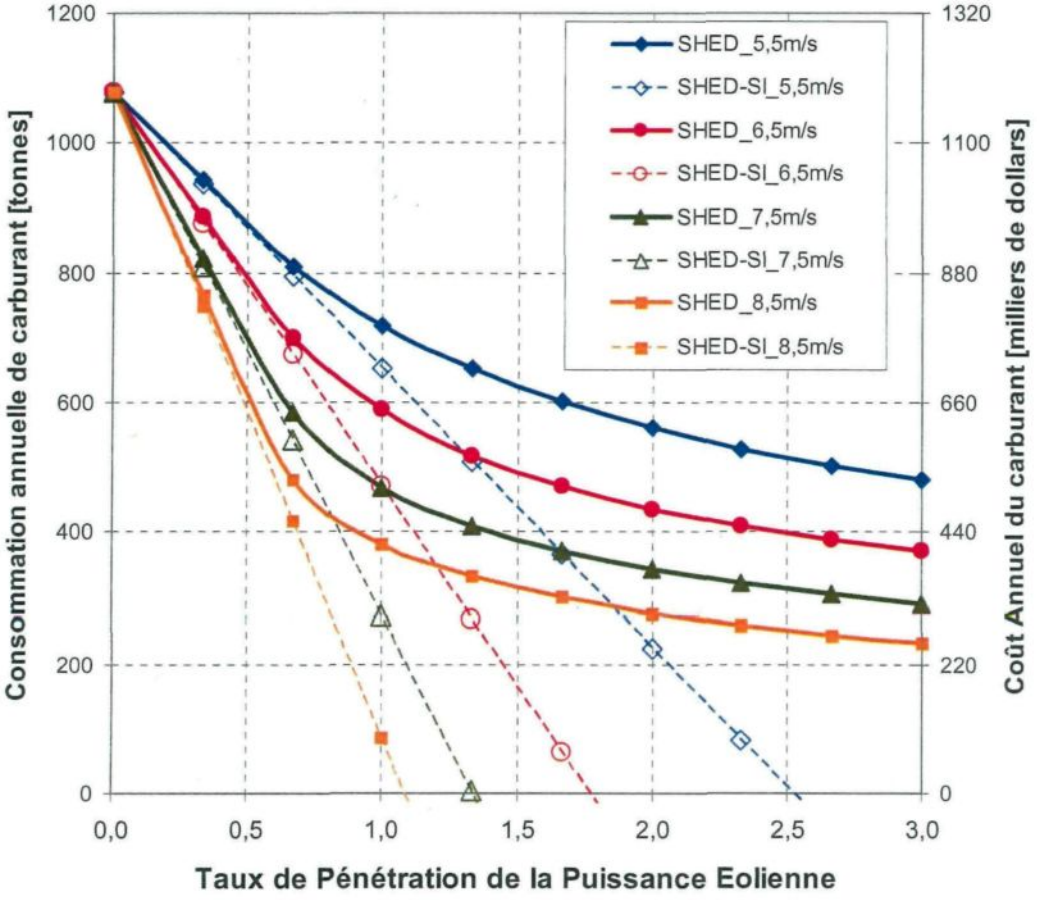

Figure I. 12 : Consommation annuelle d'un SHED et d'un SHED-SI en fonction du TPP et de la vitesse moyenne du vent

Cependant, cette opération de stockage et déstockage implique inévitablement des pertes d'énergie qui dépendent de l'efficacité du système de stockage – déstockage mis en place. Nous pouvons déjà prédire que la consommation d'un SHED avec un système de stockage réaliste se situera entre les deux courbes correspondantes à la vitesse moyenne du site. Le critère pour juger la performance énergétique du système mis en place est la proximité de sa courbe de consommation à celle du SHED avec stockage idéal.

I.2.4. Choix du système de stockage d'énergie sous forme d'air comprimé

Les possibilités techniques pour stocker l'énergie sont très vastes et concernent pratiquement toutes les formes d'énergie : mécanique, chimique ou thermique. Parmi les diverses solutions explorées, nous pouvons mentionner : volant d'inertie, stockage hydraulique, stockage sous forme d'air comprimé, batteries redox, batteries électrochimiques, stockage d'hydrogène, stockage thermique, super-condensateur, supraconductrice, etc.

Les moyens de stockage de l'énergie éolienne excédentaire envisagés présentement sont sous forme thermique (eau chaude), ou par des bancs de batteries. Ces dernières sont dispendieuses, difficiles à recycler, une source de pollution (plomb-acides) et limitées en puissance et en durée de vie. Les piles à combustible représentent une alternative viable mais la complexité technique, le prix prohibitif et le faible rendement retardent l'acceptation par le marché. De là apparaît la nécessité de choisir un dispositif de stockage assez efficace, propre, dynamique et adaptable au système hybride afin qu'il soit capable de réduire la consommation du Diesel et l'émission des GES et d'agir en temps réel en fonction des fluctuations de la puissance générée et consommée. Pour ce faire, toutes les technologies de stockage d'énergie ont été étudiées avec leurs caractéristiques techniques, économiques et environnementales de façon objective et détaillée dans plusieurs ouvrages [28-33]. Ces études ont menés à la conclusion préliminaire que le stockage d'énergie sous forme d'air comprimé est la technologie la plus appropriée et la plus performante pour être associée à un SHED à haute pénétration destiné pour l'alimentation en électricité des sites isolés.

Le stockage d'énergie sous forme d'air comprimé (CAES : Compressed Air Energy Storage) est une technologie déjà mature avec plusieurs réalisations de grande puissance. Il s'agit par exemple des centrales de Huntorf en Allemagne (210 MW) installée en 1978 et de Macintosh en Alabama aux Etats-Unis (110 MW) installée en 1991. Ces applications ne sont pas des sites isolés. La finalité du stockage d'énergie est de réguler la demande afin de permettre d'augmenter la pénétration des énergies renouvelables et nucléaires, comme illustré dans la Figure I.13. Lors les périodes de faible consommation, l'excès de l'énergie produite est stocké via un système de compresseurs à 40-70 bars, dans des cavernes souterraines géantes (310,000 m^3 pour

Huntorf et 540,000 m^3 pour Macintosh) [34] : Lors des périodes de fortes demandes, le stock de CAES est déchargé dans un turboréacteur à gaz naturel classique en réduisant significativement sa consommation de gaz. Le rendement cyclique de stockage-déstockage est de 54%, capable de croître à 80% si un système de récupération d'énergie des gaz d'échappement est mis en place.

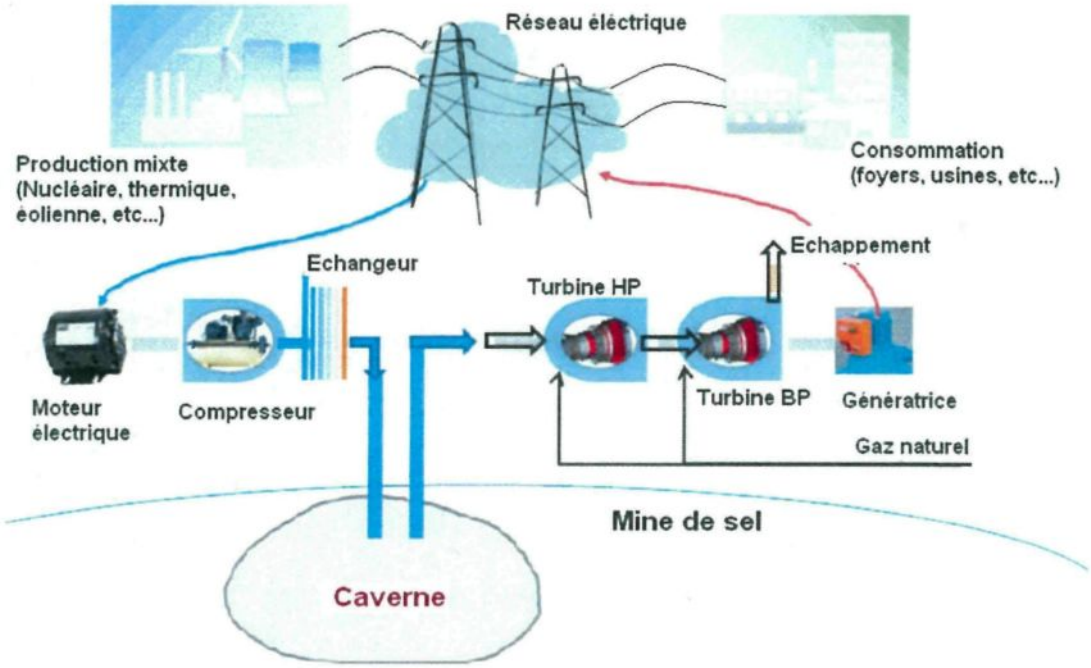

Figure I. 13 : Schéma de principe du fonctionnement du couplage turboréacteur à gaz– air comprimé pour la régulation de la production électrique (cas de Huntorf, Allemagne) [34]

On note que cette solution de combiner un stockage d'air comprimé à un turboréacteur à gaz n'est pas adaptée aux sites isolés qui sont par définition déconnectés du réseau de gaz naturel et ne peuvent ainsi pas assurer d'une façon fiable le fonctionnement d'un turboréacteur. La génératrice Diesel reste la source stable incontournable, d'où la proposition d'une solution innovante qui répond aux exigences techniques et financières de l'électrification des sites isolés tout en assurant une fiabilité d'approvisionnement électrique de ces sites. Il s'agit du système hybride Eolien-Diesel avec stockage d'air comprimé (SHEDAC).

I.3. Hybridation Pneumatique du moteur Diesel

I.3.1. Nécessité d'une hybridation pneumatique simple et efficace du moteur Diesel

Afin de stocker l'énergie éolienne sous forme d'air comprimé et ensuite la déstocker, il serait nécessaire d'avoir un Compresseur à Air (CA) et un moteur à air comprimé (MAC). Ces deux convertisseurs pourraient également être combinés en un seul dispositif fonctionnant en mode réversible. Les technologies de MAC et des CA sont matures et existent dans le marché, mais la puissance des MAC proposés ne dépasse pas quelques kilowatts [35]. Proposer l'ajout en série de plusieurs dizaines de CA et MAC aux systèmes SHED existants, ne semble pas être une solution économiquement viable. Il est donc nécessaire de trouver une autre solution plus économique.

L'alternative que nous étudions dans le cadre de cette thèse est une hybridation pneumatique des moteurs Diesels existants et les transformant en des Moteurs Hybrides Pneumatiques Diesels (MHPD). Par définition, on appelle hybridation pneumatique des moteurs Diesel toute adaptation de ces moteurs leur permettant de pouvoir être entraînés totalement ou partiellement par l'air comprimé. Les moteurs Diesels peuvent donc « tourner » sous l'effet seul de l'air comprimé (mode pneumatique) ou sous l'effet combiné de l'air comprimé et du carburant (mode hybride). Le concept visé doit aussi pouvoir fonctionner en mode compresseur afin d'économiser l'usage d'un CA.

Étant donné qu'il s'agit d'une adaptation de moteurs Diesels déjà installés, la technique d'hybridation proposée doit absolument être simple à mettre en œuvre, sans nécessiter des modifications lourdes de l'architecture initiale du moteur Diesel.

I.3.2. État de l'art et analyse critique des travaux d'antériorité sur l'hybridation pneumatique des moteurs à combustion interne

L'idée n'est pas nouvelle, elle date de plusieurs d'années. Cependant la plupart des recherches qui pont porté sur l'hybridation pneumatique des moteurs à combustion interne s'est focalisée sur l'application automobile afin de permettre au moteur de stocker l'énergie lors des décélérations du véhicule pour la restituer lors

des stabilisés ou accélérations. Certains chercheurs revendiquent également la possibilité d'augmenter la puissance spécifique des moteurs grâce à cette technique, permettant de réduire leur cylindrée et d'améliorer ainsi davantage leur efficacité. Ci-dessous nous synthétisons les recherches clés qui ont été réalisés au cours de ces dix dernières années sur ce thème.

Michael Schechter, un ingénieur de « Ford Research Laboratory », a publié une série de nouveaux cycles thermodynamiques permettant d'obtenir de meilleures performances avec un moteur à combustion interne, dont des cycles fonctionnant avec de l'air comprimé et le carburant simultanément ou séparément [36-38],

Quelques années plus tard, un concept prometteur a été étudié par Higelin et al. [39-41] puis par Donitz et al. [42-43] inspiré des cycles proposés par Schechter. Donitz a même réalisé un démonstrateur hybride pneumatique-combustion construit à partir d'un moteur à allumage commandé conventionnel. Ce concept est capable de fonctionner avec plusieurs modes dont principalement le mode conventionnel, le mode moteur pneumatique deux-temps, le mode moteur hybride pneumatique-combustion quatre-temps et le mode pompe deux-temps. Afin de réaliser ce concept à partir d'un moteur à essence ayant quatre soupapes par cylindres, Donitz a connecté un réservoir de cinquante litres à chacun des cylindres en dédiant une des soupapes d'admissions initiales à l'admission de l'air comprimé, comme le montre la Figure I.14. Les commandes de toutes les soupapes ont été transformées afin de permettre un contrôle total et indépendant de chacune d'elles [42-43]. Donitz a démontré d'abord par calcul ensuite par essais qu'une économie de carburant pouvant aller jusqu'à 28% peut être réalisée sur le cycle de roulage standard Européen NEDC (New European Driving Cycle).

En plus de ces recherches, plusieurs autres travaux ont porté sur des concepts plus simples permettant au moteur de fonctionner avec des modes moteur ou pompe à air, sans aller jusqu'au fonctionnement mixte pneumatique-combustion.

Hyungsuk et al. [44] a proposé un concept qui consiste à raccorder un réservoir d'air comprimé à l'échappement du moteur via une vanne trois-voies, comme illustré dans la Figure I.15. De la même façon que Donitz, le concept de Hyungsuk requiert un contrôle total de l'ouverture et de la fermeture des soupapes d'admission et

d'échappement du moteur, mais il a l'avantage de ne pas requérir une soupape dédiée à l'air comprimé.

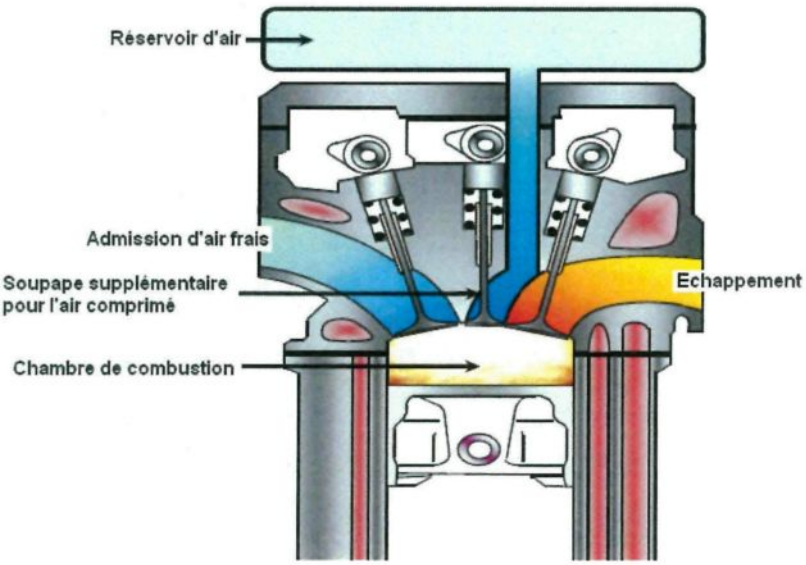

Figure I. 14 : Schéma de principe du moteur hybride combustion-pneumatique de Donitz [42]

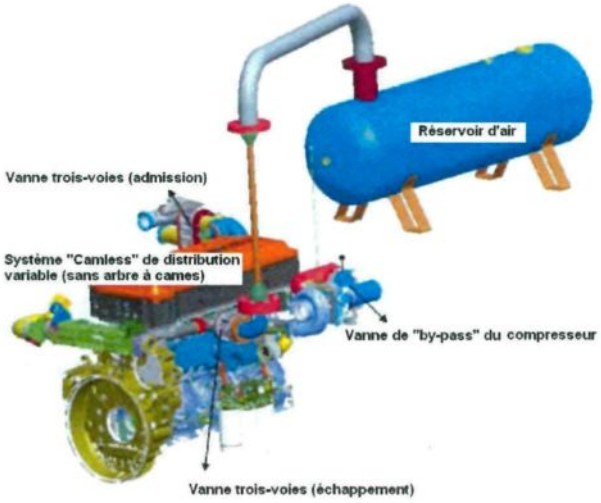

Figure I. 15 : Schéma de principe du moteur APA de Hyungsuk [44]

Hyungsuk donne à son moteur le nom APA (Air-Power-Assisted engine). Quelques essais préliminaires ont démontré la capacité du moteur à réaliser du travail

sous l'effet seul de l'air comprimé, mais aucune évaluation de l'économie de carburant globale n'a encore été réalisée.

De plus, Trajkovic [45-47] a converti un moteur Diesel monocylindre Scania D12 en un convertisseur réversible pouvant fonctionner en mode moteur pneumatique deux-temps et en mode compresseur pneumatique deux-temps. Le concept est réalisé en connectant simplement l'admission du moteur à un réservoir d'air comprimé et en prenant le contrôle total des soupapes d'admission et d'échappement. Trajkovic a procédé à une optimisation des temps d'ouvertures et de fermeture des soupapes d'admission et d'échappement. Ceci a permis de réaliser une efficacité de récupération d'énergie en mode stabilisé allant jusqu'à 48%. Il s'agit du ratio de l'énergie obtenue par l'air comprimé sur l'énergie qui a servi à le comprimer.

Pour conclure cette revue, il serait intéressant de mentionner les travaux de Lee [48] qui a travaillé sur un nouveau concept « pas cher » d'hybridation pneumatique des moteurs des bus et véhicules commerciales. Le concept requiert peu de modifications de l'architecture du moteur. Il s'agit de l'ajout de deux clapets anti retour permettant de connecter l'admission du moteur à un réservoir d'air comprimé tout en gardant la possibilité d'admettre l'air ambiant via la même soupape d'admission. Le système de distribution n'est pas changé et donc aucun contrôle supplémentaire des soupapes n'est demandé. Le moteur peut fonctionner en mode conventionnel, en mode compresseur et en mode moteur pneumatique quatre temps. Il a démontré qu'avec une pression nominale de stockage de 8 bar, il est possible d'obtenir une certaine économie de carburant, faible dans l'absolu, mais intéressante comparée au coût d'adaptation du moteur qui a permis de l'obtenir.

Une analyse critique de ces travaux de recherches antérieurs conduit à la conclusion qu'aucun de ces moteurs ne répond réellement à notre besoin d'hybridation pneumatique des génératrices Diesel existant dans les régions isolées. Le concept de Higelin et Donitz, et malgré sa performance énergétique démontrée, requiert l'ajout d'une soupape spécifique pour l'admission de l'air comprimé. Une nouvelle culasse du moteur doit donc être fabriquée, ce qui est très coûteux étant donné le nombre limité d'exemplaires qu'il faut produire, contrairement à l'application automobile qui assure via la fabrication de plusieurs centaines de milliers de moteurs, la rentabilité de ce genre d'adaptation. De plus, l'intérêt ce concept a été démontré pour une hybridation d'un moteur à allumage commandé et

non pas celle d'un moteur Diesel. En effet, pour un fonctionnement en mode hybride pneumatique-combustion, l'admission de l'air comprimé se fait dans la phase de compression, puis l'injection de carburant et l'allumage du mélange se font pendant cette même phase avant que le piston arrive à son point mort haut. Ceci est compatible avec un moteur à allumage commandé dans lequel la question du délai d'inflammation ne se pose pas, contrairement au moteur à allumage par compression pour lequel il faut laisser un temps suffisant entre l'injection du carburant et l'arrivée du piston à son point mort haut pour que la combustion et la détente se réalisent d'une façon complète et efficace ; il s'agit du fameux délai d'auto-inflammation. Pour cette raison, et tant que ça n'a pas été démontré, le concept de Higelin et Donitz est considéré non compatible avec un moteur Diesel.

Quant aux concepts de Hyungsuk et Trajkovic, ils satisfont les critères d'adaptabilité, cependant ils ne proposent pas un fonctionnement en mode hybride pneumatique-combustion, ce qui limite leur champs d'utilisation et ainsi leur efficacité globale.

Enfin, le concept de Lee n'est pas assez ambitieux quant à l'économie de carburant qu'il permet d'obtenir, et au volume de stockage d'air qu'il requiert, étant donné la relativement faible pression nominale d'air comprimé qu'il propose.

Pour ces raisons, il a été nécessaire de proposer un concept qui réponde aux critères définis dont principalement la simplicité d'adaptation d'un moteur Diesel, l'efficacité du système et la nécessité d'un volume de stockage acceptable.

I.3.3. Description du fonctionnement global du concept SHEDAC-MHPD

Le système que nous visons à concevoir et étudier, consiste simplement à combiner le système SHED à un réservoir de stockage d'air comprimé et à transformer le moteur Diesel existant en un MHPD. Dorénavant, nous appellerons ce concept multi-Hybride par SHEDAC-MHPD (SHEDAC pour Système Hybride Eolien-Diesel et MHPD pour Moteur Hybride Pneumatique Diesel).

Comme le montre le diagramme fonctionnel de la Figure I.16, les différents éléments du système SHEDAC peuvent être classés en plusieurs catégories fonctionnelles :

1) les sources d'énergies : le vent et le carburant ;

2) les convertisseurs de puissance : la ou les éoliennes et le Moteur Hybride Pneumatique-Diesel (MHPD) qui se doit, selon notre objectif visé, de pouvoir fonctionner avec le carburant et avec l'air comprimé dans les deux sens (compresseur et moteur);

3) le système de stockage d'énergie : le réservoir d'air comprimé ;

4) les consommateurs : les foyers.

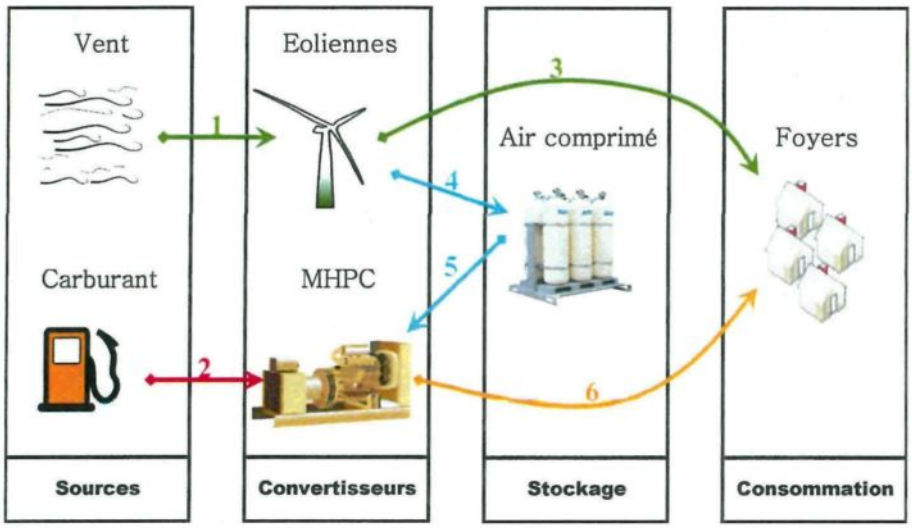

Figure I. 16 : Diagramme fonctionnel illustrant les flux énergétiques dans un SHEDAC

Tableau I. 2 : Diagramme fonctionnel illustrant les flux activés en fonction de l'État de Charge du Stockage (ECS) et de la comparaison entre la Puissance Éolienne (PE) disponible avec la Charge (CH)

	PE=0	*0<PE<CH*	*PE>CH*
PE▶ / CH▶			
ECS=0%	**2-6**	**1-2-3-6**	**1-3-4**
0%<ECS<100%	**5-6 ou 2-5-6**	**1-3-5-6 ou 1-2-3-5-6**	
ECS=100%			**1-3**

Les différents flux énergétiques réalisables entre les différents éléments du SHEDAC sont numérotés également dans la Figure I.9. Le tableau I.2 montre d'une façon synthétique les flux activés en fonction des cas possibles. L'activation ou non de chacun des flux énergétiques dépend de trois facteurs :

1) l'état de charge du système de stockage (ESC) ;
2) la puissance éolienne (PE) disponible ;
3) la charge (CH) demandée.

I.4. Objectifs et méthodologie du travail

I.4.1. Objectifs du projet de recherche global et de cette thèse

Cette thèse fait partie d'un projet de recherche global qui vise à faire l'étude, la recherche, la conception et le développement d'un Système Hybride Éolien-Diesel avec stockage d'énergie sous forme d'Air Comprimé (SHEDAC). Son objectif principal est de concevoir et évaluer une technique d'hybridation pneumatique du moteur Diesel qui lui permet d'avoir les fonctions Moteur à Air Comprimé (MAC) et Compresseur d'Air (CA). La finalité est d'assurer la rentabilité du SHEDAC en éliminant l'ajout d'un système de MAC et de CA indépendants. Cet objectif principal peut être divisé en trois sous-objectifs :

1) Explorer toutes les techniques possibles pour l'hybridation pneumatique des moteurs Diesel et retenir celle qui assure le meilleur compromis entre la complexité des changements qu'il faut apporter au moteur Diesel d'une part, et l'économie de carburant atteignable grâce à cette technique d'autre part ;
2) Optimiser le concept choisi de façon à obtenir la consommation minimale de carburant sur une année complète avec un volume de stockage le plus faible possible ;
3) Recommander la pression de stockage et le volume du réservoir de stockage pour une application cible.

I.4.2. Méthodologie

La méthodologie suivie pour la réalisation des objectifs définis est constituée de plusieurs étapes et sous-étapes :

1) Recherche du meilleur concept de Moteur Hybride Pneumatique-Combustion (MHPD) ;

   1.1) Recherche d'antériorité sur tous les travaux de recherche qui porte sur l'hybridation pneumatique des moteurs à combustion interne en général et évaluation de la portabilité de ces travaux à notre application SHEDAC ;

   1.2) Modélisation de plusieurs concepts de MHPD candidats pour le SHEDAC, en commençant par les plus simples à mettre en œuvre, et évaluation de leur potentiel ;

   1.3) Sélection du concept MHPD qui offre le meilleur compromis entre la complexité des changements qu'il faut apporter au moteur Diesel d'une part, et l'économie de carburant atteignable grâce à cette technique d'autre part;

2) Modélisation et mise au point du concept MHPD ;

   2.1) Modélisation des cycles thermodynamiques théoriques sans prise en compte des imperfections causées par des limitations ou phénomènes physiques inévitables (pertes thermiques aux parois, limitations de débits, temps de réponses de l'actuation des vannes, etc.) ;

   2.2) Optimisation des commandes du concept (ouvertures et fermetures des soupapes, injection du carburant, positions des vannes et volets, etc.) sur la base des cycles thermodynamiques théoriques dans le but d'obtenir la meilleure efficacité énergétique (consommation d'air et de carburant);

   2.3) Modélisation des cycles thermodynamiques réels prenant en compte les caractéristiques dynamiques des phénomènes de transvasement ;

   2.4) Optimisation et dimensionnement du temps de réponse des actuateurs requis pour opérer correctement le concept MHPD ;

3) Evaluation du Système Hybride Éolien-Diesel avec stockage d'énergie sous forme d'Air Comprimé (SHEDAC) combiné avec le concept MHPD, sur une application cible (site de Tuktoyaktuk) ;

   3.1) Modélisation des différents éléments du SHEDAC (Eoliennes, MHPD, réservoir de stockage, etc....) et couplage avec les données de vitesse du vent et de la consommation électrique ;

   3.2) Evaluation de l'écart de consommation de carburant annuelle entre un SHED et un SHEDAC en fonction du volume de stockage d'air disponible et du taux de pénétration de l'énergie éolienne ;

   3.3) Elaboration et évaluation d'une stratégie de gestion optimale du stock d'air permettant de maximiser l'économie de carburant et/ou de minimiser le volume requis pour le stockage ;

4) Elaboration de recommandations pour une étude de validation expérimentale des résultats théoriques obtenus.

I.5. Structure de la thèse

La présente thèse est produite « par articles ». Les différents articles soumis ou publiés dans des journaux scientifiques avec comité de lecture suivent les objectifs et la méthodologie décrits dans le chapitre I.4.

Le chapitre II présente le premier article intitulé «Pneumatic hybridization of a Diesel engine using compressed air storage for wind-Diesel energy generation» et qui est le fruit des sous-étapes 1.1 et 1.2 de la méthodologie. Il expose une évaluation du potentiel et des limites du gain en carburant espéré en remplaçant le système de suralimentation par turbocompresseur du moteur par une introduction de l'air comprimé directement à l'entrée du moteur sans changer son fonctionnement global.

Le chapitre III présente le deuxième article intitulé «A new hybrid pneumatic-combustion engine to improve fuel consumption of wind-Diesel power system for non-interconnected areas» et qui est le fruit des sous-étapes 1.3, 2.1, 2.2, 3.1 et 3.2 de la méthodologie. Il expose un nouveau concept d'une hybridation pneumatique du moteur Diesel qui peut être obtenu par une modification du circuit d'admission et d'échappement d'un moteur Diesel conventionnel en le transformant en un Moteur Hybride Pneumatique-Diesel (MHPD). Avec une modélisation simple du système,

l'économie de carburant réalisée par un SHEDAC-MHPD dans le site de Tuktoyaktuk est évaluée en fonction du TPP et du volume de stockage d'air disponible..

Le chapitre IV présente le troisième article intitulé «Fuel consumption evaluation of an optimized new hybrid pneumatic–combustion vehicle engine on several driving cycles». Cet article ressemble à l'article précédent dans sa première partie dans laquelle sont présentées la description, la modélisation et l'optimisation du fonctionnement du concept MHPD. Dans sa deuxième partie, l'article présente l'évaluation de l'économie de carburant obtenue avec ce concept, sur une application automobile, pour laquelle il est possible de stocker sous forme d'air comprimé l'énergie disponible lors des décélérations pour la restituer lors des accélérations. Ce travail, même s'il est en dehors du contexte de cette thèse, a été réalisé et soumis à ce journal pour deux raisons :

1) Avoir une reconnaissance de la crédibilité du concept, par un journal spécialisé dans les moteurs, tel que le *International Journal of Engine Research* ;
2) Démontrer que l'application du concept MHPD peut toucher d'autres domaines, tels que le domaine de l'automobile, même s'il a été réalisé pour répondre aux besoins spécifiques de la génération d'électricité pour les sites isolés.

Le chapitre V présente le quatrième article intitulé «Required time response of a variable valve actuator equipping a hybrid pneumatic-combustion engine» et qui est le fruit des sous-étapes 2.2 et 2.4 de la méthodologie. Il présente l'impact du temps de réponse du Système de Distribution Variable (SDV) requis pour le MHPD, sur la performance du système, pour en déduire le temps de réponse (TR) nécessaire pour obtenir une économie de carburant significative avec le SHEDAC-MHPD.

Le chapitre VI présente le cinquième article intitulé «Optimal management of compressed air energy storage in a hybrid wind-pneumatic-Diesel system for remote area's power generation» et qui est un rapport de synthèse dans lequel l'évaluation de l'économie de carburant réalisée par le système SHEDAC-MHPD est consolidée et une nouvelle stratégie de gestion du stock d'air comprimé est présentée, optimisée et évaluée. Cette stratégie permet de maximiser l'économie de carburant annuelle en favorisant l'optimisation de l'efficacité quand l'air comprimé est en cours d'épuisement, et la minimisation de la consommation instantanée de carburant quand l'air comprimé est abondant . Une étude de sensibilité en fonction de la vitesse

moyenne du vent sur le site en question est également réalisée. Ce travail est le fruit de l'étape 3.3 présenté dans la méthodologie.

Enfin, le chapitre VII présente la synthèse globale de tous les résultats obtenus dans le cadre de cette thèse en détaillant les économies de carburant associées au système SHEDAC-MHPD en fonction du TPP, de la vitesse moyenne du vent et du volume de stockage. Une conclusion générale ainsi qu'une perspective pour la suite des travaux est également exposée.

CHAPITRE II

Article 1

Pneumatic hybridization of a Diesel engine using compressed air storage for wind-Diesel energy generation

Publié dans Energy, Vol 38, février 2012
Energy 38 (2012) 264-275

Résumé

Cet article présente une évaluation du potentiel de l'économie de carburant obtenue en remplaçant le système de suralimentation par turbocompresseur du moteur par une introduction de l'air comprimé directement à l'entrée du moteur sans changer sont fonctionnement global. Grâce à l'air comprimé stocké, les conditions de température et de pression à l'entrée du moteur peuvent être pilotées. Cette technique est très simple à mettre en œuvre étant donné que les modifications à apporter sont seulement sur les circuits d'admission et d'échappement du moteur. L'évaluation de l'économie de carburant est réalisée à l'aide d'un modèle du cycle thermodynamique. Une étude paramétrique variant simultanément la pression et la température à l'admission et à l'échappement du moteur a été effectuée. Le travail démontre qu'un gain significatif peut être obtenu en augmentant la pression et en diminuant la température à l'admission et la pression à l'échappement. Ce gain peut aller jusqu'à 40% sur les faibles couples et décroit progressivement jusqu'à zéro sur les très forts couples. Il peut s'expliquer par trois phénomènes :

1) La réduction des pertes par transvasements et leur transformation en travail pneumatique ;
2) La réduction des pertes thermiques aux parois du fait de la réduction significative de la température moyenne des gaz de combustion ;

3) L'amélioration du rendement de cycle et du rendement de combustion du fait d'un meilleur rapport air-sur-carburant.

En revanche, cette étude démontre que la pression maximale admissible dans le moteur dans ces conditions ne peut excéder 4 bars sinon la pression maximale dans le cylindre, résultant de la compression et la combustion, dépassera 200 bars, ce qui risque de casser le moteur. Cette contrainte conduit à devoir choisir entre l'une des options suivantes :

1) Le stockage se fait à 4 bars, ce qui nécessite un volume de stockage extrêmement important pour réaliser une économie annuelle de carburant qui soit significative.

2) Le stockage se fait à une pression supérieure et l'on procède à une détente de l'air avant son introduction dans le moteur, ce qui signifie que l'efficacité de récupération globale qui est égale au rapport de l'énergie extraite de l'air comprimé sur l'énergie éolienne dépensée pour le comprimer sera très médiocre, et ainsi sera l'économie annuelle de carburant.

Pour ces raisons, le concept proposé dans cet article a été jugé plus tard comme inefficace et un nouveau concept s'affranchissant de cette limitation, présenté dans l'article 2 (chapitre 3), a été retenu.

Energy 38 (2012) 264–275

Contents lists available at SciVerse ScienceDirect

Energy

journal homepage: www.elsevier.com/locate/energy

Pneumatic hybridization of a diesel engine using compressed air storage for wind-diesel energy generation

Tammam Basbous [a,b,*], Rafic Younes [b,c], Adrian Ilinca [b], Jean Perron [a]

[a] Laboratoire International des Matériaux Antigivre, Université du Québec à Chicoutimi, Chicoutimi, Québec, Canada
[b] Laboratoire de Recherche en Energie Eolienne, Université du Québec à Rimouski, 300 allée des Ursulines, Rimouski, Québec G5L 3A1, Canada
[c] Faculté de Génie, Université Libanaise, Beyrouth, Liban

ARTICLE INFO

Article history:
Received 4 August 2011
Received in revised form
28 November 2011
Accepted 1 December 2011
Available online 29 December 2011

Keywords:
Pneumatic hybridization
Wind energy
Diesel engine
Wind-diesel hybrid system
Compressed air energy storage

ABSTRACT

In this paper, we are studying an innovative solution to reduce fuel consumption and production cost for electricity production by Diesel generators. The solution is particularly suitable for remote areas where the cost of energy is very high not only because of inherent cost of technology but also due to transportation costs. It has significant environmental benefits as the use of fossil fuels for electricity generation is a significant source of GHG (Greenhouse Gas) emissions. The use of hybrid systems that combine renewable sources, especially wind, and Diesel generators, reduces fuel consumption and operation cost and has environmental benefits. Adding a storage element to the hybrid system increases the penetration level of the renewable sources, that is the percentage of renewable energy in the overall production, and further improves fuel savings. In a previous work, we demonstrated that CAES (Compressed Air Energy Storage) has numerous advantages for hybrid wind-diesel systems due to its low cost, high power density and reliability. The pneumatic hybridization of the Diesel engine consists to introduce the CAES through the admission valve. We have proven that we can improve the combustion efficiency and therefore the fuel consumption by optimizing Air/Fuel ratio thanks to the CAES assistance. As a continuation of these previous analyses, we studied the effect of the intake pressure and temperature and the exhaust pressure on the thermodynamic cycle of the diesel engine and determined the values of these parameters that will optimize fuel consumption.

1. Introduction

1.1. Context

Most of the remote and isolated communities or technical installations (communication relays, meteorological systems, tourist facilities, farms, etc.) that are not connected to national electric distribution grids rely on diesel engines to generate electricity [1]. Electricity generated by Diesel is more expensive than large electric production plants (gas, hydro, nuclear, wind), even before taking into account the transport and environmental costs associated with this type of energy.

In Canada, approximately 200,000 people live in more than 300 remote communities (Yukon, Northwest Territories, Nunavut, etc.) that use Diesel generated electricity, which is responsible for the emission of 1.2 million tons of greenhouse gases annually [2]. In Quebec alone, there are over 14,000 subscribers scattered in about forty communities that are not connected to the main electrical grid. Each community constitutes an autonomous network that uses diesel generators for electricity production [3].

In Quebec, the total production of Diesel power generating units is approximately 300 GWh per year. The operation of these Diesel generators is extremely expensive due to the high oil price and transportation costs. Indeed, as the fuel has to be delivered to remote locations including those who are only reachable by boat during the summer, the cost of electricity in 2007 reached more than 50 cent/kWh in some communities, while in the rest of the province the electricity tariff was approximately 6 cent/kWh [1]. The resulting deficit, which is shared among all Quebecers, is far from being negligible. In 2004, the autonomous networks accounted for 144 MW of installed power, and the consumption was established at 300 GWh. Hydro-Quebec, the provincial utility, estimated the annual loss resulting from the difference between the diesel electricity production cost and the uniform electricity tariff to be approximately 133 million Canadian dollars [3].

* Corresponding author. Laboratoire de Recherche en Energie Eolienne, Université du Québec à Rimouski, 300 allée des Ursulines, Rimouski, Québec G5L 3A1, Canada. Tel.: +1 418 723 1986; fax: +1 418 724 1879.
E-mail address: el_basbous@hotmail.com (T. Basbous).

0360-5442/$ – see front matter © 2011 Elsevier Ltd. All rights reserved.
doi:10.1016/j.energy.2011.12.003

Moreover, Diesel electricity production is considered ineffective, presents significant environmental risks (spilling), pollutes local air and contributes to global warming. Overall, we estimate at 140,000 tons the annual GHG emission resulting from the use of diesel generators for the autonomous networks in Quebec. This is equivalent to the GHG emitted by 35,000 cars during one year.

While they require relatively small investments, the operating and maintenance costs of Diesel engine generators are generally very high, particularly when they function regularly at partial load [4]. Their use under weak operating factors accelerates wear and increases fuel consumption [3].

The use of Hybrid Wind-Diesel Generators solves some of the problems listed above, but their efficiency is limited due to wind intermittency. Highly fluctuating wind energy requires the Diesel engine running on idle most of the time and dissipates a part of the wind power in order to control the balance between the energy production and the energy demand [5]. Energy storage is the key to solve this issue, because it allows storing otherwise wasted energy and recover it later, when the wind power is not sufficient to cover the demand. The use of storage allows an increased penetration of the wind power in the overall system capacity [4]. The high penetration of wind energy means that the installed wind power exceeds the maximum load and, during periods of strong winds, Diesel generators may be stopped while surplus of wind energy is stored. The overall energy provided by the Diesel generator is significantly decreased with beneficial economic and environmental results. Among all energy storage techniques, Compressed Air Storage (CAES) is one of the most suitable to be used in hybrid system for remote areas application, thanks to its low cost, high power density and reliability [4].

The energy to power ratio of compressed air storage could be chosen freely. The size of the tank, a conventional industrial product, determines the energy content and the size of the motor/generator determines the power output [22]. The compressed air is usually used to drive a compressed air motor or a gas turbine to generate electricity [22]. In our project, we investigate another possibility that consists in using the Diesel engine already installed to exploit the compressed air stored. This technique is called Pneumatic Hybridization of the Diesel engine. CAES would make the Diesel engine run with less fuel consumption or even without any fuel injection at some operating points.

1.2. Objectives and methodology

Pneumatic Hybridization of the Diesel engine consists to use the stored compressed air to supercharge the Diesel engine. This could be done by several methods [1]. In a previous work [1,4] we demonstrated that with this technique, we can improve the combustion efficiency and therefore the fuel consumption through optimization of Air/Fuel ratio. Fig. 1 illustrates the link between previous and current work. Actually, we are completing previous work by studying the effect of controlling the intake air temperature and pressure, and the exhaust pressure of the Diesel engine on the thermodynamic cycle and evaluated the potential of fuel consumption reduction. It is possible to adjust these parameters by removing the turbocharger and connecting an air tank directly to the intake valve. The air in the tank has been expanded from the storage pressure to the wanted intake pressure. The intake temperature is controlled with a heating system that takes its energy from the Diesel cooling system or from Diesel exhaust gas. Our objective is to establish the maximal potential of pneumatic hybridization of the Diesel engine without any change in its architecture. Variable valve actuation has therefore not been considered. The only control parameter that we have accepted to optimize is the fuel injection timing, a minor change as it can be easily done by electronically modifying the command of the fuel injectors.

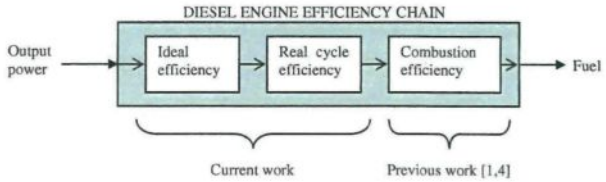

Fig. 1. Illustration of the links between previous [1,4] and current work.

The thermodynamic cycle of the diesel is simulated with a zero dimension mathematical model that is used to conduct a parametric study varying simultaneously the intake air pressure, the intake air temperature, the exhaust gas pressure and the injection timing for different engine loads. It is a classic mathematical model generally used by other authors [6,8,9]. We did not conduct any tests to calibrate or fit our parameters with a known engine but rather values available in literature [10]. We limited our study to providing guidelines for future design work by determining the resulting fuel consumption, air consumption and maximum cylinder gas pressure. The last output is important because, as will be shown later, it is the main limitation for increasing intake pressure. Actually, gas pressure in the combustion chamber has to remain under a certain limit established as a reliability criterion specific for each engine. A value of 180 bars [21] is a common limitation for Diesel engines. We have considered this value as a threshold for cylinder gas pressure.

The structure of the present article is as follows. Chapter 2 presents the state of art of pneumatic hybridization of Diesel engines and internal combustion engines in general. In chapter 3 we explain the mathematical models used to conduct the parametric study mentioned above. In chapter 4, we discuss the results obtained when parameters are varied at a partial load operating point. It presents also the results obtained for the optimization on the whole range of load operating points. Finally, chapter 5 provides a preliminary conclusion of our study and a perspective for future work.

2. State of art

2.1. Compressed air energy storage

Among all the techniques permitting the storage of intermittent renewable energy, such as Pumped hydroelectric storage, batteries, superconducting magnets, flywheels, regenerative fuel cells and Compressed Air Energy Storage (CAES), the last one has an

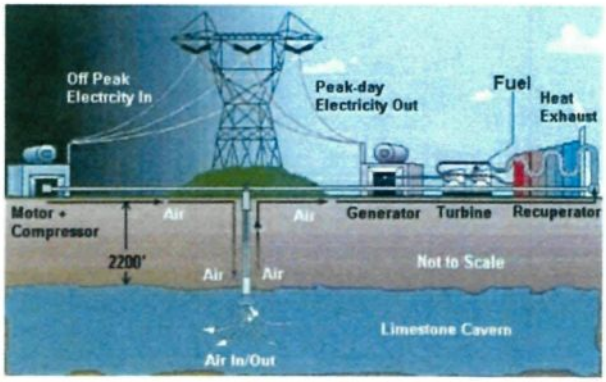

Fig. 2. Illustration of compressed air energy storage [31].

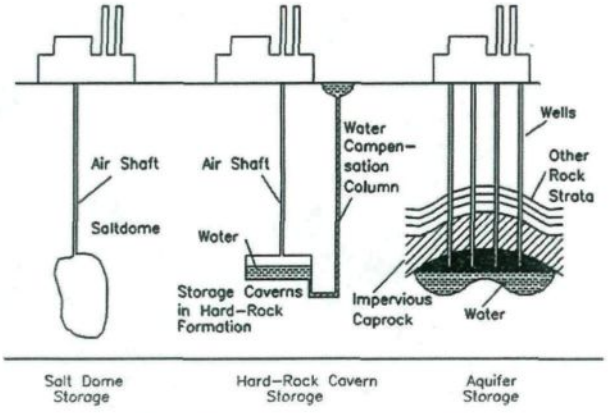

Fig. 3. Different types of CAES reservoirs [27].

overwhelming advantage considering its low cost, low environmental impact and high reliability [25].

CAES relies on relatively mature technology with several high-power projects in place [24,31]. A power plant with a standard gas turbine uses nearly two-thirds of the available power to compress the combustion air. It therefore seems possible, by separating the processes in time, to use electrical power during off-peak hours (storage hours) in order to compress the air, and then to produce, during peak hours (retrieval hours), three times the power for the same fuel consumption by expanding the air in a combustion chamber before feeding it into the turbines. Residual heat from the smoke is recovered and used to heat the air (Fig. 2).

Compressed air energy storage is achieved at high pressures (40–70 bars), at near-ambient temperatures [30] which means less volume and a smaller storage reservoir. Large caverns made of high-quality rock deep in the ground, ancient salt mines, or underground natural gas storage caves are the best options for compressed air storage, as they benefit from geostatic pressure, which facilitates the containment of the air mass (Fig. 3). A large number of studies [27] have shown that the air could be compressed and stored in underground high-pressure piping (20–100 bars). This method would eliminate the geological constraints and make the system easier to operate (Fig. 3). The energy density for this type of system is approximately 12 kWh/m^3 [31], while the estimated efficiency is around 70% [28]. The first storage station using an underground compressed air reservoir has been in operation since November 1978 in Huntorf, near Bremen, Germany [26]. In 1991, an American installation in MacIntosh,

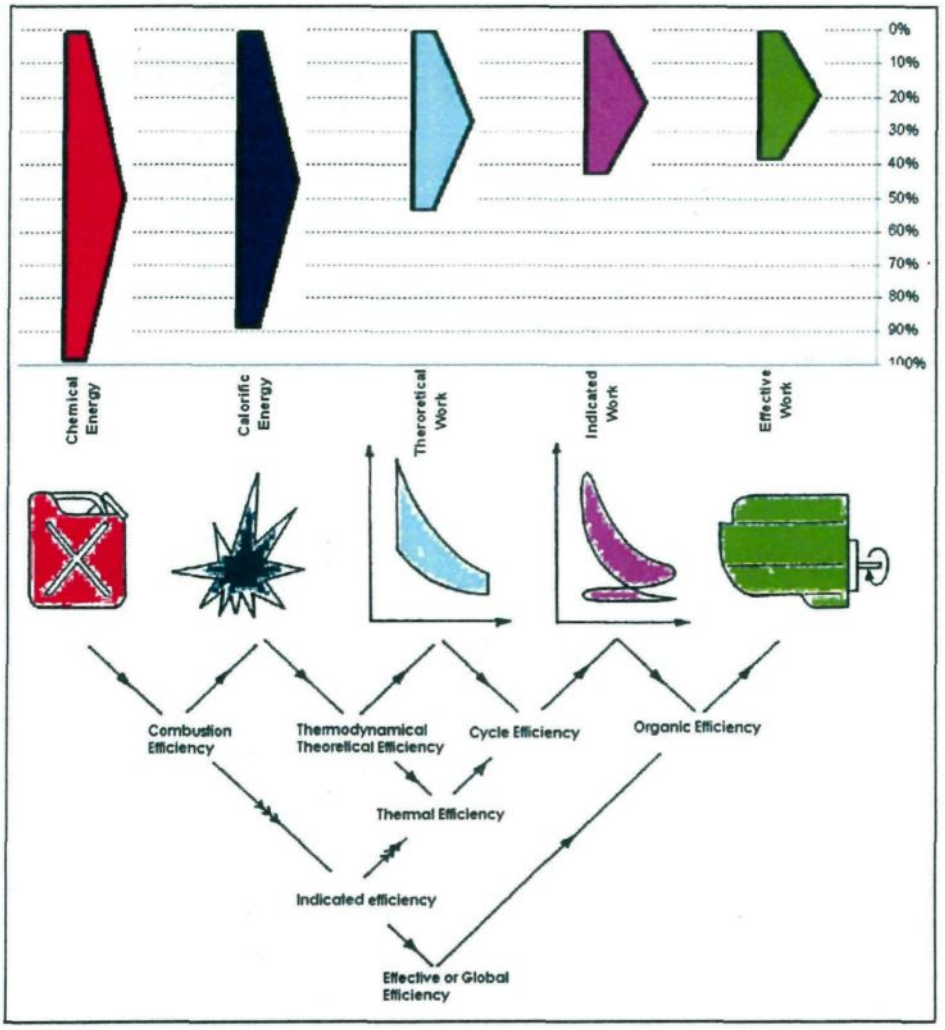

Fig. 4. Energy flow and efficiencies in a typical diesel engine.

Alabama, began to deliver 100 MW of power for 226 h. The ambient air is compressed and stored at a pressure between 40 and 70 bars in a 2555.10^3 m^3 cavern, 700 m deep in the ground [29]. During summer, the system generates energy 10 h per day on weekdays. The company using this application partially recharges the cavern weekday nights and full recharge is done on weekends. The system is in use 1770 h per year [29].

2.2. Pneumatic hybridization of diesel engines

Among the various concepts available for supplying power in autonomous grids, Diesel engines are simply stated as the most economical solution in the range of energy requirement up to 300 MW capacity, due to their efficiency, reliability, versatility and low cost [23]. In order to provide a response for pollutants and greenhouse emissions regulations, a great deal of research is conducted worldwide to improve energetic performance of Diesel engine. The efficiency of the direct injection Diesel engine has considerably increased during the last decade mainly due to turbo-charging and downsizing technique [23]. The global efficiency of a typical Diesel Engine is actually around 40% as shows Fig. 4 [6].

Since late 1990s, pneumatic hybridization of Internal Combustion Engines has been explored with a focus on automotive application. The key idea is to use the engine also as a pump to recover the vehicle's kinetic energy during braking phases, and as an expansion motor for propulsion. Donitz, Vasile, Onder and Guzzella [17] realized a fully operational hybrid pneumatic engine, able to operate under six modes as illustrated in Fig. 5.

This can be realized by connecting an air pressure tank to all cylinders via electronically fully controlled CV (Charge Valve) [7] as shown in Fig. 6. The original IV (Intake Valve) and EV (Exhaust Valve) should also be electronically controlled. Test results, supported with a modeling analysis [7] showed viability of this new concept for fuel consumption reduction, if it is combined with a strong downsizing and supercharging of the engine. Compared to a naturally aspirated engine with the same rated power, the downsized and supercharged hybrid pneumatic engine can save as much as 32% fuel [17]. The strong downsizing is possible thanks to pneumatic hybridization because the problem of the "turbo-lag" usually associated with heavily downsized and supercharged engines is completely overcome by injecting additional air from a pressure tank and more fuel during transients [17]. Experiments have confirmed the engine's instantaneous torque response resulting from applying this "supercharged" mode [17].

Earlier, Higelin, Vasile, Charlet and Chamaillard [9,18] studied a similar concept and found, using simulations of the theoretical thermodynamic cycles that fuel consumption on NEDC

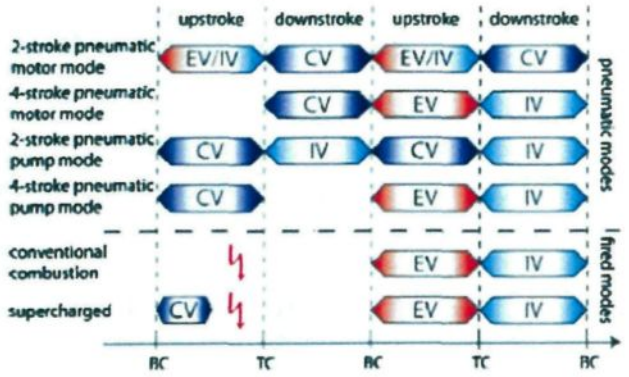

Fig. 5. Operating modes of Donitz et al. engine [17].

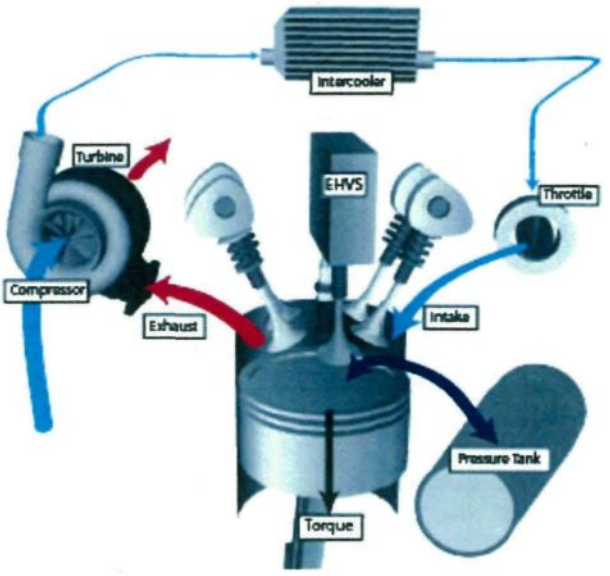

Fig. 6. Donitz et al. [17] hybrid pneumatic engine.

(Normalized European Diesel Cycle) driving cycle could be reduced up to 31 percent if all the parameters including the tank volume were optimized [18].

Hyungsuk, Tai, Smith, Wang, Tsao, Stewart et al. [19] worked on a simpler concept, the APA (Air Power Assist) engine, illustrated in Fig. 7. It consists in connecting the compressed air tank to the exhaust manifold and use a three-way valve to switch flow between turbine and air tank. No need for a specific valve to inject the compressed air. However the concept requires a complete change in valve timing for both the air compressor and air motor 2-stroke modes. This is accomplished through a cam-less HVA (*Hydraulically Actuated Valve*) system.

The APA Engine was tested at steady state in compressor mode and in motor mode. The tests confirmed the functionality of the APA engine. The APA engine demonstrated air compression and high pressure air storage in the air tank by controlling the valve timing and using the air handling system. The APA engine generated positive power by using the compressed air from the air tank without injecting fuel [19].

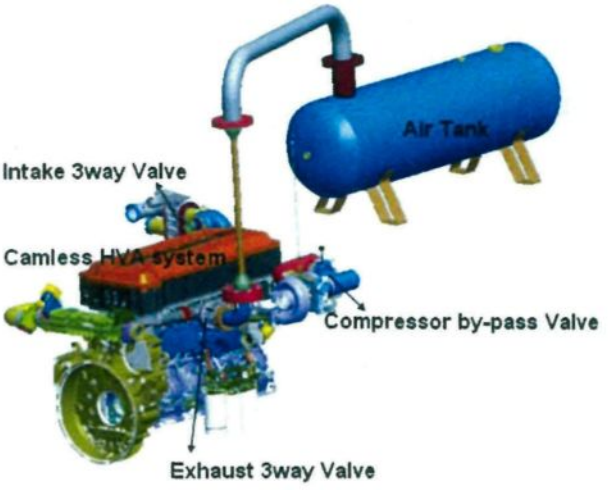

Fig. 7. Hyungsuk et al. [18] air-power-assist engine.

Ivanco, Colin, Chamaillard, Charlet and Higelin [20] recently proposed an optimal Energy Management Strategies defining the instantaneous usage of fuel energy and air tank energy, in order to maximize the global efficiency. Their work was based on an engine similar to the engine of Donitz, Vasile, Onder and Guzzella [17]. Several strategies were tested on different driving patterns combined with a pattern recognition process. The benefit was confirmed. The fuel consumptions were also compared to the best attainable obtained by Dynamic Programming, where the close to optimal results were observed.

Moreover, Trajkovic et al. [14, 15, 16] converted a single-cylinder Scania D12 Diesel engine to a pneumatic hybrid Diesel one. The concept requires having a variable valve actuation system and it can operate under conventional Diesel mode as well as two-stroke pneumatic motor and pneumatic pump modes. Trajkovic et al. conducted an optimization on valve actuation timing and obtained up to 48% of regenerative efficiency at steady state operation. Later, Trajkovic et al. compared testing measures to GT-Power simulation results. The correlation was done for both pneumatic modes and it showed a 5% error in steady state operations [16]. We indicate that this study was conducted using not more than 8 bars of tank pressure.

As we can observe, none of those studies suggests a concept of an engine that does not require an additional charge valve, and is capable in the same time to operate under hybrid mode, that is generating power simultaneously from fuel and pneumatic power. Our study deals with this possibility that aims to suggest simple adaptation of existing Diesel engines already installed for power generation, without heavy modification in the hard concept of the engine. Compressed air is therefore directly admitted through original inlet valve after bypassing the turbocharger. Fig. 8 illustrates the difference between our concept (left) and the concept of Donitz, Vasile, Onder and Guzzella [17] (right).

3. Mathematical model

Fig. 9 illustrates the system considered to calculate the evolution of the thermodynamic characteristics (pressure, temperature, specific heat constant, etc.).

The analysis is based on the following hypotheses:

1. The thermodynamic equilibrium is established for each step of the calculation.
2. The mass of gas is a homogeneous mixture of perfect gases.
3. The mass transfers occur only through the admission and exhaust valves. The blow-by flow is therefore neglected.
4. The admission back-flow is calculated and taken in consideration. The exhaust flow transferred back to the admission is readmitted in the cylinder at the exhaust temperature.

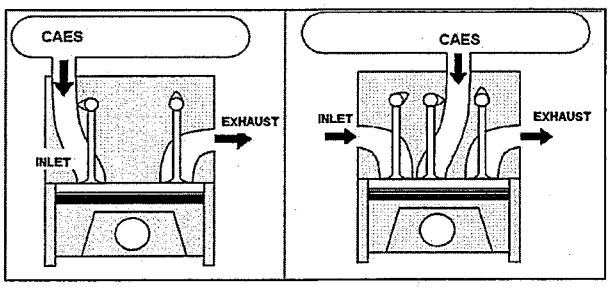

Fig. 8. Different possibilities for CAES admission in hybrid pneumatic diesel engines.

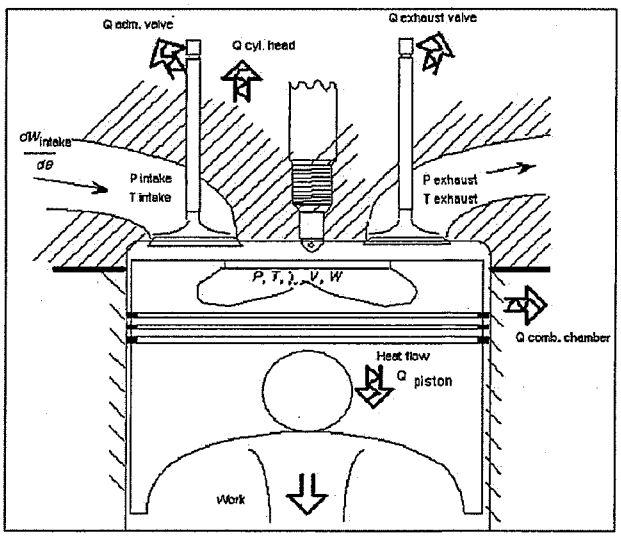

Fig. 9. Direct injection diesel engine simplified thermodynamic model.

5. The fuel is injected in the combustion chamber at a constant temperature and it is immediately burned following Wiebe law [13].
6. The heat transfers occur through the five boundary limits (cylinder head, piston, cylinder wall, exhaust valve and admission valve) that are at a constant and uniform temperature.

Main equations are issued from the mass and heat conservation as well as the ideal gas assumptions [6,13]. The application of the first law or thermodynamics and the perfect gas law to the control volume results in the differential equation (1) [13] that drives all the thermodynamic transformations.

$$m\cdot\frac{\partial u}{\partial t}\cdot\frac{dT}{dt}+m\cdot\frac{\partial u}{\partial \varphi}\cdot\frac{d\varphi}{dt}+u\cdot\frac{dm}{dt}=-\frac{m\cdot R\cdot T}{V}\cdot\frac{dV}{dt}+\sum_s\frac{dQ_s}{dt}+\sum_i h_{oi}\cdot\frac{dm_i}{dt} \quad (1)$$

This equation has to be solved iteratively, and to do so, it is necessary to solve the following sub-models.

3.1. Gas properties model

The gas properties are required as a function of temperature and composition. For individual species, the internal energy can be expressed as a function of temperature by means of a polynomial expansion with either a molar or a specific basis [13]:

$$u_i(T)=\sum_{j=0}^{n}\left(A_j\times T^j\right) \quad (2)$$

where A_j is found in JANAF thermodynamic tables [11]. For a mixture of m species, the global internal energy is calculated using the fraction method:

$$u(T)=\sum_{i=0}^{m}(x_i\times u_i(T)) \quad (3)$$

The same method is commonly used to calculate the specific stagnation enthalpy h

3.2. Mass transfer model

The mass conservation equation is used to calculate the mass and the equivalence ratio evolution in the control volume which is the combustion chamber, as illustrated in Equations (4) and (5) [10]:

$$\frac{dm}{dt} = \frac{dm_{int}}{dt} + \frac{dm_{exh}}{dt} + \frac{dm_{inj}}{dt} \tag{4}$$

where *int* refers to intake air, *exh* refers to exhaust gas and *inj* refers to injected fuel.

$$\frac{d\varphi}{dt} = \frac{\frac{dm}{dt} - (1+\varphi/\varphi_{stc}) \cdot \frac{dm_{air}}{dt}}{m_{air}} \cdot \varphi_{stc} \tag{5}$$

In Equation (5) *air* refers to fresh air in the combustion chamber and *stc* refers to stoichiometric conditions.

To solve these equations, we need to know the flow through intake and exhaust valves dm_{int}/dt and dm_{exh}/dt, as well as the variation of fresh air mass in the control volume, m_{air}. When the intake valve is open, the change of air mass in the combustion chamber is calculated by the Baré Saint-Venant model:

$$\frac{dm_{int}}{dt} = A_{int} \times P_{int} \times \sqrt{\frac{2.\gamma_{int}}{(\gamma_{int}-1) \times r_{int} \times T_{int}} \times \left[X^{\frac{2}{\gamma_{int}}} - X^{\frac{\gamma_{int}+1}{\gamma_{int}}}\right]} \tag{6}$$

where X is the maximum found between two values, as shows equation (7):

$$X = \max\left(\frac{P}{P_{int}}; \left(\frac{2}{\gamma_{int}+1}\right)^{\frac{\gamma_{int}}{\gamma_{int}-1}}\right) \tag{7}$$

When the exhaust valve is open, the change of air mass in the combustion chamber is calculated with the same model after adjusting upstream and downstream valve condition:

$$\frac{dm_{exh}}{dt} = -A_{exh} \times P \times \sqrt{\frac{2.\gamma}{(\gamma-1) \times r \times T} \times \left[Y^{\frac{2}{\gamma}} - Y^{\frac{\gamma+1}{\gamma}}\right]} \tag{8}$$

where Y is the maximum found between two values, as shows equation (9):

$$Y = \max\left(\frac{P_{exh}}{P}; \left(\frac{2}{\gamma+1}\right)^{\frac{\gamma}{\gamma-1}}\right) \tag{9}$$

Finally, the fresh air mass variation in the control volume is calculated with [10]:

$$\frac{dm_{air}}{dt} = \frac{\frac{dm_{int}}{dt}}{1+\frac{\varphi_{int}}{\varphi_{stc}}} + \frac{\frac{dm_{exh}}{dt}}{1+\frac{\varphi}{\varphi_{stc}}} \tag{10}$$

3.3. Kinematical model

The volume delimited by the piston, the cylinder wall and the cylinder head can be calculated as a function of the angular position of the crankshaft θ [6]:

$$V = \frac{\pi D^2}{8} \times L\left(1 + \frac{S}{2L} - \cos\theta - \sqrt{\left(\frac{S}{2L}\right)^2 - \sin^2\theta} + \frac{2}{\varepsilon - 1}\right) \tag{11}$$

Therefore, the volume variation can be calculated as a function of time:

$$\frac{dV}{dt} = \frac{\pi D^2}{8} \times L \times \sin\theta \times \left(\frac{\cos\theta}{\sqrt{(S/2L)^2 - \sin^2\theta}} + 1\right) \times \frac{d\theta}{dt} \tag{12}$$

3.4. Heat transfer model

Woschni [12] has developed an empirical model to describe heat transfer through cylinder walls and piston. Equation (13) gives the heat transfer through a boundary surface:

$$\frac{dQ}{dt} = \sum_{j=boundary} \left(\phi_j \times (T_j - T) \times A_j\right) \tag{13}$$

where the exchange coefficient ϕ_j is given by equation (14):

$$\phi_j = 3.26 \times D^{-0,2} \times P^{0.8} \times T^{-0,55} \times \left(C_1 \times \frac{L \times N}{30} + C_2 \times \frac{Vs \times T0}{V0 \times P0} \times (P - Psc)\right)^{0.8} \tag{14}$$

Here C_1 and C_2 are constants defined separately for each phase of the thermodynamic cycle as shown in Table 1. It is important to mention that the boundary temperatures T_j have been considered constants for all operating points, that is the cooling system is supposed perfectly designed to meet those temperatures. The temperatures values considered for cylinder head, piston head, cylinder walls, intake valve and exhaust valve are respectively 400 K, 550 K, 450 k, 400 K, and 600 K [6].

3.5. Burn rate and combustion process model

The accurate description of the combustion process in the Diesel engines requires the knowledge of different phenomena that occur starting with the fuel injection and ending with its transformation into combustion products. This knowledge needs the study of the aerodynamic motion in the combustion chamber, the penetration and the vaporization of the fuel as well as the self ignition delay and the combustion itself. Those phenomena cannot be modeled without a three dimensional study.

In this study, we have decided to simplify the modeling work in order to demonstrate a first order potential of our technical solution. A global approach of the combustion process has been modeled considering four phases:

1. The phase of the delay of self ignition: the injected fuel does not start burning before this delay ends;
2. The phase of the pre-mixed combustion, where the fuel injected during the delay of self ignition is burned;

Table 1
Constants for heat transfer exchange coefficient calculation.

	Compression	Combustion	Expansion	Exhaust
C_1	6.18	2.28	2.28	6.18
C_2	0	$3.24.10^{-3}$	0	$3.24.10^{-3}$

3. The phase of the diffusion combustion: while the injection is still ongoing and the combustion chamber is already hot, the combustion happens almost instantly and its speed is limited by the injection flow rate;
4. The final combustion phase: after the fuel injection ends, the remaining unburned fuel (relatively small quantity) burns slowly depending on the diffusion phenomena.

The global combustion model can be simplified by the combination of two Wiebe laws [13]. The first one describes the *pre-mixed combustion* and the second one describes the *diffusion combustion*. Each Wiebe law allows the calculation of the burned fuel ratio as [6]:

$$xb = 1 - \exp\left(- w \times \left(\frac{\theta - \theta_{SOI}}{\Delta\theta} \right)^{n+1} \right) \quad (15)$$

Where θ_{SOI} is the Start Of Injection Angle (SOI). The Start Of Combustion (SOC) angle θ_{SOC} is the difference between θ_{SOI} and the AID (Auto Ignition Delay) angle θ_{AID}. Several equations are proposed in the literature review for modeling the AID. We have chosen in the present work to use the following equation recommended by Heywood [6].

$$\theta_{AID} = (0.36 + 0.22 \cdot vp) \cdot \exp\left[Ea \cdot \left(\frac{1}{R_0 \cdot T} - \frac{1}{17190} \right) \cdot \left(\frac{21.2}{p - 12.4} \right)^{0.63} \right] \quad (16)$$

Where:

θ_{AID} is expressed in crank-degrees
vp is the piston mean velocity [m/s]
T is the temperature at top dead center [K]
P is the pressure at top dead center [bar]
P is the pressure at top dead center [bar]
$Ea = 618840/CN+25$; where CN is the fuel cetane number

Parameters n and w of Equation (15) are constants determined empirically. For our study, we set the values of n and w to 3 and 5 respectively, as found in literature review [10]. The combustion duration $\Delta\theta$ has been set to 70 crank-degrees [10].

4. Results and discussions

In our study, we have chosen to focus on three operating modes to study the impact of injection advance:

1. Turbo charged mode with compressed air cooling;
2. CAES charged mode with an intake temperature of 25 °C;
3. CAES charged mode with an intake temperature of −50 °C.

In a previous study [4], we have conducted a zero dimensional static model of a typical turbo charged Diesel engine and determined the downstream compressor pressure and the upstream turbine pressure for different engine loads. It is known that those values are highly dependent on turbocharger size and characteristics; however, in order to increase the intake pressure, the turbocharger increases also the exhaust pressure by almost the same amount or maybe more or, alternatively, the combustion efficiency is decreased artificially to increase exhaust temperature.

As for the CAES charged mode temperatures, we know that a temperature drop will inevitably occur when expanding the CAES from storage pressure to intake pressure. However, it is possible to heat the intake air before admitting it using engine's cooling system or exhaust temperature recovery. We have chosen not to work below intake temperature of −50 °C because it is the range of minimum external temperature that can be met in northern areas. Below this temperature, we need to investigate if the Diesel engine remains operational which exceeds the purpose of this study. These operating modes are not the only ones to be studied, but they were chosen to increase our understanding of the Diesel engine behavior regarding intake and exhaust conditions.

Finally, we have chosen the BMEP (Boost Mean Effective Pressure) as the torque indicator for our study because it is widely used by engineers to compare engines having different displacements. For a four stroke engine, the torque TQ can be written as a function of the displacement DSP and the BMEP:

$$TQ = \frac{BMEP \times DSP}{4\pi} \quad (17)$$

4.1. Detailed parametric study at BMEP = 10 bars

In order to understand its behavior, we will provide a complete analysis of the variation of the thermodynamic cycle and its efficiency, depending on the control parameters (intake pressure, intake temperature, exhaust pressure and injection advance) for a fixed load corresponding to a BMEP of 10 bars Fig. 10 illustrates the effect of intake pressure and exhaust pressure on specific fuel consumption of the engine at a BMEP of 10 bars for a fixed intake temperature of 298 K and a fixed injection advance of 6°. As we can observe, increasing intake pressure and reducing exhaust pressure highly reduces fuel consumption.

We present some qualitative explanations for this improvement, which will be completed with data in the rest of this paragraph. Actually, two main reasons are behind the fuel consumption reduction when the intake pressure is increased and exhaust pressure decreased:

1. The scavenging work, called also "the low-pressure cycle work", increases and turns out to be positive (motor). That is added to the work provided by the high pressure cycle and reduces fuel consumption. In a classic turbocharged Diesel, intake pressure is slightly lower than exhaust pressure; the scavenging work is slightly negative and requires more fuel for the same total work of the thermodynamic cycle.
2. The high-pressure cycle efficiency increases with pneumatic hybridization thanks to higher fresh air quantity. This

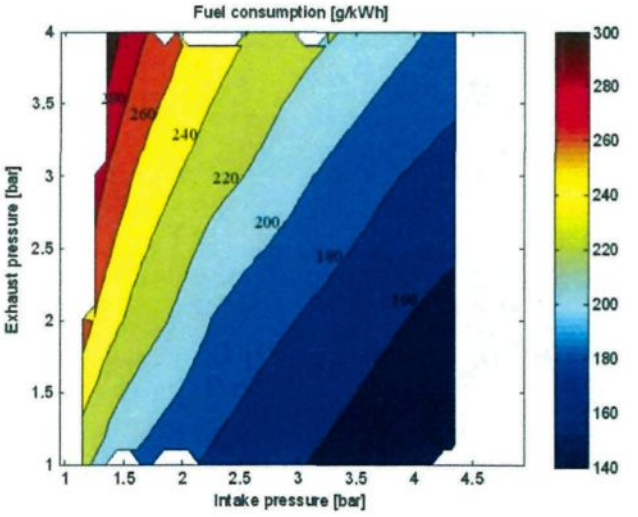

Fig. 10. Fuel consumption as a function of intake and exhaust pressures, for a fixed intake temperature of 25 °C at BMEP = 10 bars.

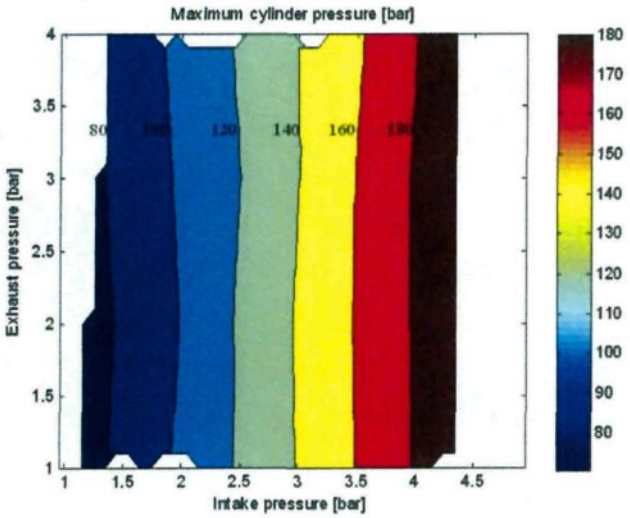

Fig. 11. Maximum gas pressure variation with intake and exhaust pressures, for a fixed intake temperature of 25 °C, at BMEP = 10 bars.

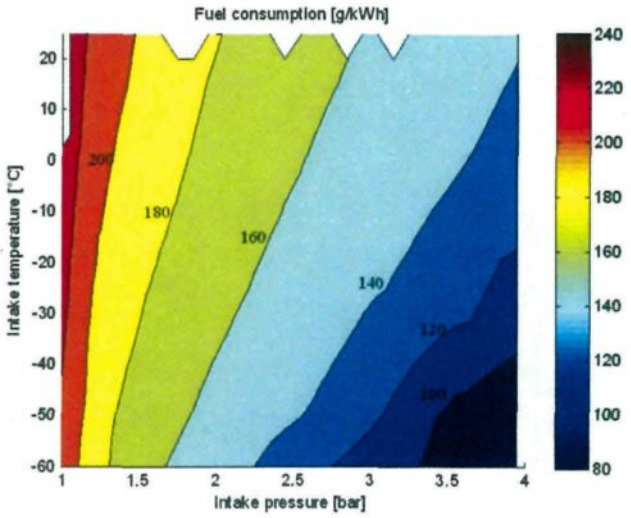

Fig. 13. Fuel consumption as a function of intake pressure and temperature, for a fixed exhaust pressure of 1 bar, at BMEP = 10 bars.

improvement is mainly due to lower thermal losses, due to the reduction of combustion temperature resulting from less fuel burned from one side, and higher air density (therefore higher calorific capacity) from the other side.

As mentioned before, the maximum pressure allowed in the cylinder limits the amount of intake pressure. Fig. 11 shows the variation of the maximum cylinder pressure as a function of the intake and exhaust pressures. We observe the maximum cylinder pressure is almost not affected by exhaust pressure but varies linearly with intake pressure with a high slope of about 40 to 1. With a 4 bars intake pressure, the maximum cylinder pressure reaches already 180 bar.

The second potential limitation that we have investigated is the exhaust temperature. Actually, exhaust valve has a threshold in terms of gas temperature not to be exceeded. As we can observe in Fig. 12, the exhaust temperature is lower when intake pressure is increased or exhaust pressure is decreased. Therefore, exhaust temperature will not limit the pneumatic hybridization.

After the analysis of the effect of intake and exhaust pressures for a fixed intake temperature and fixed injection advance, we illustrate (Fig. 13) the effect of intake temperature and pressure on fuel consumption, for a fixed exhaust pressure of 1 bar and a fixed injection advance of 6°. Fixing exhaust pressure to 1 bar assumes that the turbocharger is already by-passed. Fuel consumption is reduces as intake temperature lowers. As will be shown later with additional data, reducing intake temperature for the same intake pressure will reduce heat losses as well and improve cycle efficiency because the global gas temperature is lower (higher air density and lower initial cycle temperature).

Regarding maximum cylinder pressure, we observe in Fig. 14 that reducing the intake temperature for the same intake pressure increases the maximum cylinder pressure. This is due to higher air quantity admitted. Therefore the maximum intake pressure we can reach is lower for low intake temperature. For example, at −50 °C intake temperature, the maximum cylinder pressure reaches 180 bars for an intake pressure of 3.2 bars, which is 0.8 bars lower than the limitation at +25 °C intake temperature.

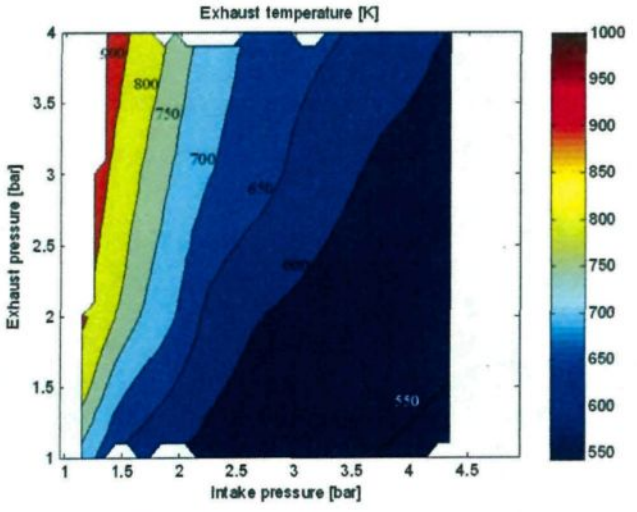

Fig. 12. Exhaust gas temperature function of intake and exhaust pressures, for a fixed intake temperature of 25 °C, at BMEP = 10 bars.

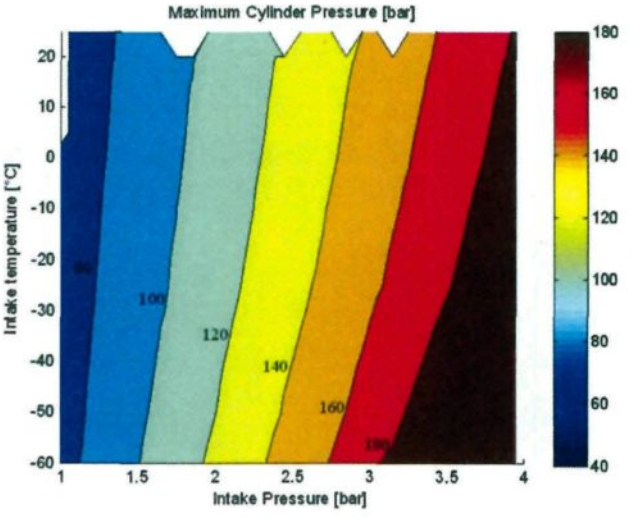

Fig. 14. Maximum gas pressure function of intake pressure and temperature, for a fixed exhaust pressure of 1 bar, at BMEP = 10 bars.

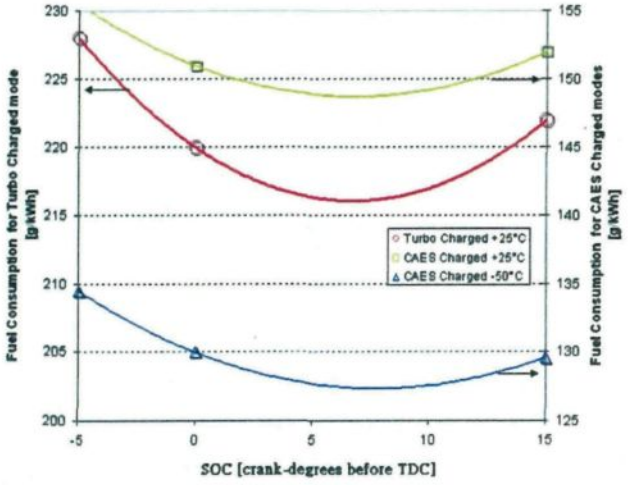

Fig. 15. Effect of SOC angle on fuel consumption, at BMEP = 10 bars, for different charging modes.

The last parameter studied is the IA (Injection Advance) which is responsible of SOC (Start of Combustion) angle. Actually, there is an optimal advance that reduces the fuel consumption to a minimum, for every condition of intake pressure, intake temperature and exhaust pressure. The reasons are:

1. The AID (Auto-Ignition Delay) depends of the intake conditions and so does the SOC because it is simply equal to the difference between the IA and the AID. It is important to have a SOC angle nearly before the TDC (Top Dead Center) in order to have good cycle efficiency.
2. The thermal loss depends of the intake temperature and pressure and the cylinder pressure profile changes consequently. To have optimal cycle efficiency, the SOC needs to be adjusted around its nominal value.

For the simplification of the study, the AID was not modeled and the effect of the SOC angle is directly studied and set to its optimal value. Fig. 15 illustrates the effect of SOC angle on fuel consumption, for the three chosen operating points. We observe that the optimal SOC angle for turbocharged mode is 6°, for CAES charged at 25 °C mode is 7° and for CAES charged at −50 °C mode, is 9°. It is important to note that increasing injection advance to reduce fuel consumption, increases the maximum cylinder pressure, and therefore decreases the maximum intake pressure. In that case, the fuel consumption may increase instead of decreasing, but the global efficiency is better because less compressed air is consumed.

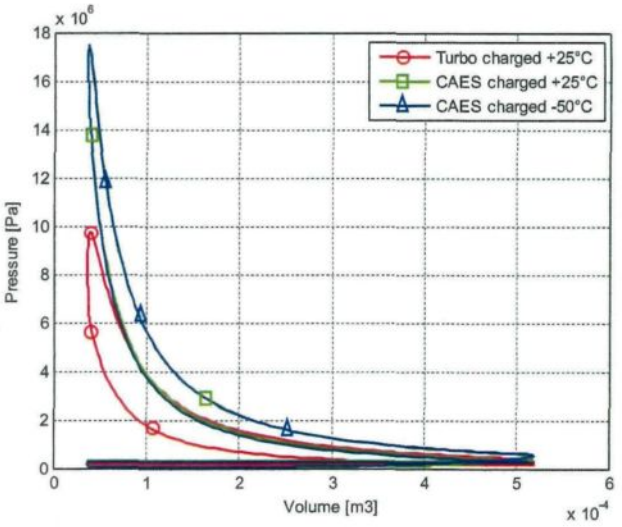

Fig. 17. P–V diagram at BMEP = 10 bars, for different charging modes.

The thermodynamic cycles of the chosen operating points are illustrated in Figs. 16 and 17. All three operating modes are working at optimal SOC angles and therefore optimal IA.

Fig. 16 illustrates the P–V diagram plotted in a logarithmic scale. It is interesting to analyze the low-pressure cycle called also the scavenging cycle. We notice that the pneumatic work witch is the area of the scavenging cycle is near zero for turbocharged mode and positive for CAES charged modes. We also notice that the scavenging work in CAES+25 °C is slightly higher than the one in CAES-50 °C because intake pressure is higher.

We notice in Fig. 17 the high increase of the maximum cylinder pressure when moving from turbocharged mode to CAES charged mode.

Figs. 18 and 19 illustrate respectively the T-θ diagram and heat exchange through boundaries for the three modes. We can see in

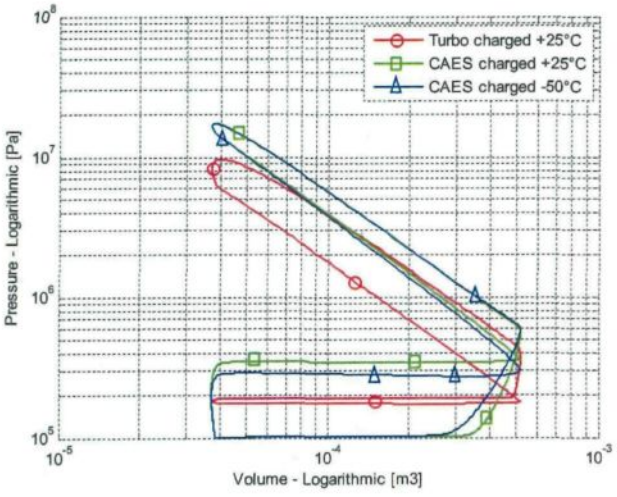

Fig. 16. Log P-log V diagrams at BMEP = 10 bars, for different charging modes.

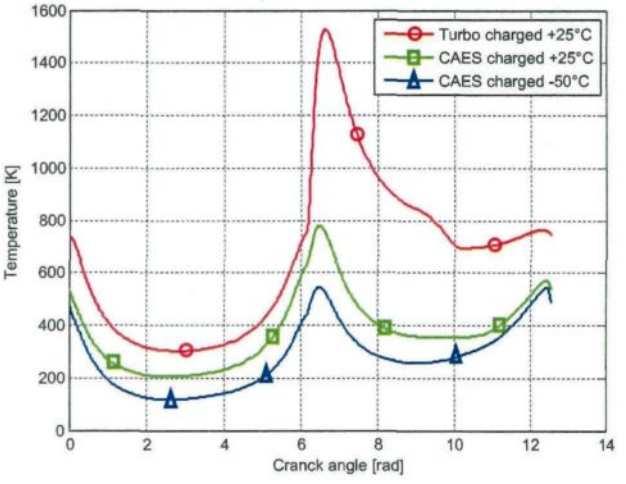

Fig. 18. T-θ diagram at BMEP = 10 bars, for different charging modes.

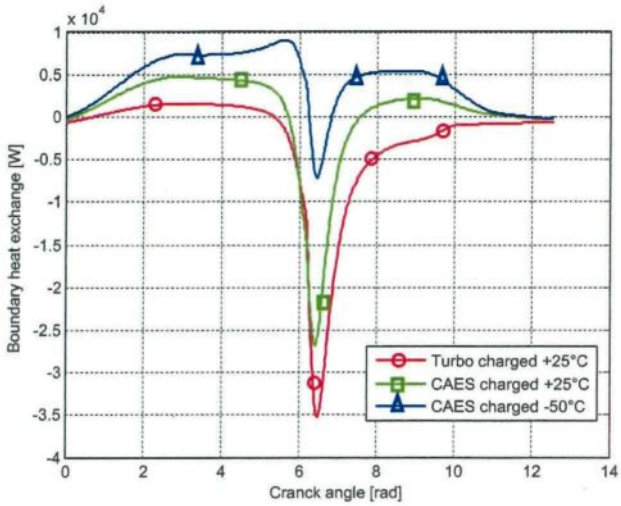

Fig. 19. Heat flow through boundary, for different charging modes, at BMEP = 10 bars.

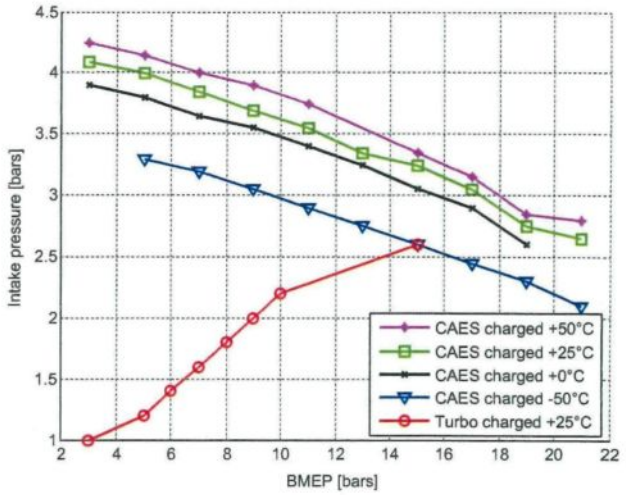

Fig. 21. Intake maximum pressure for different charging modes, function of engine load.

Fig. 18 that a significant decrease in gas temperature is obtained when moving from turbocharged mode to CAES-50 °C mode passing by CAES+25 °C charging mode. This temperature decrease is a result of the three following reasons:

1. The higher air density resulting from the higher intake pressure and/or the lower intake temperature, leads to higher calorific capacity of the in-cylinder gas and therefore lower temperature rise for a certain heat energy released by the combustion.
2. Lower heat release resulting from lower quantity of burned fuel that reduces temperature rise for CAES 25 °C and CAES -50 °C;
3. Intake air temperature is 75 °C lower for CAES -50 °C that is responsible for lower average gas temperature of this operating mode compared to CAES 25 °C.

In Fig. 19, negative flow means the gas is loosing energy through boundary and positive flow means the gas is earning energy from boundary. For turbocharged mode, the flow is positive only during intake because gas temperature at this time is lower than boundaries' temperatures. During combustion, expansion and exhaust phases, the heat flow is negative causing significant loss in energy. As for the CAES charged mode at 25 °C, we observe that heat loss decreases significantly comparing to turbocharged mode but the flow is still negative. In CAES charged mode at −50 °C, the overall heat flow is positive therefore the system is not loosing energy, on the contrary, it is recovering thermal energy from the engine. Of course, this assumes that the engine is hot and that the CAES charged mode at −50 °C occurs occasionally, after a certain time of working under standard turbocharged mode. The thermal inertia of the Diesel engine defines the minimal and maximal working time of turbocharged mode and CAES mode respectively in order to make this hypothesis valid. In case the time of operating with CAES charged mode at −50 °C exceeds a certain limit, the heat flow will stabilize to meet a global value near zero which will increase the fuel consumption by a small amount.

As a synthesis of this complete study around the operating point of BMEP 10 bars, Fig. 20 illustrates the reasons for fuel economy brought by CAES charged modes compared to turbocharged mode. We observe that 65% of the fuel consumption reduction from turbocharged mode at +25 °C to CAES charged mode at +25 °C is caused by direct pneumatic power production and 35% is caused by heat loss reduction. The heat loss reduction constitutes the only reason for the improvement from CAES charged +25 °C to CAES

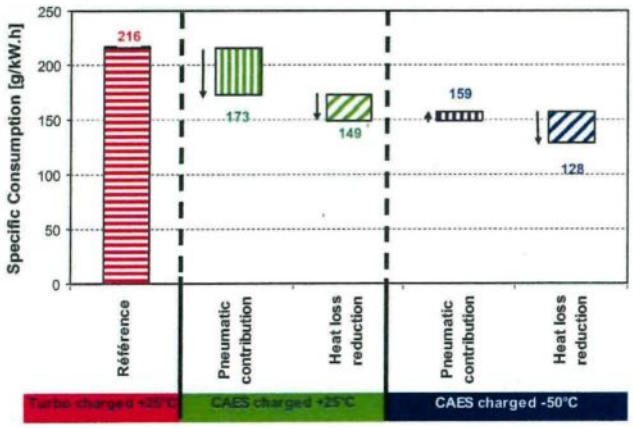

Fig. 20. Explanation of consumption change from a charging mode to another, at BMEP = 10 bars.

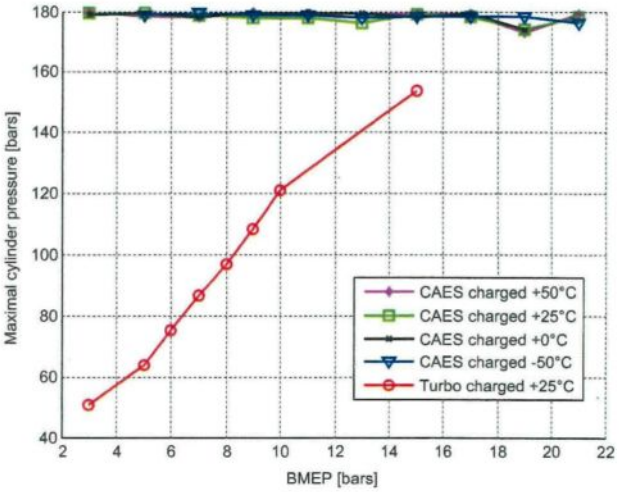

Fig. 22. Maximum cylinder pressure for different charging modes, function of engine load.

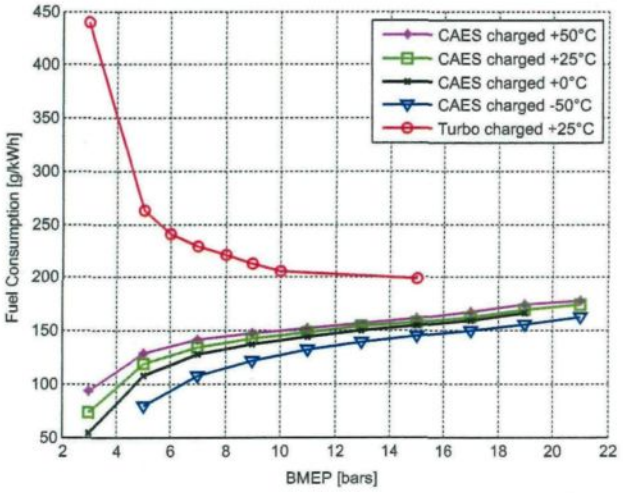

Fig. 23. Fuel specific consumption for different charging modes, function of engine load.

charged −50 °C mode, as the pneumatic contribution is higher in CAES+25 °C mode due to higher intake pressure.

4.2. Optimization result at different loads

In this section, we will compare different charging modes on different criteria, for different operating points, after optimization. The charging modes considered are:

1. CAES Charged mode at 50 °C;
2. CAES charged mode at 25 °C;
3. CAES charged mode at 0 °C;
4. CAES Charged mode at −50 °C;
5. Turbo charged mode at 25 °C.

All CAES charged modes are operating at maximum allowable intake pressure, that is intake pressure for witch maximum gas pressure during thermodynamic cycle reaches 180 bars and at an exhaust pressure of 1 bar, while turbocharged mode operates at an intake pressure and exhaust pressure both dependant on BMEP but almost equal. All operating points are set with an optimal injection

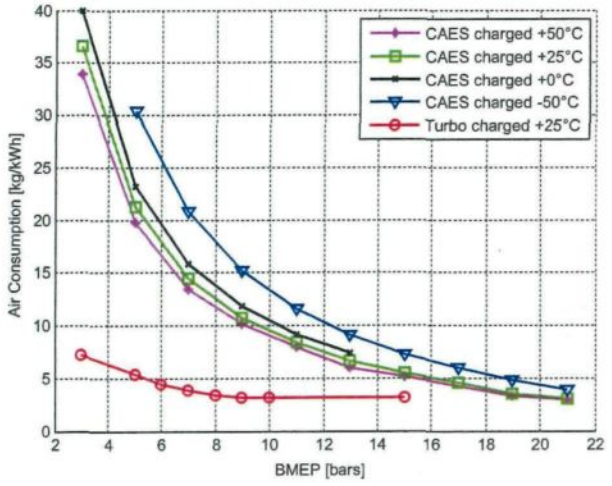

Fig. 24. Air specific consumption for different charging modes, function of engine load.

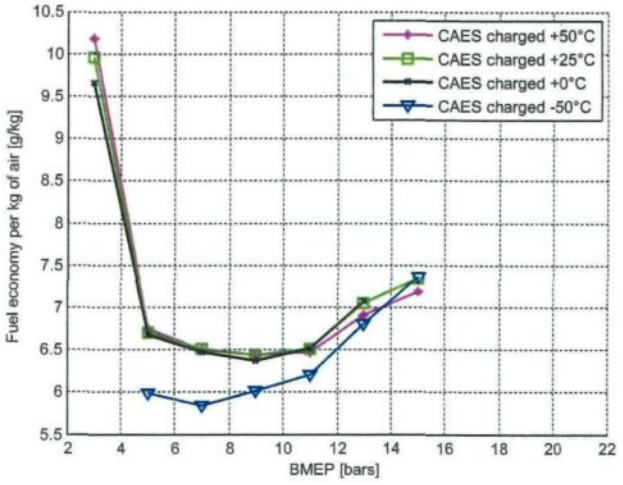

Fig. 25. Fuel economy per kilogram of air consumed, for different CAES charging modes, function of engine load.

advance, the one that maximizes the cycle efficiency, even if the intake allowed pressure has to be decreased. As mentioned before, the variation of intake pressure and exhaust pressure as a function of BMEP for a turbocharged engine depends on the design of the turbocharger. We have taken here an example provided by a previous simulation [1] conducted on a Diesel engine.

Fig. 21 illustrates the intake pressure and the injection advance at every operating point simulated. We can see that for higher loads the allowable intake pressure lowers; we can also see that a lower intake temperature will reduce the allowable intake pressure.

These intake pressures make the maximum gas pressure during Diesel cycle reach 180 bars, as shown in Fig. 22, while in turbocharged mode, maximal pressure is significantly lower.

When comparing fuel consumption of CAES charged mode with turbocharged mode, we observe in Fig. 23 that at lower loads, the reduction is higher. That is due to the more important absolute pneumatic power as intake pressure is higher, relatively to the total power of the engine. We notice also that better fuel economy for lower intake temperature for the same reasons as described in the previous paragraph.

Finally, the air consumption is one important criterion as the storage tank volume depends on it. Fig. 24 shows that air consumption increases at low loads and also at low temperature because filling is better. In order to optimize the use of stored air, another criterion is necessary. We have calculated and illustrated in Fig. 25, the fuel economy per kilogram of air consumed. This criterion has to be maximized in order to get the maximum advantage of stored air. As we can notice at Fig. 25, it is more interesting to use CAES charged mode at low and very low loads. We can also see that even if it has positive effect on fuel consumption, very low intake air temperature is less suitable when considering consumed air quantity.

In case the storage pressure is higher than the intake temperature, it is needed therefore to expand it before introducing it into the engine intake. A temperature drop will probably accompany this expansion. In that case, we recommend heating the air after its expansion, using a free of charge source as the engine cooling system or an exhaust gas exchanger.

5. Conclusion

This work is a continuation of a previous one [1] where we have demonstrated that with a simple pneumatic hybridization of Diesel

engine, we can reduce significantly its consumption by ensuring that the engine will operate under an optimal Air/Fuel ratio all the time. The simple pneumatic hybridization consists in bypassing turbocharger and increasing artificially intake air pressure. In this study, we have demonstrated some new reasons for fuel economy brought by the pneumatic hybridization. The low-pressure cycle work, called also the scavenging work, switches from a negative value to a highly positive one if we increase the intake pressure and decrease exhaust pressure by removing the turbocharger and connecting the CAES tank directly to the intake valve. A decrease of the heat loss through boundary also occurs. For those two reasons, a very significant fuel economy, up to 60% can be obtained especially at low loads. The maximum gas pressure in the combustion chamber has to stay below a certain threshold and limits the intake pressure and therefore the fuel economy that we can realize. That is why the fuel economy is higher for lower loads. If the stored air pressure is higher than the intake pressure allowed, an expansion is needed before entering the engine. A temperature drop accompanies this expansion. In this case, to maximize the efficiency of the system, we recommend heating the compressed air before admitting it in the engine. Engine cooling system can be used for this purpose.

While the present paper presents theoretical results that are valid under certain assumptions, some preliminary experimental results were published in a PhD thesis [4] and will be published shortly in a journal. The published experimental results cover CAES 25 °C operating mode, the other operating modes are presently under investigation.

Nomenclature

m	Mass [kg]
u	Internal specific energy [J kg^{-1}]
T	Temperature [K]
φ	Equivalence ratio [ ]
φ	Heat exchange coefficient [W m^{-2} K^{-1}]
R	Perfect gas constant [J mol^{-1} K^{-1}]
V	Volume [m^3]
D	Piston diameter
L	Con-rod length
S	Stroke
θ	Crankshaft angle
ε	Compression ratio [ ]
Q	Thermal energy
x_i	Molar fraction of the species i
h	Specific stagnation enthalpy [J kg^{-1}]
A_{int}	Equivalent area of intake valve section [m^2]
A_{exh}	Equivalent area of exhaust valve section [m^2]
γ	Heat capacity ratio (adiabatic index)
r	Perfect gas constant [J kg^{-1} K^{-1}]
Psc	Gas pressure in the chamber if there was no combustion [Pa]
Vs	Combustion chamber volume at bottom dead centre [m^3]
$T0$	Temperature of combustion chamber at the intake valve close [K]
$V0$	Volume of combustion chamber at the intake valve close [Pa]
$P0$	Pressure of combustion chamber at the intake valve close [Pa]
xb	Fraction of burned fuel
HLC	Maximum heat release rate [deg^{-1}]
AI	Injection Advance
AID	Auto-Ignition delay
BMEP	Boost Mean Effective Pressure [bar]
CAES	Compressed Air Energy Storage
SOC	Start Of Combustion
SOI	Start Of Injection

References

[1] Ibrahim H, Younes R, Basbous T, Ilinca A, Dimitrova M. Optimization of diesel engine performances for a hybrid wind-diesel system with compressed air energy storage. Energy 2011;36:3079–91.
[2] Liu W, Gu S, Qiu D. Techno-economic assessment for off-grid hybrid generation systems and the application prospects in China, http://www.worldenergy.org/wecgeis/publications.
[3] Ibrahim H, Ilinca A, Younes R, Basbous T. Study of a hybrid wind-diesel system with compressed air energy storage. electrical power conference 2007, "Renewable and alternative energy resources", EPC2007. Montreal, Canada: IEEE Canada; 2007. October 25-25, 2007.
[4] Ibrahim H. 2010, Etude et conception d'un générateur hybride d'électricité de type Eolien-Diesel avec élément de stockage d'air comprimé, PHD thesis, Université du Québec à Chicoutimi, 2010.
[5] Ibrahim H, Younes R, Ilinca A. Optimal conception of a hybrid generator of electricity. Toronto, Canada: CANCAM07-ETS-39; 2007.
[6] Heywood JB. Internal combustion engine Fundamentals. New York: McGraw Hill; 1988.
[7] Dönitz C, Vasile IC, Onder CH, Guzzella H. Modeling and optimizing two- and four-stroke hybrid pneumatic engines. IMechE; 2009.
[8] Lopes Correia da Silva L. Simulation of the thermodynamic processes in diesel cycle internal combustion engines. SAE; 2007. 931899.
[9] Higelin P, Charlet A, Chamaillard Y. Thermodynamic simulation of a hybrid pneumatic-combustion engine concept. Int.J Appl Thermodyn 2002;5(1): 1–11.
[10] Guibert P. Etude des cycles thermodynamiques des moteurs thermiques et modélisation, Rueil Malmaison. Ecole Nationale Supérieure du Pétrole et des Moteurs; 2002.
[11] JANAF. Thermochemical tables. 3rd ed.; 1985.
[12] Woschni G. A universally applicable equation for the instantaneous heat transfer coefficient in the internal combustion engine. SAE; 1967. 670 931.
[13] Stone R. Introduction to internal combustion engines. Department of Engineering Science, University of Oxford; 1999.
[14] Trajkovic S, Tunestal P, Johansson B. Introductory study of Variable valve actuation for Pneumanic hybridization. SAE; 2007. 2007-01-0288.
[15] Trajkovic S, Tunestal P, Johansson B. Investigation of different valve Geometries and valve timing strategies and their effect on regenerative efficiency for a pneumatic hybrid with Variable valve actuation. SAE; 2008. 2008-01-1715.
[16] Trajkovic S, Tunestal P, Johansson B. Simulation of a pneumatic hybrid Powertrain with VVT in GT-Power and Comparison with experimental data. SAE; 2009. 2009-01-1323.
[17] Donitz C, Vasile I, Onder C, and Guzzella L. Realizing a concept for high efficiency and Excellent Driveability: the downsized and supercharged hybrid pneumatic engine, SAE, 2009-01-1326.
[18] Higelin P, Vasile I, Charlet A, Chamaillard Y. Parametric optimization of a new hybrid pneumat ic ± combustion engine concept. Int J Engine Res 2004;5(2): 205.
[19] Hyungsuk K, Tai C, Smith E, Wang X, Tsao T, Stewart J, et al. Demonstration of air-Power-Assist (APA) engine technology for Clean combustion and direct energy Recovery in heavy Duty application, SAE, 2008-01-1197.
[20] Ivanco A, Colin G, Chamaillard Y, Charlet A, Higelin P. Energy Management strategies for a pneumatic-hybrid engine based on Sliding Window pattern recognition. Oil & Gas Science and Technology – Rev IFP 2010;65(1):179–90.
[21] Gheorghiu V. CO_2-emission reduction by means of enhanced thermal conversion efficiency of ICE cycles, SAE 2009-24-0081.
[22] Connolly D. A review of energy storage technologies for the integration of fluctuating renewable energy. University of Limerick; 2009.
[23] Hountalas D. Available strategies for improving the efficiency of DI diesel Engines-A theoretical investigation, SAE 2000-01-1176.
[24] Lemofouet, S., Investigation and optimisation of hybrid electricity storage systems based on compressed air and supercapacitors, École Polytechnique Fédérale de Lausanne; PHD, 2006.
[25] Cavallo A. Controllable and affordable utility-scale electricity from intermittent wind resources and compressed air energy storage (CAES). Energy 2007; 32:120–7.
[26] Anzano JP, Jaud P, Madet D. Stockage d'électricité dans le système de production électrique. Techniques de l'ingénieur, traité de Génie Electrique; 1989. D4030.
[27] Bradshaw DT, Ingram M. Pumped hydroelectric storage (PHS) and compressed air energy storage (CAES). IEEE PES summer meeting on energy storage; 2000.
[28] Robyns B. Contribution du stockage de l'énergie électrique à ka participation au système des éoliennes. Séminaire SRBE-SEE-L2EP «Eolien et réseaux: enjeux »„ 22 mars; 2005.
[29] http://www.caes.net/mcintosh.html.
[30] http://www.electricitystorage.org.
[31] Ibrahim H, Ilinca A, Perron J. Energy storage systems – Characteristics and comparisons. Renewable Sustainable Energy Rev 2008;12(5):1221–50.

CHAPITRE III

Article 2

A new hybrid pneumatic-combustion engine to improve fuel consumption of wind-Diesel power system for non-interconnected areas

Publié dans Applied Energy, Vol 96, août 2012
Applied Energy 96 (2012) 459–476

Résumé

Cet article présente un nouveau concept d'hybridation pneumatique du moteur Diesel qui peut être obtenu par une modification relativement simple d'un moteur Diesel conventionnel. Par un jeu de soupapes et de contrôle du système d'injection, il est possible d'opérer ce Moteur Hybride Pneumatique-Diesel (MHPD) selon plusieurs modes : mode moteur conventionnel, mode moteur à air comprimé, mode moteur hybride air comprimé-carburant et mode compresseur pneumatique. Une optimisation des commandes d'ouverture et de fermeture des soupapes d'admission est réalisée dans le but de maximiser le rendement pour tout couple fourni ou absorbé par moteur et pour toute pression dans le réservoir. Cette optimisation, réalisée grâce à un modèle du cycle thermodynamique théorique, conduit à la génération de cartographies de consommation spécifique d'air et de fuel pour chaque mode, en fonction du couple et de la pression dans le réservoir. Un automate permet de choisir le mode opératoire du MHPD en fonction du couple et de la pression, tout en privilégiant le mode moteur pneumatique quand celui-ci est possible, ou le cas échéant, le mode hybride pneumatique-combustion. Cette optimisation conduit à une évaluation de l'économie annuelle de carburant obtenue grâce au concept MHPD sur le site cible de Tuktoyaktuk, village isolé au nord du Canada, en fonction du volume de stockage disponible et du Taux de Pénétration de la Puissance (TPP) éolienne. La pression

maximale de stockage d'air est fixée à 20 bars. Le calcul réalisé montre que le volume de stockage est un levier important pour exploiter le plein potentiel du MHPD. Le volume optimal dépend du TPP. Par exemple, l'économie de carburant d'un SHED avec un TPP de 1, apportée par le concept MHPD combiné avec un volume de stockage de 1,000 m^3 se limite à 3% (soit 23 tonnes par an), alors que cette économie peut atteindre 9% (soit 70 tonnes par an) pour un volume de stockage de 50,000 m^3. L'augmentation de l'économie de carburant augmentant asymptotiquement par rapport au volume de stockage, il n'y a aucun intérêt pour augmenter ce volume au-delà de 100,000 m^3. Pour des TPP supérieurs, l'apport de carburant est lui aussi plus élevé ainsi que le volume de stockage permettant d'optimiser le système. A titre d'exemple, pour un TPP de 2, l'économie de carburant apportée par le concept MHPD combiné avec un volume de stockage de 50,000 m^3 est de 20% (soit 150 tonnes par an), alors que cette économie peut atteindre 26% (soit 200 tonnes par an) pour un volume de stockage de 100,000 m^3.

Applied Energy 96 (2012) 459–476

Contents lists available at SciVerse ScienceDirect

Applied Energy

journal homepage: www.elsevier.com/locate/apenergy

A new hybrid pneumatic combustion engine to improve fuel consumption of wind–Diesel power system for non-interconnected areas

Tammam Basbous [a,b,*], Rafic Younes [b,c], Adrian Ilinca [b], Jean Perron [a]

[a] Laboratoire International des Matériaux Antigivre, Université du Québec à Chicoutimi, Chicoutimi, Québec, Canada
[b] Laboratoire de Recherche en Energie Eolienne, Université du Québec à Rimouski, Rimouski, Québec, Canada
[c] Faculté de Génie, Université Libanaise, Beyrouth, Lebanon

ARTICLE INFO

Article history:
Received 12 September 2011
Received in revised form 4 January 2012
Accepted 2 March 2012
Available online 23 April 2012

Keywords:
Valves actuation
Parametric optimization
Pneumatic hybridization
Diesel engine
Wind–Diesel system
Compressed air energy storage

ABSTRACT

This paper presents an evaluation of an optimized Hybrid Pneumatic-Combustion Engine (HPCE) concept that permits reducing fuel consumption for electricity production in non-interconnected remote areas, originally equipped with hybrid Wind–Diesel System (WDS). Up to now, most of the studies on the pneumatic hybridization of Internal Combustion Engines (ICE) have dealt with two-stroke pure pneumatic mode. The few studies that have dealt with hybrid pneumatic-combustion four-stroke mode require adding a supplementary valve to charge compressed air in the combustion chamber. This modification means that a new cylinder head should be fabricated. Moreover, those studies focus on spark ignition engines and are not yet validated for Diesel engines. Present HPCE is capable of making a Diesel engine operate under two-stroke pneumatic motor mode, two-stroke pneumatic pump mode and four-stroke hybrid mode, without needing an additional valve in the combustion chamber. This fact constitutes this study's strength and innovation. The evaluation of the concept is based on ideal thermodynamic cycle modeling. The optimized valve actuation timings for all modes lead to generic maps that are independent of the engine size. The fuel economy is calculated for a known site during a whole year, function of the air storage volume and the wind power penetration rate.

1. Introduction

1.1. Power generation in remote areas

Most of the remote and isolated communities or technical installations (communication relays, meteorological systems, tourist facilities, farms, etc.) which are not connected to national electric distribution grids rely on Diesel engines to generate electricity [1]. Diesel-generated electricity is more expensive in itself than large electric production plants (gas, hydro, nuclear, wind) and, on top of that, should be added the transport and environmental cost associated with this type of energy.

In Canada, approximately 200,000 people live in more than 300 remote communities (Yukon, TNO, Nunavut, islands) and are using Diesel-generated electricity, responsible for the emission of 1.2 million tons of greenhouse gases (GHG) annually [2]. In Quebec province, there are over 14,000 subscribers distributed in about 40 communities not connected to the main grid. Each community constitutes an autonomous network that uses Diesel generators. The total production of Diesel power generating units in Quebec is approximately 300 GW h per year. In the mean time, the exploitation of the Diesel generators is extremely expensive due to the oil price increase and transportation costs. Indeed, as the fuel should be delivered to remote locations, some of them reachable only during summer periods by barge, the cost of electricity produced by Diesel generators reached in 2007 more than 50 cent/kW h in some communities, while the price for selling the electricity is established, as in the rest of Quebec, at approximately 6 cent/kW h [3]. The deficit is spread among all Quebec population as the total consumption of the autonomous grids is far from being negligible. In 2004, the autonomous networks represented 144 MW of installed power, and the consumption was established at 300 GW h. Hydro-Quebec, the provincial utility, estimated at approximately 133 millions CAD$ the annual loss, resulting from the difference between the Diesel electricity production cost and the uniform selling price of electricity [3]. Moreover, the electricity production by the Diesel is ineffective, presents significant environmental risks (spilling), contaminates the local air and largely contributes to GHG emission. In all, we estimate at 140,000 tons annual GHG emission resulting from the use of Diesel generators for the subscribers of the autonomous networks in Quebec. This is equivalent to GHG emitted by 35,000 cars during one year.

* Corresponding author at: Laboratoire International des Matériaux Antigivre, Université du Québec à Chicoutimi, Chicoutimi, Québec, Canada.
E-mail address: tammam.basbous@uqac.ca (T. Basbous).

0306-2619/$ - see front matter © 2012 Elsevier Ltd. All rights reserved.
http://dx.doi.org/10.1016/j.apenergy.2012.03.005

Nomenclature

A	area [m^2]
cp	specific heat at constant pressure [$J\,K^{-1}\,kg^{-1}$]
cv	specific heat at constant volume [$J\,K^{-1}\,kg^{-1}$]
D	displacement [l]
h	specific enthalpy [$J\,kg^{-1}$]
H	enthalpy [J]
m	mass [kg]
n	number [–]
N	engine speed [$r\,min^{-1}$]
P	pressure [Pa]
Pw	power [kW]
Qa	specific air consumption or compression [$kg\,kW^{-1}\,h^{-1}$]
Qf	specific fuel consumption [$g\,kW^{-1}\,h^{-1}$]
Qm	air consumption rate during motor mode [$kg\,h^{-1}$]
Qp	air compression rate during pump mode [$kg\,h^{-1}$]
r	gas constant [$J\,K^{-1}\,kg^{-1}$]
T	temperature [K]
Tp	compressed air temperature at the engine's outlet during pump mode [K]
Tq	torque [N m]
Tqs	specific torque [N m/l]
u	specific internal energy [$J\,kg^{-1}$]
V	volume [m^3]
ws	wind speed [$m\,s^{-1}$]
γ	specific heat ratio [–]
αv	isochoric burned fuel proportion [–]
αp	isobaric burned fuel proportion [–]
Γ	compression ratio [–]

Subscripts

air	refers to air consumed or compressed
Diesel	refers to Diesel engine
fuel	refers to injected fuel
tank	refers to tank condition
int	refers to intake conditions
ref	refers to reference conditions
WindT	refers to Wind turbine
Load	refers to consumption demand

Acronyms

BDC	Bottom Dead Center
CAES	Compressed Air Energy Storage
EVC	Exhaust Valve Close
EVO	Exhaust Valve Open
FIS	Fuel Injection Start
HPCE	Hybrid Pneumatic Combustion Engine
ICE	Internal Combustion Engine
IVC	Intake Valve Close
IVO	Intake Valve Open
TDC	Top Dead Center
WDS	Wind Diesel System
WPPR	Wind Power Penetration Rate

1.2. Hybrid Wind–Diesel systems for remote areas

The Diesel power generating units, while requiring relatively little investment, are generally expensive to exploit and maintain, particularly when are functioning regularly at partial load [4]. The use of Diesel power generators under weak operating factors accelerates wear and increases fuel consumption [5]. Therefore, the use of hybrid systems, which combine renewable sources and Diesel generators, allows reducing the total Diesel consumption, improving the operation cost and environmental benefits.

Among all renewable energies, the wind energy experiences the fastest growing rate, at more than 30% annually for the last 5 years [6,7]. Presently, wind energy offers cost effective solutions for isolated grids when coupled with Diesel generators. The Wind–Diesel System (WDS) represents a technique of generation of electrical energy by using in parallel one or several wind turbines with one or several Diesel groups. This approach is at present used in Nordic communities in Yukon [8], Nunavut [9] and in Alaska [10]. The "penetration rate" is used in reference to the rated capacity of the installed wind turbines compared to the maximum and minimum loads. A strict definition of a "low-penetration" system is one when the maximum rated capacity of the wind component of the system does not exceed the minimum load of the community. In practical terms however, a low-penetration system is one where the wind turbines are sized so as not to interfere with the Diesel generators' ability to set the voltage and frequency on the grid. In effect, the wind-generated electricity is "seen" by the Diesel plant as a negative load to the overall system. It is important to note however that, because such a system needs to be designed for the peak capacity of the wind generator, it will typically operate with an average annual output of 20–35% of its rated power, such that while low-penetration systems will have noticeable fuel and emissions savings they will be fairly minor [11,2]. In many cases it is likely that similar savings could be achieved through energy efficiency upgrades for similar capital costs. A "high-penetration" system without storage [12] is one where the output from the wind generators frequently exceeds the maximum load for extended periods of time (10 min to several hours), such that the Diesel generators can be shut off completely when there is significant wind. The Diesel generators therefore are required only during periods of low winds and/or to meet peak demands. The advantage of such systems are that very significant fuel savings can be achieved reducing import and storage costs, but also will extend the life and servicing frequency of the Diesel generators as they will log less hours. Such systems can also benefit from economies of scale for construction and maintenance, but require much more significant and expensive control systems [13,14] to regulate the grid frequency and voltage while the Diesel generators are turned off. A dispatchable or a "dump" load is required during periods when the power from the wind turbines exceeds the demand in order to maintain system frequency and voltage [10].

A medium-penetration system refers to a system in between the low- and high-penetration configurations. A medium-penetration system will have periods of time when the wind-generated electricity dominates the Diesel-generated electricity and may also be able to meet the system load for brief periods of time (30 s/min). When wind speeds are high and/or the community demand is very low, the Diesel generators may not be required at all, but are not shut off, rather they are left to idle to be able to respond quickly to load demands. A medium-penetration system is potentially subjected to both the benefits and the drawbacks of low- and high-penetration configurations. Beyond a certain penetration, the obligation to maintain idle the Diesel at any time, generally around 25–30% of its nominal output power, forces the system to function at a very inefficient regime. Indeed, for low- and medium-penetration systems, the Diesel consumes, even without load, approximately 50% of the fuel at nominal power output. These systems are easier to implant but their economic and environmental benefits are marginal [11].

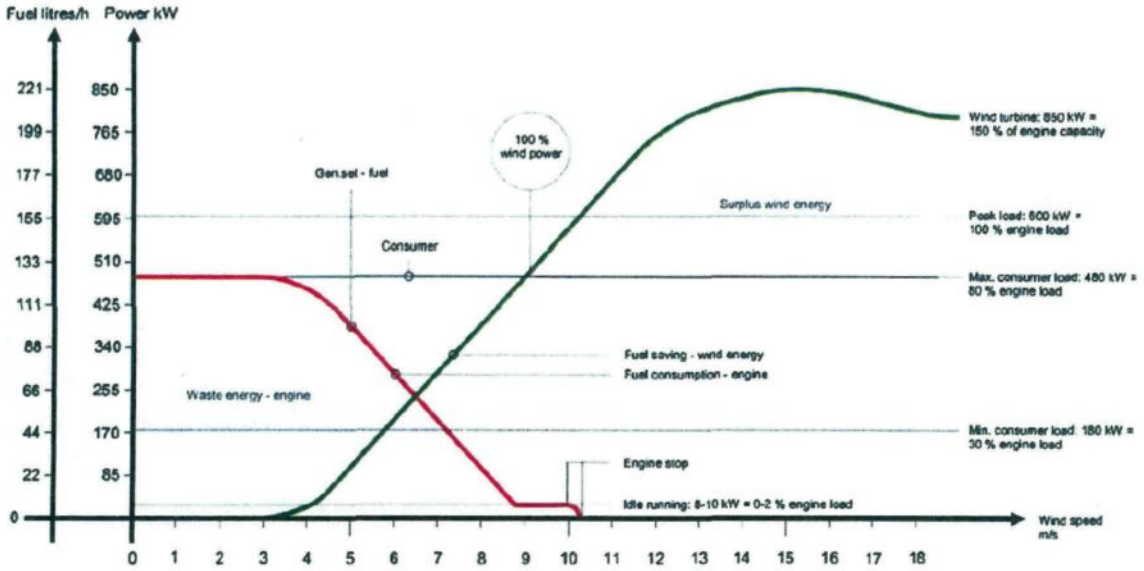

Fig. 1. example of power contribution and fuel consumption of a high penetration wind–Diesel generator [15].

The use of high-penetration systems allows the stop of the thermal groups, ideally as soon as the wind power equals the instantaneous charge, to maximize the fuel savings. However, considering the Diesel starting time as well as the instantaneous charge and wind speed fluctuations, the thermal production must be available (Diesel group to minimal regime) from the moment when the over-production passes under a threshold, named power reserve, considered as security to answer to the instantaneous requested power. The value of this reserve should be chosen so that it insures the reliability of the system and has a direct effect on the fuel consumption and the exploitation and maintenance costs of the Diesel generators. In other words, the Diesels must still idle to compensate for a sudden wind power decrease under the level of the charge. A greater value of the power reserve leads to longer periods of time during which the Diesels are functioning at inefficient regimes. During time intervals when the excess of wind energy over the charge is considerable, the Diesel engine must still be maintained on standby so that it can quickly respond to a wind speed reduction (reduce the time of starting up and consequent heating of the engine). This is an important source of over consumption because the engine could turn during hours without supplying any useful energy.

Fig. 1 [15] illustrates an example of power contribution of a high Wind Power Penetration Ratio (WPPR) in a remote area's Wind Diesel System (WDS), for a 450 kW consumer load. Fuel saving starts for wind speed higher than 4 m/s. When wind speed reaches 9 m/s, wind power is enough to cover consumers demand without Diesel engine contribution. Diesel engine is stopped, however, when a margin of 30% is reached between consumers demand and available wind power. For wind speed higher than 9 m/s, surplus wind power is lost.

1.3. Energy storage for high wind penetration system

Assuming optimum exploitation conditions [16,2] the use of energy storage with WDS can lead to better economic and environmental results, allows reduction of the overall cost of energy supply and increase the wind energy penetration rate (i.e. the proportion of wind energy as the total energy consumption on an annual basis) [2].

Presently, the excess wind energy is stored either as thermal potential (hot water), an inefficient way to store electricity as it cannot be transformed back in electricity when needed or in batteries which are expensive, difficult to recycle, a source of pollution (lead-acid) and limited in power and lifecycle. The fuel cells propose a viable alternative but due to their technical complexity, their prohibitive price and their weak efficiency, their appreciation in the market is still in an early phase. The required storage system should be easily adaptable to the hybrid system, available in real time and offer smooth power fluctuations.

In a previous work [17–21], the use of Compressed Air Energy Storage (CAES) with the hybrid WDS has been investigated. The CAES is an interesting solution to the problem of strong stochastic fluctuations of the wind power for the following reasons:

1. Its good efficiency conversion.
2. Its relatively low cost per kilowatt hour of stored energy and cost per kilowatt of peak power.
3. Its great reliability with almost infinite lifecycle number.

On the other hand, to make a hybrid WDS with CAES economically competitive, it is important not to suggest a multiplication of the Engines by adding independent air motors and compressors. That is why Pneumatic Hybridization of the existing Diesel engine is being investigated in this article. This technique consists in enabling the Diesel engine to work under pneumatic mode, conventional combustion mode or mix pneumatic-combustion mode. Diesel engine can therefore be used as a pneumatic pump during energy excess to store this energy as compressed air in the tank. The stored energy can be discharged later through a pneumatic motor operation or through a hybrid pneumatic combustion operation [22].

1.4. State of art of the pneumatic hybridization of ICE

The idea of combining pneumatic operation to combustion one whether using the same engine or using an additional one, is far from being new. However, most researchers who have studied this issue focused on automotive applications [40].

Donitz et al. [23] created a full operational hybrid pneumatic engine, theoretically able to operate under two stroke pneumatic motor mode, four stroke pneumatic motor mode, two stroke pneumatic pump mode, four stroke pneumatic pump mode, supercharged mode and conventional mode. This concept is accomplished by connecting an air pressure tank to all cylinders via electronically fully controlled Charge Valve [24]. The original Intake and Exhaust Valves should also be electronically controlled. Donitz found the efficiency data of four-stroke pneumatic modes are not significantly lower than those of the two-stroke counterpart, thus calling for their further investigation in practice [24]. Testing results on a spark ignition engine demonstrator, supported by a modeling analysis [24] showed viability of this new concept for fuel consumption reduction, when combined with a strong downsizing and supercharging of the engine. Compared to a naturally aspirated engine with the same rated power, the downsized and supercharged hybrid pneumatic engine can save 32% of fuel [23]. The strong downsizing is possible thanks to pneumatic hybridization because the problem of the "turbo-lag", usually associated with heavily downsized and supercharged engines, is completely overcome by injecting additional air from a pressure tank and more fuel during transients [23]. Experiments have verified the engine's instantaneous torque response resulting from applying this supercharged mode [23].

Earlier, Higelin et al. [25,26] studied a similar concept and concluded using simulations of the theoretical thermodynamic cycles that fuel consumption on NEDC driving cycle could be reduced up to 31% if all the parameters including the Tank volume were optimized [26]. This concept is promising in terms of energetic performance, cost and weight; it requires, however, heavy modifications in the engine's hard architecture because a charge valve has to be added. This cannot be done by simply adjusting an existing ICE. It is therefore not logical to suggest this concept as a possible modification of existing hybrid Wind Diesel power generator Moreover, this concept is validated for spark ignition engines and there are reasons to think that it might not work adequately with Diesel engines, mainly for hybrid pneumatic Diesel operations. Indeed, compressed air is charged in the cylinder during the compression phase. Afterwards, the fuel is injected and needs to start burning few degrees before piston reaches the top dead center (TDC). Considering that in Diesel engines, ignition delay has to pass before fuel starts burning; it is quite difficult to ensure the burn of enough fuel before the TDC, which will probably compromise the system efficiency. Obviously, that might be the reason why all the tests that have been conducted on this system were made on spark ignition engines.

Schechter suggested Regenerative Compression Braking as a cost effective alternative to electrification of vehicle engines [27]. He defined several new cycles [28] possible with pneumatic hybrid ICE. Two and four stroke operations with several variants are exposed. The driving cycle simulation model for the vehicle powered by an air hybrid engine has Schechter showed by modeling that for a 1531 kg vehicle, the pneumatic hybridization of the results in fuel economy improvement of 64% and 12% in city and highway driving respectively, compared to the conventional baseline vehicle [29].

In addition to that, other researchers worked on simpler concepts of pneumatic hybridization, but all of them focus on two-stroke pure pneumatic motor and pump operations.

Hyungsuk et al. [30] suggested a concept based on connecting the compressed air tank to the exhaust manifold and using a three-way valve to switch flow between turbine and air tank. It does not require a specific valve to inject the compressed air. It requires, however, a complete change in valve timing for both the air compressor and air motor two-stroke modes. This is accomplished through a cam-less Hydraulically Actuated Valve (HVA) system.

The Air-Power-Assist (APA) Engine was tested at steady state in compressor mode and in motor mode as well. The tests confirmed the functionality of the concept. The APA engine demonstrated air compression and high pressure air storage in the air tank by controlling the valve timing and using the air handling system. The APA engine generated positive power by using the compressed air from the air tank without injecting fuel [30]. APA engine can be done by applying a simple modification on an existing engine. Its performance, however, is limited to pneumatic operation. Hybrid operation that combines pneumatic power to fuel power is not possible.

Moreover, Trajkovic et al. [31–33] converted a single-cylinder Scania D12 Diesel engine to a pneumatic hybrid Diesel one. The engine can work under conventional Diesel mode as well as two-stroke pneumatic motor and pneumatic pump modes. Trajkovic et al. [31,32] conducted an optimization on valves actuation timing and obtained up to 48% of regenerative efficiency at steady state operation. Later, Trajkovic et al. [33] compared testing measures to GT-Power simulation results. The correlation was done for both pneumatic modes and it showed a 5% error in steady state operations [33]. We notice that this study was conducted using not more than 8 bars of tank pressure.

Finally, Lee et al. [34] have worked on a novel cost-effective air hybrid powertrain concept for buses and commercial vehicles. The concept is simple because it requires only a few modifications to the intake of the engine by adding two one-way valves and an air tank. The concept does not require any change to the initial intake and exhaust valves of the engine. However, the concept can only operate under conventional mode, compressor mode and cranking mode. The last mode is a four stroke pneumatic motor mode. The storage pressure is in the order of 8 bars. The simplicity and the cost effectiveness constitute the main strength of the concept, but not hoped the fuel economy.

1.5. Objectives and methodology of current study

The main objective of this study is to suggest and evaluate a new Hybrid Pneumatic-Combustion Engine (HPCE) concept that satisfies all three conditions below:

1. Require a relatively simple modification of conventional ICE including Diesel engines; concepts requiring additional air charging valve are rejected.
2. Be able to operate under pneumatic motor and pump modes, hybrid pneumatic combustion motor mode in addition to conventional mode.
3. Have good efficiency.
4. Require a feasible air tank volume.

To reach this target, after exposing the operating principles of the suggested HPCE concept and the modifications needed form a conventional ICE, a theoretical study is conducted, following the steps listed below:

1. Modeling of the ideal thermodynamic cycles of each operating mode, and mathematical expression of the fuel consumption and air consumption. The choice of using ideal cycle is justified by the need to validate the viability of this new concept regardless the imperfections that might occur because of several phenomena (such as valves opening and closing dynamics, sonic flow limitation, combustion process and boundary heat losses). The effect of those phenomena would be studied later in a future work.

2. Optimizing engine's commands (such as valves openings, valves closings and fuel injection) for every operating mode at every functioning point (torque provided), and for each possible tank pressure. This optimization aims to ensure that the engine operates under its best possible efficiency all the time.
3. Generating maps of commands resulting of previous optimization.
4. Defining a selection strategy of the operating mode function of different external or internal parameters.
5. Applying those optimized commands and mode selection strategy on a known site for evaluating fuel consumption for power generation using a WDS with HPCE concept, with different possible WPPR and tank volume, and compare the annual fuel consumption with the one obtained using a Classic Diesel engine, and with the one obtained using a WDS without energy storage.

2. Suggested concept

The suggested HPCE is based on bypassing the turbocharger and connecting air tank to intake valve using two three-way valves as shown in Fig. 2. The first three-way valve connects the ICE's inlet to either the air tank or the compressor's outlet while the second three-way valve connects the ICE's exhaust to either the turbine's

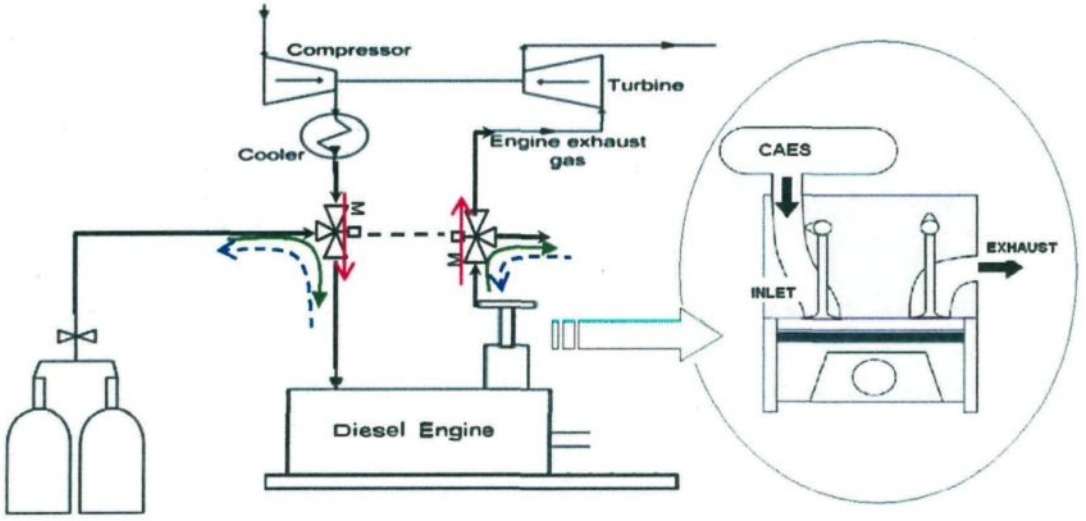

Fig. 2. Suggested HPCE concept.

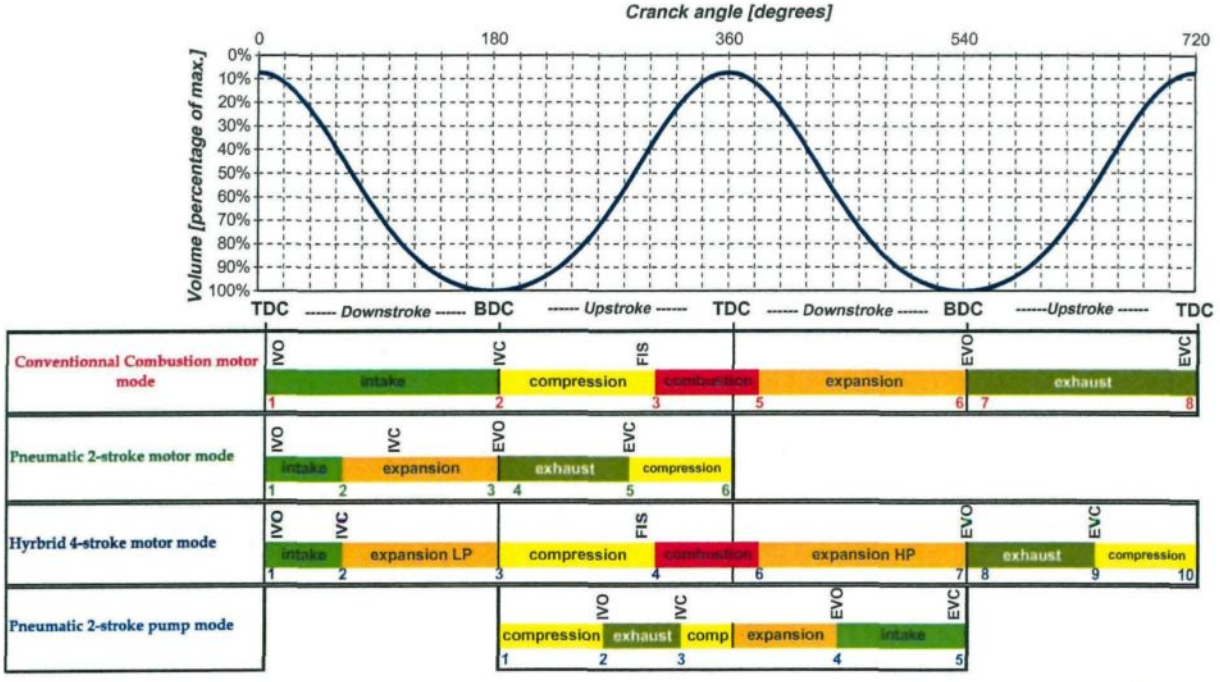

Fig. 3. Operating principles of suggested HPCE concept.

inlet or to the atmosphere. The concept requires as well a full control of the intake valves, the exhaust valves and the fuel injectors. It permits the engine to operate under the four following modes illustrated in Fig. 3.

2.1. Four-stroke conventional combustion motor mode

The three-way valves connect the turbocharger to the inlet and the exhaust of the engine. The cycle lasts during two rounds of the piston. The intake valve is open during the whole piston's way down (1 → 2) of the fist stroke. When the piston gets to the Bottom Dead Center (BDC), compression phase (2–3) starts. A few degrees before the TDC, the fuel starts to be injected (FIS). Combustion phase (3 → 5) starts a few degrees later and finishes a few degrees after the TDC. After the combustion, expansion phase (5 → 6) occurs during the piston's way down until it reaches the BDC. At BDC, the exhaust valve opens and exhaust phase (6 → 8) occurs during the piston's way up. At TDC, exhaust valve closes. The intake and exhaust pressure are set by the turbocharger. Fig. 4 illustrates the ideal thermodynamic cycle of this operating mode.

2.2. Two-stroke pneumatic motor mode

The three-way valves disconnect the turbocharger and connect the intake of the engine to the air tank and the exhaust to the atmosphere. The intake pressure is equal to the air storage pressure while exhaust pressure is equal to the atmospheric pressure. The fuel injection is disabled. The cycle lasts only one piston round. At TDC, intake valve opens and closes shortly after enabling therefore admission phase (1 → 2). Then an expansion phase (2 → 3) starts and lasts until piston reaches the BDC. Then exhaust valve opens and enables exhaust phase (3 → 5) during the piston's way up. Somewhere between BDC and TDC, exhaust valve closes and a compression phase starts (5 → 6) until piston reaches the TDC. Fig. 5 illustrates the ideal thermodynamic cycle relative to this operating mode. The interest the early Exhaust Valve Closing (EVC), i.e. closing the exhaust valve before the piston gets the TDC, will be demonstrated later in this article.

2.3. Four-stroke hybrid pneumatic-combustion motor mode

This mode is also called four-stroke air-power-assisted mode [28]. The three-way valves disconnect the turbocharger and connect the intake of the engine to the air tank. The intake pressure is equal to the air storage pressure. The intake valve is open during a part of piston's way down of the fist stroke, enabling the intake phase (1 → 2). Somewhere between TDC and BDC, intake valve closes and an expansion phase (2 → 3) starts. When the piston gets to the BDC, operation continues exactly as the conventional mode. Fig. 6 illustrates the ideal thermodynamic cycle relative to this operating mode. This mode operates normally even with Diesel engines because fuel injection can start anytime during piston compression between points 3 and 4, in order to ensure that the fuel burn starts when needed for getting the best cycle efficiency.

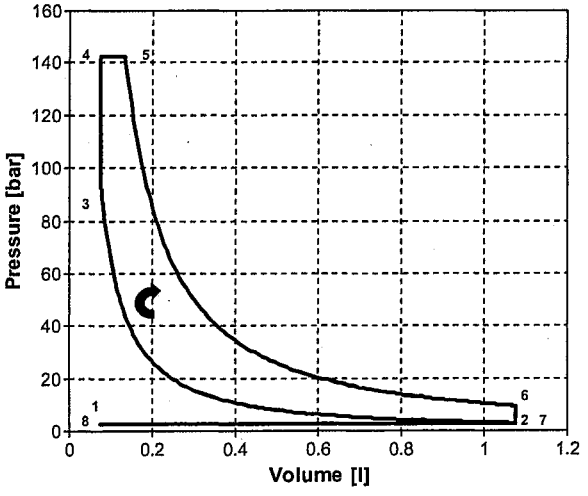

Fig. 4. Illustration of the ideal four-stroke conventional combustion cycle.

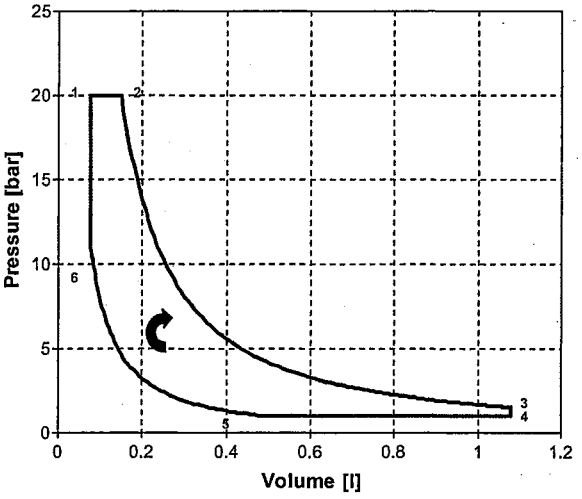

Fig. 5. Illustration of the ideal two-stroke pneumatic motor cycle.

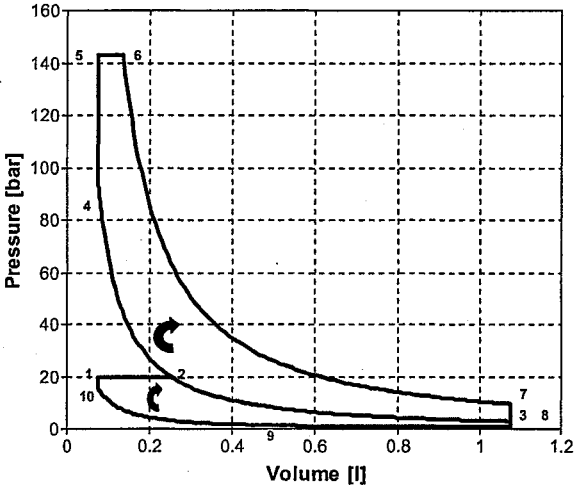

Fig. 6. Illustration of the ideal four-stroke hybrid pneumatic-combustion motor cycle.

2.4. Two-stroke pneumatic pump mode

This mode is the reverse of the two-stroke pneumatic motor mode. The three-way valve is in the same position and the engine runs in the same way. However, by changing the intake and exhaust valve timings, low-pressure air is admitted through exhaust valve and high-pressure air is rejected through intake valve. Compressed air can therefore be stored in the tank. In this mode, fuel injection is disabled. Compression phase (1 → 2) starts at BDC

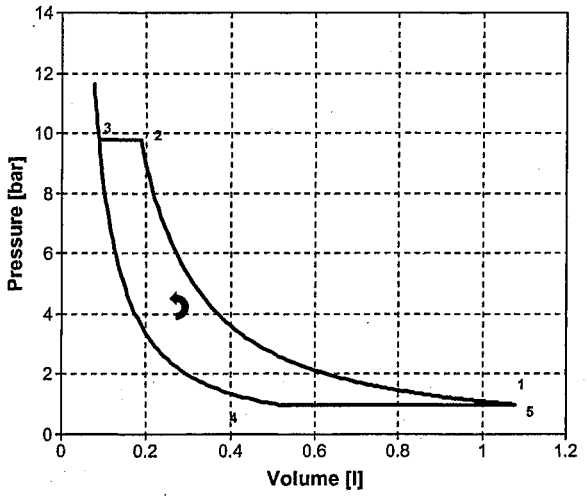

Fig. 7. Illustration of the ideal pneumatic two-stroke pump cycle.

and lasts until intake valve opens, somewhere between BDC and TDC enabling therefore exhaust phase (2 → 3). Intake valve closes a few degrees after it opens. The IVC angle will have to be dynamically adjusted for maximum braking energy recovery. If the available torque is high enough, IVC occurs at TDC in order to compress the maximum possible air quantity. If the available torque is relatively low, IVC occurs before TDC, reducing therefore the compressed air quantity as well as the work needed for the compression. After IVC, an expansion phase (3 → 4) occurs during piston's way down in the first case (IVC at TDC) and a compression phase followed by an expansion phase occur during the piston's way up then down in the second case (IVC before TDC). Somewhere between TDC and BDC, cylinder air pressure becomes exactly equal to atmospheric pressure. At that moment, exhaust valve opens and enables intake phase (4 → 5). Fresh air fills therefore the cylinder until the piston gets the BDC when exhaust valve closes. Fig. 7 illustrates the ideal thermodynamic cycle relative to this operating mode.

3. Mathematical modeling

The equations applied to characterize the thermodynamic cycles and the generated wind power model, are available in literature review [35–37].

3.1. Ideal thermodynamic cycles

The analytical equations that allow knowing the pressure, the temperature and the mass at every point of the ideal thermodynamic cycles are developed in details Appendix A.

3.1.1. Mode 1: Four-stroke combustion ideal motor cycle

The work generated during the cycle is calculated using the following equation:

$$W = \sum_{i=1}^{i=8} W_{i\to i+1} \tag{1}$$

where the work of each process $W_{i\to i+1}$ is calculated using the following equations:

$$W_{1\to 2} = -P_{int}\cdot(V_2 - V_1) \tag{2}$$
$$W_{2\to 3} = m_3\cdot(u_3 - u_2) = m_3\cdot cv\cdot(T_3 - T_2) \tag{3}$$
$$W_{3\to 4} = 0 \tag{4}$$
$$W_{4\to 5} = -P_5\cdot(V_5 - V_4) \tag{5}$$
$$W_{5\to 6} = m_5\cdot(u_6 - u_5) = m_5\cdot cv\cdot(T_6 - T_5) \tag{6}$$
$$W_{6\to 7} = 0 \tag{7}$$
$$W_{7\to 8} = -P_{exh}\cdot(V_8 - V_7) \tag{8}$$
$$W_{8\to 1} = 0 \tag{9}$$

The specific fuel consumption of the cycle is calculated using the following equation:

$$Qf = \frac{m_{fuel}}{W\cdot 3{,}6\cdot 10^{-3}} \tag{10}$$

3.1.2. Mode 2: Two-stroke pneumatic ideal motor cycle

The work generated during the cycle is calculated using the following equation:

$$W = \sum_{i=1}^{i=6} W_{i\to i+1} \tag{11}$$

where the work of each process $W_{i\to i+1}$ is calculated using the following equations:

$$W_{1\to 2} = -P_{tank}\cdot(V_2 - V_1) \tag{12}$$
$$W_{2\to 3} = m_3\cdot(u_3 - u_2) = m_3\cdot cv\cdot(T_3 - T_2) \tag{13}$$
$$W_{3\to 4} = 0 \tag{14}$$
$$W_{4\to 5} = -P_{exh}\cdot(V_5 - V_4) \tag{15}$$
$$W_{5\to 6} = m_6\cdot(u_6 - u_5) = m_6\cdot cv\cdot(T_6 - T_5) \tag{16}$$
$$W_{6\to 1} = 0 \tag{17}$$

The specific air consumption of the cycle is calculated using the following equation:

$$Qa = \frac{m_{air}}{W\cdot 3{,}6} \tag{18}$$

3.1.3. Mode 3: Four-stroke pneumatic-combustion ideal motor cycle

This cycle is simply a combination of the two previous cycles. Indeed, it is a conventional combustion mode where the scavenging cycle is replaced by two-stroke pneumatic motor cycle. The equations describing this mode are therefore the same as developed before.

The specific fuel consumption and the specific air consumption of the cycle are calculated using Eqs. (10) and (18) respectively.

3.1.4. Mode 4: Two-stroke pneumatic ideal pump cycle

The work generated during the cycle is calculated using the following equation:

$$W = \sum_{i=1}^{i=5} W_{i\to i+1} \tag{19}$$

where the work of each process $W_{i\to i+1}$ is calculated using the following equations:

$$W_{1\to 2} = m_2\cdot(u_2 - u_1) = m_2\cdot cv\cdot(T_2 - T_1) \tag{20}$$
$$W_{2\to 3} = -P_{tank}\cdot(V_3 - V_2) \tag{21}$$
$$W_{3\to 4} = m_4\cdot(u_4 - u_3) = m_4\cdot cv\cdot(T_4 - T_3) \tag{22}$$
$$W_{4\to 5} = -P_{int}\cdot(V_5 - V_4) \tag{23}$$

The specific air compression of the cycle is calculated using Eq. (18).

3.2. Tank storage and discharge ideal model

The charge and discharge operations are considered adiabatic. During storage periods, if the pump delivers a compressed air mass

rate of Qp at a temperature of Tp, the variation of the air stored mass m_{tank} and temperature T_{tank} can be calculated using the following equations:

$$dm_{tank} = Qp \cdot dt \tag{24}$$

$$dT_{tank} = \frac{\gamma \cdot Tp - T_{tank}}{m_{tank}} \cdot Qp \cdot dt \tag{25}$$

During discharge periods, if the engine consumes a compressed air mass rate of Qm, the variation of m_{tank} and T_{tank} can be calculated using the following equations:

$$dm_{tank} = -Qm \cdot dt \tag{26}$$

$$dT_{tank} = -\frac{(\gamma - 1) \cdot T_{tank}}{m_{tank}} \cdot Qm \cdot dt \tag{27}$$

After calculating m_{tank} and T_{tank}, the tank pressure P_{tank} can be calculated using perfect gas law, knowing that the tank volume V_{tank} is constant.

$$P_{tank} = \frac{m_{tank} \cdot r \cdot T_{tank}}{V_{tank}} \tag{28}$$

3.3. Model of wind power and Diesel load in Tuktoyaktuk

The power generated by one wind turbine for a certain wind speed ws can be calculated as follows:

$$Pw_{WindT}(ws) = Pw_{BETZ}(ws) \times PC_{WindT}(ws) \tag{29}$$

where Pw_{BETZ} is the maximum wind power calculated as follows:

$$Pw_{BETZ}(ws) = \frac{1}{2} \cdot \rho_a \times A_{WindT} \times ws^3 \tag{30}$$

And $PC_{WindT}(ws)$ is the power coefficient of the wind turbine. Illustrated in Fig. 8.

The Engine load is equal to the difference between load power and total wind generated power:

$$Pw_{Diesel} = Pw_{Load} - n_{WindT} \times Pw_{WindT} \tag{31}$$

where n_{WindT} is the number of installed wind turbines.

The torque provided by the engine can therefore be calculated using the following equation:

$$Tq_{Diesel} = \frac{Pw_{Diesel}}{w_{Diesel}} = \frac{30}{\pi} \cdot \frac{Pw_{Diesel}}{N_{Diesel}} \tag{32}$$

Finally, the specific torque is equal to the ratio of the torque to the engine's displacement:

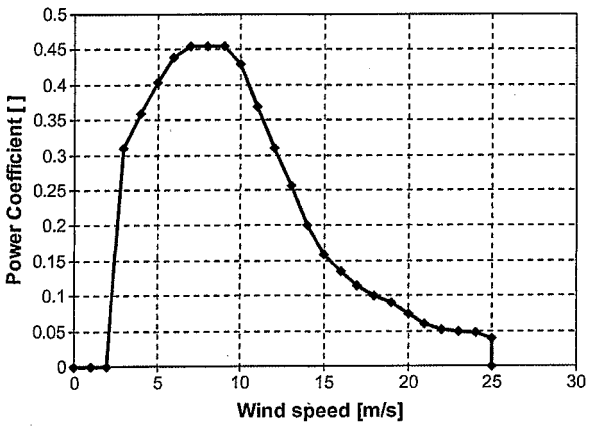

Fig. 8. Power coefficient curve of the ENERCON 330 kW wind turbine.

Table 1
Hybrid wind Diesel system parameters.

Parameter	Value	Unit
Wind turbine type	ENERCON	
Wind turbine unit power	330	kW
A_{WindT}	876	m^2
$PC_{WindT}(ws)$	See Fig. 8	
D_{Diesel}	40	l
N_{Diesel}	750	rpm
Γ_{Diesel}	14	

$$Tqs_{Diesel} = \frac{Tq_{Diesel}}{D_{Diesel}} = \frac{30}{\pi} \cdot \frac{Pw_{Diesel}}{N_{Diesel} \cdot D_{Diesel}} \tag{33}$$

The Wind Power Penetration Ratio (WPPR) is the ratio of maximal generated wind power to the maximal load, as illustrated in the following equation:

$$WPPR = \frac{n_{WindT} \times \max(Pw_{WindT})}{\max(Pw_{Load})} \tag{34}$$

The parameters used for the hybrid wind Diesel power generator are listed in Table 1.

For high WPPR, surplus wind power is transformed into electric power using wind turbines, then to mechanical power using Diesel generator Electric Machine that operates then as an electric motor.

4. Parametric optimization of the HPCE concept

4.1. Mode 1: Four-stroke combustion ideal motor cycle

This mode is the reference mode and its characterization constitutes the starting point for fuel consumption reduction. Fig. 9 shows the efficiency and the fuel consumption as a function of the specific torque, only parameter that characterizes this operating mode.

It is important to remind the reader that it is the ideal cycle efficiency and the order of 65% is therefore logical, while the real cycle efficiency is in the order of 35%.

4.2. Mode 2: Two-stroke pneumatic ideal motor cycle

First, it is important to notice that the for every intake pressure, the intake temperature considered for the calculation of the

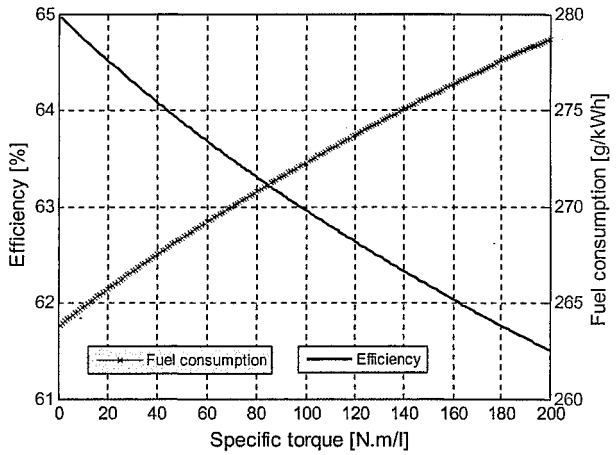

Fig. 9. Fuel specific consumption and efficiency of conventional combustion ideal cycle, as a function of specific torque.

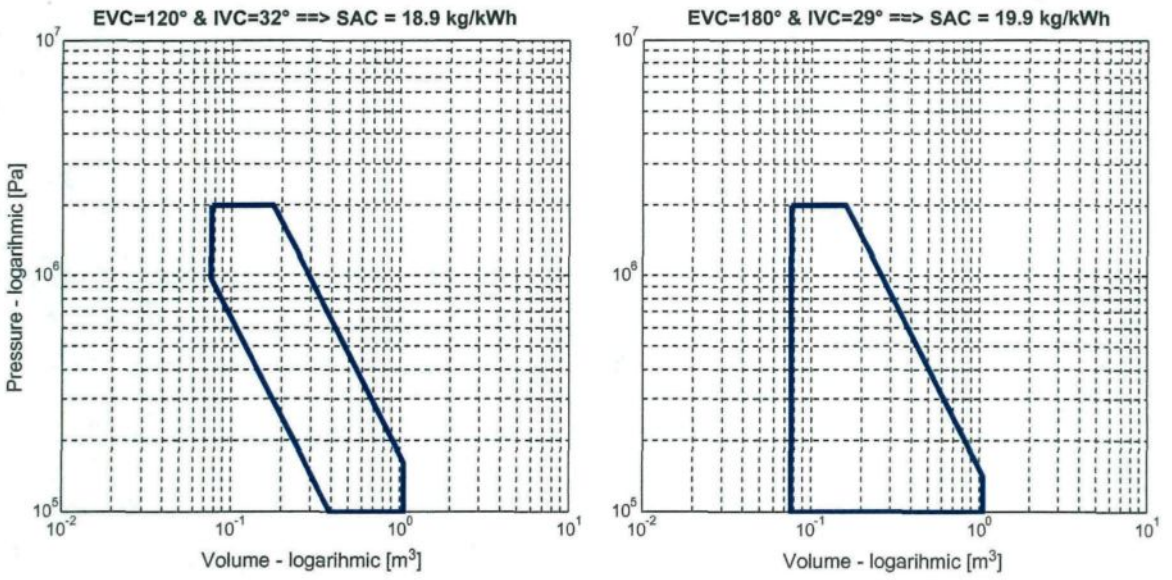

Fig. 10. Two-stroke pneumatic motor operations providing a specific torque of 80 Nm/l with early EVC (left) and without early EVC (right) for a 20 bars intake pressure.

thermodynamic cycle corresponds to the air temperature after an adiabatic compression starting from ambient conditions (P_a = 1 - bar;
T_a = 298 K) to the actual intake pressure. T_{ref} can be calculated using the following equation:

$$T_{ref} = T_a \times \left(\frac{P}{P_a}\right)^{\frac{\gamma-1}{\gamma}} \tag{35}$$

T_{ref} is therefore a reference temperature. If the intake temperature is different than T_{ref}, some of the results that will be presented below should be corrected, as will be explained later. This logic is valid for both the two-stroke pneumatic motor cycle and the four-stroke hybrid pneumatic-combustion motor cycle.

In this mode, two parameters should be set in order to meet the wanted specific torque for each tank pressure. Those parameters are the Intake Valve Close (IVC) angle and the Exhaust Valve Close (EVC) angle. Indeed, there are several possibilities to do so. Fig. 10 shows two ways to get a specific torque of 80 Nm/l while the tank pressure is 20 bars:

1. EVC angle and IVC angle respectively set to 120° and 32°, in that case, the Specific Air Consumption (SAC) is equal to 18.9 kg/kW h.
2. EVC angle and IVC angle respectively set to 180° and 29°, in that case the SAC is equal to 19.9 kg/kW h, i.e. 5% higher.

That means that early EVC is beneficial in that case in order to minimize the air consumption. We have next calculated the SAC curves and the specific torque curves for every combination of IVC and EVC. The result is shown in Fig. 11 where one can observe infinite ways to get a certain torque, but only one that ensures the minimal SAC.

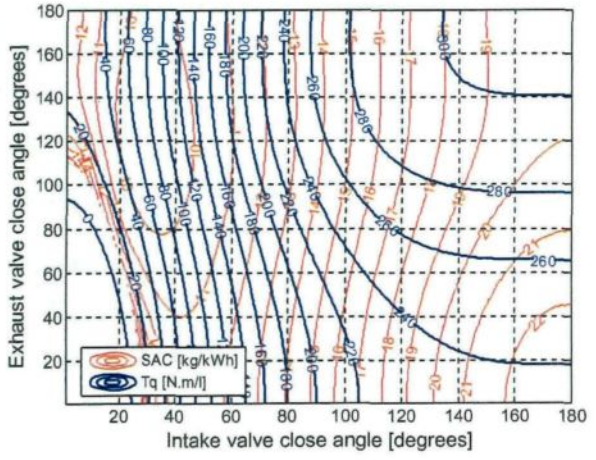

Fig. 11. Two-stroke pneumatic motor operation specific torque and efficiency with intake pressure of 20 bars, as a function of intake and exhaust close angle.

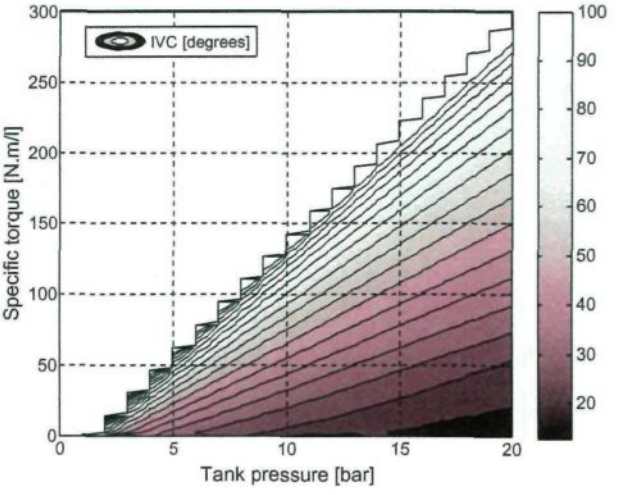

Fig. 12. Optimal intake valve close angle as a function of the tank pressure and the specific torque of a pneumatic two-stroke motor operation.

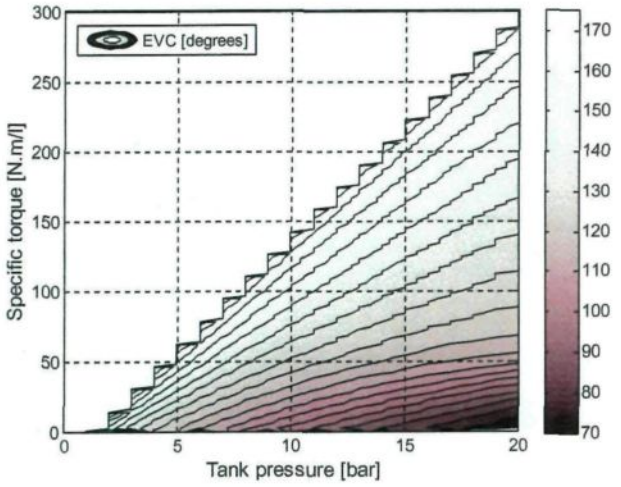

Fig. 13. Optimal exhaust valve close angle as a function of the tank pressure and the specific torque of a pneumatic two-stroke motor operation.

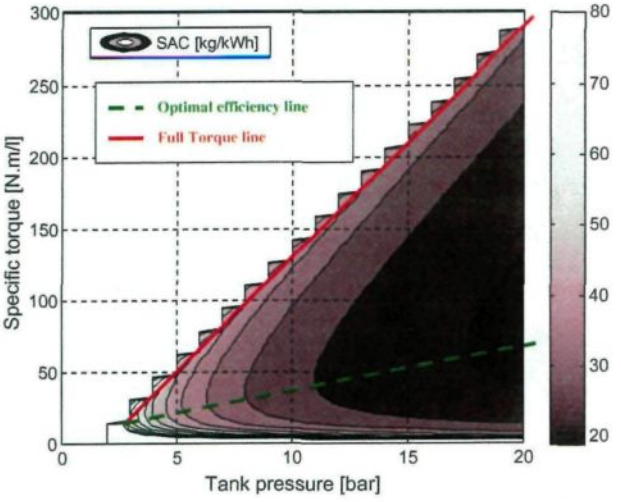

Fig. 14. Specific air consumption of an optimized pneumatic two-stroke motor mode as a function of the tank pressure and the specific torque.

Consequently, the optimal calibration of the IVC and the EVC angles that give the minimal SAC, for each combination of specific torque and tank pressure are calculated and the result is shown in Figs. 12 and 13. Early EVC is needed mainly at low loads and high tank pressure. The associated SAC is illustrated in Fig. 14. If tank pressure is equal to 5 bars, the minimal SAC is attained for a specific torque of 25 Nm/l; and if tank pressure is equal to 20 bars, the minimal SAC is attained for a specific torque of 75 Nm/l. The shape of the optimal efficiency curve is linear.

Calculus showed that optimal close valves angle and cycle efficiency are not dependant of intake temperature while air consumption is. If the tank air temperature T_{tank} is different from the reference intake temperature T_{ref} illustrated in Fig. 14, the air consumption $Q_{air}^{/T}$ is obtained by correcting the reference air consumption$Q_{air}^{/T_{ref}}$, using the following equation:

$$Q_{air}^{/T} = Q_{air}^{/T_{ref}} \times \frac{T_{ref}}{T_{tank}} \tag{36}$$

Finally, the full torque curve in this mode is also linear, function of the tank pressure.

4.3. Mode 3: Four-stroke pneumatic-combustion ideal motor cycle

The four-stroke pneumatic-combustion motor mode is an association of the two precedent modes. The ratio of the pneumatic power to the total power can be adjusted by increasing or reducing the IVC angle. The more this ratio is, the less the fuel consumption is but highest the maximal cylinder pressure is as well. Fig. 15 illustrates two possible operations to provide 150 Nm/l specific torque with 20 bars tank pressure, with two different percentages of the pneumatic power to the total power, 40% (left) and 69% (right). It can be observed that the area of the low-pressure part of the cycle is higher and the area of the high-pressure part is lower for the 69% ratio operation. It also can be remarked how the high-pressure cycle reaches much higher cylinder pressure in the 69% ratio operation. The fuel consumptions of the 40% ratio operation and the 69% ratio operation are respectively 130 g/kW h and 96 g/kW h. Fig. 16 illustrates the variation of the specific fuel consumption and the maximal cylinder pressure as functions of the ratio of the pneumatic power to the total power for a 150 Nm/l specific torque operation.

The maximal cylinder pressure cannot be increased indefinitely. Increasing this pressure exposes the engine to higher mechanical stress level. A 180 bars-pressure is a common limitation of the cylinder pressure accepted by most turbocharged Diesel engines [38]. In the present study, the threshold for maximal pressure have been considered 200 bars, considering that the modeled cycle is the ideal one and that the real cycle will produce less pressure because of different losses. This threshold is to be respected while choosing the ratio of the pneumatic power to the total power for each operation point.

For every optimized operation, the chosen EVC angle is the same than the one obtained in the two-stroke pneumatic motor mode while providing the same pneumatic torque. The results of this optimization are illustrated in the following figures. It is logical that the four-stroke pneumatic-combustion motor mode operation starts when the torque demanded is higher than the full torque possible with the two-stroke pneumatic motor mode.

Fig. 17 illustrates the optimal ratio of the pneumatic power to the total power that allows obtaining the required specific torque for a certain tank pressure, while ensuring minimal fuel consumption and without exceeding 200 bars of maximal cylinder pressure. We observe that for larger tank pressure the pneumatic contribution increases and for larger specific torque the pneumatic contribution diminishes.

Figs. 18 and 19 show respectively, the IVC and EVC angles associated to this optimized operation. Early EVC occurs mainly for very high tank pressure.

The associated SAC and SFC are illustrated in Figs. 20 and 21 respectively. SAC is lower for higher specific torque. It is important to remind that SAC should be corrected according to the intake temperature as detailed for the two-stroke pneumatic motor mode, in Eq. (36). SFC decreases significantly for higher tank pressure and for lower specific torque.

4.4. Mode 4: Two-stroke pneumatic ideal pump cycle

The two-stroke pneumatic pump cycle is possible for negative specific torque, i.e. when the engine is supplied by mechanical power. As explained previously, IVO angle is chosen in order to meet the tank pressure while IVC angle is chosen in order to meet the specific torque demanded. Figs. 22 and 23 show the IVO and the IVC as functions of tank pressure and specific torque. We remind the user that in this mode, the exhaust of the compressed

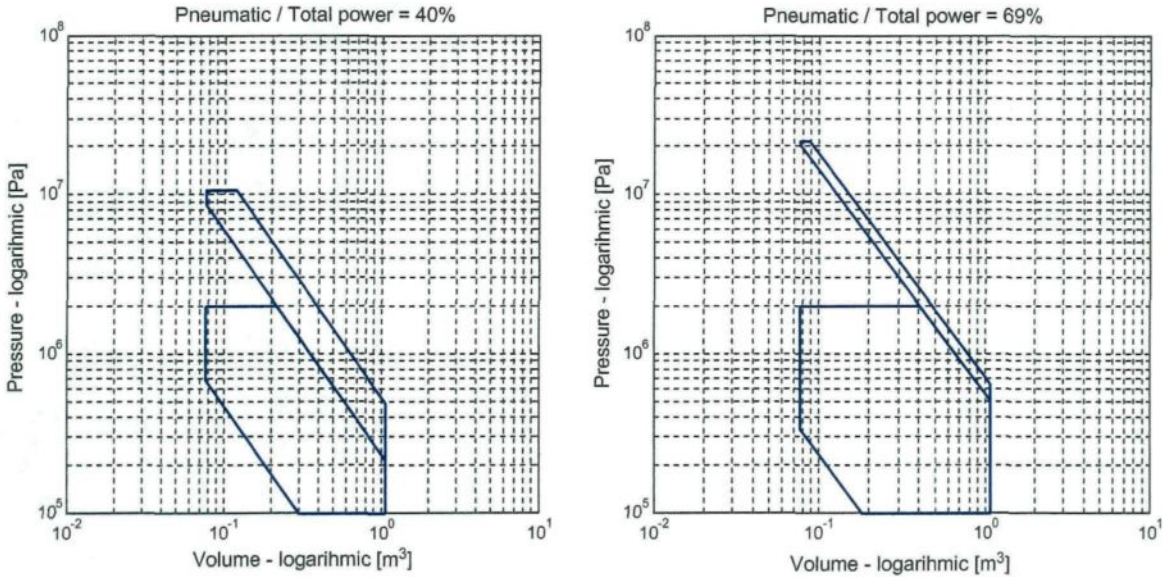

Fig. 15. Hybrid operations providing a specific torque of 150 N m/l with intake pressure of 20 bars, for 40% pneumatic contribution (left) and 69% pneumatic contribution (right).

air passes through intake valve and the intake of atmospheric air passes through exhaust valve. We observe as well in Figs. 23 and 24 the full torque curve that represents the maximal torque that the engine is able to recover. If the input torque is higher, the engine recovers a part of the mechanical energy and the rest is unfortunately dissipated. Moreover, EVO angle is chosen in order to optimize the efficiency by ensuring that the cylinder pressure when the exhaust valve opens is close to 1 bar in order not to dissipate pneumatic energy. Fig. 24 illustrates the optimal EVO as a function of tank pressure and available specific torque. As for the specific compressed air flow-rate, Fig. 25 shows that it depends only on tank pressure such that for a larger tank pressure the specific air flow-rate diminishes.

Finally, compressed air temperature is important as it will act on the tank air temperature during compression operation, as explained previously. Fig. 26 shows that this temperature depends only of the tank pressure. Tank pressure equals the compression ratio of the air pump. For highest tank pressures, the compressed air temperature increases. Exhaust temperature can rise up to 460 K if ambient temperature is 298 K.

4.5. Engine mode selection strategy

After this analysis and comprehension of the thermodynamic ideal cycles corresponding to all four modes, a strategy for choosing the engine's operation mode as a function of the tank pressure and the specific torque required can be suggested. This strategy, illustrated in Fig. 27, priories the pneumatic mode whenever it is possible. At every moment, the manager decides the operating mode depending of the instantaneous tank pressure and the instantaneous load i.e. specific torque applied to the engine. When the tank pressure is lower than 3 bars, the operation mode is forced to be conventional. During energy recovering operation,

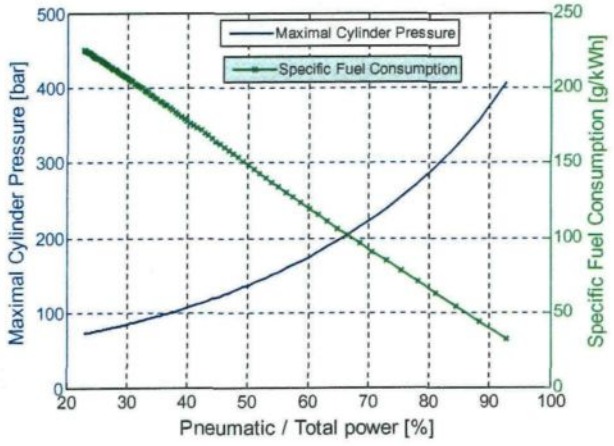

Fig. 16. Maximal gas cylinder pressure of hybrid cycle, as a function of pneumatic power contribution for 150 N m/l torque operation.

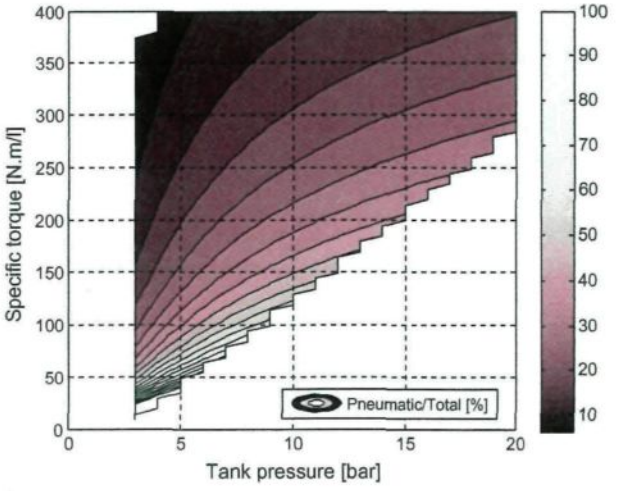

Fig. 17. Optimal pneumatic power contribution as a function of the tank pressure and the specific torque of a hybrid four-stroke operation.

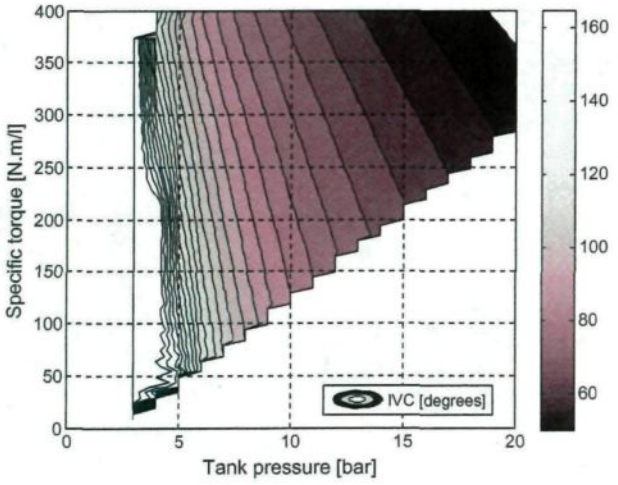

Fig. 18. Optimal intake valve close angle as a function of the tank pressure and the specific torque of a hybrid four-stroke operation.

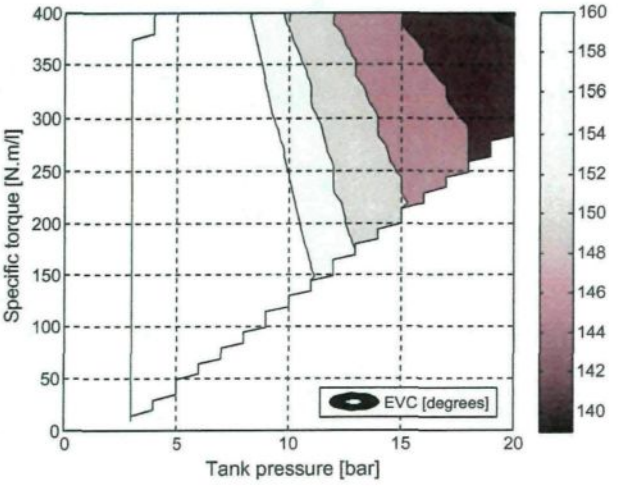

Fig. 19. Optimal exhaust valve close angle as a function of the tank pressure and the specific torque of a hybrid four-stroke operation.

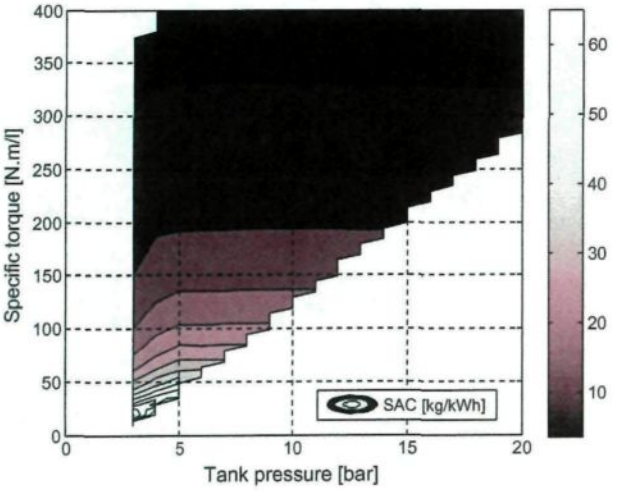

Fig. 20. Optimal specific air consumption as a function of the tank pressure and the specific torque of a hybrid four-stroke operation.

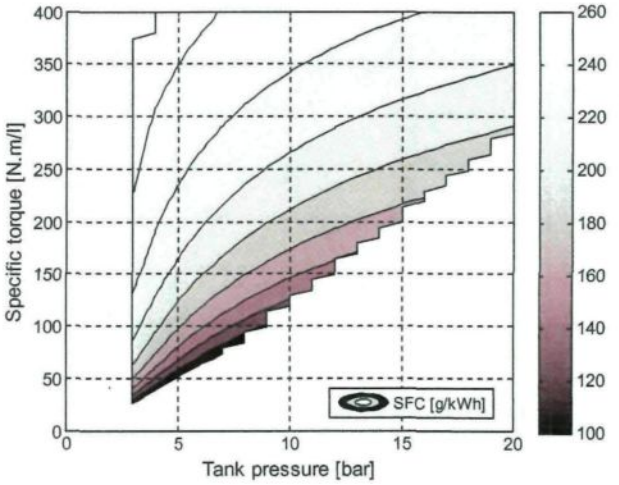

Fig. 21. Optimal specific fuel consumption as a function of the tank pressure and the specific torque of a hybrid four-stroke operation.

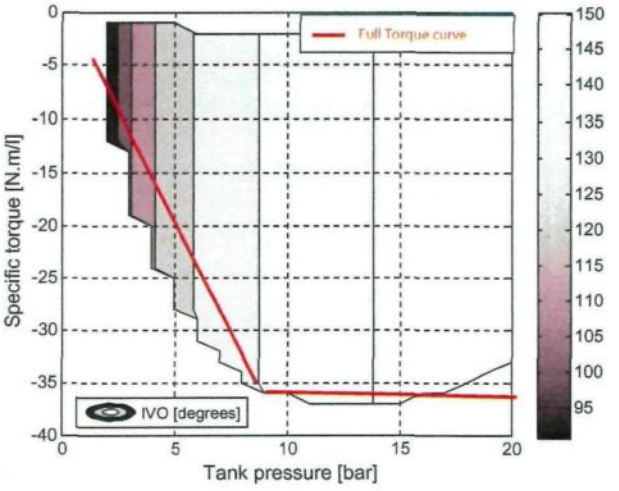

Fig. 22. Optimal intake valve open angle as a function of the tank pressure and the specific torque of a pneumatic two-stroke pump operation.

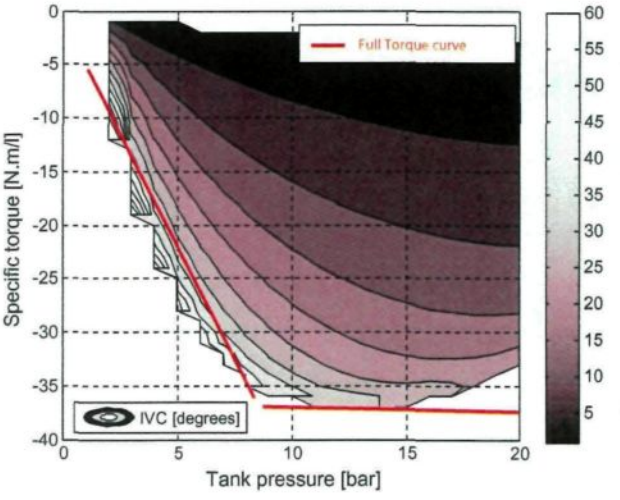

Fig. 23. Optimal intake valve close angle as a function of the tank pressure and the specific torque of a pneumatic two-stroke pump operation.

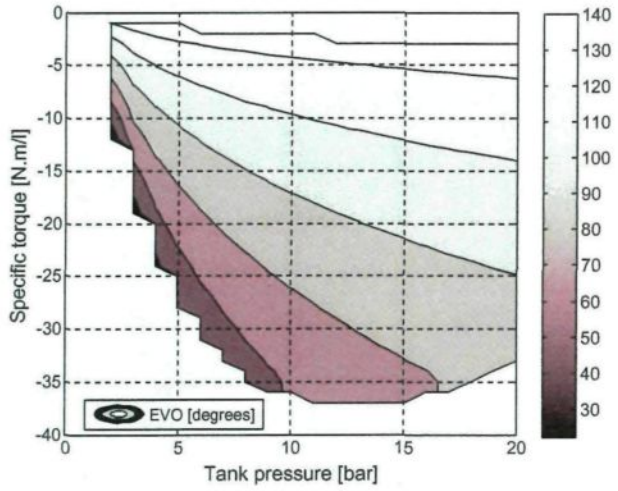

Fig. 24. Optimal exhaust valve open angle as a function of the tank pressure and the specific torque of a pneumatic two-stroke pump operation.

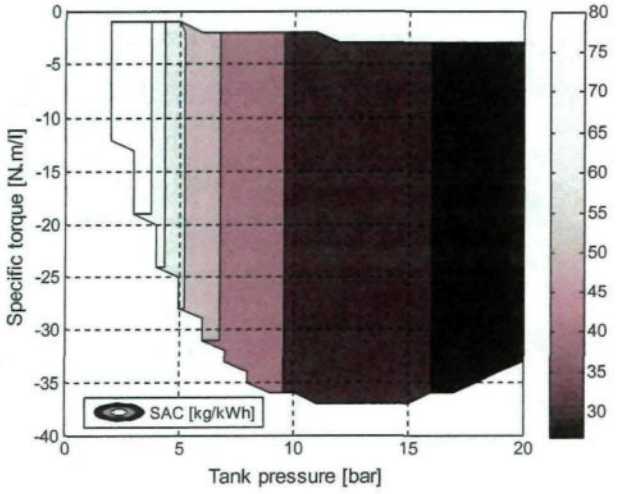

Fig. 25. Optimal specific compressed air flow-rate as a function of the tank pressure and the specific torque of a pneumatic two-stroke pump operation.

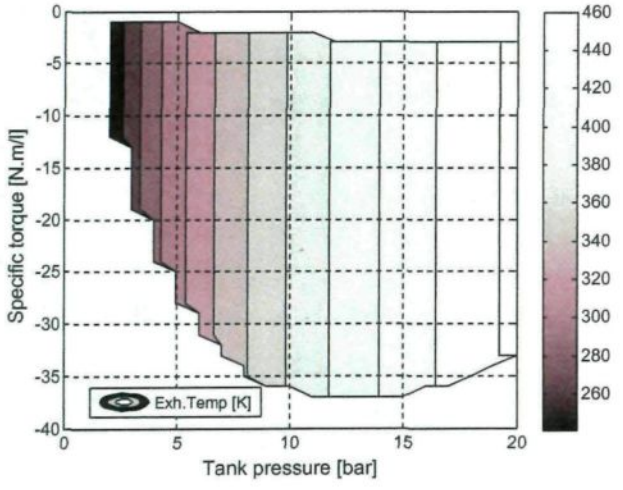

Fig. 26. Optimal exhaust air temperature as a function of the tank pressure and the specific torque of a pneumatic two-stroke pump operation.

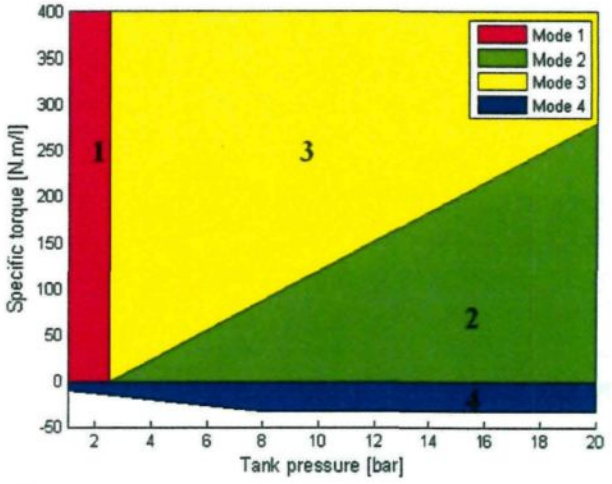

Fig. 27. Strategy used for Engine Mode selection, as a function of tank pressure and specific torque.

the maximum possible torque that can be recovered corresponds to the borders of the mode 4 zone. When the torque available is higher, the engine recovers a part of the mechanical energy and the rest is unfortunately dissipated. As one can observe, this strategy is independent from engine's size and it is therefore valid for any application.

5. Results of fuel economy obtained in Tuktoyaktuk

In this paragraph, the Hybrid-Pneumatic Combustion Concept with its mode selection strategy is evaluated during a whole year of power generation for the isolated village Tuktoyaktuk in the North of Canada. The wind speed and the consumers load data are collected for the year 2007.

5.1. Detailed results for WPPR = 1 and V_{tank} = 10,000 m^3

To start the evaluation, the tank volume and the WPPR are both fixed to respectively 10,000 m^3 and 1. a WPPR of 1 can be obtained by using three Enercon wind turbines.

Fig. 28 illustrates the wind-generated power, the consumers' load, the cumulated Diesel supplied energy and the cumulated

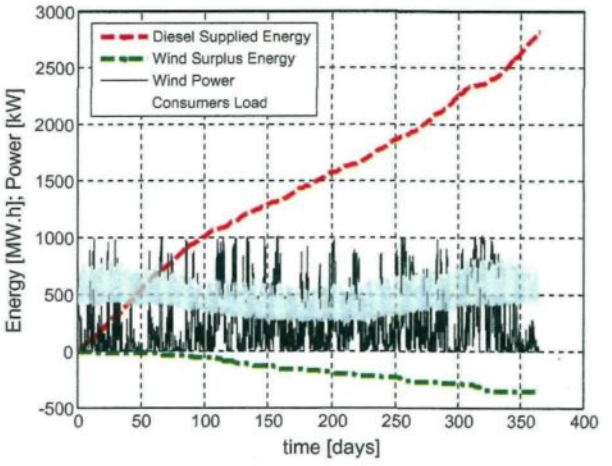

Fig. 28. Recoverable energy compared to positive energy of a WDS having a WPPR of one, at Tuktoyaktuk site during year 2007.

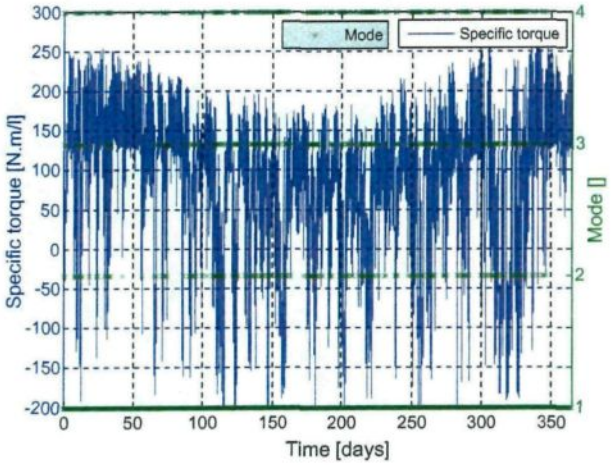

Fig. 29. Operation mode of hybrid Diesel engine over one year.

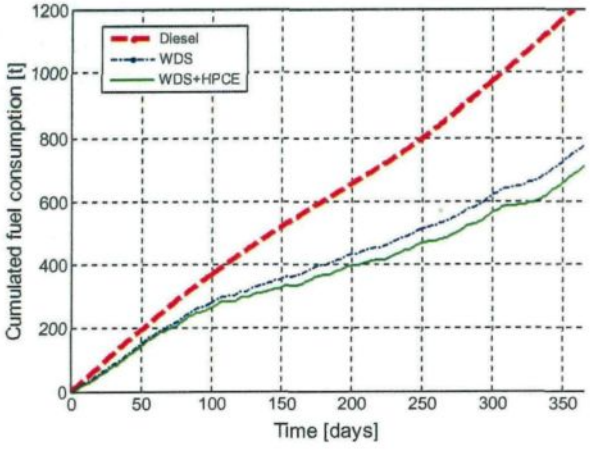

Fig. 30. One-year cumulated fuel consumption for conventional engine and pneumatic hybrid concept.

Wind surplus energy during the year 2007. Surplus wind energy represents 12% of the Diesel supplied energy.

Fig. 29, shows the Diesel specific torque that oscillates between positive values and negative values. The mode selection strategy suggested in Fig. 27 is applied to choose the operating mode as a function of instantaneous tank pressure and instantaneous specific torque. Fig. 29 illustrates as well those selected modes.

The fuel consumption during a whole year is shown in Fig. 30 in comparison with the fuel consumption obtained with a conventional Diesel working alone, and with the fuel consumption obtained with a WDS without pneumatic hybridization.

The fuel economy obtained by adding the three wind turbines to the Diesel engine is 35%. By using the pneumatic concept, another 3% is added. This might be disappointing, but considering that the recoverable energy is 12%, the recovering efficiency is therefore 25%, which is close to the one obtained with the vehicle application. In order to get higher fuel economy, we may increase the number of wind turbines and therefore wind power penetration. In that case, fuel consumption drops for two reasons: first, because Diesel engine supply demand decreases and second because the recoverable energy increases.

5.2. Synthetic results function of WPPR and V_{tank}

To complete the study, the combined effect of tank volume and WPPR on annual fuel consumption is investigated. The result is shown in Fig. 31. The variation of WPPR from 0 to 2 is obtained by increasing from 0 to 6 the number of wind turbines. The values of fuel consumption obtained for tank volume equals to zero correspond to those of the Wind Diesel System (WDS) without pneumatic hybridization.

As observed in Fig. 31, when WPPR increases, fuel consumption of WDS decreases. The improvement can reach for WPPR of 2, up to 50% comparing to a Diesel-only power generation (WPPR = 0). When WPPR increases, pneumatic hybridization permits more absolute and relative fuel economy. Finally, when tank volume increases, pneumatic hybridization permits as well more absolute and relative fuel economy. For the example, considering the case studied in the previous paragraph, where WPPR is 1, the fuel economy obtained using a 10,000 m^3 tank is only 3%, but it can reach 10% if the tank volume is 100,000 m^3.

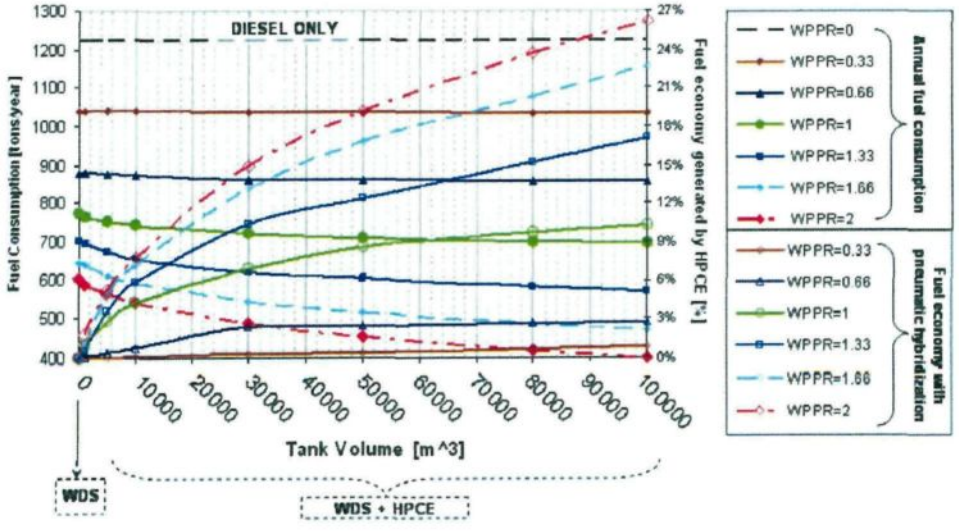

Fig. 31. Annual fuel consumption and economy generated by hybrid concept, as a function of tank volume and WPPR.

For low and medium WPPR (lower than 1), the HPCE concept has no real interest in reducing fuel consumption, whereas for high WPPR (higher than 1), fuel economy generated by HPCE concept is significant and increases with volume available for air storage. For a WPPR of 2, fuel economy generated by HPCE reaches 26% for a 100,000 m^3 tank, which represents around 200 tons per year; and for a more classical high WPPR of 1, fuel economy generated by HPCE reaches 10% for a 10^8 m^3 tank, which represents around 80 tons per year.

6. Conclusions and perspective

This article presented an optimization followed by a fuel saving evaluation of a new concept of Hybrid Pneumatic-Combustion Engine (HPCE) that can be obtained by slightly modifying a conventional Internal Combustion Engine (ICE). The evaluation of the HPCE concept was based on ideal thermodynamic cycle modeling. An optimization of the valve actuation timings for the three new modes has been conducted. This optimization led to generic maps of fuel and air consumption. Those maps are independent of the engine size therefore valid for any application. The fuel economy is calculated for the village of Tuktoyaktuk in the north of Canada, during the whole year of 2007. A parametric study of the impact of the air storage volume and the Wind Power Penetration Ratio (WPPR) on the fuel economy generated by the HPCE concept has been conducted.

For low and medium WPPR (lower than 1), the HPCE concept has no real interest in reducing fuel consumption, whereas for high WPPR (higher than 1), fuel economy generated by HPCE concept is significant and increases with volume available for air storage. For a WPPR of 2, fuel economy generated by HPCE reaches 26% for a 100,000 m^3 tank, which represents around 200 tons per year; and for a more classical high WPPR of 1, fuel economy generated by HPCE reaches 10% for a 100,000 m^3 tank, which represents around 80 tons per year.

These huge storage volumes can be obtained using large caverns made of high-quality rock deep in the ground, ancient salt mines, or underground natural gas storage caves. They actually benefit from geostatic pressure, which facilitates the containment of the air mass [17]. Some of these caverns may measure up to 1.5 km in diameter by up to almost 9 km in vertical height [39]. Depending on the depth of the cavern dome below ground surface, the caverns may hold pressure at anywhere between 70 bars to over 200 bars [39]. Electric utilities have already introduced CAES into available large caverns in the south-central USA and as well as in Germany. In an American installation in Macintosh, Alabama, ambient air is compressed and stored at a pressure between 40 and 70 bars in a 2,555,000 m^3 cavern, 700 m deep in the ground [17].

However, in the present paper, only an evaluation based on ideal cycle modeling has been conducted. Current estimation aims at bounding the hoped fuel economy. In order to be more precise, real cycle has to be studied to take in consideration several phenomena that might influence the fuel saving estimation, such as flow supersonic limitations through valves, valves response time for opening and closing, fuel injection shape, fuel burn process, heat loss through engine walls and heat loss through compressed air tank walls.

Moreover, as explained in the introduction, Diesel engine has to operate at loads higher than 30% for reliability reasons. When the demand is lower than this load, the surplus energy is usually dissipated. Using this occasional surplus energy for heating the stored air increases the benefits of the HPCE.

Last but not least, different strategies could be investigated in the future to improve the global efficiency of the system, such as deactivating some cylinders to operate the others under optimal efficiency zones or operating some cylinders in a mode while other cylinders operate in another.

Appendix A. Thermodynamic cycles modeling

A.1. Mode 1: Four-stroke Combustion ideal motor cycle

Process from 1 to 2 is isobar at intake pressureP_{int} and is characterized by:

$$P_2 = P_1 = P_{int} \tag{A.1}$$

The application of the first law of thermodynamics to this process gives:

$$m_2 \cdot u_2 - m_1 \cdot u_1 = (m_2 - m_1) \cdot h_1 - P_{int} \cdot (V_2 - V_1) \tag{A.2}$$

and:

$$m_2 \cdot cv \cdot T_2 - m_1 \cdot cv \cdot T_1 = (m_2 - m_1) \cdot cp \cdot T_1 - P_{int} \cdot (V_2 - V_1) \tag{A.3}$$

Developing this equation combined with perfect gas law results in:

$$m_2 = \frac{P_{int} \cdot V_2}{r \cdot T_{int}} - m_1 \cdot \left(\frac{T_1}{\gamma \cdot T_{int}} - 1\right) - \frac{P_{int} \cdot V_1}{cp \cdot T_{int}} \tag{A.4}$$

Therefore:

$$T_2 = \frac{P_{int} \cdot V_2}{m_2 \cdot r} \tag{A.5}$$

Process from 2 to 3 is an adiabatic compression characterized by:

$$P_3 = P_2 \cdot \left(\frac{V_2}{V_3}\right)^{\gamma} \tag{A.6}$$

Therefore,

$$T_3 = T_2 \cdot \left(\frac{V_2}{V_3}\right)^{\gamma - 1} \tag{A.7}$$

and the work generated during this process can be calculated by:

$$W_{2\to 3} = m_3 \cdot (u_3 - u_2) = m_3 \cdot cv \cdot (T_3 - T_2) \tag{A.8}$$

knowing that:

$$m_3 = m_2 \tag{A.9}$$

The process from 3 to 4 represents the premixed flame which is instantaneous isochoric combustion of a proportion αv of the total injected mass of fuel, m_f. This gives:

$$m_4 = m_3 + \alpha v \cdot m_f \tag{A.10}$$

αv is a variable depending on the operation point. For our modeling, we have considered a fixed value of αv equal to 20%. The application of the first law of thermodynamics to this process gives:

$$m_4 \cdot u_4 - m_3 \cdot u_3 = \alpha v \cdot m_f \cdot pci \tag{A.11}$$

Developing Eq. (11) gives:

$$T_4 = \frac{\alpha v \cdot m_f \cdot pci + m_3 \cdot cv \cdot T_3}{m_4 \cdot cv} \tag{A.12}$$

Moreover,

$$P_4 = \frac{m_4 \cdot r \cdot T_4}{V_4} \tag{A.13}$$

Process from 4 to 5 represents the diffusion flame witch is an isobar combustion of the remaining proportion αp of the total injected mass of fuel, m_f.

$$m_5 = m_4 + \alpha p \cdot m_f \quad (A.14)$$

The value of αp considered in this work is 80%. Process from 4 to 5 is isobaric, therefore,

$$P_5 = P_4 \quad (A.15)$$

The application of the first law of thermodynamics to this process gives:

$$m_5 \cdot u_5 - m_4 \cdot u_4 = \alpha p \cdot m_f \cdot pci - P_5 \cdot (V_5 - V_4) \quad (A.16)$$

Developing Eq. (16) gives:

$$T_5 = \frac{\alpha p \cdot m_f \cdot pci - P_5 \cdot (V_5 - V_4) + m_4 \cdot cv \cdot T_4}{m_5 \cdot cv} \quad (A.17)$$

Moreover, using the perfect gas law, we obtain:

$$V_5 = \frac{m_5 \cdot r \cdot T_5}{P_5} \quad (A.18)$$

and:

$$T_5 = \frac{\alpha_p \cdot m_f \cdot pci + P_5 \cdot V_4 + m_4 \cdot cv \cdot T_4}{m_5 \cdot cp} \quad (A.19)$$

Process from 5 to 6 is an adiabatic expansion characterized by:

$$P_6 = P_5 \cdot \left(\frac{V_5}{V_6}\right)^{\gamma} \quad (A.20)$$

and

$$T_6 = T_5 \cdot \left(\frac{V_5}{V_6}\right)^{\gamma-1} \quad (A.21)$$

Knowing that:

$$m_6 = m_5 \quad (A.22)$$

Process from 6 to 7 is an isochoric exhaust characterized by:

$$P_7 = P_{exh} \quad (A.23)$$

The application of the first law of thermodynamics to this process gives:

$$m_7 \cdot u_7 - m_6 \cdot u_6 = (m_7 - m_6) \cdot h_7 \quad (A.24)$$

The development of this equation gives:

$$T_7 = \frac{m_6 \cdot cv \cdot T + P_7 \cdot V_7}{m_6 \cdot cp} \quad (A.25)$$

Moreover, using the perfect gas law, we obtain:

$$m_7 = \frac{P_7 \cdot V_7}{r \cdot T_7} \quad (A.26)$$

Process from 7 to 8 is isobaric at intake pressure P_{exh} characterized by:

$$P_8 = P_{exh}$$

The application of the first law of thermodynamics to this process gives:

$$m_8 \cdot u_8 - m_7 \cdot u_7 = (m_8 - m_7) \cdot h_8 - P_{exh} \cdot (V_8 - V_7) \quad (A.27)$$

Therefore,

$$m_8 \cdot cv \cdot T_8 - m_7 \cdot cv \cdot T_7 = (m_8 - m_7) \cdot cp \cdot T_8 - P_{exh} \cdot (V_8 - V_7) \quad (A.28)$$

Developing this equation gives:

$$T_8 = \frac{P_{exh} \cdot V_8 + m_7 \cdot cv \cdot T - P_{exh} \cdot (V_8 - V_7)}{m_7 \cdot cp} \quad (A.29)$$

Moreover, using the perfect gas law, we obtain:

$$m_8 = \frac{P_{exh} \cdot V_8}{T_8 \cdot r} \quad (A.30)$$

Finally, process from 8 to 1 is isochoric filling characterized by:

$$P_1 = P_{int} \quad (A.31)$$

The application of the first law of thermodynamics to this process gives:

$$m_1 \cdot u_1 - m_8 \cdot u_8 = (m_1 - m_8) \cdot h_{int} \quad (A.32)$$

Therefore,

$$m_1 \cdot cv \cdot T_1 - m_8 \cdot cv \cdot T_8 = (m_1 - m_8) \cdot cp \cdot T_{int} \quad (A.33)$$

The development of this equation combined to the perfect gas law gives:

$$T_1 = \frac{P_1}{(P_1 - P_8)/(\gamma \cdot T_{int}) + P_8/T_8} \quad (A.34)$$

Moreover,

$$m_1 = m_8 + \frac{vm}{r} \cdot \left(\frac{P_1}{T_1} - \frac{P_8}{T_8}\right) \quad (A.35)$$

A.2. Mode 2: Two-stroke pneumatic ideal motor cycle

Process from 1 to 2 is isobaric intake at tank pressure, P_{tank}. This gives:

$$P_2 = P_1 = P_{tank} \quad (A.36)$$

The application of the first law of thermodynamics to this process gives:

$$m_2 \cdot u_2 - m_1 \cdot u_1 = (m_2 - m_1) \cdot h_1 - P_{tank} \cdot (V_2 - V_1) \quad (A.37)$$

Therefore,

$$m_2 \cdot cv \cdot T_2 - m_1 \cdot cv \cdot T_1 = (m_2 - m_1) \cdot cp \cdot T_1 - P_{tank} \cdot (V_2 - V_1) \quad (A.38)$$

Developing this equation gives:

$$m_2 = \frac{P_{tank} \cdot V_2}{r \cdot T_{tank}} - m_1 \cdot \left(\frac{T_1}{\gamma \cdot T_{tank}} - 1\right) - \frac{P_{tank} \cdot V_1}{cp \cdot T_{tank}} \quad (A.39)$$

Moreover, using the perfect gas law, we obtain:

$$T_2 = \frac{P_{tank} \cdot V_2}{m_2 \cdot r} \quad (A.40)$$

Process from 2 to 3 is adiabatic expansion. This gives:

$$P_3 = P_2 \cdot \left(\frac{V_2}{V_3}\right)^{\gamma} \quad (A.41)$$

Moreover,

$$T_3 = T_2 \cdot \left(\frac{V_2}{V_3}\right)^{\gamma-1} \quad (A.42)$$

The work generated during this process can be calculated by:

$$W_{2\to3} = m_3 \cdot (u_3 - u_2) = m_3 \cdot cv \cdot (T_3 - T_2) \quad (A.43)$$

Knowing that:

$$m_3 = m_2 \quad (A.44)$$

Process from 3 to 4 is an isochoric exhaust. This gives:

$$P_4 = P_{exh} \quad (A.45)$$

The application of the first law of thermodynamics to this process gives:

$$m_4 \cdot u_4 - m_3 \cdot u_3 = (m_4 - m_3) \cdot h_4 \quad (A.46)$$

The development of this equation gives:

$$T_4 = \frac{m_3 \cdot cv \cdot T_3 + P_4 \cdot V_4}{m_3 \cdot cp} \quad (A.47)$$

Moreover, using the perfect gas law, we obtain:

$$m_4 = \frac{P_4 \cdot V_4}{r \cdot T_4} \quad (A.48)$$

Process from 4 to 5 is isobaric at intake pressure P_{exh}. This gives:

$$P_5 = P_{exh} \quad (A.49)$$

The application of the first law of thermodynamics to this process gives:

$$m_5 \cdot u_5 - m_4 \cdot u_4 = (m_5 - m_4) \cdot h_5 - P_{exh} \cdot (V_5 - V_4) \quad (A.50)$$

Therefore,

$$m_5 \cdot cv \cdot T_5 - m_4 \cdot cv \cdot T_4 = (m_5 - m_4) \cdot cp \cdot T_5 - P_{exh} \cdot (V_5 - V_4) \quad (A.51)$$

The development of this equation gives:

$$T_5 = \frac{P_{exh} \cdot V_5 + m_4 \cdot cv \cdot T_4 - P_{exh} \cdot (V_5 - V_4)}{m_4 \cdot cp} \quad (A.52)$$

Moreover, using the perfect gas law, we obtain:

$$m_5 = \frac{P_{exh} \cdot V_5}{T_5 \cdot r} \quad (A.53)$$

Process from 5 to 6 is adiabatic compression. This gives:

$$P_6 = P_5 \cdot \left(\frac{V_5}{V_6}\right)^{\gamma} \quad (A.54)$$

Moreover,

$$T_6 = T_5 \cdot \left(\frac{V_5}{V_6}\right)^{\gamma - 1} \quad (A.55)$$

Knowing that:

$$m_6 = m_5 \quad (A.56)$$

Process from 6 to 1 is isochoric filling. This gives:

$$P_1 = P_{tank} \quad (A.57)$$

The application of the first law of thermodynamics to this process gives:

$$m_1 \cdot u_1 - m_6 \cdot u_6 = (m_1 - m_6) \cdot h_{tank} \quad (A.58)$$

Therefore,

$$m_1 \cdot cv \cdot T_1 - m_6 \cdot cv \cdot T_6 = (m_1 - m_6) \cdot cp \cdot T_{tank} \quad (A.59)$$

.The development of this equation gives:

$$T_1 = \frac{P_1}{(P_1 - P_6)/(\gamma \cdot T_{tank}) + P_6/T_6} \quad (A.60)$$

Moreover, using the perfect gas law, we obtain:

$$m_1 = m_6 + \frac{vm}{r} \cdot \left(\frac{P_1}{T_1} - \frac{P_6}{T_6}\right) \quad (A.61)$$

A.3. Mode 3: Four-stroke pneumatic-combustion ideal motor cycle

This cycle is simply a combination of the two preceding cycles. Indeed, it is a conventional combustion mode where the scavenging cycle is replaced by two-stroke pneumatic motor cycle. The equations describing this mode are therefore the same as developed before.

A.4. Mode 4: Two-stroke pneumatic ideal pump cycle

Process from 1 to 2 is adiabatic compression. This gives:

$$P_2 = P_1 \cdot \left(\frac{V_1}{V_2}\right)^{\gamma} \quad (A.62)$$

Moreover,

$$T_2 = T_1 \cdot \left(\frac{V_1}{V_2}\right)^{\gamma - 1} \quad (A.63)$$

Knowing that:

$$m_2 = m_1$$

Process from 2 to 3 is isobaric exhaust at tank pressure P_{tank} characterized by:

$$P_3 = P_2 = P_{tank} \quad (A.64)$$

The application of the first law of thermodynamics to this process gives:

$$m_3 \cdot u_3 - m_2 \cdot u_2 = (m_3 - m_2) \cdot h_3 - P_{tank} \cdot (V_3 - V_2) \quad (A.65)$$

Therefore,

$$m_3 \cdot cv \cdot T_3 - m_2 \cdot cv \cdot T_2 = (m_3 - m_2) \cdot cp \cdot T_3 - P_{tank} \cdot (V_3 - V_2) \quad (A.66)$$

The development of this equation gives:

$$m_3 = \frac{P_{tank} \cdot V_3}{r \cdot T_{tank}} - m_1 \cdot \left(\frac{T_2}{\gamma \cdot T_{tank}} - 1\right) - \frac{P_{tank} \cdot V_2}{cp \cdot T_{tank}} \quad (A.67)$$

Moreover, using the perfect gas law, we obtain:

$$T_3 = \frac{P_{tank} \cdot V_3}{m_3 \cdot r} \quad (A.68)$$

Process from 3 to 4 is adiabatic expansion characterized by:

$$P_4 = P_3 \cdot \left(\frac{V_3}{V_4}\right)^{\gamma} \quad (A.69)$$

where the point 4 is set to get $P_4 = P_{int}$. Therefore, the real unknown is V_4 and it is calculated by the equation:

$$V_4 = V_3 \cdot \left(\frac{P_3}{P_4}\right)^{\frac{1}{\gamma}} \quad (A.70)$$

T_4 is calculated using the perfect gas law as follows:

$$T_4 = \frac{P_{int} \cdot V_4}{m_4 \cdot r} \quad (A.71)$$

Process from 4 to 5 is isobaric filling at intake pressure P_{int} characterized by:

$$P_5 = P_4 = P_{int} \quad (A.72)$$

The application of the first law of thermodynamics to this process gives:

$$m_5 \cdot u_5 - m_4 \cdot u_4 = (m_5 - m_4) \cdot h_4 - P_{int} \cdot (V_5 - V_4) \quad (A.73)$$

Therefore,

$$m_5 \cdot cv \cdot T_5 - m_4 \cdot cv \cdot T_4 = (m_5 - m_4) \cdot cp \cdot T_4 - P_{int} \cdot (V_5 - V_4) \quad (A.74)$$

The development of this equation gives:

$$m_5 = \frac{P_{int} \cdot V_5}{r \cdot T_{int}} - m_4 \cdot \left(\frac{T_4}{\gamma \cdot T_{int}} - 1\right) - \frac{P_{int} \cdot V_4}{cp \cdot T_{int}} \quad (A.75)$$

Moreover, using the perfect gas law, we obtain:

$$T_5 = \frac{P_{int} \cdot V_5}{m_2 \cdot r} \quad (A.76)$$

References

[1] Liu W, Gu S, Qiu D. Techno-economic assessment for off-grid hybrid generation systems and the application prospects in China. <http://www.worldenergy.org/wecgeis/publications/>.
[2] Weis TM, Ilinca A. The utility of energy storage to improve the economics of wind–diesel power plants in Canada. Renew Energy 2008;33(7):1544–57.
[3] La stratégie énergétique du Québec 2006-2015. L'énergie pour construire le Québec de demain. <http://www.mrnf.gouv.qc.ca/energie/eolien>.
[4] Hunter R, Elliot G. Wind–diesel systems-a guide to the technology and its implementation. Cambridge (UK): Cambridge University Press; 1994.
[5] Forcione A. Système jumelé éolien-Diesel aux Îles-de-la-Madeleine (Cap-aux-Meules)-Établissement de la VAN optimale. Institut de Recherche, Hydro-Québec, Février; 2004.
[6] Ibrahim H, Ilinca A, Perron J. Solutions actuelles pour une meilleure gestion et intégration de la ressource éolienne. CSME/SCGM Forum 2008 at Ottawa. The Canadian Society for Mechanical Engineering, 5–8 June 2008.
[7] ACÉÉ. Association canadienne de l'énergie éolienne. <http://www.canwea.com>.
[8] Maisson JF. Wind power development in sub-arctic conditions with severe rime icing. In: Presented at the circumpolar climate change summit and exposition, Whitehorse, Yukon; 2001.
[9] www.nunavutpower.com.
[10] Reeves B. Kotzebue electric association wind projects. In: Proceedings of NREL/AWEA 2002 wind–diesel workshop, Anchorage, Alaska, USA, 2002.
[11] Singh V. Blending wind and solar into the Diesel generator market. Renewable Energy Policy Project (REPP) research report, Winter 2001, No. 12, Washington, DC.
[12] Reid R. Application de l'éolien en réseaux non reliés. Liaison Énergie-Francophonie, N°35/2e Trimestre; 1997.
[13] Jean Y, Nouaili A, Viarouge P, Saulnier B, Reid R. Développement d'un système JEDHPSS représentatif d'un village typique des réseaux non relies. Rapport IREQ-94-169-C; 1994.
[14] Gagnon R, Nouaili A, Jean Y, Viarouge P. Mise à jour des outils de modélisation et de simulation du Jumelage Éolien-Diesel à Haute Pénétration Sans Stockage et rédaction du devis de fabrication de la charge de lissage. Rapport IREQ-97-124-C; 1997.
[15] www.danvest.com.
[16] Ilinca A, Chaumel JL. Implantation d'une centrale éolienne comme source d'énergie d'appoint pour des stations de télécommunications. Colloque international sur l'énergie éolienne et les sites isolées, Îles de la Madeleine; 2005.
[17] Ibrahim H, Ilinca A, Perron J. Energy storage systems – characteristics and comparisons. Renew Sustain Energy Rev 2008;12:1221–50.
[18] Ibrahim H, Ilinca A, Perron J. Comparison and analysis of different energy storage techniques based on their performance index. In: IEEE Canada, electrical power conference 2007, "Renewable and alternative energy resources", EPC 2007, Montreal, Canada, October 25–26, 2007.
[19] Ibrahim H, Younes R, Basbous T, Ilinca A, Dimitrova M. Optimization of Diesel engine performances for a hybrid wind–diesel system with compressed air energy storage. Energy 2011;36:3079–91.
[20] Ibrahim H, Ilinca A, Younes R, Basbous T. Study of a hybrid wind–diesel system with compressed air energy storage. IEEE Canada, electrical power conference 2007, "Renewable and Alternative Energy Resources", EPC 2007, Montreal, Canada, October 25–26, 2007.
[21] Ibrahim H. Etude et conception d'un générateur hybride d'électricité de type Eolien-Diesel avec élément de stockage d'air comprimé, PhD thesis. Université du Québec à Chicoutimi.; 2010.
[22] Basbous T, Younes R, Ilinca A, Perron J. Fuel consumption evaluation of an optimized new hybrid pneumatic-combustion vehicle engine on several driving cycles. Int J Engine Res. http://dx.doi.org/10.1177/1468087411433250.
[23] Donitz C, Vasile I, Onder C, Guzzella L. Realizing a concept for high efficiency and excellent driveability: the downsized and supercharged hybrid pneumatic engine. SAE 2009-01-1326; 2009.
[24] Dönitz C, Vasile IC, Onder CH, Guzzella H. Modelling and optimizing two- and four-stroke hybrid pneumatic engines. IMechE Part D – J Automob Eng 2009;223(2):255–80. xii, 27, 28, 30.
[25] Higelin P, Charlet A, Chamaillard Y. Thermodynamic simulation of a hybrid pneumatic-combustion engine concept. Int J Appl Thermodynam 2002; 5(1):1–11.
[26] Higelin P, Vasile I, Charlet A, Chamaillard Y. Parametric optimization of a new hybrid pneumatic ± combustion engine concept. Int J Engine Res 2004; 5(2):205.
[27] Schechter M. Regenerative compression braking–a low cost alternative to electric hybrids. SAE 2000-01-1025.
[28] Schechter M. New cycles for automobile engines. SAE 1999-01-0623; 1999.
[29] Tai C, Tsao T, Levin M, Barta G, Schechter M. Using Camless Valvetrain for air hybrid optimization. SAE 2003-01-0038.
[30] Hyungsuk KH, Tai C, Smith E, Wang X, Tsao T, Stewart J, et al. Demonstration of air-power-assist (APA) engine technology for clean combustion and direct energy recovery in heavy duty application. SAE 2008-01-1197; 2008.
[31] Trajkovic S, Tunestal P, Johansson B. Introductory study of variable valve actuation for pneumanic hybridization. SAE 2007-01-0288; 2007.
[32] Trajkovic S, Tunestal P, Johansson B. Investigation of different valve geometries and valve timing strategies and their effect on regenerative efficiency for a pneumatic hybrid with variable valve actuation. SAE 2008-01-1715; 2008.
[33] Trajkovic S, Tunestal P, Johansson B. Simulation of a pneumatic hybrid powertrain with VVT in GT-power and comparison with experimental data. SAE 2009-01-1323; 2009.
[34] Lee CY, Zhao H, Ma T. Pneumatic regenerative engine braking technology for buses and commercial vehicles. SAE 2011-01-2176.
[35] Heywood JB. Internal combustion engine fundamentals. New York: McGraw Hill; 1988.
[36] Stone R. Introduction to internal combustion engines. Department of Engineering Science, University of Oxford; 1999.
[37] Manwell JF, McGowan JG, Rogers AL. Wind energy explained–theory, design and application. John Wiley & Sons Ltd.; 2002. ISBNs: 0-471-49972-2.
[38] Gheorghiu V. CO_2-emission reduction by means of enhanced thermal conversion efficiency of ICE cycles. SAE 2009-24-0081; 2009.
[39] http://www.maritime-executive.com.
[40] Basbous T, Younes R, Ilinca A, et al. A new hybrid pneumatic combustion engine to improve fuel consumption of Wind-Diesel power system for non-interconnected areas. Appl Energy 2012;96:459–76.

CHAPITRE IV

Article 3

Fuel consumption evaluation of an optimized new hybrid pneumatic–combustion vehicle engine on several driving cycles

Publié dans International Journal of Engine Research, juin 2012, vol. 13
DOI: 10.1177/1468087411433250

Résumé

Cet article démontre la possibilité d'appliquer le concept Moteur Hybride Pneumatique-Diesel (MHPD) à l'automobile. L'énergie est stockée sous forme d'air comprimé pendant les phases de décélérations du véhicule et restituée pendant les phases d'accélération ou de maintien de vitesse. Lé travail présenté dans cet article démontre que l'économie de carburant réalisée sur un véhicule de 1500 kg, pour un volume de stockage d'air de 100 litres, est de 17% sur le cycle d'homologation Européen NEDC, 60% sur le cycle standard international ARTEMIS type urbain, et de 23% sur le cycle ARTEMIS type extra-urbain.

International Journal of ENGINE RESEARCH

Original Article

International J of Engine Research
0(0) 1–21

DOI: 10.1177/1468087411433250
jer.sagepub.com
SAGE

Fuel consumption evaluation of an optimized new hybrid pneumatic–combustion vehicle engine on several driving cycles

Tammam Basbous[1,2], Rafic Younes[2,3], Adrian Ilinca[2] and Jean Perron[1]

Abstract

In this paper, we describe an optimization followed by a fuel-saving evaluation of a new concept of a hybrid pneumatic–combustion engine that can be obtained by modifying a conventional internal combustion engine without developing a new cylinder head. Until now, most studies on the pneumatic hybridization of internal combustion engines have dealt with a two-stroke pure pneumatic mode. The few concept studies that have dealt with a hybrid pneumatic–combustion four-stroke mode required a supplementary valve to be added to charge compressed air in the combustion chamber. This heavy modification cannot be carried out by simply adjusting an existing internal combustion engine because a new cylinder head should be developed. It is therefore not logical to suggest this concept as an option in vehicle powertrains to reduce fuel consumption. Moreover, those studies focus on spark-ignition engines; there are reasons to think that their concepts might not work adequately for diesel engines. Our concept is capable of making a diesel engine operate under two-stroke pneumatic motor modes, two-stroke pneumatic pump modes and four-stroke hybrid modes, without requiring an additional valve in the combustion chamber. This fact constitutes our study's strength and innovation. The evaluation of our concept is based on ideal thermodynamic cycle modeling. The optimized valve actuation timings for all modes lead to generic maps that are independent of the engine size. The fuel economy is calculated based on the new European driving cycle and on the assessment and reliability of transport emission models and inventory system urban and rural cycles.

Keywords

Valve actuation, parametric optimization, pneumatic hybridization, hybrid vehicle, diesel engine, compressed air energy storage

Date received: 06 September 2011; accepted: 18 November 2011

Introduction

The problem

Energy recovery constitutes one of the key solutions to improve the energetic performance of internal combustion engines (ICEs) on vehicles, as excess of mechanical energy frequently occurs during driving cycles. Conventional engines consume fuel to generate power during acceleration and steady-state modes, whereas in the deceleration mode, energy is usually dissipated in brakes.[1–3] Through a dynamic model that will be shown in the section on vehicle model and engine specific torque calculation, we have calculated the ratio of the deceleration energy to the acceleration energy for a 1500 kg vehicle and found, for different driving cycles,

(a) the new European driving cycle (NEDC): 31%, as illustrated in Figure 1;
(b) the assessment and reliability of transport emission models and inventory system (ARTEMIS) urban cycle: 70%, as illustrated in Figure 2;
(c) the ARTEMIS rural cycle: 35%, as illustrated in Figure 3.

This means that the fuel consumption may decrease proportionally with the energy recovered, stored and

[1]Laboratoire International des Matériaux Antigivre, Université du Québec à Chicoutimi, Canada
[2]Laboratoire de Recherche en Energie Eolienne, Université du Québec à Rimouski, Canada
[3]Faculté de Génie, Université Libanaise, Liban

Corresponding author:
Tammam Basbous, Laboratoire International des Matériaux Antigivre, Université du Québec à Chicoutimi, Chicoutimi, Québec, Canada.
Email: tammam.basbous@uqac.ca

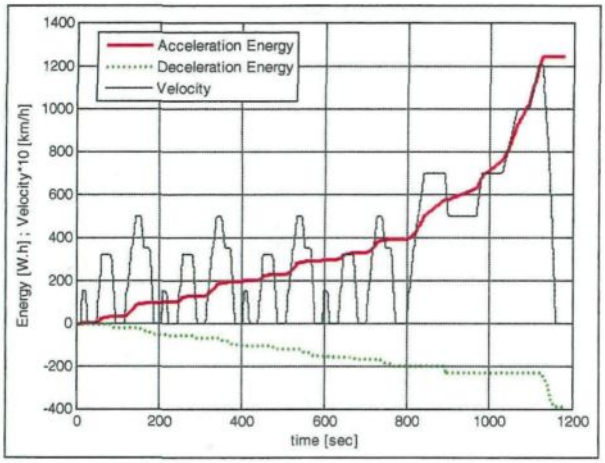

Figure 1. Deceleration energy compared to acceleration energy on the NEDC.

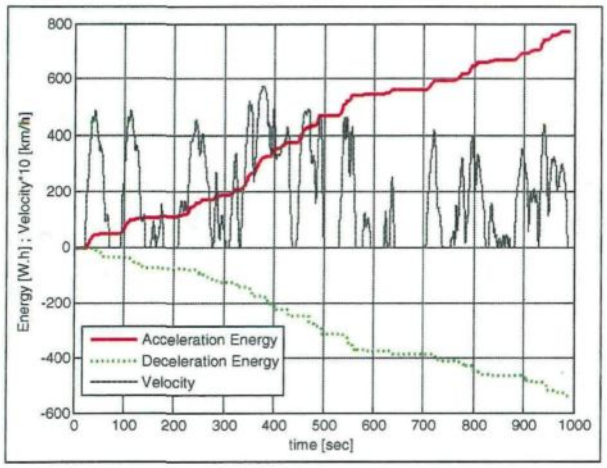

Figure 2. Deceleration energy compared to acceleration energy on the ARTEMIS urban cycle.

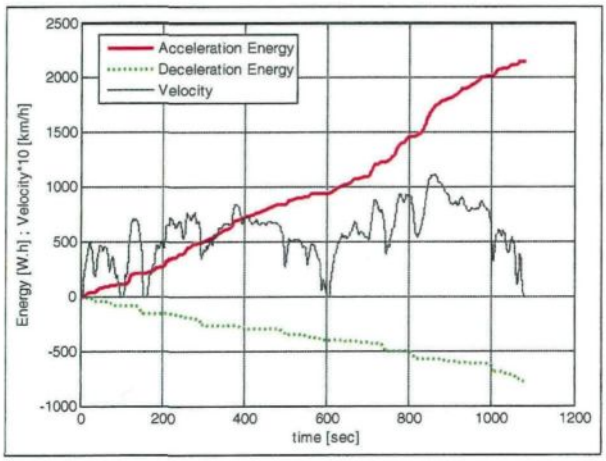

Figure 3. Deceleration energy compared to acceleration energy on the ARTEMIS rural cycle.

later used when needed. In order to ensure energy recovery, additional electric motors and battery energy storage are usually combined with the ICE. This solution has numerous drawbacks, both for automotive applications and power generation. Weight is the major weakness of this solution for automotive applications. The mass of the added components offsets a significant part of fuel reduction.[1] Another major issue to be considered is added cost. Reliable battery packs and electric motors are expensive. This means that the return on investment would be very low.[4–6] For this reason, hybrid vehicles are less popular without fiscal reductions or ecologic bonuses offered by governments for those who decide to drive a hybrid.

In the present work, we suggest a modification to the powertrain to store and recover energy. In order to make the solution economically interesting, the modifications from original technical specifications should be kept to a minimum in order to limit the investment.

Pneumatic hybridization of the ICE

One solution to the problem of energy recovery exposed in the section above is to use the ICE as a hybrid engine combining a conventional combustion motor operation and a pneumatic motor and pump operation and to connect it to an air storage tank. Therefore, the engine can be used as a pneumatic pump when energy is in excess and store this energy as compressed air in the tank. The stored energy can be discharged later through a pneumatic operation of the engine or through a hybrid pneumatic–combustion operation. Pneumatic hybridization of ICEs is an alternative to electric hybridization that requires the use of expensive, sensitive and heavy batteries.

State-of-art of pneumatic hybridization of the ICE

Recently, different concepts of pneumatic hybridization have been studied.[7–10] Dönitz et al.[1] created a fully operational hybrid pneumatic engine that was able to operate under the following modes:

(a) two-stroke pneumatic motor mode (non-fired);
(b) four-stroke pneumatic motor mode (non-fired);
(c) two-stroke pneumatic pump mode (non-fired);
(d) four-stroke pneumatic pump mode (non-fired);
(e) supercharged mode (fired);
(f) conventional mode (fired).

This concept was accomplished by connecting an air pressure tank to all cylinders via an electronic fully controlled charge valve.[4] The original intake and exhaust valves should also be electronically controlled. Test results on a spark-ignition engine demonstrator, supported by modeling analysis,[4] showed the viability of this new concept for fuel consumption reduction,

when combined with strong downsizing and supercharging of the engine. Compared to a naturally aspirated engine with the same rated power, the downsized and supercharged hybrid pneumatic engine can save 32% of the fuel.[1] The strong downsizing is possible owing to pneumatic hybridization because the problem of the 'turbo-lag', usually associated with heavily downsized and supercharged engines, is completely overcome by injecting additional air from a pressure tank and more fuel during transients.[1] Experiments have verified the engine's instantaneous torque response resulting from applying this supercharged mode.[1]

Earlier, Higelin et al.[5,6] studied a similar concept and concluded, using simulations of theoretical thermodynamic cycles, that fuel consumption on the NEDC could be reduced by up to 31% if all the parameters, including the tank volume, were optimized.[6] This concept is promising in terms of energetic performance, cost and weight; however, it requires heavy modifications of the engine's hard architecture because a charge valve has to be added. This cannot be done by simply adjusting an existing ICE. It is therefore not possible to suggest this concept as an option in vehicle powertrains for reducing fuel consumption. Moreover, this concept is validated for spark-ignition engines, and there are reasons to think that it might not work adequately with diesel engines, mainly for hybrid pneumatic–combustion operations. Compressed air is charged in the cylinder during the compression phase. Then, the fuel is injected and needs to start burning a few degrees before the piston reaches top dead center (TDC). Considering that, in diesel engines, the ignition delay has to elapse before the fuel starts burning, it is quite difficult to ensure that enough fuel is burnt before TDC, which will probably compromise the system efficiency. This might be the reason why all the tests conducted on this system were made on spark-ignition engines. In addition, other researchers worked on simpler concepts of pneumatic hybridization, but all of them focused on two-stroke pure pneumatic motor and pump operations.

Hyungsuk et al.[11] suggested a concept based on connecting the compressed air tank to the exhaust manifold and using a three-way valve to switch flow between the turbine and air tank. It does not require a specific valve to inject the compressed air. However, it requires a complete change in valve timing for both the air compressor and the air motor two-stroke modes. This is accomplished through a cam-less hydraulically actuated valve system.

The air-power-assist (APA) engine was tested at steady state in compressor mode and in motor mode. The tests confirmed the functionality of the concept. The APA engine demonstrated air compression and high-pressure air storage in the air tank by controlling the valve timing and using the air handling system. The APA engine generated positive power by using the compressed air from the air tank without injecting fuel.[11] The APA engine can be obtained by applying a simple modification to an existing engine. Its performance, however, is limited to pneumatic operation. Hybrid operation, which combines pneumatic power and fuel power, is not possible.

Trajkovic et al.[2,3,12] converted a single-cylinder Scania D12 diesel engine to a pneumatic hybrid diesel one. The concept requires having a variable valve actuation system, and it can operate under a conventional diesel mode as well as two-stroke pneumatic motor and pneumatic pump modes. Trajkovic et al. conducted an optimization on valve actuation timing and obtained up to 48% regenerative efficiency under steady-state operation. Later, Trajkovic et al. compared test results to GT-Power simulation results. The correlation was carried out for both pneumatic modes, and it showed a 5% error in steady-state operations.[12] We notice that this study was conducted using not more than 8 bar of tank pressure.

Finally, Lee et al.[13] have worked on a novel cost-effective air hybrid powertrain concept for buses and commercial vehicles. The concept is simple because it requires only a few modifications to the intake of the engine by adding two one-way valves and an air tank. The concept does not require any change to the initial intake and exhaust valves of the engine. However, the concept can only operate under conventional mode, compressor mode and cranking mode. The last mode is a four-stroke pneumatic motor mode. The storage pressure is of the order of 8 bar. The simplicity and the cost effectiveness constitute the main strength of the concept, but not the hoped for fuel economy.

Objective of our study

Through our study, we aim to propose a new concept of pneumatic hybridization of ICEs that satisfies all three conditions below:[7,10]

(a) to require a simple modification of ICEs including diesel engines;
(b) the ability to operate under pneumatic motor and pump modes, hybrid pneumatic–combustion motor modes, in addition to conventional modes;
(c) to be efficient and require a reasonable air tank volume.

Suggested concept

The concept that we suggest is based on bypassing the turbocharger and connecting the air tank to the intake valve using two three-way valves, as shown in Figure 4.

The first three-way valve connects the ICE's inlet to either the air tank or the compressor's outlet, while the second three-way valve connects the ICE's exhaust to either the turbine's inlet or to the atmosphere. The concept also requires full control of the intake valves, the exhaust valves and the fuel injectors. It is assumed that the volume of the compressed air energy storage (CAES) tank is much higher than the displacement of

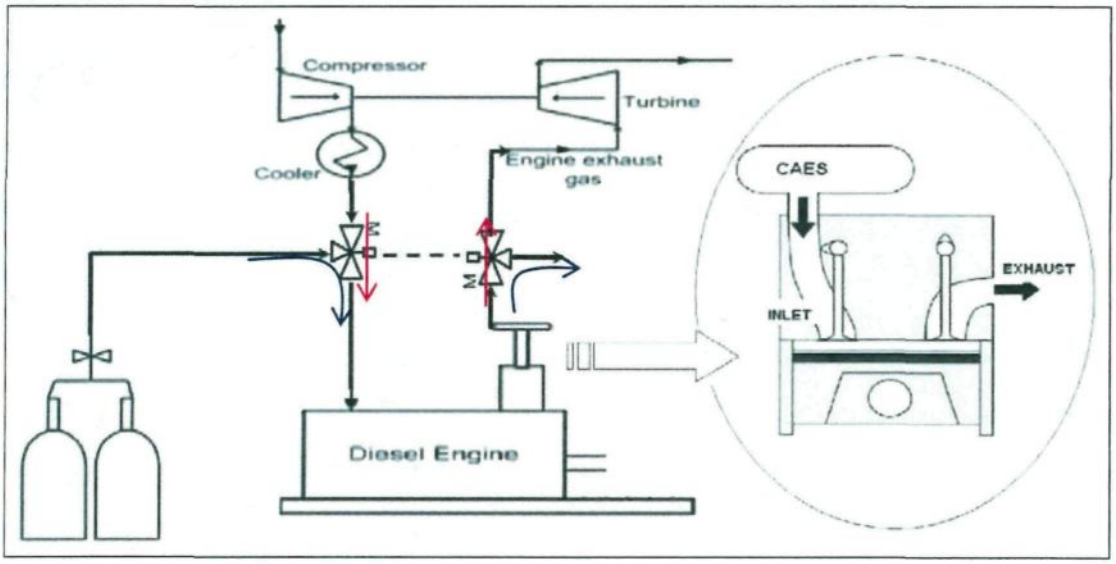

Figure 4. Suggested pneumatic concept.

the engine. The concept may operate under the four modes illustrated in Figure 5.

Mode 1: four-stroke conventional combustion motor mode. The three-way valves connect the turbocharger to the inlet and the exhaust of the engine. The cycle lasts for two rounds of the piston. The intake valve is open during the whole piston's way down (1→2) of the fist stroke. When the piston gets to bottom dead center (BDC), the compression phase (2→3) starts. A few degrees before TDC, the fuel starts to be injected (FIS). The combustion phase (3→5) starts a few degrees later, and finishes a few degrees after TDC. After combustion, the expansion phase (5→6) occurs during the piston's way down until it reaches BDC. At BDC, the exhaust valve opens and exhaust phase (6→8) occurs during the piston's way up. At TDC, the exhaust valve closes. The intake and exhaust pressure are set by the turbocharger. Figure 6 illustrates the ideal thermodynamic cycle of this operating mode.

Mode 2: two-stroke pneumatic motor mode. The three-way valves disconnect the turbocharger and connect the intake of the engine to the air tank and the exhaust

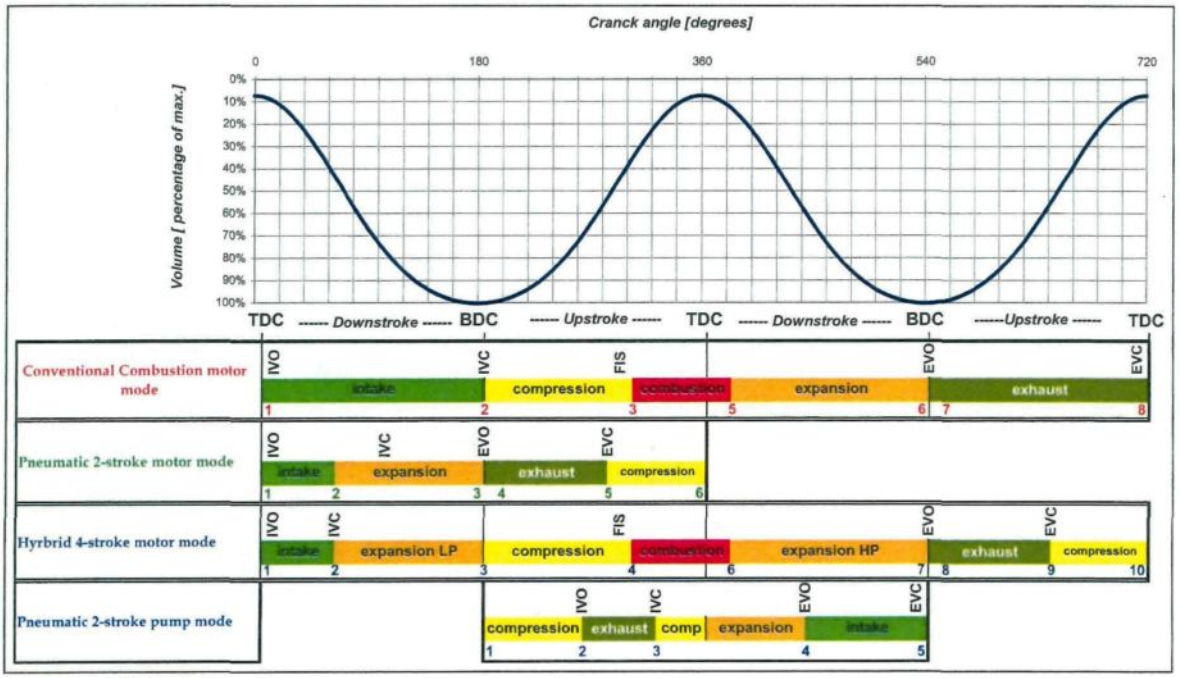

Figure 5. Operating principles of suggested pneumatic concept.

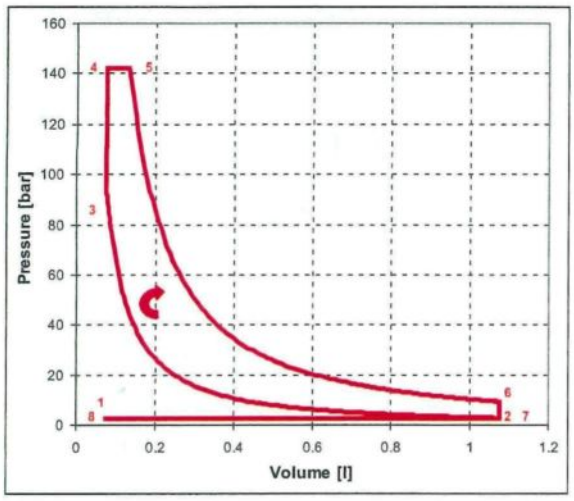

Figure 6. Illustration of the ideal four-stroke conventional combustion cycle.

to the atmosphere. The intake pressure is equal to the air storage pressure, while the exhaust pressure is equal to the atmospheric pressure. The fuel injection is disabled. The cycle lasts only one piston round. At TDC, the intake valve opens and closes shortly after, therefore enabling the admission phase (1→2). Then, an expansion phase (2→3) starts and lasts until the piston reaches BDC. Then, the exhaust valve opens and enables the exhaust phase (3→5) during the piston's way up. Somewhere between BDC and TDC, the exhaust valve closes and a compression phase starts (5→6) until the piston reaches TDC. Figure 7 illustrates the ideal thermodynamic cycle relative to this operating mode. The interest in early exhaust valve closing (EVC), i.e. closing the exhaust valve before the piston gets to TDC, will be demonstrated later in this article.

Mode 3: four-stroke hybrid pneumatic–combustion motor mode. The three-way valves disconnect the turbocharger and connect the intake of the engine to the air tank. The intake pressure is equal to the air storage pressure. The intake valve is open during part of the piston's way down on the first stroke, enabling the intake phase (1→2). Somewhere between TDC and BDC, the intake valve closes, and an expansion phase (2→3) starts. When the piston gets to BDC, the operation continues exactly as the conventional mode. Figure 8 illustrates the ideal thermodynamic cycle relative to this operating mode. This mode operates normally, even with diesel engines, because fuel injection can start anytime during the piston compression between points 3 and 4, in order to ensure that the fuel burn starts when needed for obtaining the best cycle efficiency.

Mode 4: two-stroke pneumatic pump mode. This mode is the reverse of the two-stroke pneumatic motor mode. The three-way valve is in the same position, and the engine runs in the same way. However, by changing the intake and exhaust valve timings, low-pressure air is admitted through the exhaust valve, and high-pressure air is rejected through the intake valve. Compressed air can therefore be stored in the tank. In this mode, fuel injection is disabled. The compression phase (1→2) starts at BDC and lasts until the intake valve opens, somewhere between BDC and TDC, enabling the exhaust phase (2→3). The intake valve closes a few degrees after it opens. The intake valve close (IVC) angle will have to be dynamically adjusted for maximum braking energy recovery. If the available torque is high enough, IVC occurs at TDC in order to compress the maximum possible air quantity. If the available torque is relatively low, IVC occurs before TDC, therefore reducing the compressed air quantity as well as the work needed for the compression. After IVC, an expansion phase (3→4) occurs during the piston's way down

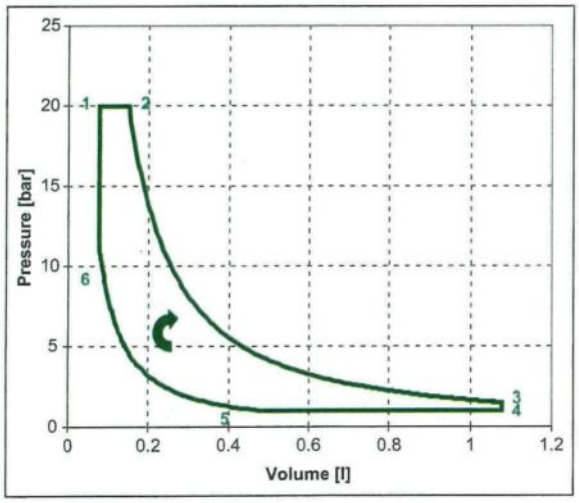

Figure 7. Illustration of the ideal two-stroke pneumatic motor cycle.

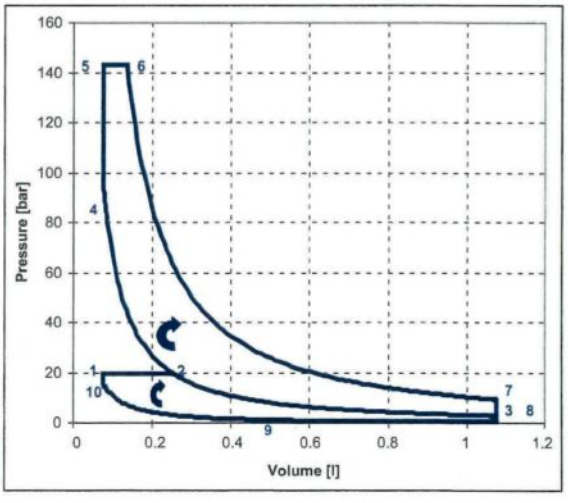

Figure 8. Illustration of the ideal four-stroke hybrid pneumatic–combustion motor cycle.

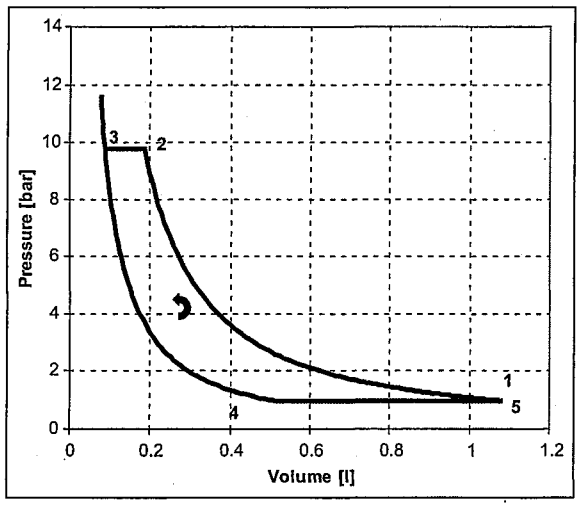

Figure 9. Illustration of the ideal pneumatic two-stroke pump cycle.

in the first case (IVC at TDC), and a compression phase followed by an expansion phase occur during the piston's way up, then down in the second case (IVC before TDC). Somewhere between TDC and BDC, the cylinder air pressure becomes exactly equal to atmospheric pressure. At that moment, the exhaust valve opens and enables the intake phase (4→5). Fresh air fills therefore the cylinder until the piston gets to BDC when the exhaust valve closes. Figure 9 illustrates the ideal thermodynamic cycle relative to this operating mode.

Mathematical modeling

We apply the equations available in the literature[14–16] to characterize the thermodynamic cycles of the different operating modes.

Ideal thermodynamic cycles

The analytical equations that allow the calculation of the pressure, temperature and mass at every point of the ideal thermodynamic cycles are developed in detail in Appendices 2–4.

Mode 1: four-stroke combustion ideal motor cycle. The work generated during the cycle is calculated using

$$W = \sum_{i=1}^{i=8} W_{i\to i+1} \tag{1}$$

where the work of each process $W_{i\to i+1}$ is calculated using the following equations

$$W_{1\to 2} = -P_{\text{int}} \cdot (V_2 - V_1) \tag{2}$$
$$W_{2\to 3} = m_3 \cdot (u_3 - u_2) = m_3 \cdot c\_v \cdot (T_3 - T_2) \tag{3}$$
$$W_{3\to 4} = 0 \tag{4}$$
$$W_{4\to 5} = -P_5 \cdot (V_5 - V_4) \tag{5}$$
$$W_{5\to 6} = m_5 \cdot (u_6 - u_5) = m_5 \cdot c\_v \cdot (T_6 - T_5) \tag{6}$$
$$W_{6\to 7} = 0 \tag{7}$$
$$W_{7\to 8} = -P_{\text{exh}} \cdot (V_8 - V_7) \tag{8}$$
$$W_{8\to 1} = 0 \tag{9}$$

The specific fuel consumption (SFC) of the cycle is calculated using

$$Q\_f = \frac{m_{\text{fuel}}}{|W| \cdot 3,6 \cdot 10^{-3}} \tag{10}$$

Mode 2: two-stroke pneumatic ideal motor cycle. The work generated during the cycle is calculated using

$$W = \sum_{i=1}^{i=6} W_{i\to i+1} \tag{11}$$

where the work of each process $W_{i\to i+1}$ is calculated using the following equations

$$W_{1\to 2} = -P_{\text{tank}} \cdot (V_2 - V_1) \tag{12}$$
$$W_{2\to 3} = m_3 \cdot (u_3 - u_2) = m_3 \cdot c\_v \cdot (T_3 - T_2) \tag{13}$$
$$W_{3\to 4} = 0 \tag{14}$$
$$W_{4\to 5} = -P_{\text{exh}} \cdot (V_5 - V_4) \tag{15}$$
$$W_{5\to 6} = m_6 \cdot (u_6 - u_5) = m_6 \cdot c\_v \cdot (T_6 - T_5) \tag{16}$$
$$W_{6\to 1} = 0 \tag{17}$$

The specific air consumption (SAC) of the cycle is calculated using

$$Q\_a = \frac{m_{\text{air}}}{|W| \cdot 3.6} \tag{18}$$

Mode 3: four-stroke pneumatic–combustion ideal motor cycle. This cycle is simply a combination of the two previous cycles. Indeed, it is a conventional combustion mode where the scavenging cycle is replaced by a two-stroke pneumatic motor cycle. The equations describing this mode are therefore the same as developed previously.

The SFC and the SAC of the cycle can be calculated using equations (10) and (18), respectively.

Mode 4: two-stroke pneumatic ideal pump cycle. The work generated during the cycle is calculated using

$$W = \sum_{i=1}^{i=5} W_{i\to i+1} \tag{19}$$

where the work of each process $W_{i\to i+1}$ is calculated using the following equations

$$W_{1\to 2} = m_2 \cdot (u_2 - u_1) = m_2 \cdot c\_v \cdot (T_2 - T_1) \tag{20}$$
$$W_{2\to 3} = -P_{\text{tank}} \cdot (V_3 - V_2) \tag{21}$$
$$W_{3\to 4} = m_4 \cdot (u_4 - u_3) = m_4 \cdot c\_v \cdot (T_4 - T_3) \tag{22}$$

$$W_{4\to5} = -P_{\text{int}} \cdot (V_5 - V_4) \quad (23)$$

The specific air compression of the cycle is calculated using equation (18).

Tank storage and discharge ideal model

We consider that the charge and discharge operations are adiabatic. During storage periods, if the pump delivers a compressed air mass rate of Q_p at a temperature of T_p, the variation of the air stored mass m_{tank} and temperature T_{tank} can be calculated using the following equations

$$dm_{\text{tank}} = Q\_p \cdot dt \quad (24)$$

$$dT_{\text{tank}} = \frac{\gamma \cdot T\_p - T_{\text{tank}}}{m_{\text{tank}}} \cdot Q\_p \cdot dt \quad (25)$$

During discharge periods, if the engine consumes a compressed air mass rate of Q_m, the variation of m_{tank} and T_{tank} can be calculated using the following equations

$$dm_{\text{tank}} = -Q\_m \cdot dt \quad (26)$$

$$dT_{\text{tank}} = -\frac{(\gamma - 1) \cdot T_{\text{tank}}}{m_{\text{tank}}} \cdot Q\_m \cdot dt \quad (27)$$

After calculating m_{tank} and T_{tank}, the tank pressure P_{tank} can be calculated using the ideal gas law, knowing that the tank volume V_{tank} is constant,

$$P_{\text{tank}} = \frac{m_{\text{tank}} \cdot r \cdot T_{\text{tank}}}{V_{\text{tank}}} \quad (28)$$

Vehicle model and engine's specific torque calculation

The total resistance applied to a vehicle moving on a flat road is the sum of the inertial acceleration resistance, the drag resistance and the rolling resistance, as can be calculated in

$$F = m \cdot \frac{d(v\_s)}{dt} + \frac{\rho \cdot A \cdot C\_d \cdot v\_s^2}{2} + C\_r \cdot m \cdot g \quad (29)$$

The three added terms of equation (29) are the acceleration force, the aerodynamic force and the friction force, respectively.

The output power of the engine should therefore be equal to the power needed to move the vehicle forward. It is calculated as

$$Pw = F \cdot vs = m \cdot vs \cdot \frac{d(v\_s)}{dt} + \rho \cdot A \cdot C\_d \cdot vs^3 + C\_r \cdot m \cdot g \cdot vs \quad (30)$$

Engine rotational speed, if the position of the gear is i, can be calculated using

$$N = \frac{30 \cdot w}{\pi} = \frac{v\_s}{k(i)} \quad (31)$$

where k is a ratio given for each gear position. The torque provided by the engine can therefore be calculated using

$$T\_q = \frac{P\_w}{w} = \frac{30}{\pi} \cdot k(i) \cdot \left(m \cdot \frac{d(v\_s)}{dt} + \rho \cdot A \cdot C\_d \cdot v\_s^2 + C\_r \cdot m \cdot g \right) \quad (32)$$

Finally, the specific torque is equal to the ratio of the torque to the engine's displacement

$$T\_qs = \frac{T\_q}{D} \quad (33)$$

Hybrid concept optimized control

Parametric optimization of the thermodynamic cycles

Mode 1: four-stroke combustion ideal motor cycle. This mode is the reference mode, and its characterization constitutes the starting point for fuel consumption reduction. Figure 10 shows the efficiency and the fuel consumption as a function of the specific torque, the only parameter that characterizes this operating mode.

The efficiency drawn in Figure 10 is calculated using

$$\eta = \frac{|W|}{m_{\text{fuel}} \cdot p\_ci} \quad (34)$$

Mode 2: Two-stroke pneumatic ideal motor cycle. First, it is important to notice that for every intake pressure, the intake temperature considered for the calculation of the thermodynamic cycle corresponds to the air temperature after an adiabatic compression starting from ambient conditions (P_a = 1 bar; T_a = 298 K) to the actual intake pressure. T_{ref} can be calculated using

$$T_{\text{ref}} = T_a \times \left(\frac{P}{P_a} \right)^{\frac{\gamma-1}{\gamma}} \quad (35)$$

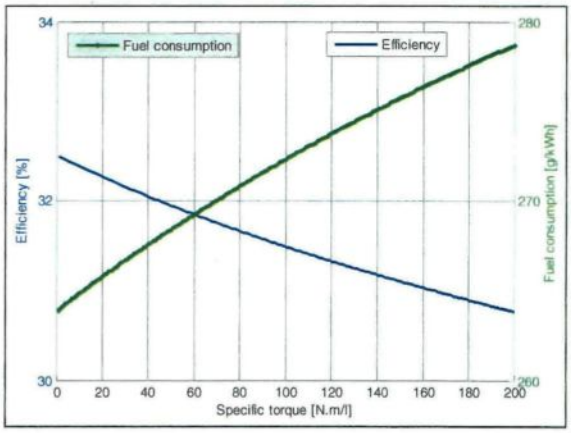

Figure 10. Fuel specific consumption and efficiency of the conventional combustion ideal cycle, as a function of specific torque.

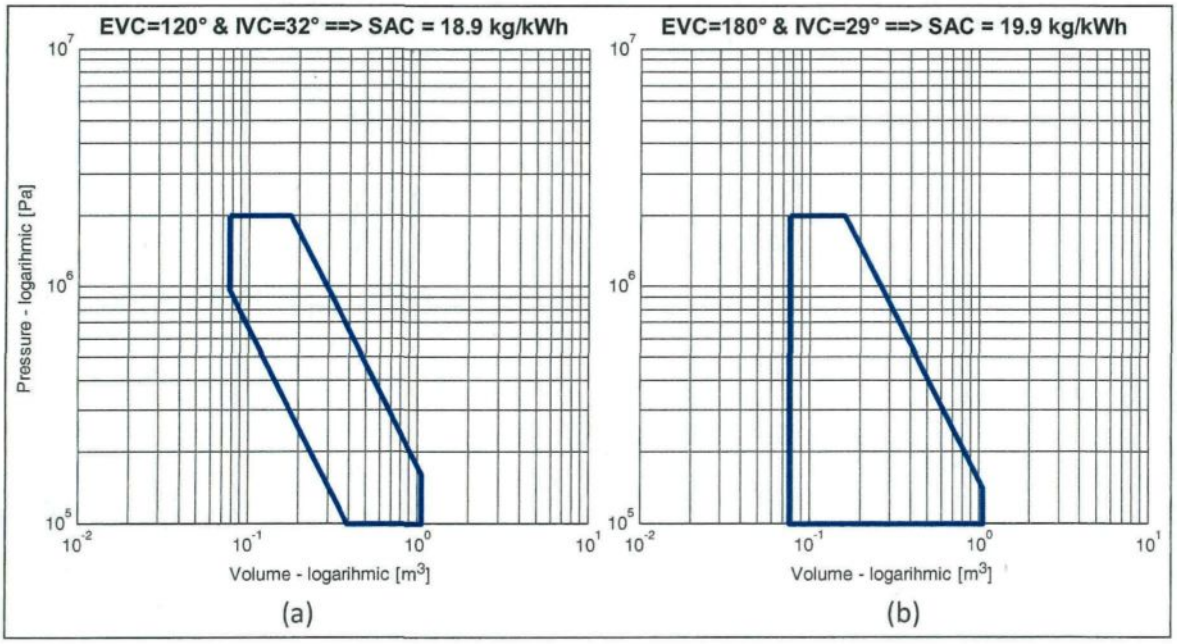

Figure 11. Two-stroke pneumatic motor operations providing a specific torque of 80 Nm/l with (a) early EVC and (b) without early EVC for a 20 bar intake pressure.

T_{ref} is therefore a reference temperature. If the intake temperature is different to T_{ref}, some of the results that will be presented below should be corrected, as we will explain later. This logic is valid for both the two-stroke pneumatic motor cycle and the four-stroke hybrid pneumatic–combustion motor cycle.

In this mode, two parameters should be set in order to meet the required specific torque for each tank pressure. Those parameters are the IVC angle and the EVC angle. Indeed, there are several possibilities to do so. Figure 11 shows two ways to obtain a specific torque of 80 Nm/l, while the tank pressure is 20 bar:

(a) EVC angle and IVC angle, respectively, set to 120° and 32°, in this case, the SAC is equal to 18.9 kg/kWh;
(b) EVC angle and IVC angle, respectively, set to 180° and 29°, in this case, the SAC is equal to 19.9 kg/kWh, i.e. 5% higher.

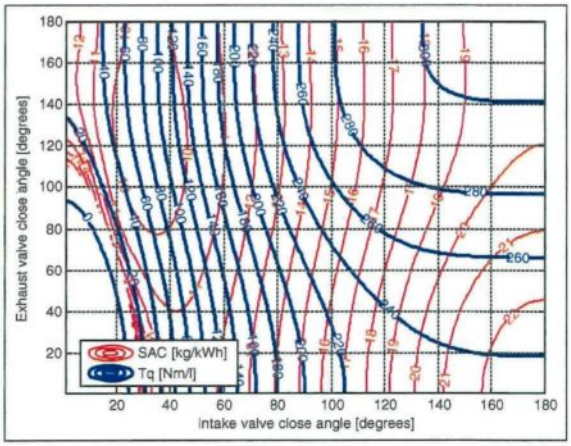

Figure 12. Two-stroke pneumatic motor operation specific torque and efficiency with intake pressure of 20 bar, as a function of IVC and EVC angles.

This means that early EVC results in reducing the air consumption. We next calculated the SAC curves and the specific torque curves for every combination of IVC and EVC. The results are shown in Figure 12, where we observe infinite ways to obtain a certain torque, but only one that ensures minimal SAC.

Consequently, we have calculated, using an adequate optimization algorithm, the optimal calibration of the IVC and the EVC angles that give the minimal SAC, for each combination of specific torque and tank pressure. Figures 13 and 14 show, respectively, the IVC angle and the EVC angle that allow a specific torque to be attained for a certain tank pressure, while ensuring an optimal efficiency and therefore minimal air consumption. We observe that early EVC is needed mainly at low loads and high tank pressure. The associated SAC is illustrated in Figure 15. If the tank pressure is equal to 5 bar, the minimal SAC is attained for a specific torque of 25 Nm/l; and if the tank pressure is equal to 20 bar, the minimal SAC is attained for a specific torque of 75 Nm/l. The shape of the optimal efficiency curve is linear.

Our analysis revealed that optimal valve closing angles and cycle efficiency do not depend on intake temperature, but air consumption does. If the tank air temperature T_{tank} is different to the reference intake temperature T_{ref} illustrated in Figure 14, the air

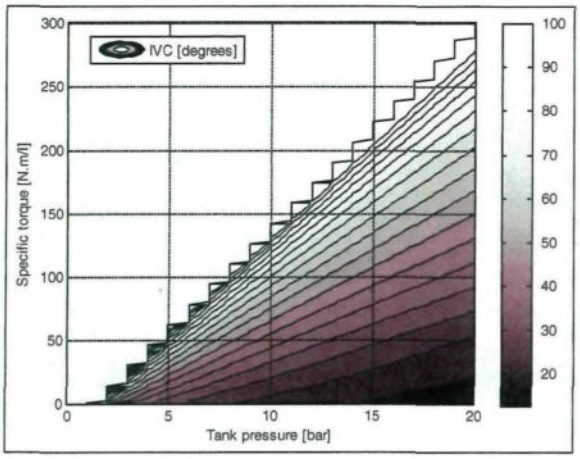

Figure 13. Optimal IVC angle as a function of the tank pressure and the specific torque of a pneumatic two-stroke motor operation.

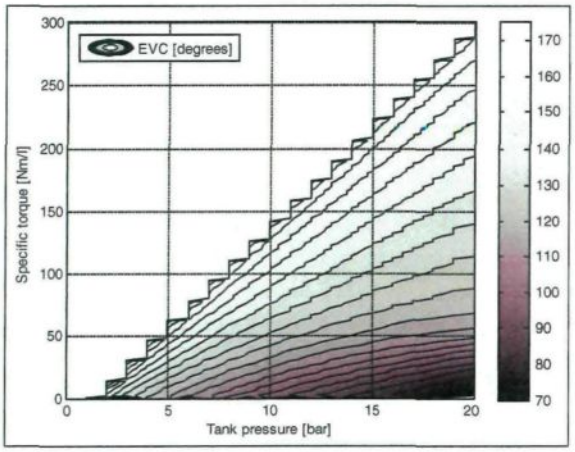

Figure 14. Optimal EVC angle as a function of the tank pressure and the specific torque of a pneumatic two-stroke motor operation.

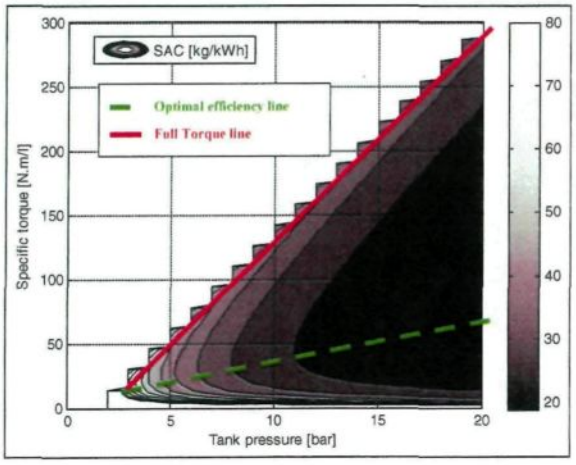

Figure 15. SAC of an optimized pneumatic two-stroke motor mode as a function of the tank pressure and the specific torque.

consumption Q'^{T}_{air} is obtained by correcting the reference air consumption $Q'^{T_{\text{ref}}}_{\text{air}}$, using

$$Q'^{T}_{\text{air}} = Q'^{T_{\text{ref}}}_{\text{air}} \times \frac{T_{\text{ref}}}{T_{\text{tank}}} \tag{36}$$

Finally, we can observe the full torque curve in this mode, which is also linear with respect to tank pressure.

Mode 3: four-stroke pneumatic–combustion ideal motor cycle. The four-stroke pneumatic–combustion motor mode is an association of the two precedent modes. The ratio of the pneumatic power to the total power can be adjusted by increasing or reducing the IVC angle. The higher this ratio is, the less the fuel consumption is, but also the higher the maximum cylinder pressure is. Figure 16 illustrates two possible operations to provide 150 Nm/l specific torque with 20 bar tank pressure, with two different percentages of the pneumatic power to the total power, 40% (a) and 69% (b). We can observe that the area of the low-pressure part of the cycle is higher and the area of the high-pressure part is lower for the 69% ratio operation. We can also observe how the high-pressure cycle reaches a much higher cylinder pressure in the 69% ratio operation. The fuel consumptions of the 40% ratio operation and the 69% ratio operation are 130 g/kWh and 96 g/kWh, respectively. In Figure 17, we can observe the variation of the SFC and the maximum cylinder pressure as functions of the ratio of the pneumatic power to the total power for a 150 Nm/l specific torque operation.

The maximum cylinder pressure cannot be increased indefinitely. Increasing this pressure exposes the engine to a higher mechanical stress level. A pressure of 180 bar is a common limitation of the cylinder pressure accepted by most turbocharged diesel engines.[17] In our study, we have considered 200 bar as a threshold to be respected while choosing the ratio of the pneumatic power to the total power for each operation point. The reason why we have increased the threshold is that we are dealing with an ideal cycle, which tends to overestimate real cylinder pressure.

For every optimized operation, the chosen EVC angle is the same as the one obtained in the two-stroke pneumatic motor mode while providing the same pneumatic torque. The results of this optimization are illustrated in the following figures. It is logical that the four-stroke pneumatic–combustion motor mode operation starts when the torque demanded is higher than the full torque possible with the two-stroke pneumatic motor mode.

Figure 18 illustrates the optimal ratio of the pneumatic power to the total power that allows the required specific torque to be obtained for a certain tank pressure, while ensuring minimal fuel consumption and without exceeding the 200 bar maximum cylinder pressure. We observe that for larger tank pressures, the pneumatic contribution increases, and for larger specific torque, the pneumatic contribution diminishes.

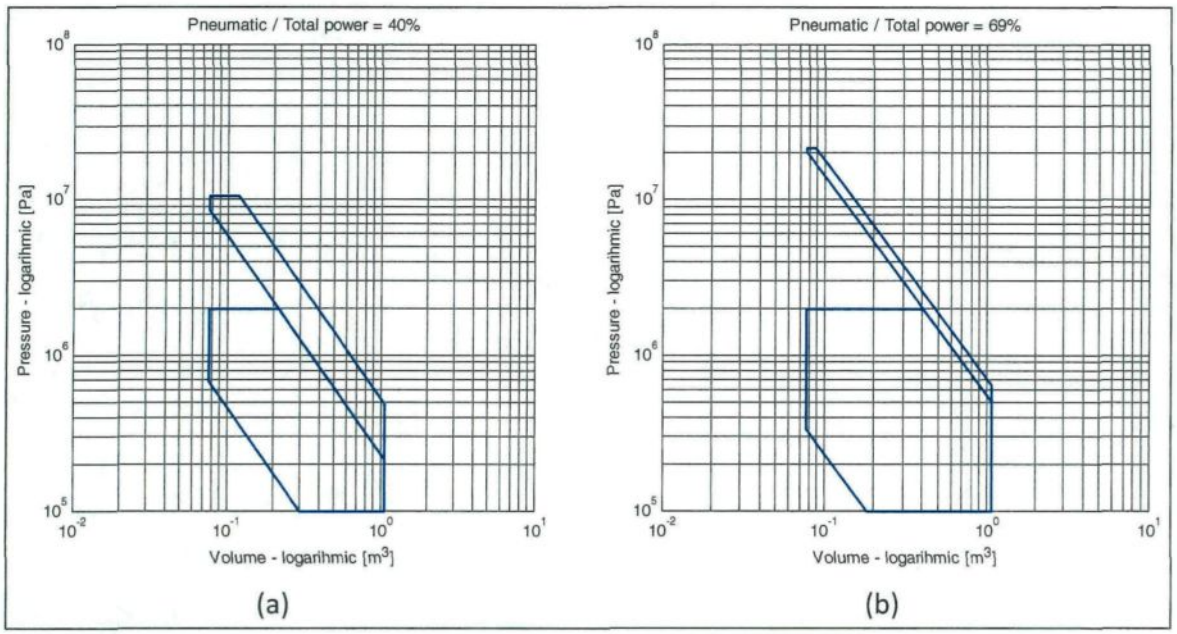

Figure 16. Hybrid operations providing a specific torque of 150 Nm/l with intake pressure of 20 bar, for (a) 40% pneumatic contribution and (b) 69% pneumatic contribution.

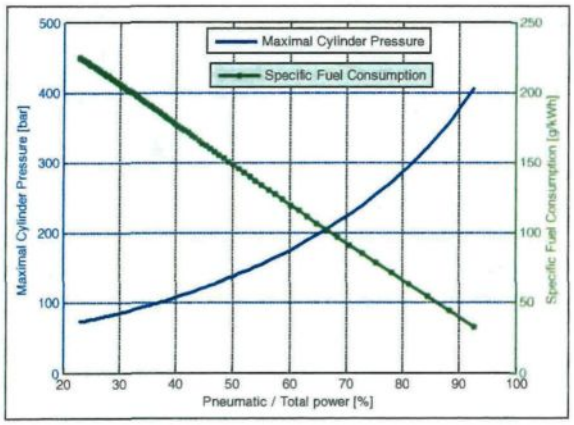

Figure 17. Maximum gas cylinder pressure of hybrid cycle, as a function of pneumatic power contribution for 150 Nm/l torque operation.

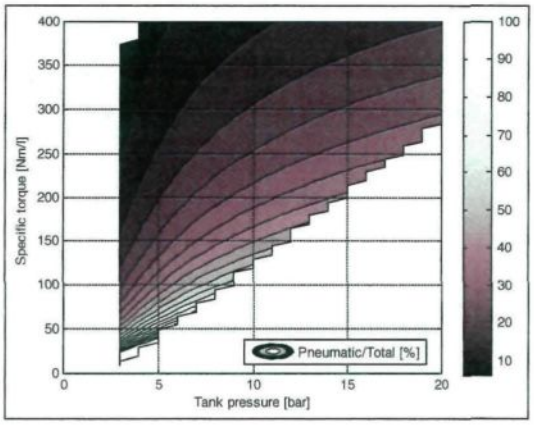

Figure 18. Optimal pneumatic power contribution as a function of the tank pressure and the specific torque of a hybrid four-stroke operation.

Figures 19 and 20 show, respectively, the IVC and EVC angles associated with this optimized operation. Early EVC occurs, mainly for very high tank pressure.

The associated SAC and SFC are illustrated in Figures 21 and 22, respectively. SAC is lower for higher specific torque. It is important to note that SAC should be corrected according to the intake temperature, as detailed for the two-stroke pneumatic motor mode in equation (33). SFC decreases significantly for higher tank pressure and for lower specific torque.

Mode 4: two-stroke pneumatic ideal pump cycle. The two-stroke pneumatic pump cycle is possible for negative specific torque, i.e. when the engine is supplied by mechanical power. As explained in the suggested concept section, the intake valve open (IVO) angle is chosen in order to meet the tank pressure, while the IVC angle is chosen in order to meet the specific torque demanded. Figures 23 and 24 show the IVO and IVC as functions of tank pressure and specific torque. We remind the reader that in this mode, the exhaust of the compressed air passes through the intake valve, and the intake of atmospheric air passes through the exhaust valve. We also observe in Figures 23 and 24 the full torque curve, which represents the maximum torque that the engine is able to recover. If the input torque is higher, the engine recovers a part of the mechanical energy, and the rest is unfortunately dissipated.

In addition, the exhaust valve opening (EVO) angle is chosen in order to optimize the efficiency by ensuring

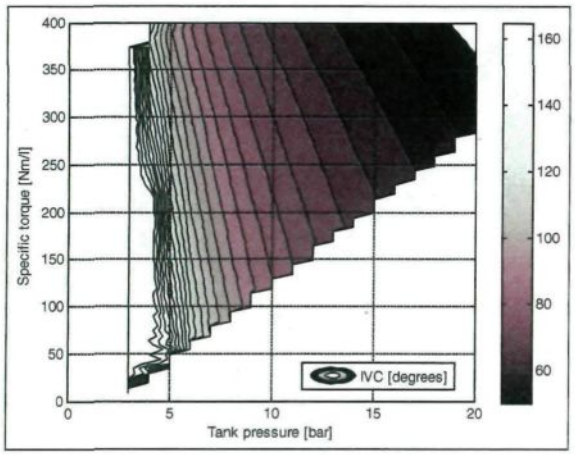

Figure 19. Optimal IVC angle as a function of the tank pressure and the specific torque of a hybrid four-stroke operation.

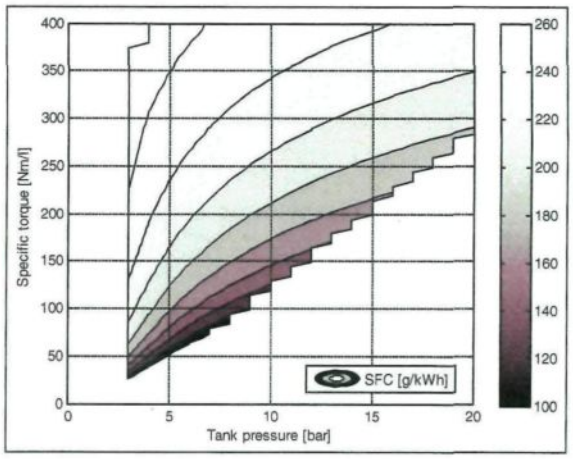

Figure 22. Optimal SFC as a function of the tank pressure and the specific torque of a hybrid four-stroke operation.

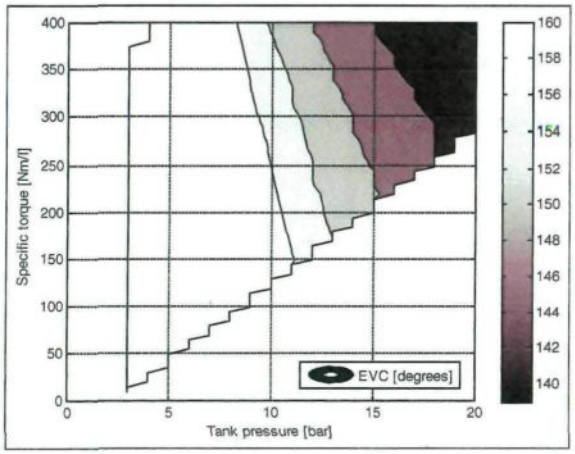

Figure 20. Optimal EVC angle as a function of the tank pressure and the specific torque of a hybrid four-stroke operation.

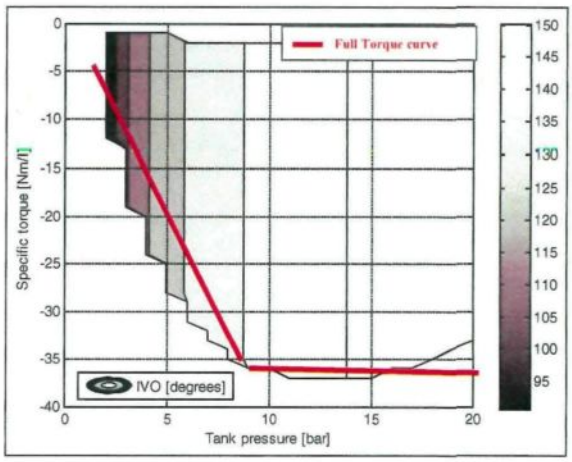

Figure 23. Optimal IVO angle as a function of the tank pressure and the specific torque of a pneumatic two-stroke pump operation.

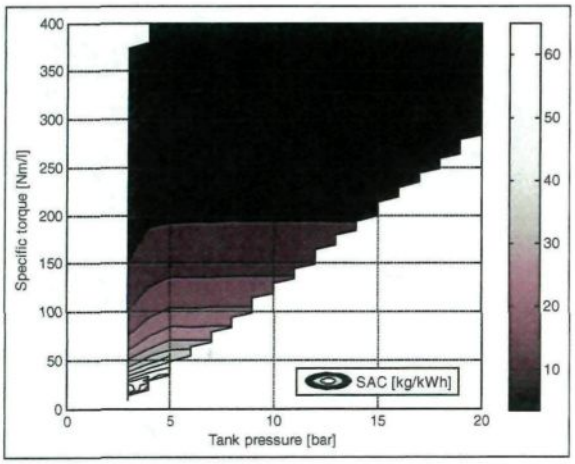

Figure 21. Optimal SAC as a function of the tank pressure and the specific torque of a hybrid four-stroke operation.

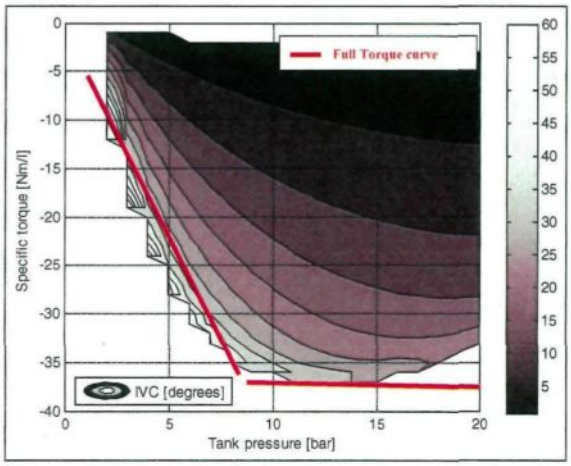

Figure 24. Optimal IVC angle as a function of the tank pressure and the specific torque of a pneumatic two-stroke pump operation.

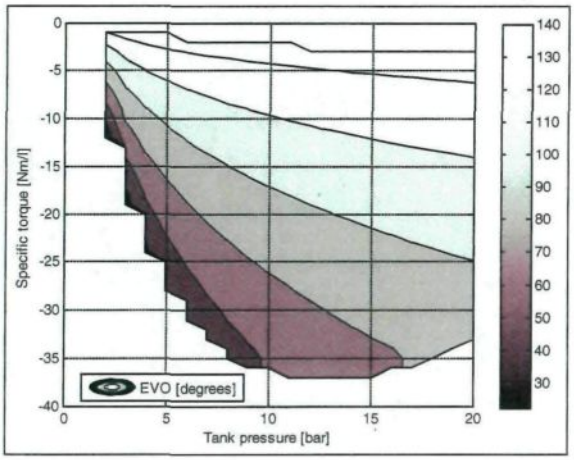

Figure 25. Optimal EVO angle as a function of the tank pressure and the specific torque of a pneumatic two-stroke pump operation.

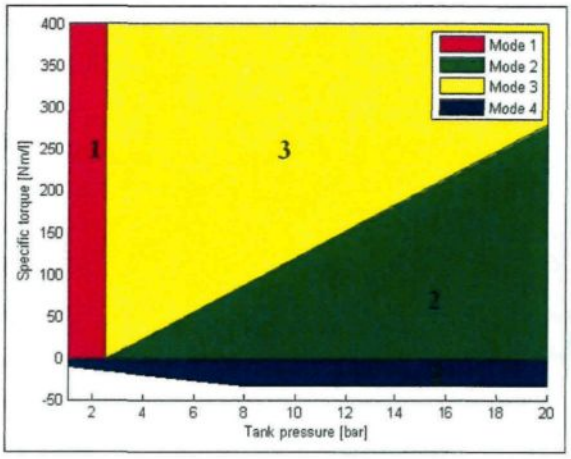

Figure 28. Strategy used for engine mode selection, as a function of tank pressure and specific torque.

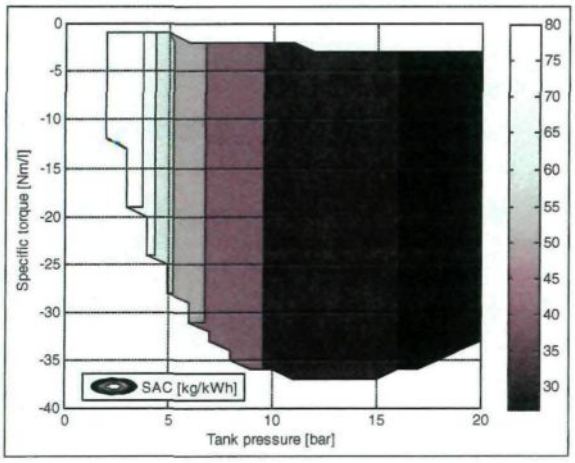

Figure 26. Optimal specific compressed air flow-rate as a function of the tank pressure and the specific torque of a pneumatic two-stroke pump operation.

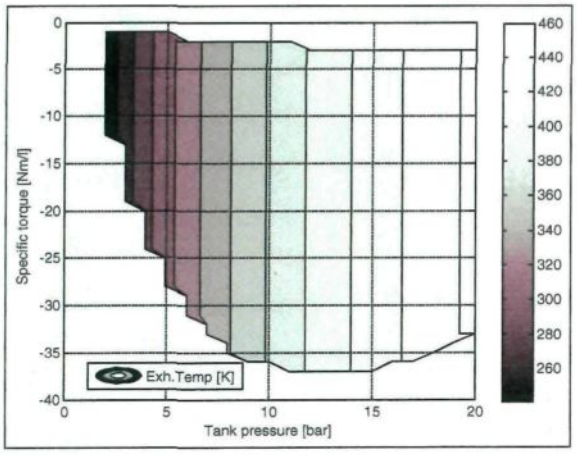

Figure 27. Optimal exhaust air temperature as a function of the tank pressure and the specific torque of a pneumatic two-stroke pump operation.

that the cylinder pressure when the exhaust valve opens is close to 1 bar in order not to dissipate pneumatic energy. Figure 25 illustrates the optimal EVO as a function of tank pressure and available specific torque. For the specific compressed air flow-rate, Figure 26 shows that it depends only on tank pressure, such that for a larger tank pressure, the specific air flow-rate diminishes.

Finally, the compressed air temperature is important as it will act on the tank air temperature during compression operation, as explained previously. Figure 27 shows that this temperature depends only on the tank pressure. Tank pressure equals the compression ratio of the air pump. For the highest tank pressures, the compressed air temperature increases. The exhaust temperature can rise up to 460 K if the ambient temperature is 298 K.

Engine mode selection strategy

After this analysis and comprehension of the thermodynamic ideal cycles corresponding to all four modes, we suggest the strategy illustrated in Figure 28 for choosing the engine's operation mode as a function of the tank pressure and the specific torque required. The strategy prioritizes the pneumatic mode whenever possible. When the tank pressure is lower than 3 bar, the operation mode is forced to be conventional. During energy recovering operation, the maximum possible torque that can be recovered corresponds to the borders of the mode 4 zone. When the available torque is higher, the engine recovers a part of the mechanical energy, and the rest is unfortunately dissipated. As can be observed, this strategy is independent from engine size, and is therefore valid for any application.

Complete fuel economy analysis on driving cycles for fixed tank volume

For the current application, the vehicle parameters are listed in Table 1 and the powertrain parameters are listed in Table 2.

Table 1. Vehicle parameters.

Parameter	Value	Unit
m	1500	kg
A	2.06	m^2
C_d	0.312	
C_r	0.00863	

Table 2. Powertrain parameters.

Parameter	Value	Unit
Γ	14	
D	0.750	l
$k(1)$	0.007	km/h or r/min
$k(2)$	0.014	km/h or r/min
$k(3)$	0.020	km/h or r/min
$k(4)$	0.030	km/h or r/min
$k(5)$	0.040	km/h or r/min
$k(6)$	0.045	km/h or r/min

It is worth noting that the modeling of the thermodynamic cycles performed previously, the parametric optimization of those cycles and the generated maps remain valid for any engine displacement, as long as the tank volume is much higher than the displacement. The generated maps, a function of the specific torque not the absolute one, are independent of the engine displacement. The tank volume is set to 50 l, which satisfies the condition of being significantly higher than the engine displacement.

To evaluate accurately the fuel economy obtained with the hybrid concept, the tank pressure, which is the image of the tank state of charge (TSOC), should reach at the end of the driving cycle, the same value as the one settled at the beginning of the cycle.

The concept is evaluated on the New European Drinving Cycle (ARTEMIS) and on the Assessment and Reliability of Transport Emission Models and Inventory System (ARTEMIS) urban and rural driving cycles. The cycles' specifications and engine associated load are illustrated in Figures 40 to 48.

The NEDC

On the NEDC, we have found that it is allowed to start the cycle with a full charged tank because the long deceleration at the end of the cycle fills the tank to the maximum, as shown in Figure 29. The operation modes selected by the strategy are shown in Figure 30. We observe that mode 2 is activated much more often than mode 3, which means that the displacement is suitable for the application on this cycle. Mode 4 is well activated during decelerations, as long as the tank is not full. The result of fuel consumption on the NEDC is shown in Figure 31 in comparison with the fuel consumption obtained with a conventional combustion engine. The fuel economy between the two engines is 39 g, which represents 12% less consumption.

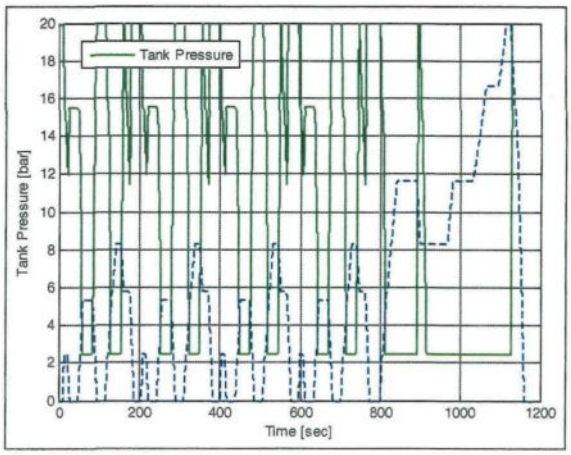

Figure 29. Tank pressure on the NEDC.

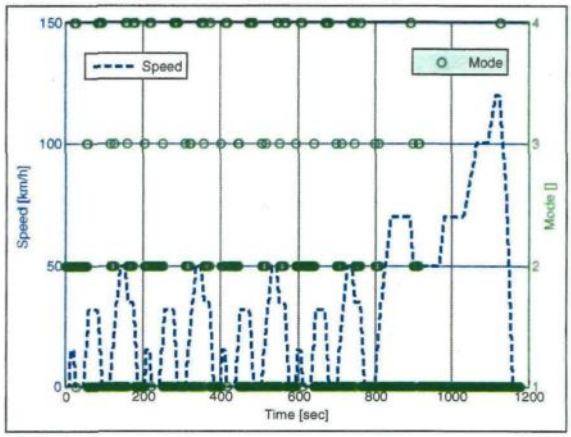

Figure 30. Operating modes of hybrid engine on the NEDC.

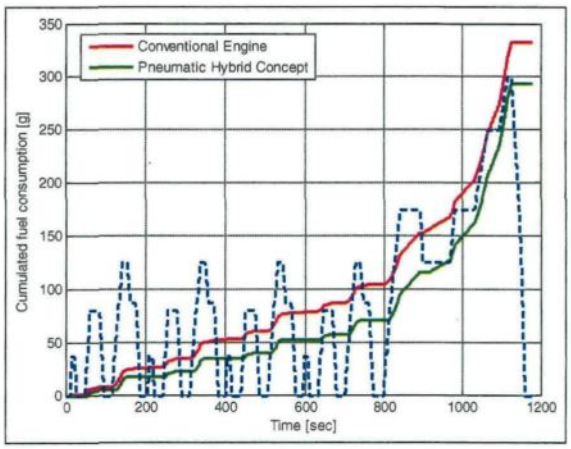

Figure 31. Fuel consumption on the NEDC for the conventional engine and pneumatic hybrid concept.

The ARTEMIS urban cycle

On the ARTEMIS urban cycle, we have found that the initial tank pressure that allows the same value to be reached at the end of the cycle is 18 bar, as shown in

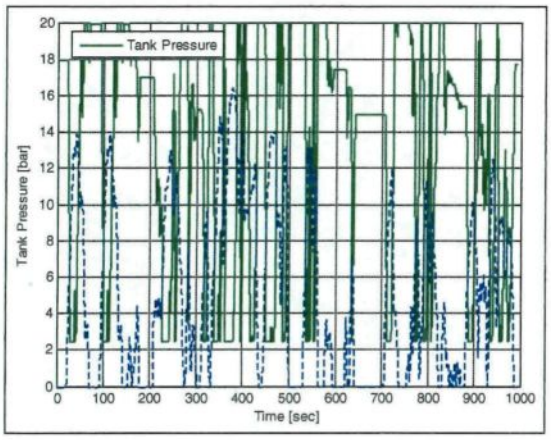

Figure 32. Tank pressure on the ARTEMIS urban cycle.

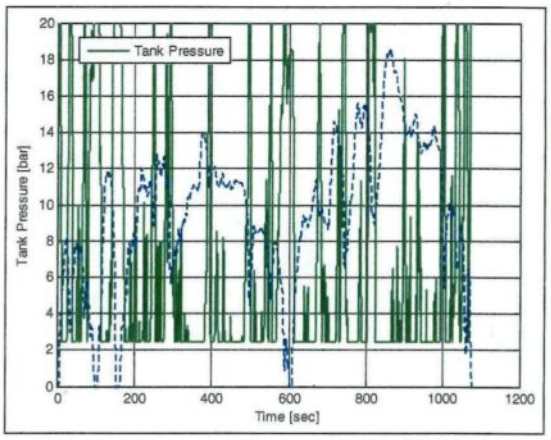

Figure 35. Tank pressure on the ARTEMIS rural cycle.

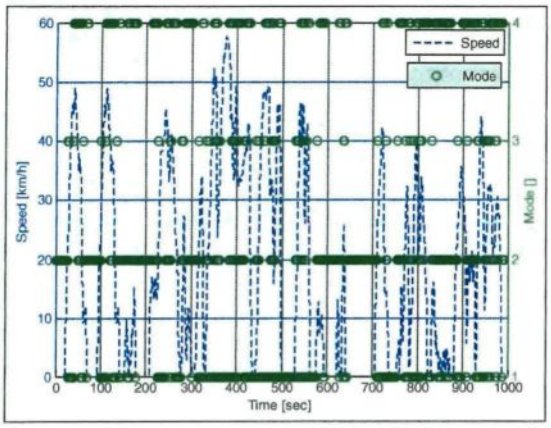

Figure 33. Operating modes of the hybrid engine on the ARTEMIS urban cycle.

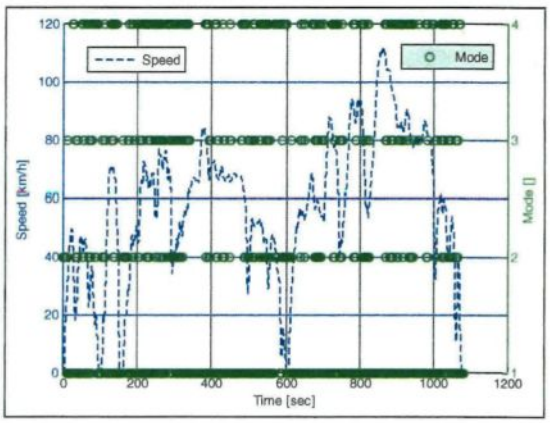

Figure 36. Operating modes of the hybrid engine on the ARTEMIS rural cycle.

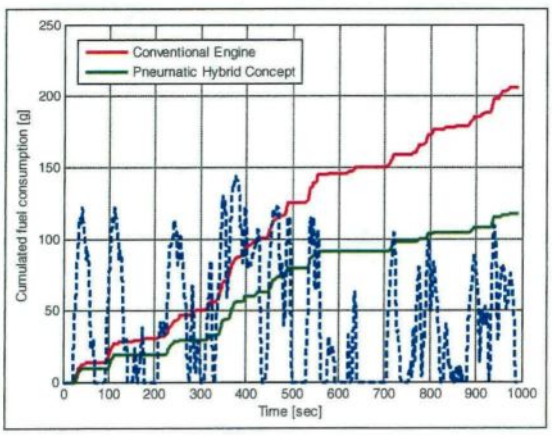

Figure 34. Fuel consumption on the ARTEMIS urban cycle for the conventional engine and pneumatic hybrid concept.

Figure 32. The operation modes chosen are shown in Figure 33, and the fuel economy obtained is shown in Figure 34. We can observe that the hybrid concept consumes 88 g less fuel, which represents a fuel economy of 43%.

The ARTEMIS rural cycle

On the ARTEMIS rural cycle, we have found that it is also allowed to start the cycle with a full tank, as shown in Figure 35. The chosen operation modes are shown in Figure 36, and the fuel economy is shown in Figure 37. We can observe that the hybrid concept consumes 94 g less fuel, which represents a fuel economy of 16%.

Study of impact of the air storage tank volume

In order to complete the study, we have investigated the effect of the tank volume on the fuel economy obtained between the conventional engine and our hybrid concept. The vehicle parameters and the powertrain parameters are the same as in the previous section (Tables 1 and 2). The tank volume is varied. We ensure that the initial tank pressure is equal to the final tank pressure in order to accurately evaluate the fuel economy.

Figure 38 shows this initial pressure as a function of the tank volume, for all the driving cycles analyzed. We observe that for both ARTEMIS cycles, the larger the tank volume is, the less the initial pressure should be,

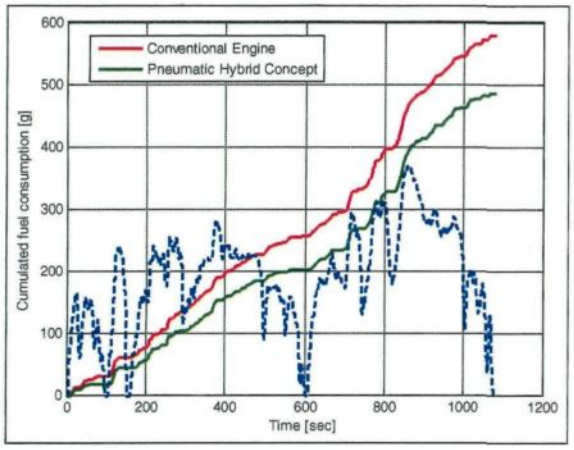

Figure 37. Fuel consumption on the ARTEMIS rural cycle for the conventional engine and pneumatic hybrid concept.

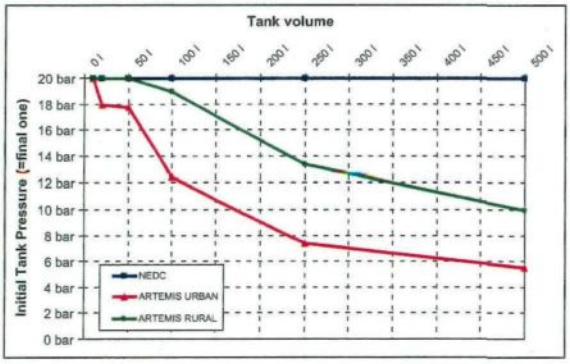

Figure 38. Settled initial tank pressure as a function of tank volume, for different cycles.

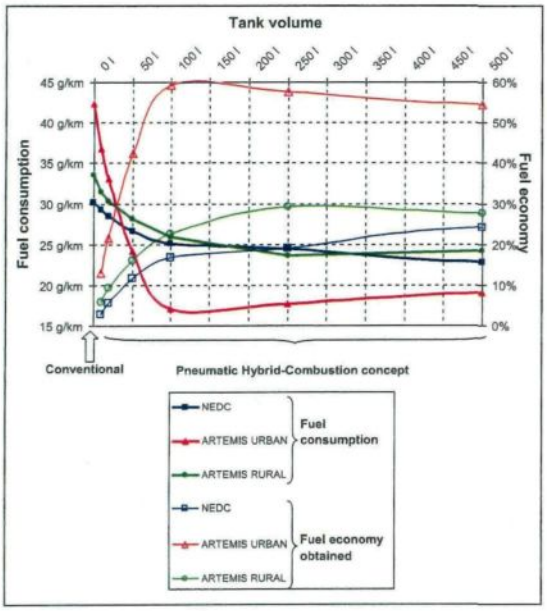

Figure 39. Fuel consumption and economy from the conventional engine of the hybrid concept as a function of tank volume, for different driving cycles.

whereas for the NEDC, the initial pressure can be set to the maximum (20 bar), even for a 500 l volume tank. This is due to the high amount of energy available during the last deceleration of the NEDC.

Figure 39 illustrates the effect of tank volume on the absolute fuel consumption (left axis) and on the fuel economy (right axis) compared to the one obtained with a conventional engine, as a function of tank volume and for different driving cycles. The initial pressure for each cycle is the one illustrated in Figure 38. The starting points of the fuel consumption curves (corresponding to a 0 l tank) represent the conventional engine operation. We have found that there is an optimal value of the tank volume that ensures the best fuel economy for all three cycles. For our application, this optimal value is around 100 l. The fuel economy can therefore reach 17% on the NEDC, 60% on the ARTEMIS urban cycle and 23% on the ARTEMIS rural cycle, as shown in Figure 39.

Conclusions and perspective

In this paper, we have presented an optimization followed by a fuel-saving evaluation of a new concept of a pneumatic hybrid–combustion engine that can be obtained by slightly modifying a conventional ICE. The evaluation of our concept was based on ideal thermodynamic cycle modeling. We have conducted optimization of the valve actuation timing for three possible operation modes in addition to the conventional mode. This optimization led to generic maps of fuel and air consumption. These maps are independent of the engine size and are therefore valid for any application.

We have evaluated this concept for a 1500 kg vehicle on the NEDC and on the ARTEMIS urban and rural driving cycles. We demonstrated that the fuel saving on these cycles reaches 17%, 60% and 23%, respectively, using a 100 l volume tank. The fuel economy is lower with a smaller tank. It is important to bear in mind that packaging is a first-order constraint for automotive engineering design. In order to be feasible, the pneumatic concept should require a reasonable tank volume.

This evaluation, however, was based on ideal cycle modeling and aimed to bound hoped fuel saving generated by the concept. A real cycle needs to be investigated by taking into consideration other phenomena that might influence the fuel-saving estimation, such as supersonic flow limitations through valves, valve response times for opening and closing, fuel injection shape, fuel burn process and heat exchanges through boundaries. The next phase of this study will be to perform a more accurate evaluation of the fuel economy by real cycle modeling using commercial software such as GT-Power, then to perform engine bench tests to validate the models.

Funding

This research received no specific grant from any funding agency in the public, commercial, or not-for-profit sectors.

References

1. Dönitz C, Vasile I, Onder C, et al. Realizing a concept for high efficiency and excellent driveability: the downsized and supercharged hybrid pneumatic engine. SAE paper 2009-01-1326, 2009.
2. Trajkovic S, Tunestal P and Johansson B. Introductory study of variable valve actuation for pneumanic hybridization. SAE paper 2007-01-0288, 2007.
3. Trajkovic S, Tunestal P and Johansson B. Investigation of different valve geometries and valve timing strategies and their effect on regenerative efficiency for a pneumatic hybrid with variable valve actuation. SAE paper 2008-01-1715, 2008.
4. Dönitz C, Vasile IC, Onder CH, et al. Modeling and optimizing two- and four-stroke hybrid pneumatic engines. Proc. IMechE Vol. 223 Part D: J. Automobile Engineering; DOI: 10.1243/09544070JAUTO972; 2009.
5. Higelin P, Charlet A and Chamaillard Y. Thermodynamic simulation of a hybrid pneumatic-combustion engine concept. *Int J App Thermo* 2007; 5(1): 1–11.
6. Higelin P, Vasile I, Charlet A, et al. Parametric optimization of a new hybrid pneumatic combustion engine concept. *Int J Engine Res*earch 2004; 5(2): 205.
7. Ibrahim H, Younes R, Basbous T, et al. Optimization of diesel engine performances for a hybrid wind-diesel system with compressed air energy storage. *Energy* 2011; 36: 3079–3091.
8. Ibrahim H, Ilinca A, Younes R, et al. Study of a hybrid wind-diesel system with compressed air energy storage. In: *IEEE Canada, Electrical Power Conference 2007, Renewable and Alternative Energy Resources, EPC2007*, Montreal Canada, 25 October 2007.
9. Ibrahim H. *Etude et conception d'un générateur hybride d'électricité de type Eolien-diesel avec élément de stockage d'air comprimé*. PhD Thesis, Université du Québec à Chicoutimi, 2010.
10. Basbous T, Younes R, Ilinca A, et al. Pneumatic hybridization of a diesel engine using compressed air storage for wind-diesel energy generation. Energy 2012; 38: 264–275.
11. Hyungsuk KH, Tai C, Smith E, et al. Demonstration of air-power-assist (APA) engine technology for clean combustion and direct energy recovery in heavy duty application. SAE paper 2008-01-1197, 2008.
12. Trajkovic S, Tunestal P and Johansson B. Simulation of a pneumatic hybrid powertrain with VVT in GT-power and comparison with experimental data. SAE paper 2009-01-1323, 2009.
13. Lee CY, Zhao H and Ma T. Pneumatic regenerative engine braking technology for buses and commercial vehicles. SAE paper 2011-01-2176, 2011.
14. Heywood JB. *Internal combustion engine fundamentals*. New York: McGraw Hill, 1988.
15. Stone R. *Introduction to internal combustion engines*. Department of Engineering Science, University of Oxford, 1999.
16. Manwell JF, McGowan JG and Rogers AL. *Wind energy explained – theory design and application*. John Wiley & Sons Ltd, 2002.
17. Gheorghiu V. CO2-emission reduction by means of enhanced thermal conversion efficiency of ICE cycles. SAE paper 2009-24-0081, 2009.
18. Lopes Correia da Silva L. Simulation of the thermodynamic processes in diesel cycle internal combustion engines. SAE paper 931899, 2007.

Appendix I

Notation

A	area (m^2)
c_p	specific heat at constant pressure (J/(K kg))
c_v	specific heat at constant volume (J/(K kg))
C_d	drag coefficient
C_r	rolling coefficient
D	displacement (l)
g	acceleration of gravity (m/s)
h	specific enthalpy (J/kg)
H	enthalpy (J)
k	gearbox ratio
m	mass (kg)
N	engine speed (r/min)
P	pressure (Pa)
P_w	power (kW)
Q_a	specific air consumption or compression (kg/(kW h))
Q_f	specific fuel consumption (g/(kW h))
Q_m	air consumption rate during motor mode (kg/h)
Q_p	air compression rate during pump mode (kg/h)
r	gas constant (J/(K kg))
T	temperature (K)
T_p	compressed air temperature at the engine's outlet during pump mode (K)
T_q	torque (Nm)
T_qs	specific torque (Nm/l)
u	specific internal energy (J/kg)
v_s	vehicle speed (m/s)
V	volume (m^3)
w_s	wind speed (m/s)
α_v	isochoric burned fuel Work [joules] proportion
α_p	isobaric burned fuel proportion
γ	specific heat ratio
Γ	geometric compression ratio
η	efficiency

Subscripts

a	ambient conditions
air	air consumed or compressed
exh	exhaust conditions
fuel	injected fuel
int	intake conditions
ref	reference conditions
tank	tank conditions

Abbreviations

ARTEMIS	assessment and reliability of transport emission models and inventory system
BDC	bottom dead center
CAES	compressed air energy storage

EVC	exhaust valve close
EVO	exhaust valve open
FIS	fuel injection start
ICE	internal combustion engine
IVC	intake valve close
IVO	intake valve open
NEDC	new European driving cycle
SAC	specific air consumption
SFC	specific fuel consumption
SOC	state of charge
TDC	top dead center
TSOC	tank state of charge

Appendix 2

Thermodynamic cycle calculations

Mode 1: four-stroke combustion ideal motor cycle. The ideal four-stroke combustion cycle is shown in Figure 8. The following equations describe the cycle.

The process from 1 to 2 is isobaric at intake pressure P_{int}, and is characterized by

$$P_2 = P_1 = P_{int} \tag{37}$$

The application of the first law of thermodynamics to this process gives

$$m_2 \cdot u_2 - m_1 \cdot u_1 = (m_2 - m_1) \cdot h_1 - P_{int} \cdot (V_2 - V_1) \tag{38}$$

and

$$m_2 \cdot c\_v \cdot T_2 - m_1 \cdot c\_v \cdot T_1 = (m_2 - m_1) \cdot c\_p \cdot T_1 - P_{int} \cdot (V_2 - V_1) \tag{39}$$

Developing this equation, and combining with the perfect gas law, results in

$$m_2 = \frac{P_{int} \cdot V_2}{r \cdot T_{int}} - m_1 \cdot \left(\frac{T_1}{\gamma \cdot T_{int}} - 1\right) - \frac{P_{int} \cdot V_1}{c\_p \cdot T_{int}} \tag{40}$$

Therefore,

$$T_2 = \frac{P_{int} \cdot V_2}{m_2 \cdot r} \tag{41}$$

The process from 2 to 3 is an adiabatic compression characterized by

$$P_3 = P_2 \cdot \left(\frac{V_2}{V_3}\right)^{\gamma} \tag{42}$$

Therefore,

$$T_3 = T_2 \cdot \left(\frac{V_2}{V_3}\right)^{\gamma - 1} \tag{43}$$

knowing that

$$m_3 = m_2 \tag{44}$$

The process from 3 to 4 represents the premixed flame, which is instantaneous isochoric combustion of a proportion αv of the total injected mass of fuel, m_f. This gives

$$m_4 = m_3 + \alpha\_v \cdot m_f \tag{45}$$

where α_v is a variable depending on the operation point. For our modeling, we have considered a fixed value of $\alpha\_v = 20\%$. The application of the first law of thermodynamics to this process gives

$$m_4 \cdot u_4 - m_3 \cdot u_3 = \alpha\_v \cdot m_f \cdot p\_ci \tag{46}$$

Developing equation (47) gives

$$T_4 = \frac{\alpha\_v \cdot m_f \cdot pci + m_3 \cdot c\_v \cdot T_3}{m_4 \cdot c\_v} \tag{47}$$

Moreover,

$$P_4 = \frac{m_4 \cdot r \cdot T_4}{V_4} \tag{48}$$

The process from 4 to 5 represents the diffusion flame, which is isobaric combustion of the remaining proportion αp of the total injected mass of fuel, m_f

$$m_5 = m_4 + \alpha\_p \cdot m_f \tag{49}$$

The value of αp considered in this work is 80%. The process from 4 to 5 is isobaric, therefore,

$$P_5 = P_4 \tag{50}$$

The application of the first law of thermodynamics to this process gives

$$m_5 \cdot u_5 - m_4 \cdot u_4 = \alpha\_p \cdot m_f \cdot p\_ci - P_5 \cdot (V_5 - V_4) \tag{51}$$

Developing this equation (60) gives

$$T_5 = \frac{\alpha\_p \cdot m_f \cdot p\_ci - P_5 \cdot (V_5 - V_4) + m_4 \cdot c\_v \cdot T_4}{m_5 \cdot c\_v} \tag{52}$$

Moreover, using the perfect gas law, we obtain

$$V_5 = \frac{m_5 \cdot r \cdot T_5}{P_5} \tag{53}$$

and

$$T_5 = \frac{\alpha_p \cdot m_f \cdot p\_ci + P_5 \cdot V_4 + m_4 \cdot c\_v \cdot T_4}{m_5 \cdot c\_p} \tag{54}$$

The process from 5 to 6 is an adiabatic expansion characterized by

$$P_6 = P_5 \cdot \left(\frac{V_5}{V_6}\right)^{\gamma} \tag{55}$$

and

$$T_6 = T_5 \cdot \left(\frac{V_5}{V_6}\right)^{\gamma - 1} \tag{56}$$

knowing that

$$m_6 = m_5 \tag{57}$$

The process from 6 to 7 is an isochoric exhaust characterized by

$$P_7 = P_{exh} \tag{58}$$

The application of the first law of thermodynamics to this process gives

$$m_7 \cdot u_7 - m_6 \cdot u_6 = (m_7 - m_6) \cdot h_7 \tag{59}$$

The development of this equation gives

$$T_7 = \frac{m_6 \cdot c\_v \cdot T_6 + P_7 \cdot V_7}{m_6 \cdot c\_p} \tag{60}$$

Moreover, using the perfect gas law, we obtain

$$m_7 = \frac{P_7 \cdot V_7}{r \cdot T_7} \tag{61}$$

The process from 7 to 8 is isobaric at intake pressure P_{exh}, and is characterized by

$$P_8 = P_{exh} \tag{62}$$

The application of the first law of thermodynamics to this process gives

$$m_8 \cdot u_8 - m_7 \cdot u_7 = (m_8 - m_7) \cdot h_8 - P_{exh} \cdot (V_8 - V_7) \tag{63}$$

Therefore,

$$m_8 \cdot c\_v \cdot T_8 - m_7 \cdot c\_v \cdot T_7 = (m_8 - m_7) \cdot c\_p \cdot T_8 - P_{exh} \cdot (V_8 - V_7) \tag{64}$$

Developing this equation gives

$$T_8 = \frac{P_{exh} \cdot V_8 + m_7 \cdot c\_v \cdot T - P_{exh} \cdot (V_8 - V_7)}{m_7 \cdot c\_p} \tag{65}$$

Moreover, using the perfect gas law, we obtain

$$m_8 = \frac{P_{exh} \cdot V_8}{T_8 \cdot r} \tag{66}$$

Finally, the process from 8 to 1 is isochoric filling, characterized by

$$P_1 = P_{int} \tag{67}$$

The application of the first law of thermodynamics to this process gives

$$m_1 \cdot u_1 - m_8 \cdot u_8 = (m_1 - m_8) \cdot h_{int} \tag{68}$$

Therefore,

$$m_1 \cdot c\_v \cdot T_1 - m_8 \cdot c\_v \cdot T_8 = (m_1 - m_8) \cdot c\_p \cdot T_{int} \tag{69}$$

The development of this equation combined to the perfect gas law gives

$$T_1 = \frac{P_1}{(P_1 - P_8)/(\gamma \cdot T_{int}) + P_8/T_8} \tag{70}$$

Moreover,

$$m_1 = m_8 + \frac{v\_m}{r} \cdot \left(\frac{P_1}{T_1} - \frac{P_8}{T_8}\right) \tag{71}$$

Mode 2: two-stroke pneumatic ideal motor cycle. The ideal two-stroke ideal pneumatic motor mode cycle is shown in Figure 9. The following equations describe the cycle.

The process from 1 to 2 is isobaric intake at tank pressure, P_{tank}. This gives

$$P_2 = P_1 = P_{tank} \tag{72}$$

The application of the first law of thermodynamics to this process gives

$$m_2 \cdot u_2 - m_1 \cdot u_1 = (m_2 - m_1) \cdot h_1 - P_{tank} \cdot (V_2 - V_1) \tag{73}$$

Therefore,

$$m_2 \cdot c\_v \cdot T_2 - m_1 \cdot c\_v \cdot T_1 = (m_2 - m_1) \cdot c\_p \cdot T_1 - P_{tank} \cdot (V_2 - V_1) \tag{74}$$

Developing this equation gives

$$m_2 = \frac{P_{tank} \cdot V_2}{r \cdot T_{tank}} - m_1 \cdot \left(\frac{T_1}{\gamma \cdot T_{tank}} - 1\right) - \frac{P_{tank} \cdot V_1}{c\_p \cdot T_{tank}} \tag{75}$$

Moreover, using the perfect gas law, we obtain

$$T_2 = \frac{P_{tank} \cdot V_2}{m_2 \cdot r} \tag{76}$$

The process from 2 to 3 is adiabatic expansion. This gives

$$P_3 = P_2 \cdot \left(\frac{V_2}{V_3}\right)^{\gamma} \tag{77}$$

Moreover,

$$T_3 = T_2 \cdot \left(\frac{V_2}{V_3}\right)^{\gamma - 1} \tag{78}$$

knowing that

$$m_3 = m_2 \tag{79}$$

The process from 3 to 4 is an isochoric exhaust. This gives

$$P_4 = P_{exh} \tag{80}$$

The application of the first law of thermodynamics to this process gives

$$m_4 \cdot u_4 - m_3 \cdot u_3 = (m_4 - m_3) \cdot h_4 \tag{81}$$

The development of this equation gives

$$T_4 = \frac{m_3 \cdot c\_v \cdot T_3 + P_4 \cdot V_4}{m_3 \cdot cp} \tag{82}$$

Moreover, using the perfect gas law, we obtain

$$m_4 = \frac{P_4 \cdot V_4}{r \cdot T_4} \tag{83}$$

The process from 4 to 5 is isobaric at intake pressure P_{exh}. This gives

$$P_5 = P_{exh} \tag{84}$$

The application of the first law of thermodynamics to this process gives

$$m_5 \cdot u_5 - m_4 \cdot u_4 = (m_5 - m_4) \cdot h_5 - P_{exh} \cdot (V_5 - V_4) \tag{85}$$

Therefore,

$$m_5 \cdot c\_v \cdot T_5 - m_4 \cdot c\_v \cdot T_4 = (m_5 - m_4) \cdot c\_p \cdot T_5 - P_{exh} \cdot (V_5 - V_4) \tag{86}$$

The development of this equation gives

$$T_5 = \frac{P_{exh} \cdot V_5 + m_4 \cdot c\_v \cdot T_4 - P_{exh} \cdot (V_5 - V_4)}{m_4 \cdot c\_p} \tag{87}$$

Moreover, using the perfect gas law, we obtain

$$m_5 = \frac{P_{exh} \cdot V_5}{T_5 \cdot r} \tag{88}$$

The process from 5 to 6 is adiabatic compression. This gives

$$P_6 = P_5 \cdot \left(\frac{V_5}{V_6}\right)^{\gamma} \tag{89}$$

Moreover,

$$T_6 = T_5 \cdot \left(\frac{V_5}{V_6}\right)^{\gamma - 1} \tag{90}$$

knowing that

$$m_6 = m_5 \tag{91}$$

The process from 6 to 1 is isochoric filling. This gives

$$P_1 = P_{tank}$$

The application of the first law of thermodynamics to this process gives

$$m_1 \cdot u_1 - m_6 \cdot u_6 = (m_1 - m_6) \cdot h_{tank} \tag{93}$$

Therefore,

$$m_1 \cdot c\_v \cdot T_1 - m_6 \cdot c\_v \cdot T_6 = (m_1 - m_6) \cdot c\_p \cdot T_{tank} \tag{94}$$

The development of this equation gives

$$T_1 = \frac{P_1}{(P_1 - P_6)/(\gamma \cdot T_{tank}) + P_6/T_6} \tag{95}$$

Moreover, using the perfect gas law, we obtain

$$m_1 = m_6 + \frac{v\_m}{r} \cdot \left(\frac{P_1}{T_1} - \frac{P_6}{T_6}\right) \tag{96}$$

Mode 3: four-stroke pneumatic–combustion ideal motor cycle. This cycle is simply a combination of the two preceding cycles. Indeed, it is a conventional combustion mode where the scavenging cycle is replaced by a two-stroke pneumatic motor cycle. The equations describing this mode are therefore the same as developed before.

Mode 4: two-stroke pneumatic ideal pump cycle. The ideal two-stroke ideal pneumatic motor mode cycle is shown in Figure 11. The following equations describe the cycle.

The process from 1 to 2 is adiabatic compression. This gives

$$P_2 = P_1 \cdot \left(\frac{V_1}{V_2}\right)^{\gamma} \tag{97}$$

Moreover,

$$T_2 = T_1 \cdot \left(\frac{V_1}{V_2}\right)^{\gamma - 1} \tag{98}$$

knowing that

$$m_2 = m_1$$

The process from 2 to 3 is isobaric exhaust at tank pressure P_{tank} characterized by

$$P_3 = P_2 = P_{tank} \tag{99}$$

The application of the first law of thermodynamics to this process gives

$$m_3 \cdot u_3 - m_2 \cdot u_2 = (m_3 - m_2) \cdot h_3 - P_{tank} \cdot (V_3 - V_2) \tag{100}$$

Therefore,

$$m_3 \cdot c\_v \cdot T_3 - m_2 \cdot c\_v \cdot T_2 = (m_3 - m_2) \cdot c\_p \cdot T_3 - P_{tank} \cdot (V_3 - V_2) \tag{101}$$

The development of this equation gives

$$m_3 = \frac{P_{tank} \cdot V_3}{r \cdot T_{tank}} - m_1 \cdot \left(\frac{T_2}{\gamma \cdot T_{tank}} - 1\right) - \frac{P_{tank} \cdot V_2}{c\_p \cdot T_{tank}} \tag{102}$$

Moreover, using the perfect gas law, we obtain

$$T_3 = \frac{P_{tank} \cdot V_3}{m_3 \cdot r} \tag{103}$$

The process from 3 to 4 is adiabatic expansion characterized by

$$P_4 = P_3 \cdot \left(\frac{V_3}{V_4}\right)^{\gamma} \tag{104}$$

where the point 4 is set to obtain $P_4 = P_{int}$. Therefore, the real unknown is V_4 and is calculated by

$$V_4 = V_3 \cdot \left(\frac{P_3}{P_4}\right)^{\frac{1}{\gamma}} \tag{105}$$

T_4 is calculated using the perfect gas law as

$$T_4 = \frac{P_{int} \cdot V_4}{m_4 \cdot r} \tag{106}$$

The process from 4 to 5 is isobaric filling at intake pressure P_{int} characterized by

$$P_5 = P_4 = P_{int} \tag{107}$$

The application of the first law of thermodynamics to this process gives

$$m_5 \cdot u_5 - m_4 \cdot u_4 = (m_5 - m_4) \cdot h_4 - P_{int} \cdot (V_5 - V_4) \tag{108}$$

Therefore,

$$m_5 \cdot c\_v \cdot T_5 - m_4 \cdot c\_v \cdot T_4 = (m_5 - m_4) \cdot c\_p \cdot T_4 - P_{int} \cdot (V_5 - V_4) \tag{109}$$

The development of this equation gives

$$m_5 = \frac{P_{int} \cdot V_5}{r \cdot T_{int}} - m_4 \cdot \left(\frac{T_4}{\gamma \cdot T_{int}} - 1 \right) - \frac{P_{int} \cdot V_4}{c\_p \cdot T_{int}} \tag{110}$$

Moreover, using the perfect gas law, we obtain

$$T_5 = \frac{P_{int} \cdot V_5}{m_2 \cdot r} \tag{111}$$

Appendix 3

Some equation clarifications

Equations (3), (6), (13), (16) and (20) used for calculating work provided by adiabatic process are driven by the application of the first principle of thermodynamics

$$du = dw + dq \tag{112}$$

$$m \cdot c\_v \cdot dt = -P \cdot dv + dq \tag{113}$$

Assuming adiabatic transformation ($dq = 0$), the work w can be written as illustrated in equations (3), (6), (13), (16) and (20).

Equation (25) used for calculating the temperature evolution of the air tank during the charging process can be demonstrated as follows: the variation of the internal energy of the air tank equals the enthalpy of the compressed air provided by the pump

$$du_{tank} = dh_{in} \tag{114}$$

$$\Rightarrow d(m_{tank} \cdot c\_v \cdot T_{tank}) = Q_p \cdot c\_p \cdot T\_p \cdot dt \tag{115}$$

$$\Rightarrow d(m_{tank}) \cdot c\_v \cdot T_{tank} + m_{tank} \cdot c\_v \cdot d(T_{tank}) = Q_p \cdot c\_p \cdot T\_p \cdot dt \tag{116}$$

$$\Rightarrow Q_p \cdot c\_v \cdot T_{tank} \cdot dt + m_{tank} \cdot c\_v \cdot d(T_{tank}) = Q_p \cdot c\_p \cdot T\_p \cdot dt \tag{117}$$

$$\Rightarrow d(T_{tank}) = \frac{Q_p \cdot \left(\frac{c\_p}{c\_v} \cdot T\_p - T_{tank} \right)}{m_{tank}} \cdot dt = \frac{Q_p \cdot (\gamma \cdot T\_p - T_{tank})}{m_{tank}} \cdot dt \tag{118}$$

The same logic is applied to demonstrate equation (27) for calculating the temperature evolution of the air tank during the discharging process. The variation of the internal energy of the air tank equals the enthalpy transmitted to the engine.

$$du_{tank} = dh_{out} \tag{119}$$

$$\Rightarrow d(m_{tank} \cdot c\_v \cdot T_{tank}) = -Q_m \cdot c\_p \cdot T_{tank} \cdot dt \tag{120}$$

$$\Rightarrow d(m_{tank}) \cdot c\_v \cdot T_{tank} + m_{tank} \cdot c\_v \cdot d(T_{tank}) = -Q_m \cdot c\_p \cdot T_{tank} \cdot dt \tag{121}$$

$$\Rightarrow -Q_m \cdot c\_v \cdot T_{tank} \cdot dt + m_{tank} \cdot c\_v \cdot d(T_{tank}) = -Q_m \cdot c\_p \cdot T_{tank} \cdot dt \tag{122}$$

$$\Rightarrow d(T_{tank}) = -\frac{Q_m \cdot \left(\frac{c\_p}{c\_v} - 1 \right) \cdot T_m}{m_{tank}} \cdot dt = -\frac{Q_m \cdot (\gamma - 1) \cdot T_m}{m_{tank}} \cdot dt \tag{123}$$

Appendix 4

Vehicle driving cycles

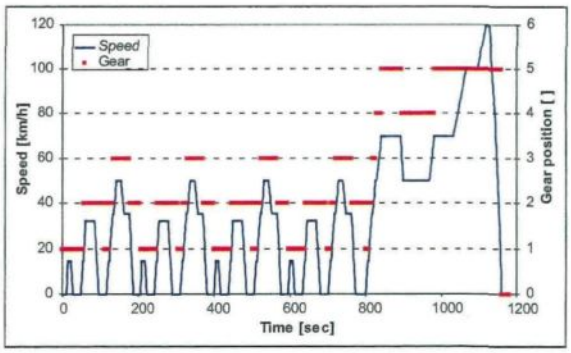

Figure 40. The NEDC.

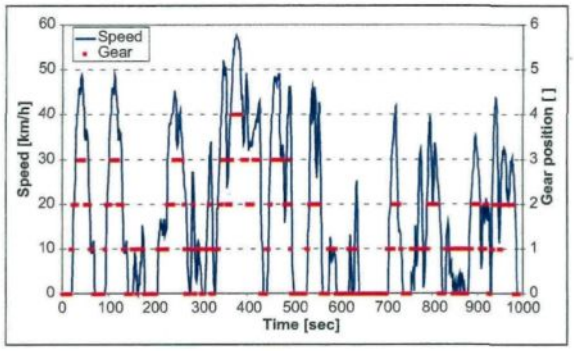

Figure 41. The ARTEMIS urban cycle.

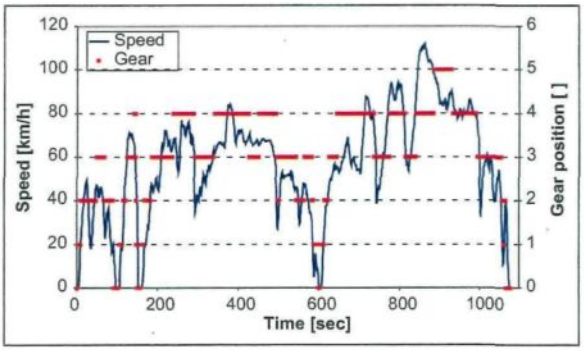

Figure 42. The ARTEMIS rural cycle.

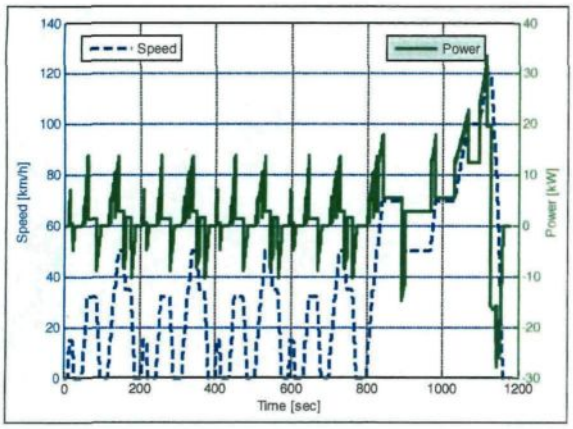

Figure 43. Power needed or available to drive the vehicle on the NEDC.

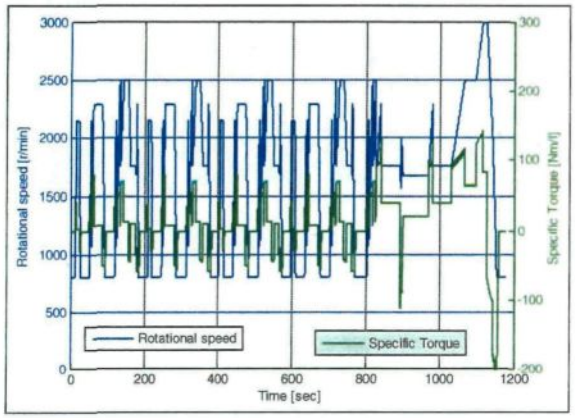

Figure 44. Specific torque and engine speed on the NEDC.

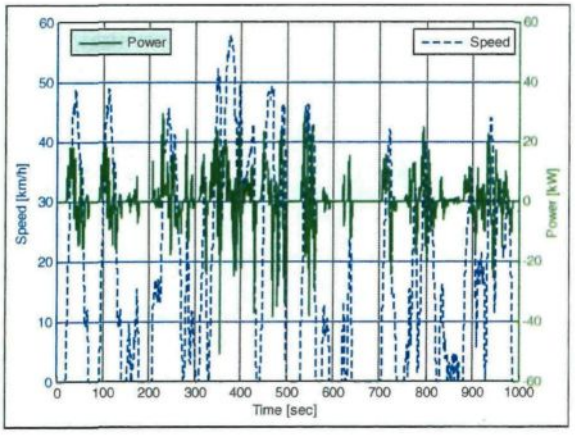

Figure 45. Power needed or available to drive the vehicle on the ARTEMIS urban cycle.

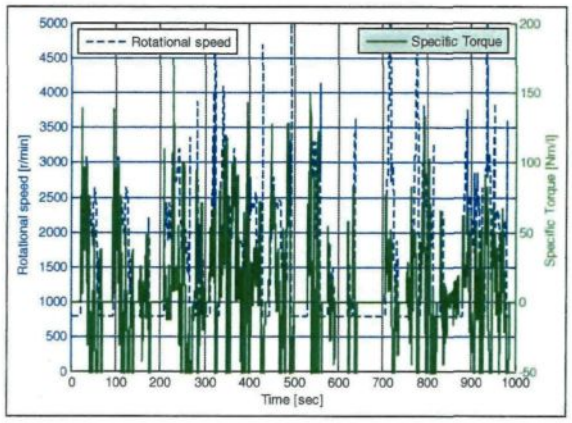

Figure 46. Specific torque and engine speed on the NEDC.

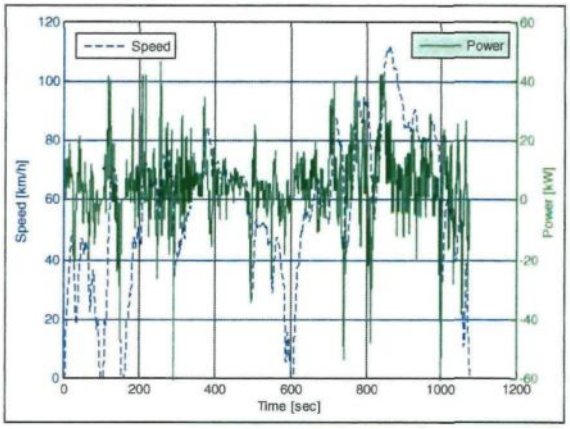

Figure 47. Power needed or available to drive the vehicle on the ARTEMIS rural cycle.

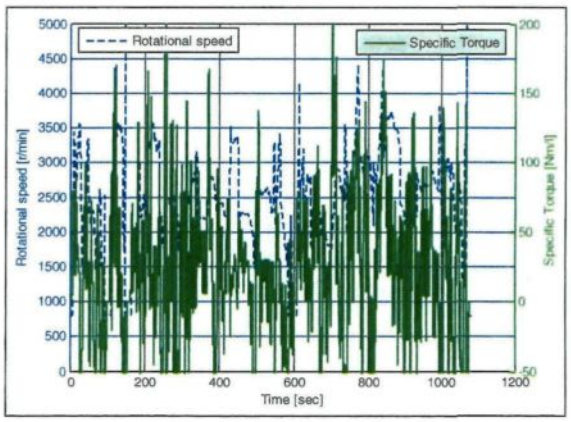

Figure 48. Specific torque and engine speed on the ARTEMIS rural cycle.

CHAPITRE V

Article 4

Required time response of a variable valve actuator equipping a hybrid pneumatic-combustion engine

Publié dans International Journal of Engine Research, octobre 2012
DOI: 10.1177/1468087412450812

Résumé

Cet article présente un dimensionnement du Système de Distribution Variable (SDV) nécessaire pour opérer correctement le Moteur Hybride Pneumatique Diesel (MHPD). Un modèle dynamique d'un SDV électromagnétique, couplé avec un modèle thermodynamique du cycle réel du MHPD, permet de réaliser une étude paramétrique afin d'observer l'impact du Temps de Réponse (TR) du SDV sur l'étendue de l'utilisation possible de chaque mode du MHPD. Cette étude démontre que le couple minimal réalisable en mode moteur pneumatique dépend du TR du SDV. Plus ce TR est élevé plus le moteur aura des difficultés à réaliser les faibles couples en mode moteur pneumatique ; dans ce cas ces points de fonctionnement devraient être réalisé en mode conventionnel, ce qui est clairement un manque d'efficacité du système. Le TR limite au dessus duquel le mode moteur pneumatique ne se comporte plus correctement est inversement proportionnelle au régime de rotation du moteur. Il est de 5 millisecondes pour un moteur fonctionnant à 750 tours par minutes. De la même façon, mais avec une exigence cinq fois plus sévère, le mode pompe pneumatique requiert un TR minimal afin de fonctionner dans des conditions acceptables qui lui permettent de récupérer le maximum d'énergie possible. Pour un MHPD fonctionnant à 750 tr/min le TR minimal requis est de 1 milliseconde.

Original Article

International Journal of ENGINE RESEARCH

International J of Engine Research
13(5) 514–528

DOI: 10.1177/1468087412450812
jer.sagepub.com
SAGE

Required time response of a variable valve actuator equiping a hybrid pneumatic–combustion engine

Tammam Basbous[1,2], Rafic Younes[2,3], Adrian Ilinca[2] and Jean Perron[1]

Abstract

This work is a part of a research program that aims to modify a conventional internal combustion engine and turn it into a hybrid pneumatic–combustion engine. The hybrid pneumatic–combustion engine should be able to convert mechanical energy into compressed air and convert compressed air back into mechanical energy. The potential application for the concept is any use of the internal combustion engine where the load oscillates between a negative and a positive value, such as automobiles and hybrid wind diesel systems for remote area power generation. In the first application, during vehicle decelerations, an excess of power occurs, and a negative load could be applied to the engine, whereas during vehicle accelerations, a positive load is applied. In the second application, if the generated wind power is higher than consumption demand, then the load applied to the engine could be negative, and if the generated wind power is lower than consumption demand, then the load is positive. In previous work, we exposed an optimization followed by a fuel-saving evaluation of a new hybrid pneumatic–combustion engine concept that uses a variable valve actuator system. The optimization of the valve actuation was based on ideal thermodynamic cycle modeling, assuming therefore an instant response of the variable valve actuator system. In the present work, a more realistic analysis of the system is provided by taking into consideration the dynamic response of the variable valve actuator system.

Variable valve actuators have been widely studied for optimizing performance and fuel consumption of the internal combustion engine, especially in spark-ignition engines. For these engines, it is possible to reduce the pumping losses and to optimize the engine filling by controlling the intake and exhaust valve opening and closing angles, as well as their lifts. However, the variation of valve actuation crank angles required in a conventional internal combustion engine is significantly smaller than the one required in the hybrid pneumatic–combustion engine. This paper describes, through simulation, how the valve time response affects the performance of the hybrid pneumatic–combustion engine and recommends a required valve time response.

Keywords

Variable valve actuation, valve time response, pneumatic hybridization, wind diesel system, compressed air energy storage

Date received: 24 November 2011; accepted: 11 May 2012

Introduction

Context

Energy recovery constitutes one of the key solutions to improve the energetic performance of internal combustion engines for different applications where an excess of mechanical energy frequently occurs, such as in automobiles and hybrid wind diesel systems (HWDSs) for power generation.

In automotive applications, conventional engines consume fuel to generate power during acceleration and steady-state modes, whereas in deceleration mode, energy is usually dissipated in brakes.[1–3] Through a dynamic model of a 1500 kg commercial vehicle,[4] we have found that the deceleration energy on the new European driving cycle (NEDC) is about 31% of the

[1]Laboratoire International des Matériaux Antigivre, Université du Québec à Chicoutimi, Canada
[2]Laboratoire de Recherche en Energie Eolienne, Université du Québec à Rimouski, Canada
[3]Faculté de Génie, Université Libanaise, Liban

Corresponding author:
Tammam Basbous, Laboratoire International des Matériaux Antigivre, Université du Québec à Chicoutimi, Chicoutimi, Québec, Canada.
Email: tammam.basbous@uqac.ca

total mechanical energy necessary to move this vehicle. The result of the cumulated energy used for vehicle acceleration and the cumulated recoverable deceleration energy is shown in Figure 1. This means that the fuel consumption may decrease in the same proportion if part of this energy is recovered, stored and used later when needed.

In HWDS applications, diesel engines consume fuel to provide power when the wind power is not sufficient to cover the demand, while a surplus wind electrical power exists during high-wind or low-demand periods.[5,6] This surplus of energy is wasted unless it is recovered and stored for later use. Through a model of a 1 MW HWDS at Tuktoyaktuk, the northern Canadian community, considering a wind power penetration ratio of 1; we have found that wind energy excess during phases of high wind speed and/or low power demand weights up to 12% in total energy demand, as shown in Figure 2. Dissipating this energy means increasing the fuel consumption by approximately the same proportion.[7]

In order to ensure this need for energy storage and recovery, additional electric motors and battery energy storage are usually combined with a diesel engine. This solution is far from being satisfactory, for automotive applications or for power generation applications. For instance, weight is the major weakness of this solution for automotive applications. The mass of the added components offsets a part of the reduction in fuel consumption that they are designed to produce.[1] Another major issue to be considered is the added cost. Reliable battery packs and electric motors are expensive, which means that a return on investment would be very difficult.[8–10] For this reason, hybrid vehicles would be less popular without fiscal reductions or ecologic bonuses offered by governments for those who decide to drive a hybrid. The same issue occurs in power generation where battery packs that can deliver hundreds of kilowatts and store dozens of megawatts hours are extremely expensive and are, in addition, not reliable.

Objectives of the research program

One solution to the problem of energy recovery discussed above is to use the internal combustion engine as a hybrid engine combining a conventional combustion operation and a pneumatic operation and to connect it to an air storage tank. The engine can therefore be used as a pneumatic pump when energy is in excess and store this energy as compressed air in the tank. This stored energy can be discharged later, either through a pneumatic operation or through a hybrid pneumatic–combustion operation of the engine. Pneumatic hybridization of internal combustion engines is an alternative to electric hybridization, which requires the use of expensive, sensitive and heavy batteries.

Our research program aims at suggesting the modification of a conventional internal combustion engine (ICE) to turn it into a hybrid pneumatic–combustion engine (HPCE). In order to make the solution economically feasible, the modification rate from the original specification should be as low as possible. Any solution that requires modification of the architecture (cylinder block, cylinder head, etc.) of the engine should be aborted.

Suggested concept

The concept that we suggest is based on bypassing the turbocharger and connecting an air tank to the intake valve by using two three-way valves, as shown in Figure 3.

The first three-way valve connects the ICE's inlet to either the air tank or the compressor's outlet, while the second three-way valve connects the ICE's exhaust

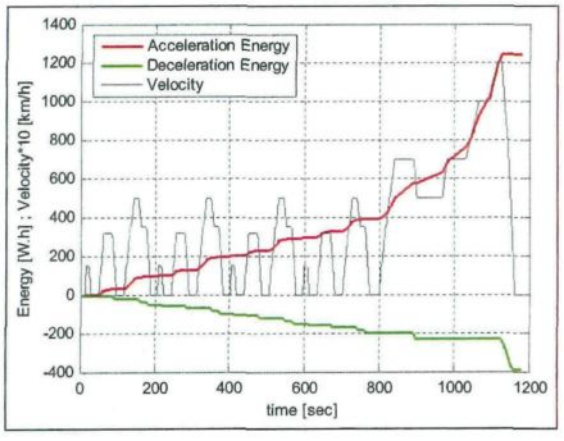

Figure 1. Recoverable energy compared to positive energy on the NEDC.

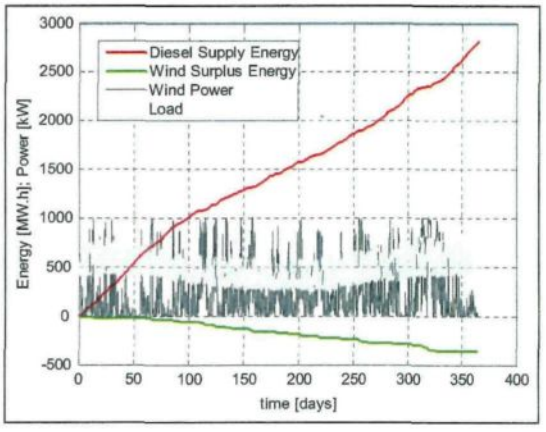

Figure 2. Recoverable energy compared to positive energy for power generation application on Tuktoyaktuk site – wind speed measured during the year 2007.

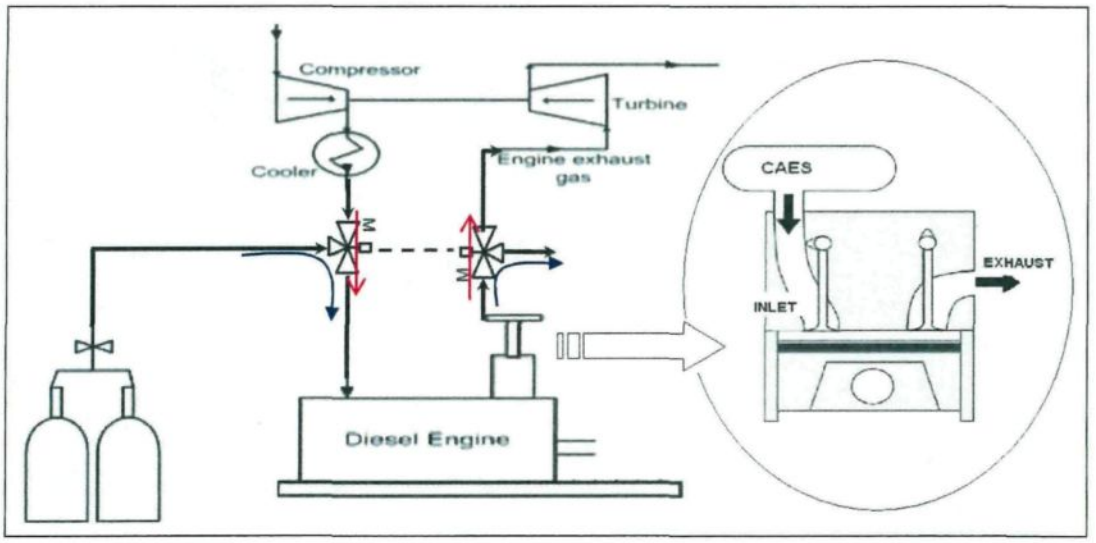

Figure 3. Suggested pneumatic concept.

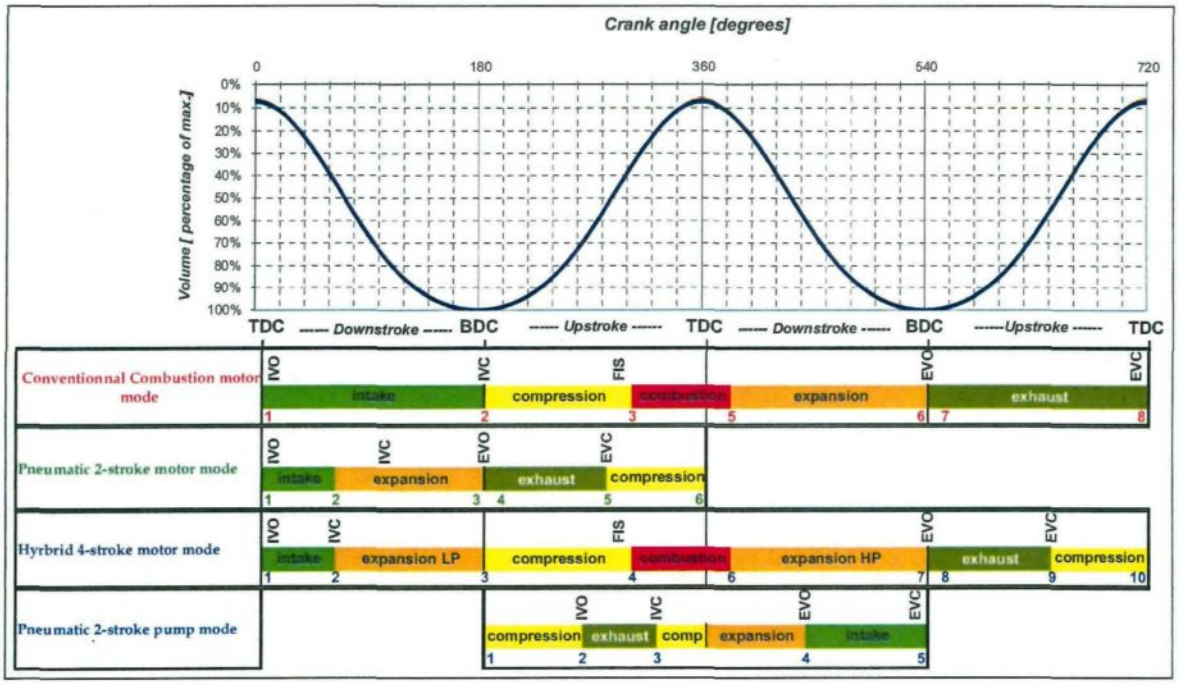

Figure 4. Operating principles of suggested pneumatic concept.

either to the turbine's inlet or to the atmosphere. The concept requires full control of the intake valves, the exhaust valves and the fuel injectors. The concept is able to operate with the four modes illustrated in Figure 4.

Mode 1: four-stroke conventional combustion motor mode. The three-way valves connect the turbocharger to the inlet and the exhaust of the engine. The cycle lasts for two rounds of the piston. The intake valve is open during the whole piston's way down (1→2) of the first stroke. When the piston gets to the bottom dead center (BDC), the compression phase (2—3) starts. A few degrees before the top dead center (TDC), the fuel starts to be injected (FIS). The combustion phase (3→5) starts a few degrees later and finishes a few degrees after TDC. After combustion, the expansion phase (5→6) occurs during the piston's way down until it reaches the BDC. At BDC, the exhaust valve opens and the exhaust phase (6→8) occurs during the piston's way up. At TDC, the exhaust valve closes. The intake and exhaust pressure are set by the turbocharger.

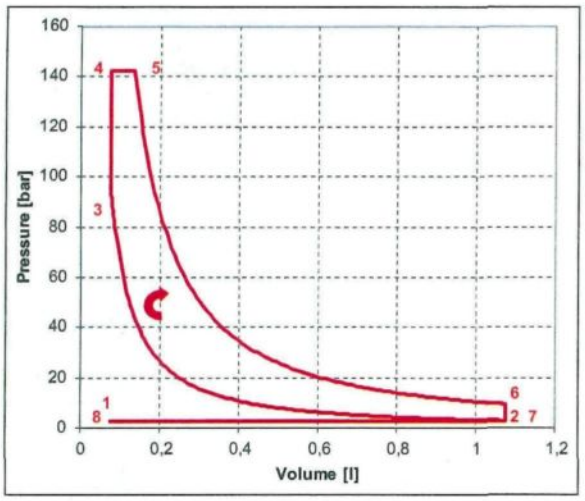

Figure 5. Illustration of the ideal four-stroke conventional combustion cycle.

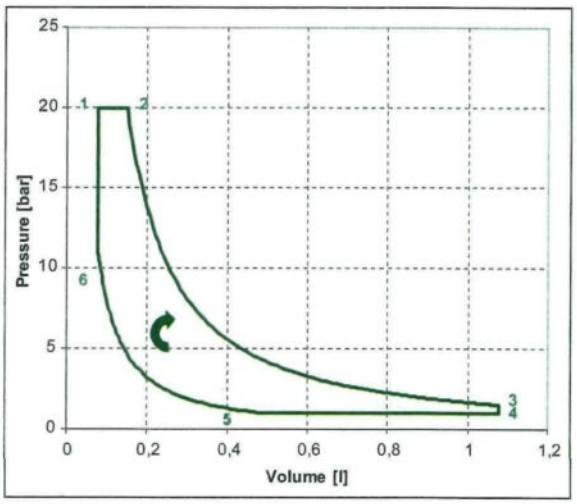

Figure 6. Illustration of the ideal two-stroke pneumatic motor cycle.

Figure 5 illustrates the ideal thermodynamic cycle of this operating mode.

Mode 2: two-stroke pneumatic motor mode. The three-way valves disconnect the turbocharger and connect the intake of the engine to the air tank and the exhaust to the atmosphere. The intake pressure is equal to the air storage pressure, while the exhaust pressure is equal to the atmospheric pressure. The fuel injection is disabled. The cycle lasts only one piston round. At TDC, the intake valve opens and closes shortly after, therefore enabling an admission phase (1→2). Then, an expansion phase (2→3) starts and lasts until the piston reaches BDC. Then, the exhaust valve opens and enables the exhaust phase (3→5) during the piston's way up. Somewhere between BDC and TDC, exhaust valve closes and a compression phase starts (5→6) until the piston reaches TDC. Figure 6 illustrates the ideal thermodynamic cycle relative to this operating mode.

Mode 3: four-stroke hybrid pneumatic–combustion motor mode. The three-way valves disconnect the turbocharger and connect the intake of the engine to the air tank. The intake pressure is equal to the air storage pressure. The intake valve is open during part of the piston's way down of the first stroke, enabling the intake phase (1→2). Somewhere between TDC and BDC, the intake valve closes, and an expansion phase (2→3) starts. When the piston gets to BDC, the operation continues exactly as in the conventional mode. Figure 7 illustrates the ideal thermodynamic cycle relative to this operating mode. This mode operates normally, even with diesel engines because fuel injection can start any time during the piston compression between points 3 and 4, in order to ensure that the fuel burn starts when required for obtaining the best cycle efficiency.

Mode 4: Two-stroke pneumatic pump mode. This mode is the reverse of the two-stroke pneumatic motor mode. The three-way valve is in the same position, and the engine runs in the same way. However, by changing

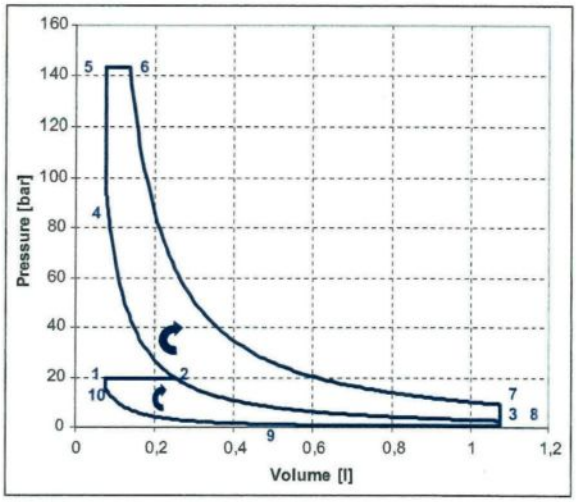

Figure 7. Illustration of the ideal four-stroke hybrid pneumatic–combustion motor cycle.

the intake and exhaust valve timings, low-pressure air is admitted through the exhaust valve, and high-pressure air is rejected through intake valve. Compressed air can therefore be stored in the tank. In this mode, fuel injection is disabled. The compression phase (1→2) starts at BDC and lasts until the intake valve opens, somewhere between BDC and TDC, therefore enabling the exhaust phase (2→3). The intake valve closes a few degrees after it opens. The intake valve closing (IVC) angle will have to be dynamically adjusted for maximum braking energy recovery. If the available torque is high enough, IVC occurs at TDC in order to compress the maximum possible air quantity. If the available torque is relatively low, IVC occurs before TDC, therefore reducing the compressed air quantity, as well as the work needed for the

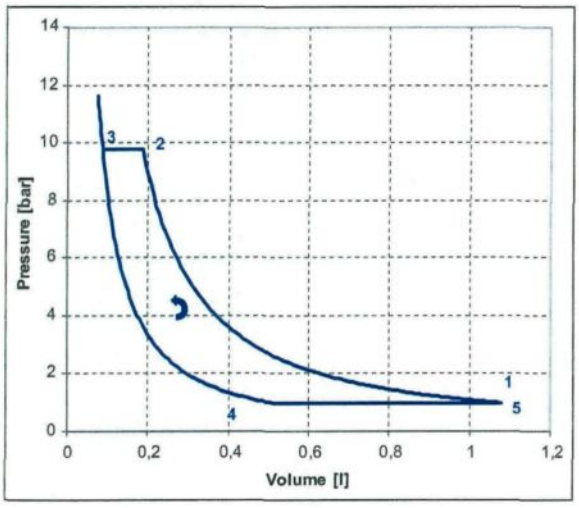

Figure 8. Illustration of the ideal pneumatic two-stroke pump cycle.

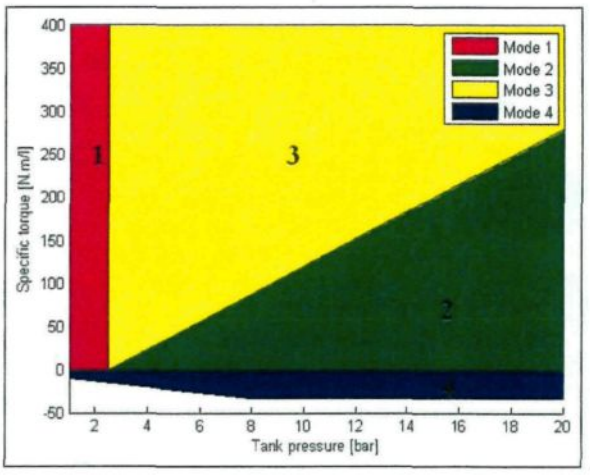

Figure 9. Mode selection for an ideal HPCE.

compression. After IVC, an expansion phase (3→4) occurs during the piston's way down in the first case (IVC at TDC), and a compression phase followed by an expansion phase occurs during the piston's way up then down in the second case (IVC before TDC). Somewhere between TDC and BDC, the cylinder air pressure becomes exactly equal to atmospheric pressure. At that moment, the exhaust valve opens and enables the intake phase (4→5). Fresh air therefore fills the cylinder until the piston gets to BDC when the exhaust valve closes. Figure 8 illustrates the ideal thermodynamic cycle relative to this operating mode.

Finally, Table 1 presents a synthesis of the optimizing parameters and the fixed commands in each of the four modes.

Objective and methodology of current paper

In previous work,[4] a parametric optimization based on ideal cycle modeling of the HPCE concept has been conducted and led to the definition of the zones of each mode's operation as a function of tank pressure and specific torque needed, as illustrated in Figure 9.

It has been stated[4] that the fuel consumption on the NEDC of a 1500 kg vehicle could be reduced by 17% if the conventional ICE is turned into an HPCE operating with this strategy (Figure 9) and combined with a 100 l tank. In the ideal cycle modeling used for this evaluation, the valves opening and closing, as well as the mass transfer, are considered to be instantaneous. Nevertheless, it is known that a valve's actuation is never instantaneous, but it has a time response that depends on the characteristics of the actuators and on the engine speed. It is also known that the flow rate through the valves is not instantaneous, but it depends on the differential pressure and on the valve's effective area. The objective of the present paper is to define the minimum requirement of the valve's actuation time response to have an acceptable performance of the HPCE and thus, a significant fuel economy.

To reach this objective, a real cycle model of modes 2 and 4 is established. This model takes into consideration the intake and exhaust valve dynamics as well as the flow rate through these valves. Different possible values of valve time response (VTR) are investigated. For each VTR, the maximum and minimum possible torque is calculated as a function of the tank pressure. Once the operating domains of modes 2 and 4 are drawn, the zones of operation of modes 1 and 3 can be deduced.

Table 1. Parameters for each mode of the HPCE concept.

Mode	Parameters				
	Qf	IVO	IVC	EVO	EVC
Conventional	o	x	x	x	x
Two-stroke pneumatic motor mode	-	x	o	x	o
Four-stroke hybrid motor mode	o	x	o	x	o
Two-stroke pneumatic mode	-	o	o	o	o

EVC: exhaust valve closing; EVO: exhaust valve opening; IVC: intake valve closing; IVO: intake valve opening; Qf: quantity of injected fuel.
o: optimizing parameter; x: fixes parameter; - not concerned.

State of art review

Review of recent work on HPCE concepts

Lately, different concepts of pneumatic hybridization have been studied. Donitz et al.[1] created a fully operational hybrid pneumatic engine, able to operate under a two-stroke pneumatic motor mode (non-fired), four-stroke pneumatic motor mode (non-fired), two-stroke pneumatic pump mode (non-fired), four-stroke pneumatic pump mode (non-fired), supercharged mode (fired) and conventional mode (fired). This concept is accomplished by connecting an air pressure tank to all cylinders via an electronic fully controlled charge valve.[8] The original intake and exhaust valves should also be electronically controlled. Test results on a spark-ignition engine demonstrator, supported by modeling analysis,[8] showed viability of this new concept for fuel consumption reduction, when combined with a strong downsizing and supercharging of the engine. Compared to a naturally aspirated engine with the same rated power, the downsized and supercharged hybrid pneumatic engine can save 32% of the fuel.[1] The strong downsizing is possible owing to pneumatic hybridization because the problem of the 'turbo-lag', usually associated with heavily downsized and supercharged engines, is completely overcome by injecting additional air from a pressure tank and more fuel during transients.[1] Experiments have verified the engine's instantaneous torque response resulting from applying this supercharged mode.[1]

Higelin et al.[9,10] studied a similar concept and concluded, using simulations of the theoretical thermodynamic cycles, that fuel consumption on the NEDC could be reduced by up to 31% if all the parameters, including the tank volume, were optimized.[10] This concept is promising in terms of energetic performance, cost and weight; however, it requires heavy modifications of the engine's hard architecture because a charge valve has to be added. This cannot be done by simply adjusting an existing ICE. It is therefore not possible to suggest this concept as an option in vehicle power train in order to reduce fuel consumption. Moreover, this concept is validated for spark-ignition engines, and there are reasons to believe that it might not work adequately with diesel engines, mainly for hybrid pneumatic–combustion operations. Indeed, compressed air is charged in the cylinder during the compression phase. Then, the fuel is injected and needs to start burning few degrees before the piston reaches the TDC. Considering that in diesel engines, the ignition delay has to pass before the fuel starts burning, it is quite difficult to ensure the burn of enough fuel before the TDC, which will probably compromise the system efficiency. Obviously, this might be the reason why all the tests conducted on this system were made on spark-ignition engines. In addition, other researchers worked on simpler concepts of pneumatic hybridization, but all of them focused on two-stroke pure pneumatic motor and pump operations.

Kang et al.[11] suggested a concept based on connecting the compressed air tank to the exhaust manifold and using a three-way valve to switch flow between the turbine and the air tank. It does not require a specific valve to inject the compressed air. It requires, however, a complete change in valve timing for both the air compressor and air motor two-stroke modes. This is accomplished through a cam-less hydraulically actuated valve system.

The air-power-assist (APA) engine was tested at steady state in compressor mode and in motor mode. The tests confirmed the functionality of the concept. The APA engine demonstrated air compression and high-pressure air storage in the air tank by controlling the valve timing and using the air handling system. The APA engine generated positive power by using the compressed air from the air tank without injecting fuel.[11] The APA engine can be converted by applying a simple modification to an existing engine. Its performance, however, is limited to pneumatic operation. Hybrid operation, which combines pneumatic power with fuel power, is not possible.

Moreover, Trajkovic et al.[2,3,12] converted a single-cylinder Scania D12 diesel engine to a pneumatic hybrid diesel one. The concept requires having a variable valve actuator (VVA) system, and it can operate under conventional diesel mode as well as two-stroke pneumatic motor and pneumatic pump modes. Trajkovic et al. conducted an optimization on valve actuation timing and obtained up to 48% of regenerative efficiency under steady-state operation. Later, Trajkovic et al. compared testing measures to GT-Power simulation results. The correlation was carried out for both pneumatic modes, and it showed a 5% error in steady-state operations.[12] We notice that this study was conducted using a tank pressure of not more than 8 bar.

Lee et al.[13] worked on a novel cost-effective air hybrid powertrain concept for buses and commercial vehicles. The concept is simple because it requires only a few modifications to the intake of the engine by adding two one-way valves and an air tank. The concept does not require any change to the initial intake and exhaust valves of the engine. However, the concept can only operate under conventional mode, compressor mode and cranking mode. The last mode is a four-stroke pneumatic motor mode. The storage pressure is of the order of 8 bar. The simplicity and the cost effectiveness constitute the main strength of the concept, but not the hoped for fuel economy.

Review of recent works on VVA systems

VVAs have been widely studied for optimizing performance and fuel consumption of ICEs, especially spark-ignition engines, where reducing the pumping losses and optimizing the engine filling can be obtained by controlling the intake and exhaust valves opening and closing angle, as well as their lift. The devices may generally be included in four main categories: mechanical (includes cam phasers and three-dimensional cams), electro-hydraulic, electro-mechanical and motor driven

systems.[14] The degree of flexibility of the various systems is different. It may include: valve timing variation, valve lift and event variation, single port deactivation and cylinder deactivation.[14]

Most of this research has been driven by the automotive industry. Among the first developed arrangements are the cam phasers, often combined with profile switching systems,[15–17] in order to obtain some flexibility for both timing and lift variation demands. This technique is currently applied in more than one production engine. Different systems capable of continuously variable lift and timing are proposed or still under development[18–21] by BMW (Valve-tronic), Meta (VVH system), Nissan (VEL) and Fiat (Uni-Air). All the mentioned systems are cam driven. A further improvement of the VVA concept application is then represented by the development of cam-less devices, based on electromagnetic, electro-hydraulic or electro-pneumatic systems. While the first ones present some problems, such as those related to the valve position in failure mode or to the seating velocity, systems based on hydraulic actuators (Lotus-Eaton, AVL-Bosch, Sturman, Cargine Engineering, Ford[22–27]) appear to be more promising, showing potentially good performances in terms of lift and time control, along with other operative advantages, while the main drawback is represented by the power consumption limitation.

Model of the HPCE pneumatic operations

The main equations originate from mass and heat conservation, as well as the ideal gas assumptions.[28,29] The application of the first law of thermodynamics and the ideal gas law to the control volume results in a differential equation[29] that drives all the thermodynamic transformations

$$m \cdot du + u \cdot dm = -\frac{m \cdot R \cdot T}{V} \cdot dV + \sum_s dQ_s + \sum_i h_{oi} \cdot dm_i \quad (1)$$

This equation has to be solved iteratively, and so it is necessary to solve the following sub-models.

Gas properties

The gas properties are required as a function of temperature and composition. For individual species, the internal energy can be expressed as a function of temperature by means of a polynomial expansion with either a molar or a specific basis[29]

$$u_i(T) = \sum_{j=0}^{n} (a_j \cdot T^j) \quad (2)$$

where a_j is found in the JANAF thermodynamic tables.[30] For a mixture of z species, the global internal energy is calculated using the fraction method

$$u(T) = \sum_{i=0}^{z} (\alpha_i \cdot u_i(T)) \quad (3)$$

The same method is commonly used to calculate the specific stagnation enthalpy h.

Valve dynamic model

The electro-magnetic valve can be modeled using a simple mechanical system composed of a mass coupled through spring and damping elements to a fixed position, as shown in Figure 10.

Assuming that the reference of the valve position is the equilibrium of the system without applying any electro-magnetic force, the differential equation that drives the displacement of the valve is

$$m \cdot \frac{d^2x}{dt^2} + k \cdot x + c \cdot \frac{dx}{dt} = F \quad (4)$$

The homogeneous equation of this open-loop second-order system can be written as

$$\frac{d^2x}{dt^2} + 2 \cdot \zeta \cdot w_n \cdot \frac{dx}{dt} + w_n^2 \cdot x = 0 \quad (5)$$

where the natural frequency w_n can be expressed as

$$w_n = \sqrt{\frac{k}{m}} \quad (6)$$

and the damping ratio ζ can be expressed as

$$\zeta = \frac{c}{2\sqrt{k \cdot m}} \quad (7)$$

In order to prevent overshoot and have a smooth landing of the valve, the damping coefficient c needs to be chosen adequately to have a critically damped system($\zeta = 1$), which gives

$$c = 2\sqrt{k \cdot m} \quad (8)$$

under the following assumptions:

(a) the electro-magnetic time response of the flux's establishment is very small compared to the mechanical time response of the system's motion;
(b) the force applied by the pressurized gas on the valve is not significant.

The response of this critically damped system for a unit step order can be written as

$$x = \frac{1}{w_n^2} \cdot (1 - e^{-w_n t} - w_n t \cdot e^{-w_n t}) \quad (9)$$

The VTR is defined as the time needed until the valve reaches 95% of its final value. The VTR of a critically damped second-order system is illustrated in Figure 11. It can be calculated using

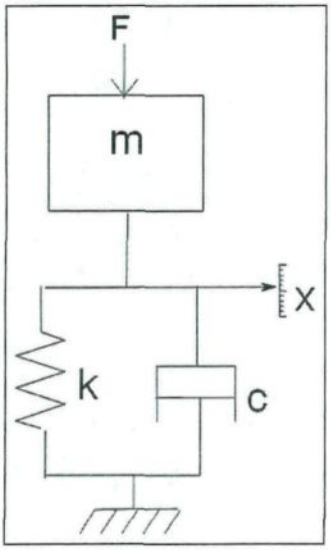

Figure 10. Electro-magnetic valve simplified dynamic model.

$$\mathrm{VTR} = \frac{5}{w_n} \tag{10}$$

The value of w_n and k are therefore defined to reach the required VTR

$$w_n = \frac{5}{\mathrm{VTR}} \tag{11}$$

$$k = \frac{25m}{\mathrm{VTR}^2} \tag{12}$$

Finally, the electro-magnetic force (F) to be applied can be set to meet the required valve lift (l) using

$$l = \lim_{t\to\infty}(F \cdot x) = F \cdot \frac{1}{w_n^2} = \frac{F \cdot m}{k} \tag{13}$$

Therefore,

$$F = \frac{k \cdot l}{m} \tag{14}$$

Unlike conventional engines where the valves are driven by a camshaft hardly connected to the crankshaft, the HPCE's valves are driven by a cam-less VVA system. The motion of the valves is therefore not strictly connected to the crankshaft angular position. The valve's position function of the angular position depends on the valve energizing time (VET) and the rotational speed. The valve angular response (VAR) is defined as the equivalent of the VTR, expressed in terms of crank angular variation. The VAR can be written as a function of the VTR and the engine speed N as

$$\mathrm{VAR} = 6 \times N \times \mathrm{VTR} \tag{15}$$

where VAR is expressed in crank degrees, VTR in seconds and N in revolutions per minute.

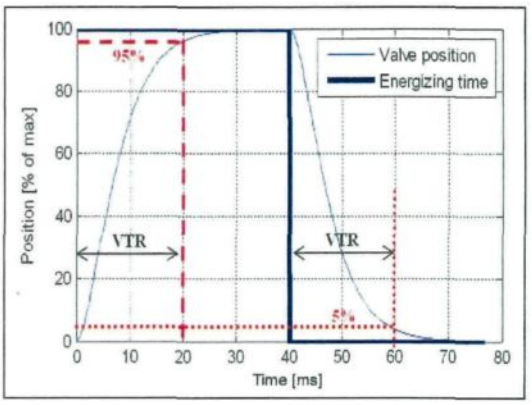

Figure 11. Illustration of VTR during valve opening and closing.

Mass-transfer model

The mass conservation equation is used to calculate the mass and the equivalence ratio evolution in the control volume, which is the combustion chamber,[28]

$$\frac{dm}{dt} = \frac{dm_{\mathrm{int}}}{dt} + \frac{dm_{\mathrm{exh}}}{dt} \tag{16}$$

where int refers to the intake air and exh refers to the exhaust gas.

When a valve, either the intake or exhaust one, is opened, the air flow circulates from the highest pressure to the lowest pressure side of this valve. The air flow rate can be calculated using the Barré Saint-Venant model[29]

$$\frac{dm}{dt} = A \times P_{\mathrm{high}} \times \sqrt{\frac{2\gamma_{\mathrm{high}}}{(\gamma_{\mathrm{high}} - 1) \times r_{\mathrm{high}} \times T_{\mathrm{high}}}} \times \left[X^{\frac{2}{\gamma_{\mathrm{high}}}} - X^{\frac{\gamma_{\mathrm{high}}+1}{\gamma_{\mathrm{high}}}}\right] \tag{17}$$

where X is the maximum found between two values,

$$X = \max\left(\frac{P_{\mathrm{low}}}{P_{\mathrm{high}}}; \left(\frac{2}{\gamma_{\mathrm{high}} + 1}\right)^{\frac{\gamma_{\mathrm{high}}}{\gamma_{\mathrm{high}}-1}}\right) \tag{18}$$

where high and low refer, respectively, to the highest pressure side and the lowest pressure side of the valve.

Kinematical model

The volume delimited by the piston, the cylinder wall and the cylinder head can be calculated as a function of the angular position of the crankshaft θ[32]

$$V = \frac{\pi D^2}{8} \times L\left(1 + \frac{S}{2L} - \cos\theta - \sqrt{\left(\frac{S}{2L}\right)^2 - \sin^2\theta} + \frac{2}{\varepsilon - 1}\right) \tag{19}$$

Therefore, the variation of the volume can be calculated as a function of time using

$$\frac{dV}{dt} = \frac{\pi D^2}{8} \times L \times \sin\theta \times \left(\frac{\cos\theta}{\sqrt{\left(\frac{S}{2L}\right)^2 - \sin^2\theta}} + 1 \right) \times \frac{d\theta}{dt} \quad (20)$$

In the current simulation, the characterizing parameters are $S/L = 0.33$, $S/D = 0.82$, $\varepsilon = 14$ and $N = 750$ r/min.

Results

Understanding the response of the VVA system, the function of VTR and engine speed

The valve opening profile (VOP) is a function describing the valve lift function of the crank angle. Unlike the conventional ICE, the VOP of the HPCE depends on the rotational speed. Figure 12 illustrates the VOP for a 1 ms VTR valve, at different engine speeds, for a valve energizing angle (VEA) of 10 crank degrees. One can observe that the angular delay to open the valve and to close it is higher, and the maximal valve position is lower, when the engine speed is higher.

Indeed, it is the VAR, and not the VTR, that defines the form of the thermodynamic cycle. The requirement to have a good performance of the HPCE should therefore be expressed in terms of VAR. The required VTR is deduced taking into consideration the engine speed.

The maximal engine speed varies from one application to another. It is around 8000 r/min for a conventional vehicle gasoline engine, 6000 r/min for a conventional vehicle diesel engine, 1500 r/min for a medium-speed diesel power plant engine, and 750 r/min for a low-speed diesel power plant engine.

In the rest of the study, the engine speed is fixed at 750 r/min. The minimum VTR is calculated for 750 r/min, then deduced for each application as a function of its own maximal speed using equation (15)

Figure 13 shows the VOP of different VTR valves, for 30° VEA, at 750 r/min. The full valve opening is reached only for VTR values lower than 5 ms. For 20 ms VTR, the open-loop control of the VVA appears to be delicate as the angular delay between the VEA and VOP is very high.

Figure 14 illustrates the response of a VVA having 10 ms VTR for different VEA values. The valve lift and opening angle both increase when the VEA increases. The maximum lift is reached for an VEA higher than 50 crank degrees.

Figures 15 and 16 show, respectively, the valve effective open angle (VEOA) and the valve maximal position as functions of the VEA, for different VTR values.

As observed in Figure 15, the higher the VTR, the harder the control of the brief valve openings. For instance, if a VTR of 20 ms is used, a brief VEA of 3 crank degrees (equivalent to a VET of 100 μs at 750 r/min) results in 80 crank degrees of effective valve opening. Consequently, the controllable range of the valve corresponds to the near-linear part of each curve

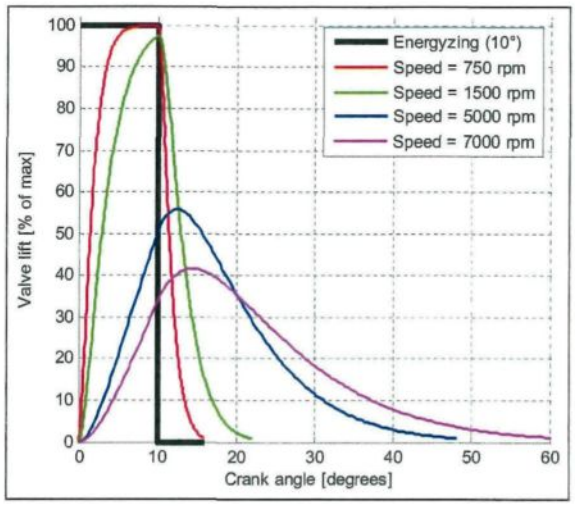

Figure 12. VOP of a 1 ms VTR valve, for 10° VEA, at different engine speeds.

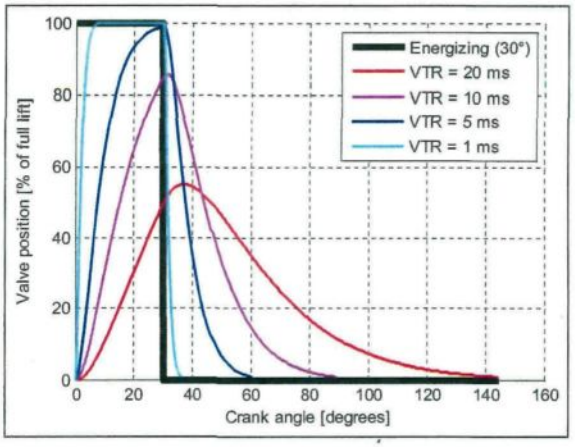

Figure 13. VOP of different VTR valves, for 30° VEA, at 750 r/min.

of Figure 15. Thus, the minimal energizing crank angles for a 20 ms VTR valve, a 10 ms VTR valve, a 5 ms VTR and a 1 ms VTR valve are, respectively, 10°, 5°, 3° and 0.5° for a 750 r/min engine. The effective opening angles are then, respectively, 110°, 55°, 30° and 5°. Moreover, one can observe in Figure 16 that the slower the valve actuator, the lower the maximal valve position for a certain VEA. Full valve opening is reached for a minimal VEA of 5°, 30°, 60° and 110°, for the different values of VTR, respectively.

Effect of VTR on the two-stroke pneumatic motor mode, at 750 r/min

As explained in the previous section, the minimal possible IVC and exhaust valve closing (EVC) angles depend on the VTR. This limitation results in a limitation for

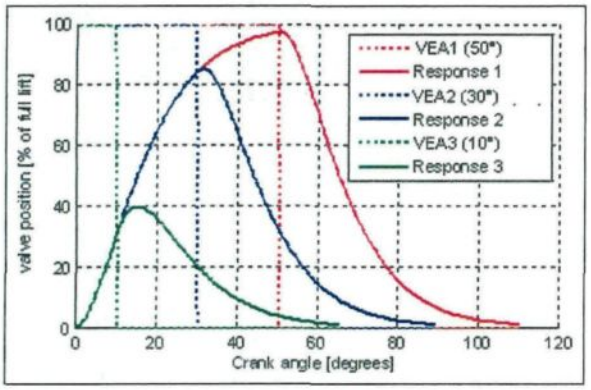

Figure 14. VOP of a 10 ms VTR valve, for different VEA valves, at 750 r/min.

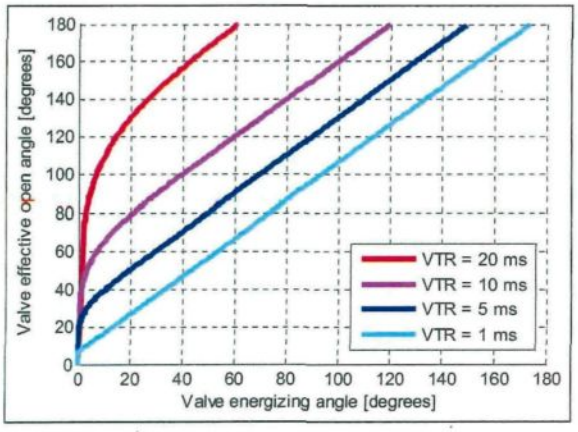

Figure 15. VEOA as a function of VEA, at 750 r/min, for different VTR valves.

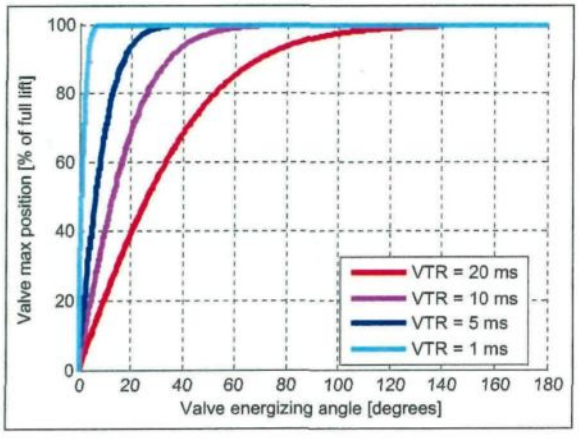

Figure 16. Valve maximal position as a function of VEA, at 750 r/min, for different VTR valves.

the minimal possible torque in the two-stroke pneumatic motor mode. Note that to reduce the torque, the IVC angle is reduced. When the IVC angle is at its minimal value, it is still possible to reduce the EVC angle to further reduce the torque. The minimal IVC angle reached when at least one of the following conditions is satisfied:

(a) the VEA reaches the minimum identified above;
(b) the pressure at the end of the expansion phase is lower than the atmospheric pressure. In this case, the cycle efficiency and therefore the specific air consumption (SAC) are highly decreased.

The minimal EVC angle is reached when at least one of the following conditions is satisfied:

(a) the VEA reaches the minimum identified above;
(b) the pressure at the end of the compression phase is higher than the tank pressure. If so, the cycle efficiency and therefore the SAC are highly decreased.

Under these assumptions, the minimal specific torque (TS) obtained for a tank pressure of 20 bar using a VTR of 1ms, 5 ms, 10 ms and 20 ms are, respectively, 26 N.m/l, 26 N.m/l, 46 N.m/l and 126 N.m/l, as shown in Figures 17 and 18.

It is worth noting that it is theoretically possible to further reduce the torque if the second condition for the minimal EVC is omitted. The thermodynamic cycle that we would obtain has a clockwise part and an anticlockwise part, as illustrated in Figure 19. As shown in Figure 19, it is possible to achieve a specific torque of 35 N.m/l by using a 20 ms VTR valve, yet the SAC is three times higher than the one obtained with a 5 ms VTR valve. For that reason, this type of operation is forbidden as dissipates the stored energy.

After this detailed analysis, it is possible to draw the zone of operation with a two-stroke pneumatic motor mode, for different possible VTR values, as illustrated in Figure 20. As can observed, the VTR that ensures a maximal zone of operation, nearly equal to the ideal cycle, is 1 ms. However, a VTR of 5 ms is still acceptable because the unfeasible zone is relatively small.

Effect of VTR on the two-stroke pneumatic pump mode, at 750 r/min

In the two-stroke pneumatic pump mode, the minimal possible IVC angle results in limiting the maximal compression ratio and the minimal torque.

During the compression phase, the intake valve remains closed until the pressure in the cylinder reaches the tank pressure. At this precise moment, the intake valve starts opening, while it has to be closed completely at TDC. In other words, the valve should be able to open and close within an angular margin that depends on the compression ratio, as shown in Figure 21. When the minimal IVC angle is higher than the margin that corresponds to a certain compression ratio, this

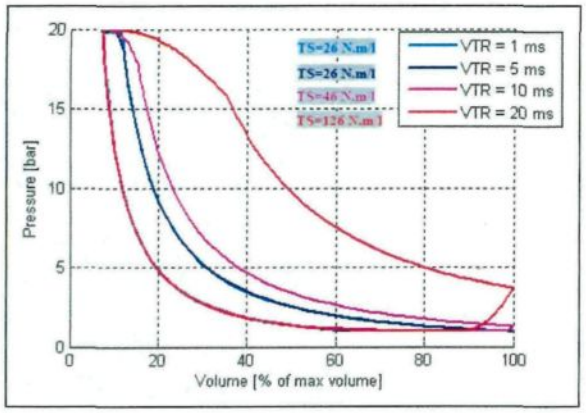

Figure 17. *P–V* diagram of the minimal torque operation in two-stroke pneumatic motor mode for different VTR values, for 20 bar tank pressure, at 750 r/min.

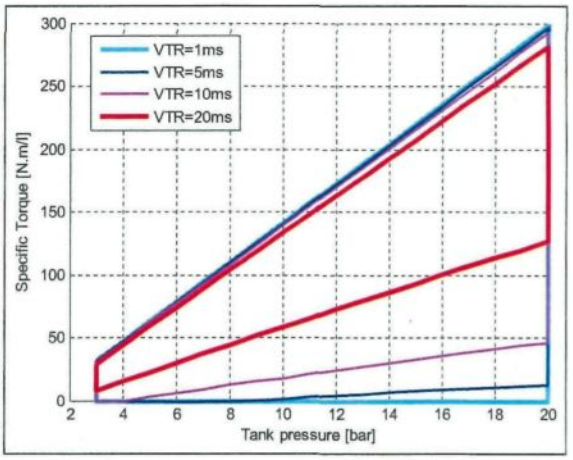

Figure 20. Operation domain of two-stroke pneumatic motor mode for different possible VTR values, at 750 r/min.

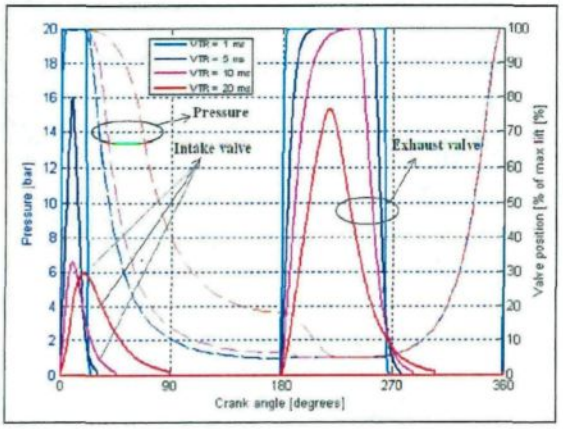

Figure 18. *P–θ* diagram and valve profiles of the minimal torque operation in two-stroke pneumatic motor mode for different VTR values, for 20 bar tank pressure, at 750 r/min.

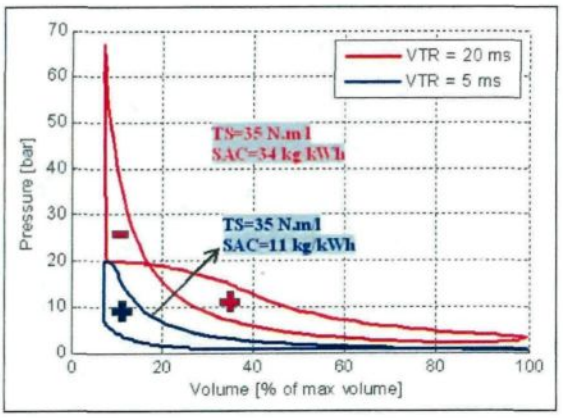

Figure 19. *P–V* diagram of the two-stroke pneumatic motor mode providing 35 N.m/l for 20 bar tank pressure, for VTR = 20 ms and VTR = 5 ms, at 750 r/min.

compression ratio cannot be achieved. Consequently, the higher the VTR, the higher the maximum achievable compression ratio. For instance, the maximal compression ratio using a 20 ms VTR is only 4, and the one using a 10 ms VTR is 18.

Moreover, the minimal torque under which the HPCE is unable to operate is limited by the minimal IVC angle. Indeed, the difference between the margin explained previously and the minimal IVC is an indicator of the flexibility for varying the torque. As shown in Figure 21, for a certain VTR, the higher the compression ratio, the lower the flexibility for controlling the torque.

Figures 22 and 23 illustrate pressure–volume (*P–V*) and pressure–crank angle (*P–θ*) diagrams of maximal and minimal torque operations in pneumatic pump mode for a tank pressure of 20 bar, with a VTR of 10 ms. The dashed lines represent the maximal torque operation and the solid lines represent the minimal torque operation. As one can observe, the flexibility for controlling the torque is much reduced.

After this detailed analysis, it is possible to draw the zone of operation with a two-stroke pneumatic pump mode, for different possible VTR values, as illustrated in Figure 24. It can be observed that the impact of the VTR is essential. The optimal value of the VTR for the two-stroke motor mode, which was 5 ms, is not sufficient to achieve an acceptable performance of the two-stroke pneumatic pump mode. The required VTR for this mode would be 1 ms.

Synthesis and recommendations

The ideal HPCE mode selection strategy, which was illustrated in Figure 9, may now be adjusted to take into consideration the VTR. Figure 25 illustrates the real HPCE mode selection strategy, for different VTR valves, at 750 r/min.

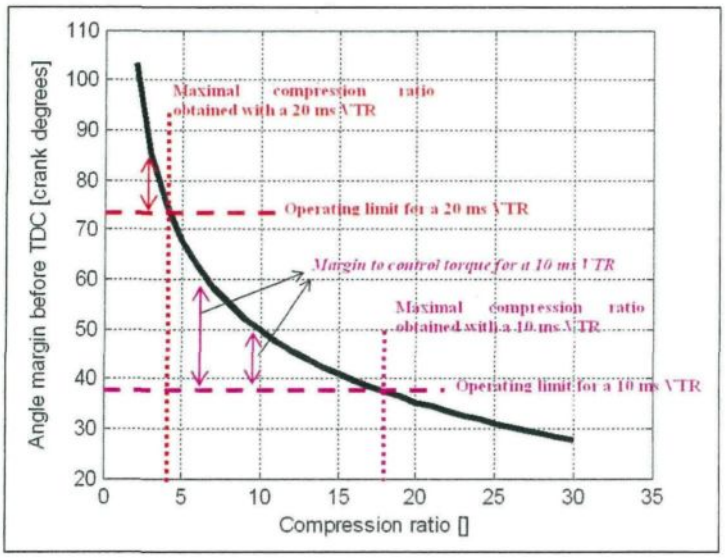

Figure 21. Angular margin to control torque as a function of compression ratio, for a two-stroke pneumatic pump mode, at 750 r/min.

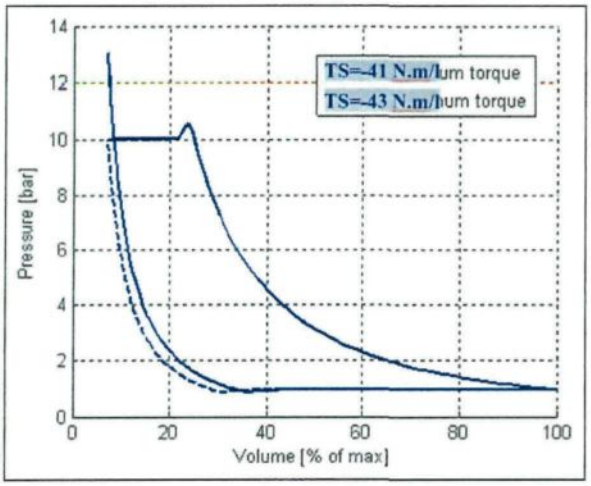

Figure 22. *P–V* diagram of the minimal and maximal torque operation in two-stroke pneumatic pump mode for 10 ms VTR and 10 bar pressure, at 750 r/min.

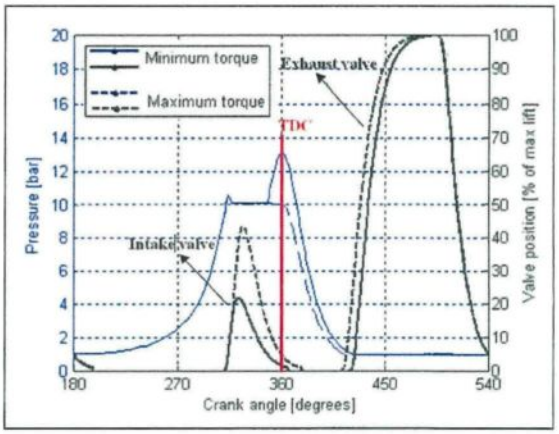

Figure 23. *P–θ* diagram and valve profiles of the minimal and maximal torque operation in two-stroke pneumatic pump mode for 10 ms VTR and 10 bar pressure, at 750 r/min.

Assuming that the optimal VTR is the one that maximizes the zone of mode 2 and mode 4 and minimizes the zone of mode 1, one can conclude that the minimal required VTR at 750 r/min is 1 ms (VAR of 4.5 crank degrees). However, if an additional air compressor is added, then the minimal required VTR is only 5 ms (VAR of 22.5 crank degrees), as mode 4 will no longer be considered.

All these VTR requirements are valid for a 750 r/min operation. Assuming that the combustion process and the mass transfer through the valves does not significantly affect the thermodynamic cycle, we could say in a first-order approach, that the thermodynamic cycle operates in the crank angular domain, while only the valve motion is in the time domain. The required VTR can be calculated for speeds other than 750 r/min by

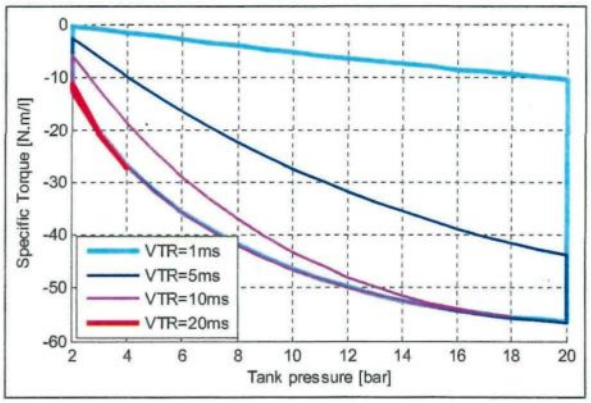

Figure 24. Operation domain of two-stroke pneumatic pump mode for different possibilities of VTR values, at 750 r/min.

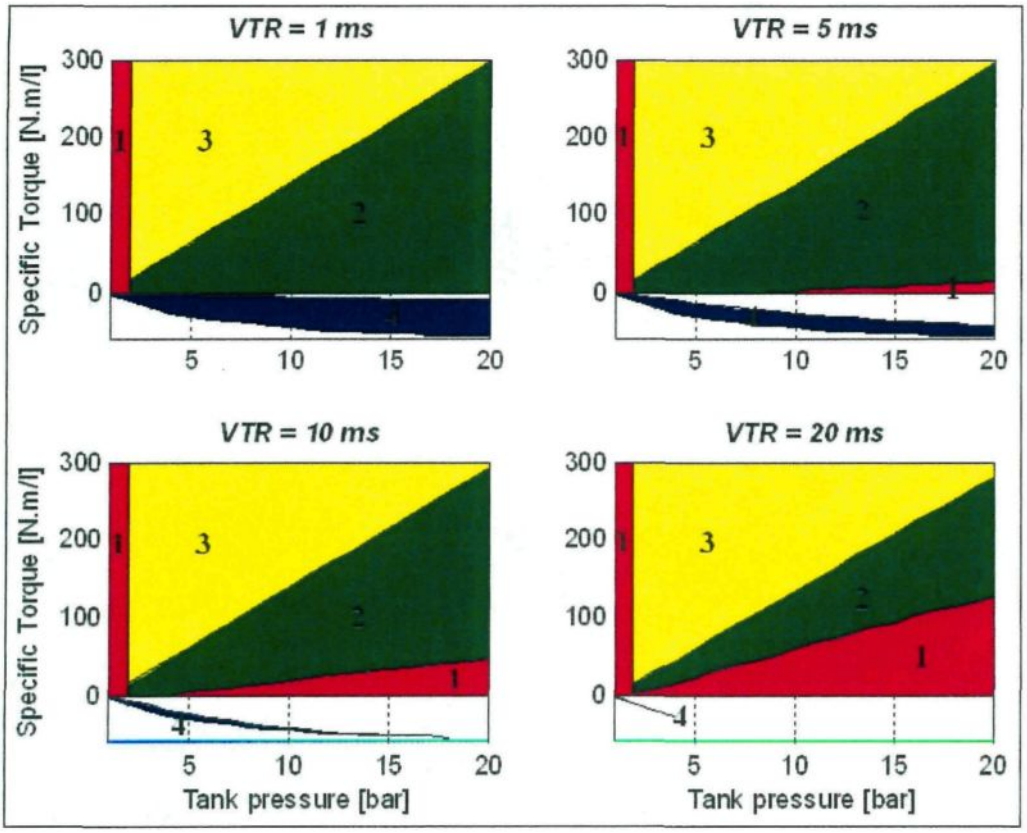

Figure 25. Mode selection strategy of the HPCE for different possibilities of VTR, at 750 r/min.

Table 2. Minimal required VTR for different applications.

Application	Hybrid wind diesel system		Automobile	
Category	Low-speed diesel engine	Medium-speed diesel engine	Diesel engine	Gasoline engine
Maximal speed	750 r/min	1500 r/min	6000 r/min	8000 r/min
Required VTR without compressor	1 ms	0.5 ms	0.12 ms	0.09 ms
Required VTR with compressor	5 ms	2.5 ms	0.62 ms	0.47 ms

keeping the same VAR as the one found for the 750 r/min engine. Equation (15) can be used for this purpose. The result is graphically illustrated in Figure 26 and reported in Table 2.

Unlike HWDSs, which operate at constant speed, automotive powertrains operate at a speed range that varies from idle speed (around 750 r/min) to the maximal speed. The required VTR for an automotive application illustrated in Table 2 is therefore the one that permits the optimal operation for the whole speed range. If the VTR is lower than the required one, optimal HPCE operation is ensured up to a certain speed, above which downgrade operation occurs. For example, with a 0.2 ms VTR valve, the optimal HPCE operation is ensured up to 4000 r/min, without the use of compressor, which is likely to be sufficient to satisfy most frequent uses.

Moreover, it is possible to find alternatives in the case of difficulty obtaining the required VTR. One of these alternatives is the use of the cylinder deactivation technique. Diesel power generators are mostly multi-cylinder engines. This offers the possibility for deactivating some cylinders to be able to provide low torque if the VTR is not low enough. Deactivating some cylinders increases the specific torque required for the other activated cylinders. This technique is well known for conventional multi-cylinder engines in order to optimize fuel consumption at low loads.

Conclusion

This work is a part of a research program that aimed to modify a conventional ICE and turn it into an HPCE. The HPCE should be able to convert

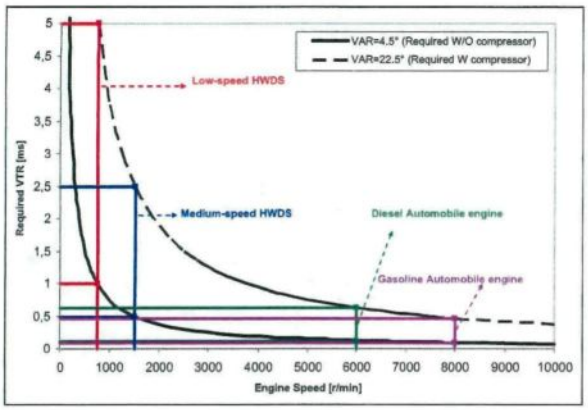

Figure 26. Required VTR for HPCE, as a function of the engine speed.

mechanical energy into compressed air and convert compressed back air into mechanical energy. The HPCE concept could be useful for several applications such as in automobiles and HWDSs. In previous work, we exposed an optimization followed by a fuel-saving evaluation of a new HPCE concept that used a VVA system. The optimization of the valve actuation was based on ideal thermodynamic cycle modeling, assuming an instant response of the VVA system. In the present work, a more realistic analysis of the system was provided by taking into consideration the dynamic response of the VVA system. The impact of the VTR on the performance of the HPCE concept was studied, and a minimal VTR defined to operate it adequately.

This work is important for the next phase of the research program, which consists of equipping a diesel engine test bench to confirm the theoretical benefits obtained through modeling. The importance of choosing the correct VTR, as recommended in the present article, has been proved.

Funding

This research received no specific grant from any funding agency in the public, commercial, or not-for-profit sectors.

References

1. Donitz C, Vasile I, Onder C, et al. Realizing a concept for high efficiency and excellent driveability: the downsized and supercharged hybrid pneumatic engine. SAE paper 2009-01-1326, 2009.
2. Trajkovic S, Tunestal P and Johansson B. Introductory study of variable valve actuation for pneumatic hybridization. SAE paper 2007-01-0288, 2007.
3. Trajkovic S, Tunestal P and Johansson B. Investigation of different valve geometries and valve timing strategies and their effect on regenerative efficiency for a pneumatic hybrid with variable valve actuation. SAE paper 2008-01-1715, 2008.
4. Basbous T, Younes R, Ilinca A, et al. Fuel consumption evaluation of an optimized new hybrid pneumatic–combustion vehicle engine on several driving cycles. *Int J Engine Res*, published online ahead of print May 11, 2012. DOI: 10.1177/1468087411433250.
5. Ibrahim H, Younes R, Basbous T, et al. Optimization of diesel engine performances for a hybrid wind-diesel system with compressed air energy storage. *Energy* 2011; 36: 3079–3091.
6. Ibrahim H, Ilinca A, Younes R, et al. Study of a hybrid wind-diesel system with compressed air energy storage. In: *IEEE Canada, electrical power conference 2007, Renewable and alternative energy resources, EPC2007*, Montreal, Canada, 25 October 2007.
7. Ibrahim H. *Etude et conception d'un générateur hybride d'électricité de type Eolien-Diesel avec élément de stockage d'air comprimé*. PhD Thesis, Université du Québec à Chicoutimi, 2010.
8. Donitz C, Vasile IC, Onder CH, et al. Modeling and optimizing two- and four-stroke hybrid pneumatic engines. *Proc. IMechE Part D: J. Automobile Engineering* 2009; 223. DOI: 10.1243/09544070JAUTO972.
9. Higelin P, Charlet A and Chamaillard Y. Thermodynamic simulation of a hybrid pneumatic-combustion engine concept. *Int J App Thermo* 2002; 5(1): 1–11.
10. Higelin P, Vasile I, Charlet A, et al. Parametric optimization of a new hybrid pneumatic-combustion engine concept. *Int J Engine Res* 2004; 5: 205–217.
11. Kang H, Tai C, Smith E, et al. Demonstration of air-power-assist (APA) engine technology for clean combustion and direct energy recovery in heavy duty application. SAE paper 2008-01-1197, 2008.
12. Trajkovic S, Tunestal P and Johansson B. Simulation of a pneumatic hybrid powertrain with VVT in GT-Power and comparison with experimental data. SAE paper 2009-01-1323, 2009.
13. Lee CY, Zhao H and Ma T. Pneumatic regenerative engine braking technology for buses and commercial vehicles. SAE paper 2011-01-2176, 2011.
14. Diana S, Iorio B, Giglio V, et al. The effect of valve lift shape and timing on air motion and mixture formation of DISI engines adopting different VVA actuators. SAE paper 2001-01-3553, 2001.
15. Fukuo K, Iwata T, Sakamoto Y, et al. Honda 3.0 liter new V6 engine. SAE paper 970916, 1997.
16. Brüstle C and Schwarzenthal D. VarioCam plus – a highlight of the Porsche 911 turbo engine. SAE paper 2001-01-0245, 2001.
17. Sellnau M and Rask E. Two-step variable valve actuation for fuel economy emissions and performance. SAE paper 2003-01-0029, 2003.
18. Flierl R and Klüting M. The third generation of valvetrains – new fully variable valvetrains for throttle-free load control. SAE paper 2000-01-1227, 2000.
19. Kreuter P, Heuser P, Reinicke-Murmann J, et al. The meta VVH system – the advantages of a continuously mechanical variable valve timing. SAE paper 1999-01-0329, 1999.
20. Takemura S, Aoyama S, Sugiyama T, et al. A study of a continuous variable valve event and lift (VEL) system. SAE paper 2001-01-0243, 2001.
21. Bernard L, Ferrari A, Rinolfi R, et al. Fuel economy improvements potential of UniAir throttleless technology. In: *ATA conference*, Venice, 27–29 November 2002.

22. Allen J and Law D. Production electro-hydraulic variable valve-train for a new generation of IC engines. SAE paper 2002-01-1109, 2002.
23. Turner JWG, Kenchington SA and Stretch DA. Production AVT development: Lotus and Eaton's electrohydraulic closed-loop fully variable valve train system. In: *25th Vienna Motor Symposium*, 2004.
24. Denger D and Mischker K. The electro-hydraulic valvetrain system EHVS – system and potential. SAE paper 2005-01-0774, 2005.
25. Turner CW, Babbitt GR, Balton CS, et al. Design and control of a two-stage electro-hydraulic valve actuation system. SAE paper 2004-01-1265, 2004.
26. Schechter MM and Levin MB. Camless engine. SAE paper 960581, 1996.
27. Herranen M, Huntala K, Vilenius M, et al. The electrohydraulic valve actuation (EHVA) for medium speed diesel engine – development steps with simulation and measurements. SAE paper 2007-01-1289, 2007.
28. Heywood JB. *Internal combustion engine fundamentals.* New York: McGraw Hill, 1988.
29. Stone R. *Introduction to internal combustion engines.* Oxford: Department of Engineering Science, University of Oxford, 1999.
30. JANAF thermochemical tables, 3rd ed. 1985.
31. Magnesense. Electromagnetic engine valves, http://www.magnesense.com.
32.

Appendix I

Notation

a_j	coefficient for calculation of the specific energy
A	equivalent area of intake or exhaust valve (m^2)
c	damping coefficient (N.s/m)
D	piston diameter
F	electro-magnetic force (N)
h	specific stagnation enthalpy ($J.kg^{-1}$)
k	spring rod stiffness (N/m)
l	valve lift
L	con-rod length
m	mass (kg)
P	pressure (Pa)
N	engine speed (r/min)
Q	thermal energy (J)
r	ideal air thermodynamic constant ($J.kg^{-1}.K^{-1}$)
R	ideal gas constant ($J.mol^{-1}.K^{-1}$)
S	stroke
T	temperature (K)
u	internal specific energy ($J.kg^{-1}$)
V	volume (m^3)
t	time (sec)
x	valve displacement (m)
α_i	molar fraction of species i
ε	engine volumetric ratio
ζ	damping ratio
γ	gas constant
θ	crank angle
w_n	natural frequency (Hz)

Abbreviations

APA	air-power-assist
BDC	bottom dead center
CAES	compressed air energy storage
EVC	exhaust valve closing
EVO	exhaust valve opening
FIS	fuel injection start
HPCE	hybrid pneumatic–combustion engine
HWDS	hybrid wind diesel system
ICE	internal combustion engine
IVC	intake valve closing
IVO	intake valve opening
NEDC	new European driving cycle
Qf	quantity of injected fuel
SAC	specific air consumption
TDC	top dead center
TS	specific torque
VAR	valve angular response
VEA	valve energizing angle
VEOA	valve effective open angle
VET	valve energizing time
VOP	valve opening profile
VTR	valve time response
VVA	variable valve actuator

CHAPITRE VI

Article 5

Optimal management of compressed air energy storage in a hybrid wind-pneumatic-Diesel system for remote area's power generation

Soumis à Applied Energy (APEN-D-12-03587)

Résumé

Cet article est un rapport de synthèse qui consolide les études précédentes d'optimisation et d'évaluation de l'économie de carburant réalisée par le système SHEDAC-MHPD. Il présente et évalue également une stratégie innovante de gestion du stock d'air comprimé permettant de maximiser l'économie de carburant sur une base annuelle. Une modélisation du cycle thermodynamique réel conduit à démontrer qu'un couple demandé au moteur peut être réalisé suivant une infinité de possibilités correspondant à une infinité de valeurs de la Contribution de la Puissance Pneumatique (CPP). Ainsi, cette CPP est choisie comme étant le paramètre d'ajustement de la stratégie de gestion. Deux réglages sont mis en évidence :

1) Un réglage R1 qui minimise la consommation de carburant : il s'agit du même réglage qui a servi à l'évaluation réalisée dans l'article 2. Ce réglage impose au CPP d'être constamment à sa valeur maximale. Pour une grande majorité de cas, le CPP est de 100% indiquant donc qu'il s'agit du mode moteur pneumatique ;

2) Un réglage R2 qui maximise le rendement global, même si la consommation de carburant n'est pas minimale. Le CPP est mis à une valeur intermédiaire entre 0% et 100%, indiquant qu'il s'agit du mode hybride pneumatique combustion, avec un équilibre entre la puissance pneumatique et la puissance thermique défini de façon à garantir une efficacité maximale.

Comme pour l'article 2, l'étude de cas est faite sur le site de Tuktoyaktuk. L'économie de carburant réalisée grâce au MHPD avec chacun des deux réglages ci-dessus est évaluée en fonction du volume de stockage disponible. Fonctionnant avec le réglage R1, et pour un volume de stockage de 50,000 m^3, le MHPD réduit de 17% (soit 95 tonnes par an) la consommation de carburant d'un SHED ayant un TPP de 1. L'économie de carburant d'un SHED avec un TPP de 1. Fonctionnant avec le réglage R2, l'économie de carburant est de 20% (soit 110 tonnes par an).

Comme complément à ce résultat, l'étude explore une nouvelle d'optimisation de la gestion du stock d'air, basée sur la prédiction de la vitesse du vent et de la consommation électrique. Plusieurs logiciels de prédiction peuvent effectivement être utilisés pour cette finalité. La stratégie proposée consiste à choisir à chaque instant entre la loi R1 et la loi R2 en fonction de la connaissance de l'énergie éolienne et de la consommation dans les dix heures à venir. Le critère consiste simplement à dire que si cette énergie éolienne est supérieure au double de la consommation, le réglage R1 est utilisé, sinon le réglage R2 est utilisé. Le travail démontre que la consommation obtenue par cette stratégie, qui n'est qu'une combinaison des deux réglages R1 et R2, est meilleure que celle obtenue par chacun de ces deux réglages. Plus de 3 tonnes de carburants peuvent être encore gagnés pour une SHED ayant un TPP de 1 et un volume de stockage de 50,000 m^3.

Pour compléter ces résultats intéressants, une étude de sensibilité de l'apport du MHPD en fonction de la vitesse moyenne du vent est réalisée. Ceci permet de prévoir le gain réalisable dans des sites ayant un plus fort potentiel éolien que celui de Tuktoyaktuk qui a une vitesse moyenne du vent seulement de 5.5 m/s.

OPTIMAL MANAGEMENT OF COMPRESSED AIR ENERGY STORAGE IN A HYBRID WIND-PNEUMATIC-DIESEL SYSTEM FOR REMOTE AREA'S POWER GENERATION

Tammam **BASBOUS*** [a,b], Rafic **YOUNES** [b,c], Adrian **ILINCA** [b], Jean **PERRON** [a]

[a] *Laboratoire International des Matériaux Antigivre, Université du Québec à Chicoutimi, Chicoutimi, Québec, Canada*
[b] *Laboratoire de Recherche en Energie Eolienne, Université du Québec à Rimouski, Rimouski, Québec, Canada*
[c] *Faculté de Génie, Université Libanaise, Beyrouth, Liban*

Abstract

The power generation for remote areas is historically ensured with Diesel engines generators. The economical cost of energy is therefore very high not only due to inherent cost of fuel but also due to transportation and maintenance costs. The environmental cost of energy is also high as the use of fossil fuels for electricity generation is a significant source of greenhouse gas emissions. The use of hybrid systems that combine renewable sources, especially wind, and Diesel generators, reduces fuel consumption, operational cost and pollution. Adding a storage element to the hybrid system increases the penetration level of the renewable sources, which is the percentage of renewable energy in the overall production, and further improves fuel savings. Compressed Air Energy Storage (CAES) has several advantages for hybrid Wind-Diesel Systems (WDS) due to its low cost, high power density and reliability. In a previous work, we have exposed and evaluated a new technique to transform the existing Diesel engine to a Hybrid Pneumatic Combustion Engine (HPCE), able to operate as a bi-source engine (compressed air and fuel). A first order annual fuel economy obtained with this multi-hybrid system (WDS-HPCE), based on ideal cycle modeling, was provided. As a continuity of these previous works, we are comparing several strategies of management of the CAES. One alternative is the use of an algorithm based on the prediction of the wind speed, which we demonstrate to be the most effective way to reduce the fuel consumption. We provide an evaluation of the fuel economy generated by the WDS-HPCE, as a function of the wind power penetration ratio, the air-storage capacity, and the average wind speed on site.

* Corresponding author : *tammam.basbous@uqac.ca*

Keywords: Pneumatic Hybridization; Diesel Engine; Wind-Diesel System; Compressed Air Energy Storage, Storage Capacity, Optimal Management of Energy

Nomenclature

A	Area [m^2]
A_FC	Annual fuel consumption [tons]
c_p	Specific heat at constant pressure [$J.K^{-1}.kg^{-1}$]
c_v	Specific heat at constant volume [$J.K^{-1}.kg^{-1}$]
D	Displacement [m^3]
H	Enthalpy [J]
h	Specific enthalpy [$J.kg^{-1}$]
h_v	Heat value [$J.kg^{-1}$]
N	Engine revolution [$round.min^{-1}$]
Q	Heat [J]
r	Specific gas constant [$J.K^{-1}.kg^{-1}$]
p	Pressure [Pa]
P	Power [kW]
P_max	Maximal power [kW]
T	Temperature [K]
Γ	Torque [N.m]
Γ_s	Specific torque [$N.m.l^{-1}$]
U	Internal energy [J]
u	Specific internal energy [$J.kg^{-1}$]
W	Work [J]
V	Speed [$m.s^{-1}$]
v	Volume [m^3]
v_m	Dead volume [m^3]
n	Number []
θ	Prediction's number of hours [hours]
ϕ	Flow [$kg.h^{-1}$]
η	Efficiency []
α_v	Proportion of the isochoric combustion []
α_p	Proportion of the isobaric combustion []

Subscripts

air	Refers to air consumed or compressed
Betz	Refers to Betz's limit
cycle	Refers to consumption demand
charge	Refers to the compressed air at the engine's outlet
discharge	Refers to the compressed air at the tank's outlet
eng	Refers to the engine
fuel	Refers to injected fuel

int	Refers to intake conditions
load	Refers to consumption demand
ref	Refers to reference conditions
tank	Refers to air-tank
windT	Refers to the wind turbine
wind	Refers to the wind

Acronyms

AFR	Air to Fuel Ratio
CAES	Compressed Air Energy Storage
EFF	Efficiency
EVC	Exhaust Valve Close
EVO	Exhaust Valve Open
FT	Filling Time
GHG	Greenhouse gas
HPCE	Hybrid Pneumatic Combustion Engine
ICE	Internal Combustion Engine
IVC	Intake Valve Close
IVO	Intake Valve Open
L	Load
PPC	Pneumatic Power Contribution
SAC	Specific Air Consumption
SFC	Specific Fuel Consumption
TDC	Top Dead Center
TSOC	Tank State Of Charge
WDS	Wind Diesel System
WP	Wind Power
WPPR	Wind Power Penetration Rate

1. Introduction

In Canada, more than 200,000 people live in more than 300 remote communities (Yukon, TNO, Nunavut, islands ...). It is necessary to add to that the many technical installations (towers and communications relays, weather systems), tourist facilities, farms which are not connected to the provincial or national electric distribution grids [1]. This is the result of economic decisions related to the cost of transmission and distribution lines over a vast territory [2]. These isolated sites are equipped with diesel power generators. This electricity production method is more expensive in itself than large electric production plants (gas, hydro, nuclear, wind ...) and, on top of that, to which should be added significantly higher fuel transport costs. Thus, the diesel electricity production is relatively inefficient, expensive and responsible for the emission of 1.2 million tons of GHG annually in Canada only [3]. Indeed, the exploitation of these remote isolated grids shows a deficit in the order of hundreds of million of dollars per year that the government should support in a way or another. In Quebec alone, where the electricity tariff is uniform independent of the production price, Hydro-Quebec estimates at approximately 133 million dollars the annual losses for the supply of 14,000 subscribers divided in forty communities not connected to the main grid. These deficits reflect the gap between the high costs of electricity produced from the diesel in these regions and the uniform price of the electricity [4]. Furthermore, we estimate at 140,000 tons the GHG emission resulting from the use of generators for the subscribers of the Quebec autonomous networks. This quantity of GHG is equivalent to the one emitted by 35,000 cars during one year. The majority of these communities are located in coastal areas and benefit of a good wind resource. The exploitation of the wind resource in these autonomous networks could reduce the deficits of exploitation by privileging the wind, a "local fuel", rather than the diesel, an imported fuel.

The use of hybrid systems, which combine renewable sources with the diesel generators, allows reducing the total consumption of fuel, an environmental and economic advantage. Among all renewable energies, the wind energy experiences the fastest growing rate, at more than 30% annually for the last ten years [5, 6]. Low penetration wind – diesel systems (WDS), have been already implemented in Nordic communities in

Yukon [7], Nunavut [8] and in Alaska [9]. By low penetration systems we understand that the instantaneous wind power is maximum of 20-35% of the diesel rated power and the overall energy from wind do not exceed 10-15% of total consumption [10, 11]. Generally, the WDS uses an existing diesel power plant and add a wind farm containing a single model of turbine.[12] To these two principal elements are added logic and the components necessary to the hybrid exploitation of the system: secondary loads for smoothing, regulator and automated command. The increase of the wind penetration level allows better fuel reduction. However, the first obstacle with this perspective results from the operation constraints of diesels. Beyond a certain penetration level, it is necessary to maintain the diesel on stand by at over 30% of its nominal power output in order to respond to a sudden reduction of the wind. This limits the wind energy to a level of too weak penetration and the wind turbines act only as a negative charge for the network.

The high-penetration wind diesel systems without storage are those where the wind power production exceeds the charge for large periods of time [13]. This allows the complete stop of the diesels during those periods and conduct to a significant reduction of fuel consumption. In the mean time, this design is subject to complex technical problems [14, 15] which did that a single project of this type, without any electrical storage, is presently operational in Alaska [9]. During some periods when the excess of wind energy over the charge is reduced, the diesel engine still must be maintained on stand by so that it could quickly respond to a wind speed reduction (reduce the time of starting up and heating of the engine). This is an important source of over consumption because the engine could turn during hours without supplying any useful energy.

Figure 1 illustrates an operation example of a high penetration WDS [16], for a 480 kW consumer load. Fuel savings start when wind speed gets higher than 4 m/s. When wind speed reaches 9 m/s, wind power is enough to cover consumers demand without Diesel engine contribution. Diesel engine is stopped, however, when a margin of 30% is reached between consumers demand and available wind power. For wind speed higher than 9 m/s, surplus wind power is lost.

Combining a storage element to a high penetration WDS allows storing the excess of wind energy that frequently occurs and is otherwise dissipated, then use it later when

needed. The request for fuel energy is therefore reduced. Assuming optimum exploitation conditions [17, 3] the use of energy storage with WDS can lead to better economic and environmental results, allows reduction of the overall cost of energy supply and increase the wind energy penetration rate (i.e., the proportion of wind energy as the total energy consumption on an annual basis) [3].

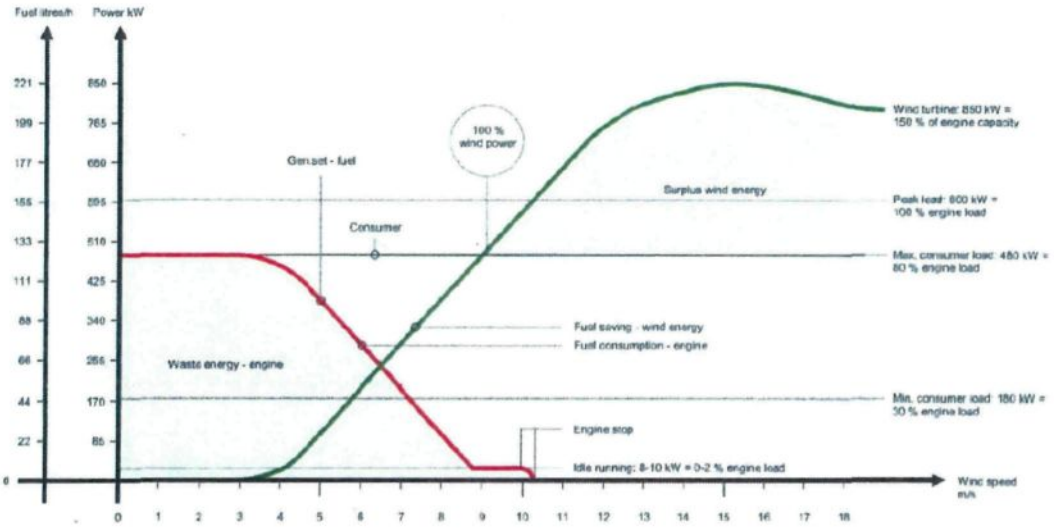

Figure 1: example of power contribution and fuel consumption of a high penetration Wind-Diesel generator [16]

2. Our concept: Hybrid Wind-Diesel-Compressed Air Energy Storage

Among all the techniques allowing the storage of intermittent renewable energy, such as pumped hydroelectric storage, batteries, superconducting magnets, flywheels, regenerative fuel cells and Compressed Air Energy Storage (CAES), the last one has an overwhelming advantage considering its low cost, low environmental impact and high reliability [18, 19, 20]. This leads us to suggest a multi-hybrid system composed of one or more wind turbines, one or more Diesel engines and a CAES system.

To make this system economically competitive, it is important not to suggest a multiplication of the Engines by adding independent air motors and compressors. That is why Pneumatic Hybridization of the existing Diesel engine is being investigated. This technique consists in enabling the Diesel engine to operate as an air compressor and as an

air motor along with its conventional operation. The Diesel engine is turned into a Hybrid Pneumatic Combustion Engine (HPCE). The components of out multi-hybrid WDS-HPCE as well as the energy flows are described in Figures 2 and 3.

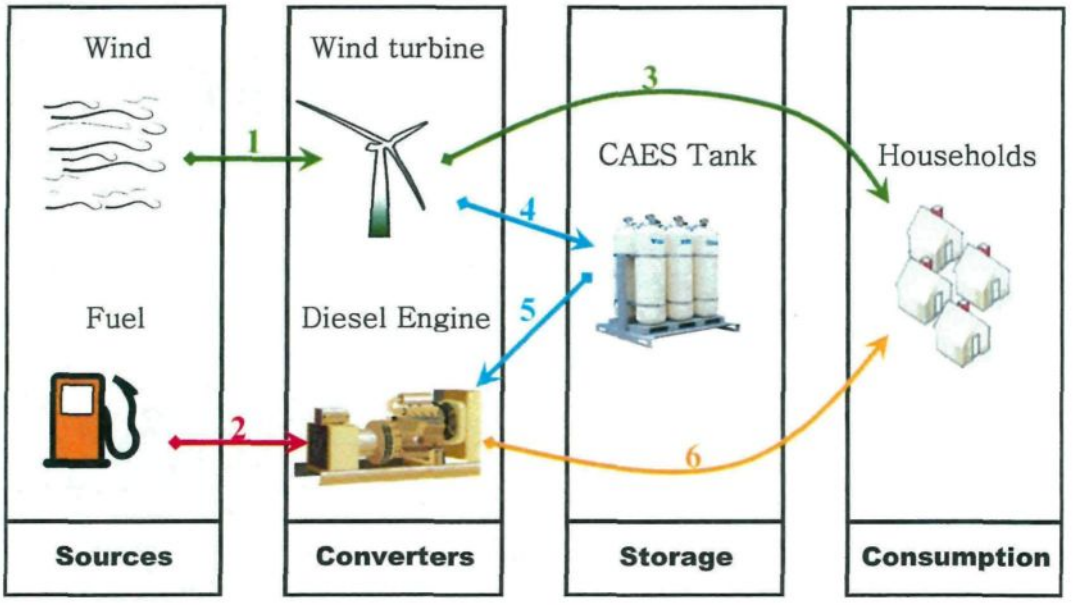

Figure 2: The components of the Hybrid WDS-HPCE and the energy flow chart

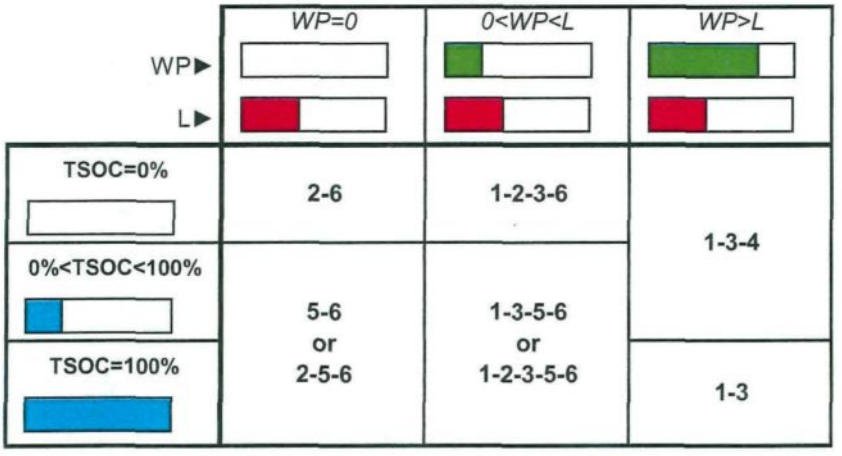

Figure 3: Active energy flows as a function of Tank State Of Charge (TSOC) and Wind Power (WP) compared to Load (L)

Figure 3 illustrates the active energy flows as a function of the Tank State Of Charge (TSOC), and the comparison between Wind Power (WP) and Load (L). For example,

when the tank is partially filled (0%<TSOC<100%) and the Wind Power is lower than the load (0<WP<L), the generated wind power (flow 1 active) provides a part of the load (flow 3 active) and the engine provides the remaining needed load (flow 6 active). The engine operates as an air motor using the compressed air (flow 5 active) or as a hybrid air-fuel motor using both compressed air and fuel (flows 2 and 5 active).

We have already presented the design of a new concept of HPCE [21, 22, 23, 24]. The concept is based on bypassing the turbocharger and connecting the air tank to intake valve using two three-way valves as shown in Figure 4.

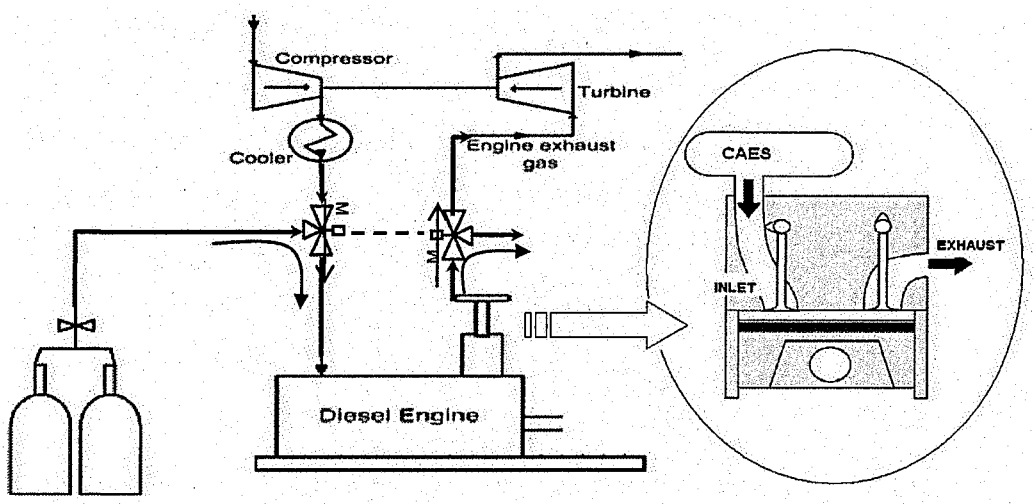

Figure 4: Suggested pneumatic concept

The first three-way valve connects the engine's inlet to either the air tank or the compressor's outlet while the second three-way valve connects the engine's exhaust to either the turbine's inlet or to the atmosphere. It also requires a full control of the intake valves, the exhaust valves and the fuel injectors. It is assumed that the volume of the CAES tank is much higher than the displacement of the engine. Using a specific control of the opening and the closing angles of the intake and exhaust valves, the engine may operate under one of the following four modes:

Mode 1: Four-stroke conventional Combustion motor mode;

Mode 2: Two-stroke pneumatic motor mode;

Mode 3: Four-stroke hybrid Pneumatic-Combustion motor mode;

Mode 4: Two-stroke pneumatic pump mode.

The principle of each mode is described in details in a previous publication [23, 24]

3. Mathematical modeling

3.1. Thermodynamic cycles

We have conducted the modeling of the ideal thermodynamic cycles using the equations of the first principle of thermodynamics, applied to all phases of the cycles [25, 26, 27]:

$$dU = dW + dQ \tag{1}$$

$$dH = dU + pdv + vdp \tag{2}$$

where dU, dH and dW can be calculated using the following equations:

$$dU = m \cdot c\_v \cdot dT + dm \cdot c\_v \cdot T \tag{3}$$

$$dH = m \cdot c\_p \cdot dT + dm \cdot c\_p \cdot T \tag{4}$$

$$dW = -pdv \tag{5}$$

Since ideal thermodynamic cycle is being modeled, dQ is zero for all phases except for combustion where it can be expressed using Equation 6:

$$dQ = dm_{fuel} \cdot h\_v \tag{6}$$

The ideal torque Γ_{ideal} can be calculated using Equation 7

$$\Gamma_{ideal} = \frac{-W}{n_s \cdot \pi} = \frac{\oint pdv}{n_s \cdot \pi} \tag{7}$$

where n_s is the number of stroke ($n_s = 2$ in Mode 2 and 4 and $n_s = 4$ in Mode 1 and 3)

The real torque, which takes into consideration all the losses, can be approximated using Equation 8:

$$\Gamma_{real} = \eta_{cycle} \cdot \Gamma_{ideal} - \Gamma_{fric} \tag{8}$$

where η_{cycle} is a quadratic function of Air to Fuel ratio, illustrated in the Appendix (Figure A.1) and the friction loss Γ_{fric} is constant since the engine is running at a fixed speed.

3.2. Tank storage and discharge model

The air storage is considered adiabatic. When the engine is charging the tank with an air mass rate of ϕ_{charge} at a temperature of T_{charge}, the variation of the air stored mass m_{tank} and temperature T_{tank} can be calculated using the following Equations 9 and 10 [25, 28, 29]:

$$dm_{\text{tank}} = \phi_{\text{charge}} \cdot dt \tag{9}$$

$$dT_{\text{tank}} = \frac{\gamma \cdot T_{\text{charge}} - T_{\text{tank}}}{m_{\text{tank}}} \cdot \phi_{\text{charge}} \cdot dt \tag{10}$$

When the engine is discharging the tank with a mass rate of $\phi_{\text{discharge}}$, the variation of m_{tank} and T_{tank} can be calculated using the following Equations 11 and 12 [25, 28, 29].

$$dm_{\text{tank}} = -\phi_{\text{discharge}} \cdot dt \tag{11}$$

$$dT_{\text{tank}} = -\frac{(\gamma - 1) \cdot T_{\text{tank}}}{m_{\text{tank}}} \cdot \phi_{\text{discharge}} \cdot dt \tag{12}$$

After calculating m_{tank} and T_{tank}, the tank pressure p_{tank} can be determined using perfect gas law (Equation 13), knowing that the tank volume v_{tank} is constant:

$$p_{\text{tank}} = \frac{m_{\text{tank}} \cdot r \cdot T_{\text{tank}}}{v_{\text{tank}}} \tag{13}$$

3.3. Model of Wind Power and Diesel load

The power generated by one wind turbine for a certain wind speed V_{wind} can be calculated using Equation 14 [30]:

$$P_{windT}(V_{wind}) = P_{AvailableWind}(V_{wind}) \times C_{windT}(V_{wind}) \tag{14}$$

Where $P_{AvailableWind}$ is the maximum available wind power calculated using Equation 15 [30]:

$$P_{AvailableWind}(V_{wind}) = \frac{1}{2} \cdot \rho_{air} \times A_{windT} \times V_{wind}^{3} \quad (15)$$

And $C_{windT}(V_{wind})$ is the power coefficient of the wind turbine, as given by the manufacturer (Appendix, Figure A.2).

The power required from the engine (P_{eng}) is equal to the difference between load power and total wind generated power.

$$P_{eng} = P_{load} - n_{windT} \times P_{windT} \quad (16)$$

where n_{windT} is the number of the wind turbines.

The torque provided by the engine can therefore be calculated using Equation 17:

$$\Gamma_{eng} = \frac{30}{\pi} \cdot \frac{P_{eng}}{N_{eng}} \quad (17)$$

Finally, the specific torque is equal to the ratio of the torque to the engine's displacement. This gives:

$$\Gamma\_s_{eng} = \frac{30}{\pi} \cdot \frac{P_{eng}}{N_{eng} \cdot D_{eng}} \quad (18)$$

The Wind Power Penetration Ratio (WPPR) is the ratio of maximal generated wind power to the maximal load, as illustrated in Equation 19.

$$WPPR = \frac{n_{windT} \times P\_\max_{windT}}{P\_\max_{load}} \quad (19)$$

3.4. Application settings and system model structure

We suggest to optimize and evaluate the concept for the north-Canadian village Tuktoyaktuk for which the electric consumption and wind speed data are known (data registered in 2009). The characteristics of the WDS-HPCE are listed in Table 1.

Parameter	Value	Unit	Comment
Wind turbine type	**ENERCON**		
$P\_\max_{WindT}$	**330**	kW	
A_{WindT}	**876**	m^2	
C_{WindT}	**Function of wind speed**		Appendix B, Figure B.2
n_{WindT}	**3**		Default value, but will be varied
WPPR	**1**		Default value, but will be varied
V_{tank}	**30000**	m^3	Default value, but will be varied
D_{Diesel}	**60**	l	
N_{Diesel}	**1800**	rpm	

Table 1: Hybrid Wind Diesel system parameters

The structure of the model is illustrated in Figure 5. The sub-model entitled "strategy" defines the mode that will be used by the engine to provide the required torque, depending on the tank pressure and temperature. This strategy is described in detail later in this article.

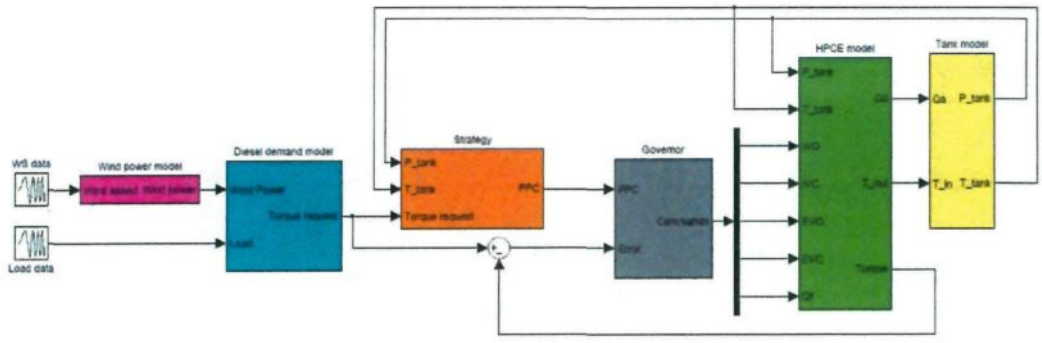

Figure 5: Structure of the WDS-HPCE power generator model

3.5. Fine-tuning the HPCE

Tuning the HPCE consists in defining the parameters illustrated in Table 2 for every requested torque and every possible combination of tank pressure and tank temperature. In a previous work [23, 24], tuning maps were calculated ensuring the minimal fuel consumption at every operating point. In the present study, a finer tuning is suggested in order to maximize the global efficiency of the system.

	$\emptyset_{fuel}$	IVO	IVC	EVO	EVC
Mode 1	o	x	x	x	x
Mode 2	-	x	o	x	o
Mode 3	o	x	o	x	o
Mode 4	-	o	o	o	o

Legend:
o : tuning parameter
x : fixed parameter
- : not concerned

Table 2: Tuning parameters for each mode

Indeed, for a certain tank pressure and temperature, there are several ways to obtain any requested torque. The Pneumatic Power Contribution (PPC) is defined as the ratio of the pneumatic power to the total power of the cycle. The PPC may take values going from 0% to 100% included. If Mode 1 is chosen, the PPC is equal to 0%; if Mode 2 is chosen, the PPC is equal to 100%; and if Mode 3 is chosen the PPC is somewhere between 0% and 100%. The efficiency (EFF) of the HPCE at a certain operating point is defined the ratio of the output power to the input power, where input and output power for each mode are expressed in Table 3.

	Input Power	Output Power
Mode 1	$\phi_{fuel} \cdot h\_v$	$\frac{\Gamma_{HPCE} \cdot N_{HPCE} \cdot \pi}{30}$
Mode 2	$\phi_{discharge} \times c\_p \times T_{tank}$	$\frac{\Gamma_{HPCE} \cdot N_{HPCE} \cdot \pi}{30}$
Mode 3	$\phi_{fuel} \cdot h\_v + \phi_{discharge} \times c\_p \times T_{tank}$	$\frac{\Gamma_{HPCE} \cdot N_{HPCE} \cdot \pi}{30}$
Mode 4	$\frac{\Gamma_{HPCE} \cdot N_{HPCE} \cdot \pi}{30}$	$\phi_{charge} \times c\_p \times T_{compression}$

Table 3: Input and Output power expressions for each mode

Figure 6 illustrates numerous possibilities to obtain 120N.m/l knowing that the tank pressure and temperature are 20 bars and 575K respectively. If Mode 1 is chosen (PPC=0%), the Specific Air Consumption (SAC) is null (no tank-air consumption), the Specific Fuel Consumption (SFC) is 341 g/kWh and the efficiency (EFF) is 23.5%; if Mode 2 is chosen (PPC=100%), the SFC is null, the SAC is 39 kg/kWh and the EFF is 31.6%; and if Mode 3 is chosen, as PPC increases, SAC increases and SFC decreases. Three examples of PPC are illustrated in Mode 3 operation: 30%, 38% and 46%.

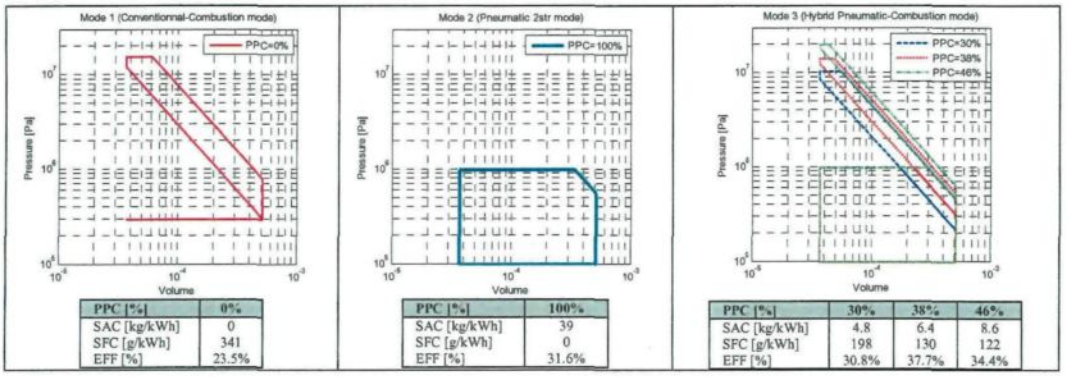

Figure 6: five possibilities of obtaining a torque of 120 N.m/l, with a tank pressure and temperature of 20 bars and 575K respectively

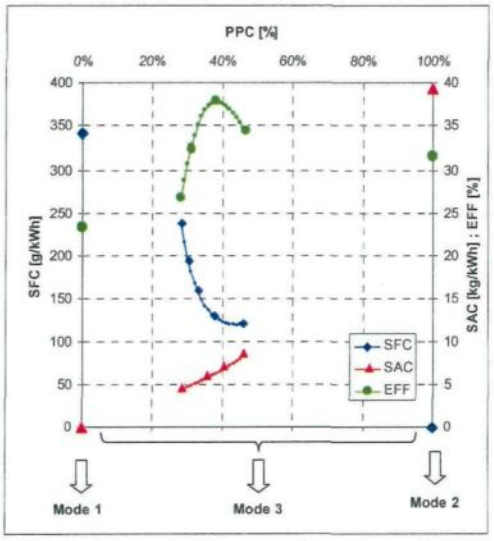

Figure 7: Variation of SFC, SAC and EFF as a function of PPC, for a torque of 120 N.m/l, obtained with a tank pressure and temperature of 20 bars and 575K respectively

The EFF is respectively 30.8%, 37.7% and 34.4%. It can also be noticed that the higher the PPC, the higher the maximal cylinder gas pressure. For a PPC of 46%, the threshold of 200 bars is reached and the PPC cannot therefore be further increased. On the other hand, as PPC decreases, the Air over Fuel Ratio (AFR) decreases. For a PPC of 24%; the threshold of 15 is reached and the PPC cannot therefore be further decreased.

This analysis enables plotting the SFC, the SAC and the EFF as a function of the PPC for this operating point (120 N.m/l, 20 bars, 575K) as shown in Figure 7. The discontinuity

in the curves is explained by the maximal and the minimal PPC that can be used as explained previously.

It can be noticed that two interesting choices can be made:

1. PPC = 0% (Mode 2) where the SFC is guaranteed to be at its lowest value
2. PPC=38% (Mode 3) where the EFF is guaranteed to be at its highest value

3.6. Characterization maps of HPCE

Similar fine-tuning is conducted for all possible combinations of torque, tank pressure and tank temperature. At each operating point; the "Minimal SFC" and the "Maximal EFF" is selected as possible tuning strategies. It is worth noting that the "Minimal SFC" corresponds sometimes to an operation in Mode 3, since some high torque values are not feasible in Mode 1 in case the tank pressure is too low.

Figures 8 to 13 show the characterizing maps of the "Minimal SFC" strategy and the "Maximal EFF" strategy. Every operating point is defined by the specific torque and the tank pressure. The temperature at each operating point is calculated by considering an adiabatic compression starting from the normal conditions (1 bar; 298K), up to this tank pressure. This choice was made only for the illustration since 2D graphs are simple to understand. Indeed, 3D maps are calculated varying simultaneously the three variables: the tank pressure, the tank temperature and the specific torque. Those maps were used in the calculation of the annual fuel economy that will be exposed in the next section.

Figures 8, 9 and 10 illustrate the PPC, the SAC and the SFC for minimal SFC tuning strategy, as a function of the tank pressure and the specific torque. It can be observed that Mode 1 is used for tank pressure lower than 3 bars. Mode 2 is used in most cases where tank pressure is higher than 3 bars except for high torque request and relatively low tank pressure where Mode 3 needs to be used, as explained previously.

Figures 11, 12 and 13 illustrate the PPC, the SAC and the SFC for maximal EFF tuning strategy, as a function of the tank pressure and the specific torque. It can be observed that Mode 3 or Mode 1 is privileged in several cases where Mode 2 was also possible. Also, the Mode 1 is surprisingly privileged in some operating points where Mode 2 and Mode 3 were possible (the zone around 6 bars, 40N.m/l).

As for the pump mode, there is only one possible tuning map. The IVO angle is defined to meet the compression ratio. The compressed air flow, the compressed air temperature and the mechanical torque are simply a result of this operation. Figures 14 and 15 illustrate respectively the Specific Air Compression (SAC) and the compressed air temperature.

It can be noticed that there are two unfeasible zones:

1. The one corresponding to low absolute values of specific torque which are not able to compensate the friction losses.
2. The one corresponding to high absolute value of specific torque which cannot be accomplished by the concept due to present design. When the recoverable power is too high, unfortunately only a part of it can be recovered. It is also noticed that the maximal recoverable power occurs when the tank pressure is between 10 bars and 15 bars.

Indeed, this is the major handicap of this concept because, as will be explained in the next section, any recoverable power that corresponds to a torque out of ability of the HPCE is partially lost, which will reduce significantly the efficiency of the system.

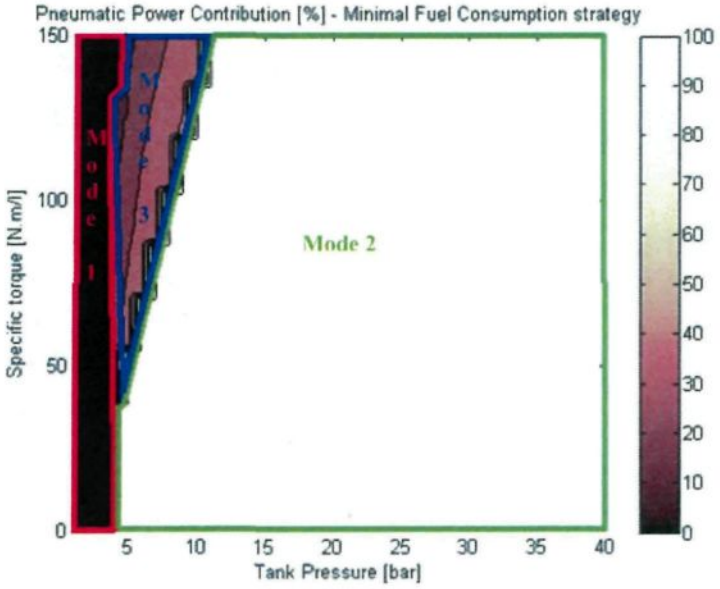

Figure 8: Pneumatic Power Contribution as a function of tank pressure and specific torque for minimal SFC tuning strategy

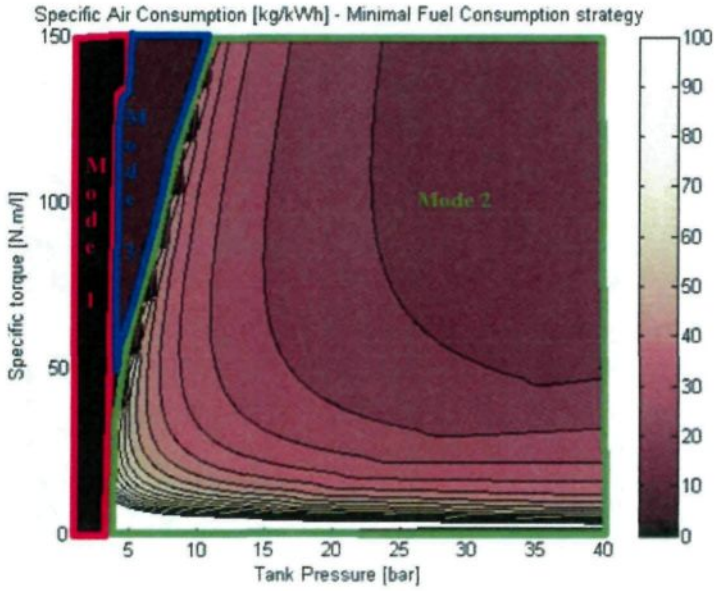

Figure 9: Specific Air Consumption as a function of tank pressure and specific torque for minimal SFC tuning strategy

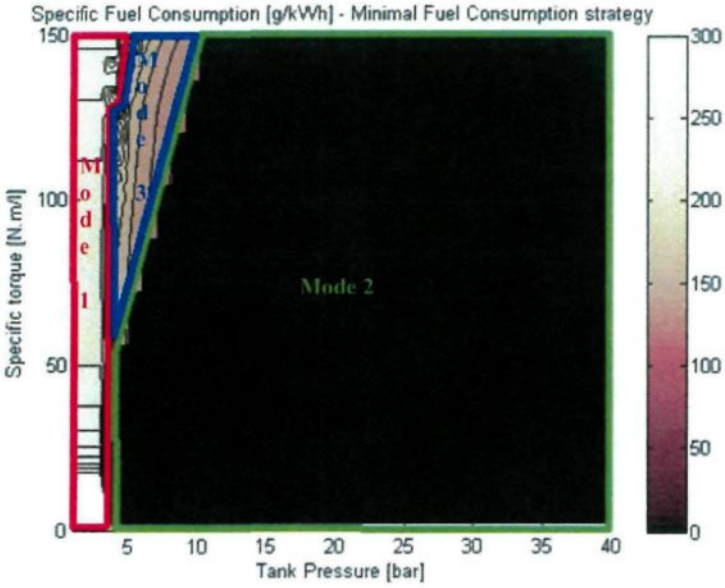

Figure 10: Specific Fuel Consumption as a function of tank pressure and specific torque for minimal SFC tuning strategy

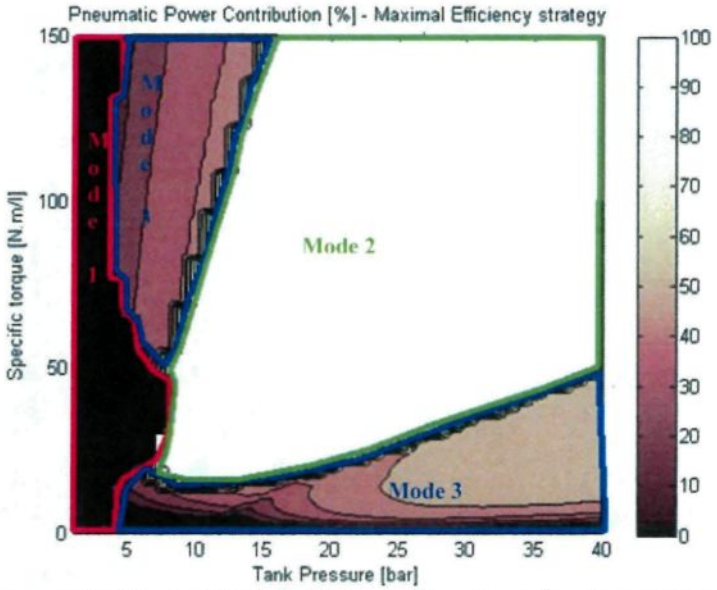

Figure 11: Pneumatic Power Contribution as a function of tank pressure and specific torque for maximal EFF tuning strategy

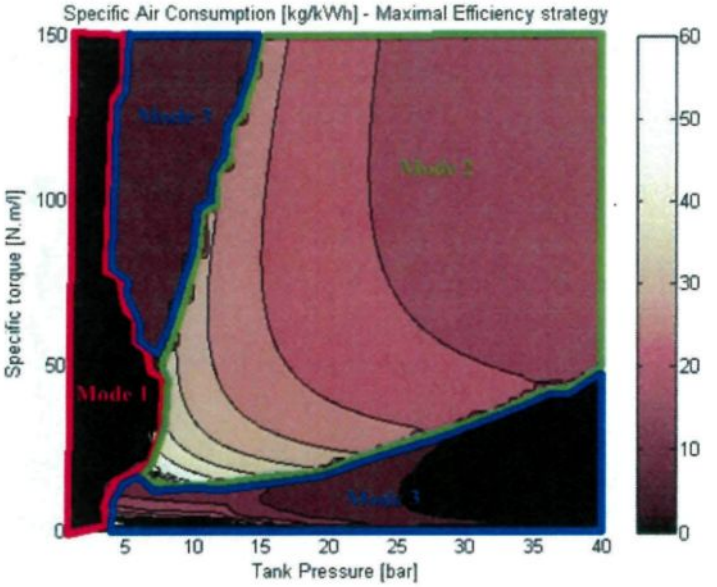

Figure 12: Specific Air Consumption as a function of tank pressure and specific torque for maximal EFF tuning strategy

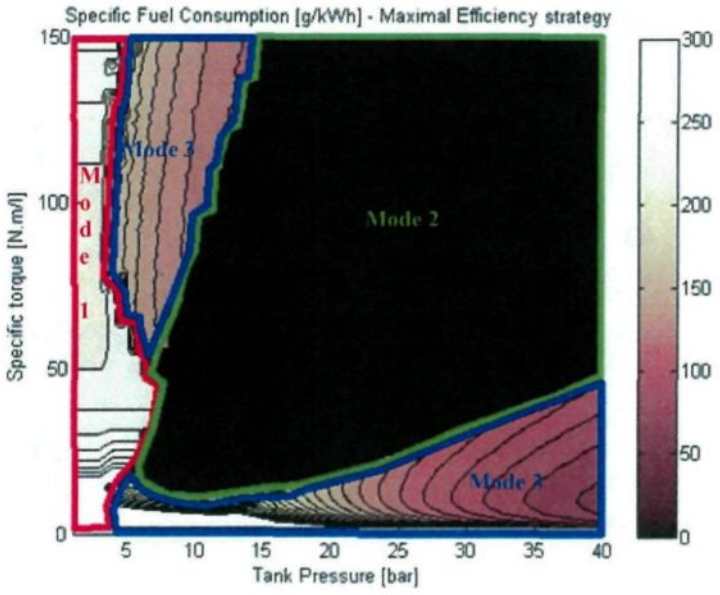

Figure 13: Specific Fuel Consumption as a function of tank pressure and specific torque for maximal EFF tuning strategy

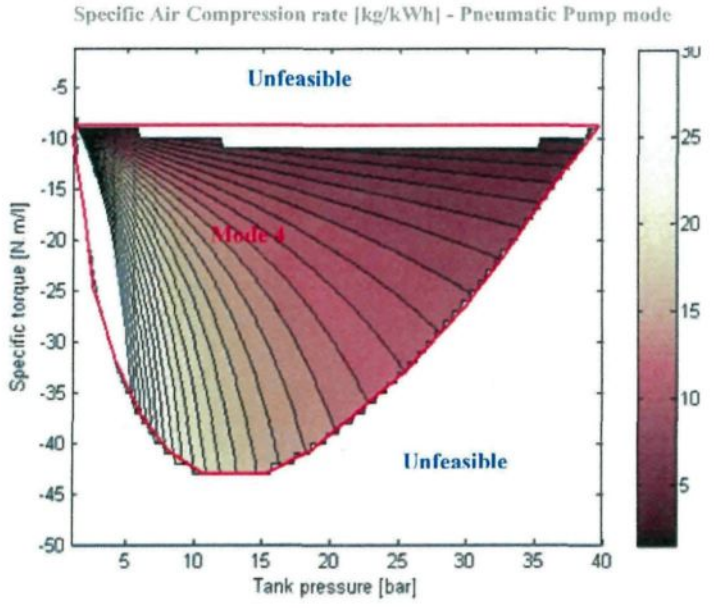

Figure 14: Specific Air Compression rate as a function of tank pressure and specific torque for maximal EFF strategy

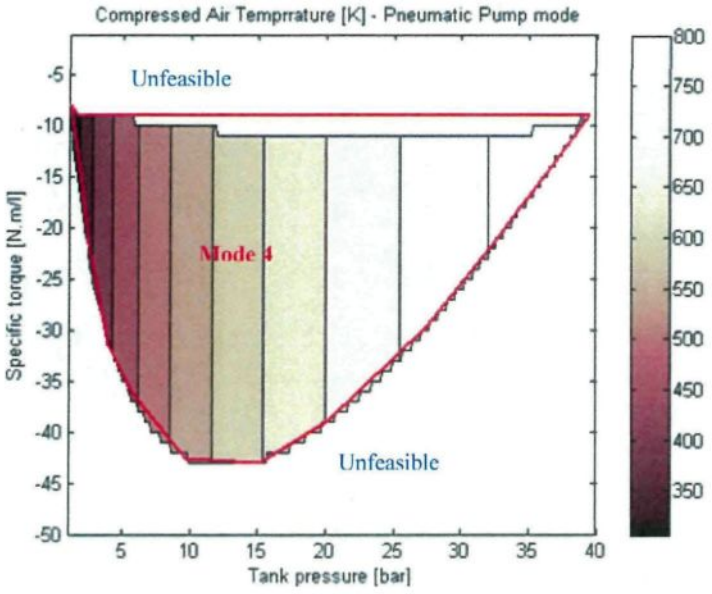

Figure 15: Compressed Air Temperature as a function of tank pressure and specific torque for maximal EFF strategy

4. Evaluation of annual fuel consumption

4.1. Strategies for CAES management

We have evaluated three strategies of CAES management:

1. The "minimal SFC strategy", where the engine constantly operates with the "minimal SFC tuning map";
2. The "maximal EFF strategy", where the engine constantly operates with the "maximal EFF tuning map";
3. The "optimal combined strategy", where the engine controller switches between the "minimal SFC map" and the "maximal EFF map" depending on a defined criterion.

The criterion that we suggest to use to manage the "optimal combined strategy" is based on the forecasting of the wind power and the load during the coming hours. There are several statistical models that may be used for this purpose. The idea is to minimize the lost energy that occurs when the wind is high but the air tank is full. If the prediction of the tank filling shows that the tank will be full during the coming hours, the engine

should operate with the "minimal SFC map", otherwise the "maximal EFF map" is privileged. The mathematical expression of the criterion that should be evaluated at every moment (t) is illustrated in Equation 10:

$$\text{Criterion} = \frac{\int_{t}^{t+\theta(p,V_{tank})} P_{wind}(t)\cdot dt}{\int_{t}^{t+\theta(p,V_{tank})} P_{load}(t)\cdot dt} \qquad (20)$$

Where (P_{load}) is the load-power; (θ) is the prediction's number of hours and (P_{wind}) is the wind-power.

The duration of the prediction (θ) represents the minimal time (in hours) needed to fill the air tank. This depends of the tank volume (V_tank) and of the actual tank pressure (p). The curve illustrating the tank filling minimal time from its lowest level, using a 60-liters-displacement engine, is illustrated in Figure 16.The required filling period (θ) is defined as the number of hours needed to increase the tank pressure from its current pressure up to 3 MPa, according to Figure 16. The resulting variation is shown in Figure 17.

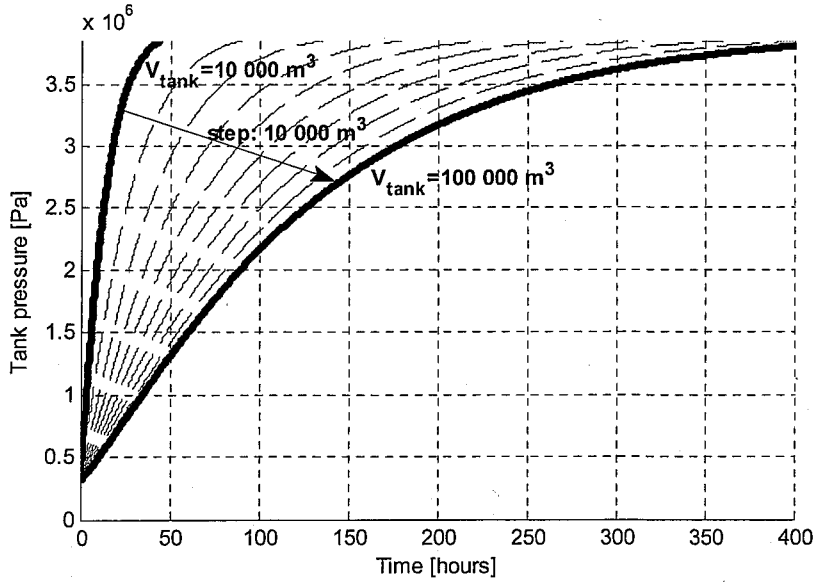

Figure 16: Air tank minimal filling time for different tank-volumes, using a 60-liters-displacement HPCE

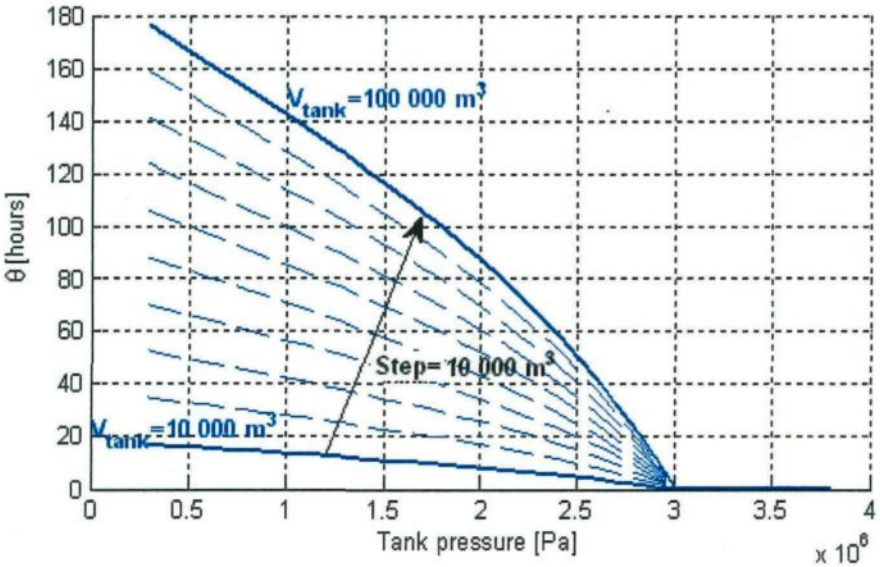

Figure 17: Required filling time as a function of actual tank pressure, for different tank-volumes, using a 60-liters-displacement HPCE

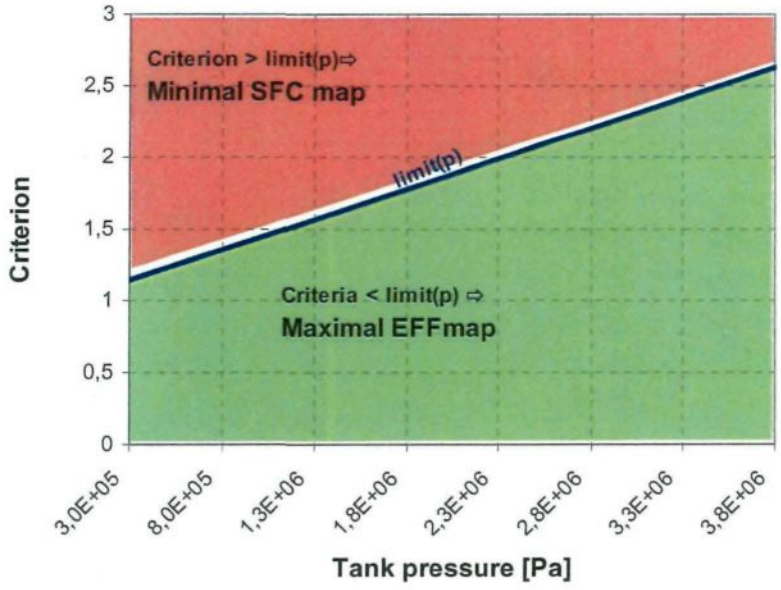

Figure 18: optimal threshold for selecting maps for a 30000-m^3-air-tank

Now that the criterion is evaluated, it should be compared to a threshold. If the criterion is higher than this threshold, the "minimal SFC map" is selected, otherwise the "maximal EFF map" is selected. The threshold is a function of the actual tank pressure. This function is optimized using mathematical algorithms such as "*fminbnd*" or "*ga*" of

Matlab, to minimize the annual fuel consumption. The result of this optimization for a 30000 m^3-air-tank shows that the best function is linear, increasing with tank pressure as shown in Figure 18.

4.2. Fuel consumption results for Tuktoyaktuk village

4.2.1. *Fuel economy analysis for a fixed air- tank capacity*

The simulation is conducted for Tuktoyaktuk village where the maximal load is 1 MW. We have considered a WPPR of one, i.e. composed of three wind turbines ENERCON 330 kW. Also we have considered an air storage capacity of 30000 m^3.

Figure 19 (supplemented by Figure A.3 in the appendix) illustrates the cumulated fuel consumption for power generation with Diesel only, wind-diesel system (WDS) and WDS-HPCE using the three strategies listed in the section 6. The performance is compared with one of an ideal storage system (WDS-IS).

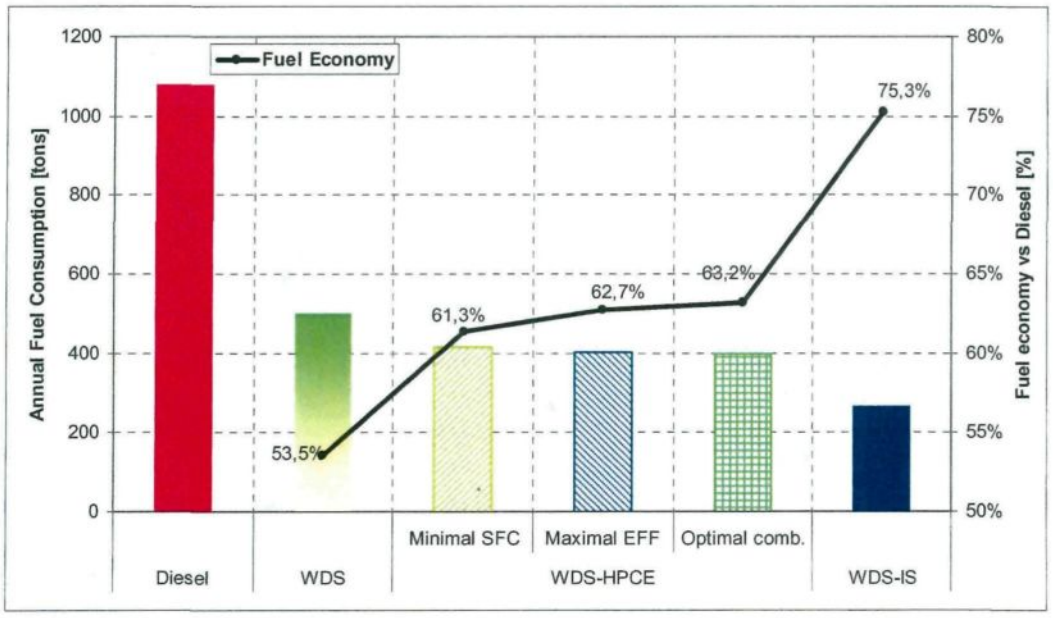

Figure 19: Annual fuel consumption for different case studies and fuel economy compared to a Diesel-only generation

It can be observed that the 53% fuel economy generated by WDS may be improved significantly by adding the HPCE concept. Another 7.8% of fuel economy can be

obtained with the minimal SFC strategy which makes a total fuel economy of 61.3%. By using maximal EFF strategy instead of minimal SFC strategy, another 1.4% of fuel economy can be obtained which makes a total fuel economy of 62.7%. This result is very interesting and it is quite new compared to our previous results [24] because it highlights the interest of not using "at all costs" the compressed air.

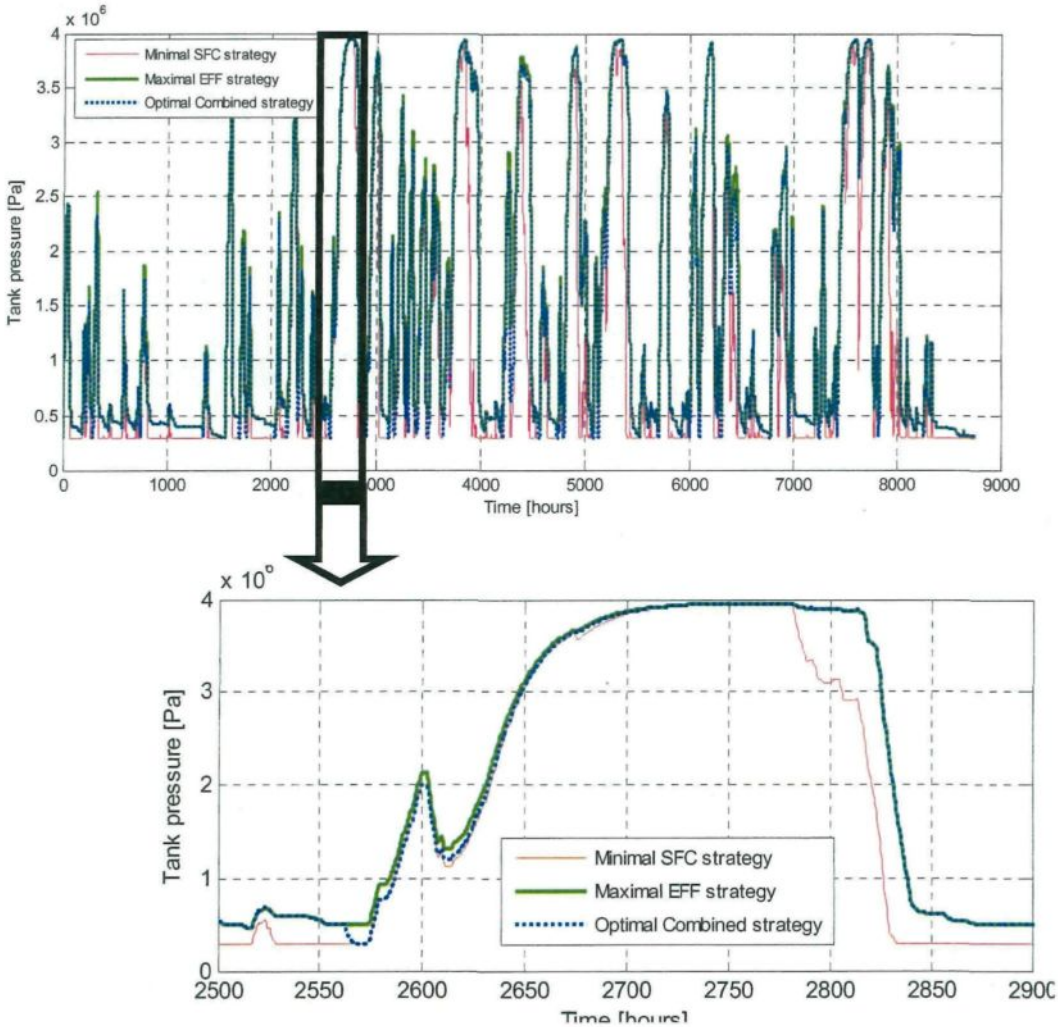

Figure 20: Variation of the tank pressure in WDS-HPCE, for different strategies

Another interesting result concerns the use of the "Optimal combined strategy' where another 0.5% of fuel economy can be obtained to reach a total fuel economy of 63.2%. This result is quite innovative because it proofs that by combining two strategies, the fuel economy obtained is better than the one obtained by each one of those strategies.

The annual fuel consumption (A_FC) of a WDS-IS is 12% lower than that of the HPCE. This is mainly due to the waste that occurs when the surplus of wind power to be stored is higher than the maximal power at which HPCE can operate in Mode 4 (as a pneumatic pump). The charge-discharge efficiency of the HPCE (η_{cd}) indicates the performance of the system compared to an ideal storage system. It can be calculated using the equation

$$\eta_{cd} = \frac{A\_FC_{WDS} - A\_FC_{WDS-HPCE}}{A\_FC_{WDS} - A\_FC_{WDS-IS}} \tag{21}$$

Thus, the charge-discharge efficiency of an HPCE (optimal combined strategy) used with a 30000 m^3 air-tank, and a WPPR of one is approximately 44%.

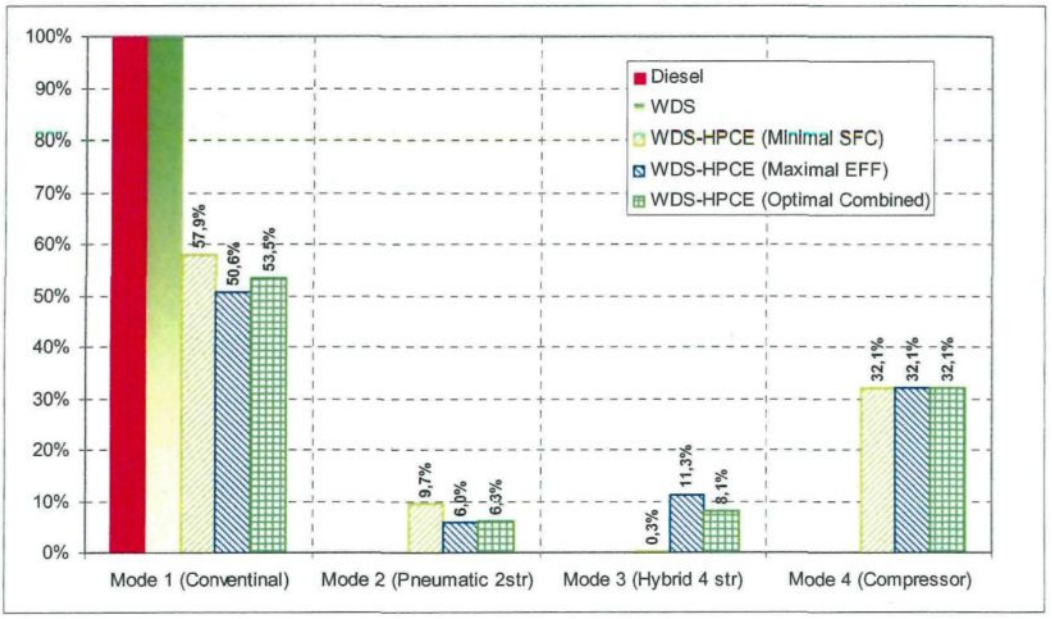

Figure 21: Annual variation of the Tank pressure for different strategies of HPCE

To understand the behavior of each strategy, Figure 20 illustrates the tank pressure during one year, with a focus on a typical zone where the "optimal combined strategy" is useful. As one can observe, the "empty tank" status occurs very often and the tank pressure drops very fast when using "minimal SFC strategy" whereas the opposite happens when using "maximal EFF strategy". Since operating with pneumatic modes with a low tank pressure is not efficient, as shown in section 6.2, the "maximal EFF strategy" keeps the tank pressure above 0.5 MPa by selecting conventional mode. On the other hand, the

"optimal combined strategy" activates the "minimal SFC map" when it predicts that a high amount of compressed air will be generated in the few coming hours. The tank is therefore emptied as illustrated in Figure 20, at x-coordinate value of 2560.

Furthermore, Figure 21 illustrates the temporal distribution of each mode used in the different concepts simulated. While Diesel-only and WDS use continually Mode 1, WDS-HPCE uses the other modes as well. It can be observed that with "minimal SFC strategy", Mode 3 is rarely used (0.3%) because Mode 2 is privileged, while in "maximal EFF strategy", Mode 3 (11.3%) is used significantly more often than Mode 2 (6%). It is also interesting to note that Mode 1 is more often used in "Minimal SFC strategy" than in "Maximal EFF strategy". This is explained by the fact that in Minimal EFF strategy, the air stock is consumed faster and the periods where tank is empty are higher than in "Maximal EFF strategy". As for "Optimal Combined strategy", it is clear that, comparing to "Maximal EFF strategy", the use of Mode 2 and Mode 1 were increased to the detriment of the use of Mode 3. This is logical because Optimal Combined strategy privileges the use of Mode 2 during the excess of wind energy.

4.2.2. Fuel economy as a function of air-tank capacity

Previous evaluation was made using an air storage capacity of 30000 m^3. This capacity has a significant influence on the fuel economy generated by the pneumatic hybridization of Diesel Engines, as shown in Figure 22. An asymptotic fuel economy of 120 tons, i.e. 24% compared to WDS, is obtained for a 100000 m^3-capacity.

It can be noticed that "Optimal Combined Strategy" looses its interest, as tank capacity is increases. This is logical because then the occurrence of "full tank" status gets lower.

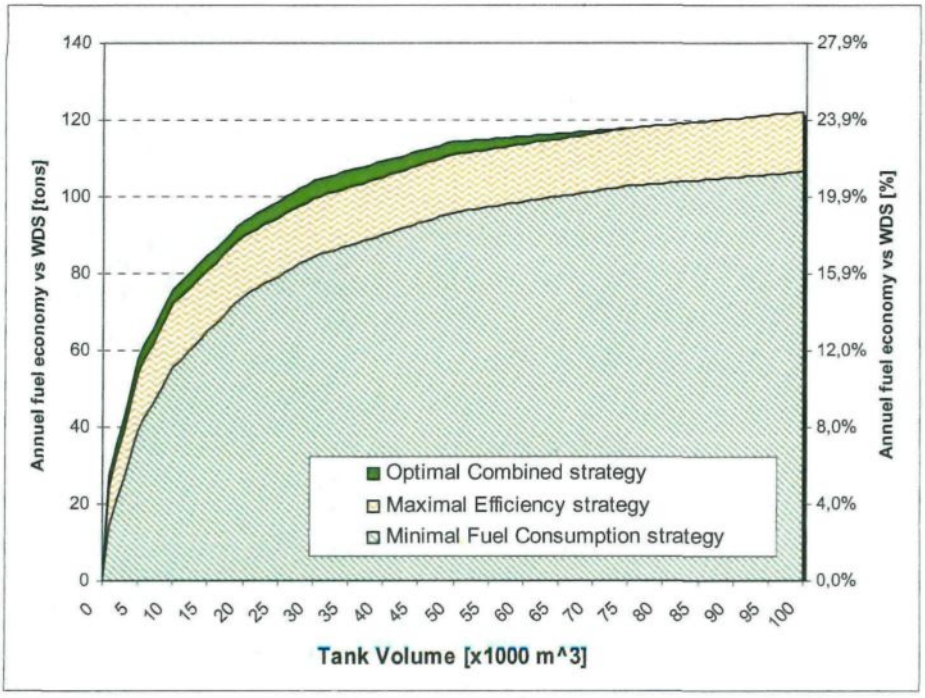

Figure 22: Fuel economy generated by WDS-HPCE compared to a WDS, as a function of the air-tank volume, and for different strategies for CAES management

4.3. Fuel economy as a function of WPPR and the average Wind Speed in the area

Similar analysis was conducted for different WPPR and for different wind speed to establish a general vision of the performance of the HPCE system. The WPPR is varied by changing the number of ENERCON wind turbines. The average wind speed is varied by multiplying by a constant the wind speed data registered in Tuktoyaktuk area. We have drawn in Figure 23, the fuel consumption of the considered systems as a function of the WPPR. The first point of each curve corresponds to a Diesel only power generation. For every "average wind speed", we have plotted the fuel consumption curves of a WDS, a WDS-IS and a WDS-HPCE working under optimal conditions. It is worth noting that for each average wind speed, there is one WPPR where the fuel consumption of a WDS-IS is null, i.e. that the stored energy during the wind excess periods fully compensates the lack of wind energy during low wind speed. On the other hand, the WDS-HPCE cannot reach the "zero fuel consumption" for a reasonable WPPR.

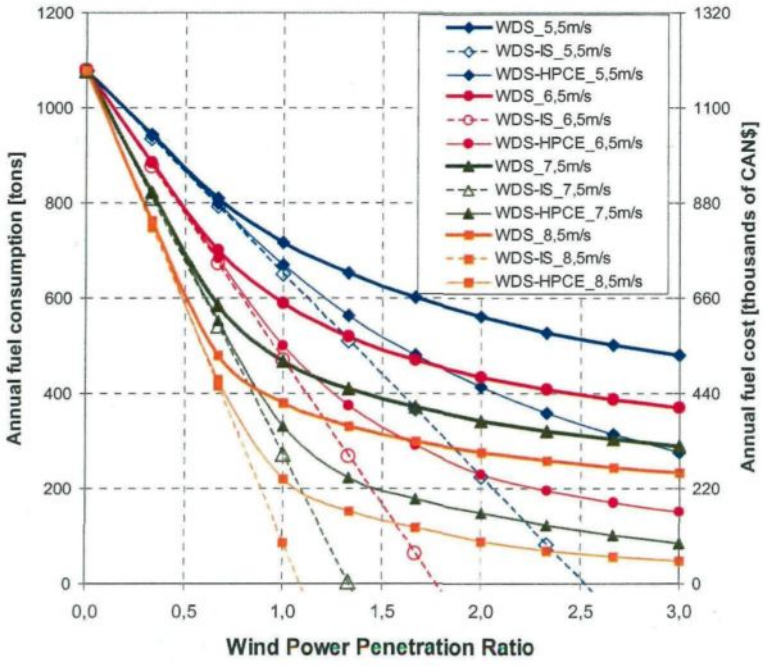

Figure 23: Annual fuel consumption for various average wind speed as a function of WPPR

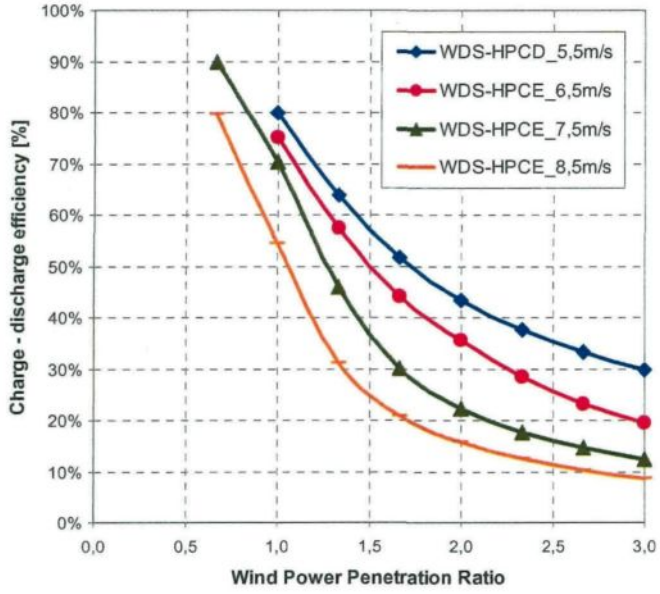

Figure 24: Charge-discharge efficiency of HPCE concept for various average wind speed, as a function of WPPR

The charge-discharge efficiency of the HPCE can be evaluated by comparing the relative position of the WDS-HPCE curve with the one of WDS-IS. Figure 24 illustrates the result. It can be observed that the higher the WPPR, the lower is the charge-discharge efficiency of the WDS-HPCE. Similarly, the higher the wind average speed, the lower the charge-discharge efficiency of the HPCE. The reason of this efficiency drop is the inability of the HPCE to recover very high wind power excess because the maximal specific torque in pneumatic pump mode is limited to 45 Nm/l. To increase the efficiency of charge-discharge, an additional compressor should be added to the system. The operations of the HPCE would be limited then to motor modes.

5. Conclusion and perspectives

This paper is a continuation of previous work [21, 22, 23, 24] were we have given a first order evaluation of the fuel economy generated by a new Hybrid Pneumatic Combustion Engine (HPCE), combined to a hybrid Wind-Diesel System (WDS) for power generation in remote areas. We are seeking at optimizing the WDS-HPCE concept and evaluating the annual fuel economy function of different parameters, such as the storage volume, the average wind speed, the relative size of the wind farm compared to the Diesel engine. We also investigate the potential of implementing a smart strategy for the management of CAES stock in order to maximize the annual benefits.

Two tuning maps are established for managing the HPCE's operation:

1) the first map minimizes the Specific Fuel Consumption (SFC) at every moment by getting the maximum power of the stored compressed air, whatever the discharge efficiency is;
2) the second map optimizes the efficiency (EFF) at every moment even if has to privilege fuel power while air-tanks are not empty yet

An evaluation of the annual fuel consumption for providing the power is provided for three strategies for HPCE control:

1) the "minimal SFC strategy" that enables the engine to operate with the minimal SFC tuning map all the time;

2) the "maximal EFF strategy" that enables the engine to operate with the maximal EFF tuning map all the time;

3) the "optimal combined strategy" that enables the engine to switch between both two tuning maps depending on the prediction of storable energy in the few coming hours.

Compared to a Diesel-only power generation, which is the current power generation method used in Tuktoyaktuk north Canadian village, a WDS power generation with a WPPR of one reduces the annual fuel consumption by 53.5%. Adding the HPCE concept with an air storage capacity of 30000 m^3, the fuel economy raises up to 61.3% if the "minimal SFC strategy" is used, up to 62.7% if the "maximal EFF strategy", and up to 63.2% if the "optimal combined strategy" is used.

Two important and innovative conclusions can be deduced from theses results:

1) The "maximal EFF strategy" is more interesting than the "minimal SFC strategy". This conclusion gives more credit to our HPCE concept compared to the other concepts of pneumatic hybridization of internal combustion engines that allow the engines to operate as air motors only.

2) By combining two strategies, the fuel economy is better than the one obtained by each one of those strategies. Indeed, the "optimal combined strategy" takes the advantages of the two other strategies and is therefore better than both of them.

The air storage capacity is very important for obtaining significant fuel economy. The optimal air capacity depends on the WPPR. For a WPPR of 1, the storage capacity that permits obtaining the maximal fuel economy in Tuktoyaktuk is 100000 m^3. With this capacity, the fuel economy generated with a WDS-HPCE is 64% compared to a Diesel generation and 24% compared to a WDS generation. Moreover, the "optimal combined strategy" is more interesting when the air-storage capacity is low.

Depending on the site exposure to the wind, these conclusions can be different. The higher the wind speed, the higher the fuel economy generated by a WDS. However, the WDS-HPCE is less effective when the average wind speed is higher. The same tendency is observed when WPPR is higher. The charge-discharge efficiency of the WDS-HPCE is about 80% for a WPPR of 1 and an average wind speed of 5.5 m/s, but it drops to 10%

for a WPPR of 3 and an average wind speed of 8.5 m/s. The reason of this efficiency drop is the inability of the HPCE to recover very high wind power excess because the maximal specific torque in pneumatic pump mode is limited to 45 Nm/l. To increase the efficiency of charge-discharge, an additional compressor should be added to the system. The operations of the HPCE would be limited then to motor modes.

Finally, it is important to note that the evaluation provided in the present paper is based on theoretical models and is not confirmed yet by testing measurement. It aimed only at bounding the fuel economy generated by the WDS-HPCE concept. The models used are simplistic and need to be reevaluated by using more sophisticated models such as one-dimensional engine model to take in consideration several phenomena that might influence the fuel saving estimation, such as flow supersonic limitations through valves, valves response time for opening and closing, fuel injection shape, fuel burn process, heat loss through engine walls and heat loss through compressed air tank walls.

References

[1] Ibrahim H., Ilinca A., Younes R., Basbous T, Study of a Hybrid Wind-Diesel System with Compressed Air Energy Storage, IEEE Canada, electrical power conference 2007, "Renewable and Alternative Energy Resources", EPC2007,, Montreal, Canada; October 25-25, 2007

[2] Liu W, Gu S, Qiu D. Techno-economic assessment for off-grid hybrid generation systems and the application prospects in China. http://www.worldenergy.org/wecgeis/publications/.

[3] Weis TM, Ilinca A. The utility of energy storage to improve the economics of wind-Diesel power plants in Canada. Renewable Energy 2008; 33(7):1544-57.

[4] La stratégie énergétique du Québec 2006-2015. L'énergie pour construire le Québec de demain. http://www.mrnf.gouv.qc.ca/energie/eolien.

[5] Ibrahim H, Ilinca A, Perron J. Solutions actuelles pour une meilleure gestion et intégration de la ressource éolienne. CSME/SCGM Forum 2008 at Ottawa. The Canadian Society for Mechanical Engineering, 5-8 June 2008.

[6] ACÉÉ. Association canadienne de l'énergie éolienne. http://www.canwea.com

[7] Maisson JF. Wind power development in sub-arctic conditions with severe rime icing. In: Presented at the circumpolar climate change summit and exposition, Whitehorse, Yukon; 2001.

[8] www.nunavutpower.com.

[9] Reeves B. Kotzebue electric association wind projects. In: Proceedings of NREL/AWEA 2002 wind-Diesel workshop, Anchorage, Alaska, USA, 2002.

[10] Ibrahim, H., Younes, R., Ilinca, A., Ramdenee, D., Dimitrova, M., and Perron, J.; Potential of a Hybrid Wind-Diesel-CAES System for Nordic Remote Canadian Areas; Energy Procedia, v.6, pp. 795-804, 2011

[11] Ibrahim, H., Dimitrova, M., Ilinca, A., and Perron, J.; Étude et conception d'un système hybride éolien-diesel-stockage d'air comprimé pour l'électrification d'une station de télécommunication isolée; European Journal of Electrical Engineering (Revue Internationale de Génie Électrique), numéro spécial sur les réseaux isolés, vol.12, pp. 701-731, 2009

[12] Ibrahim, H., Ghandour, M., Dimitrova, M., Ilinca, A., and Perron, J.; Integration of Wind Energy into Electricity Systems: Technical Challenges and Actual Solutions, Energy Procedia, v.6, pp. 815-824, 2011

[13] Reid R. Application de l'éolien en réseaux non reliés. Liaison Énergie-Francophonie, N°35/2e Trimestre; 1997.

[14] Jean Y, Nouaili A, Viarouge P, Saulnier B, Reid R. Développement d'un système JEDHPSS représentatif d'un village typique des réseaux non relies. Rapport IREQ-94-169-C; 1994.

[15] Gagnon R, Nouaili A, Jean Y, Viarouge P. Mise à jour des outils de modélisation et de simulation du Jumelage Éolien-Diesel à Haute Pénétration Sans Stockage et rédaction du devis de fabrication de la charge de lissage. Rapport IREQ-97- 124-C; 1997.

[16] www.danvest.com.

[17] Ilinca A, Chaumel JL. Implantation d'une centrale éolienne comme source d'énergie d'appoint pour des stations de télécommunications. Colloque international sur l'énergie éolienne et les sites isolées, Îles de la Madeleine; 2005.

[18] Cavallo, A., Controllable and affordable utility-scale electricity from intermittent wind resources and compressed air energy storage (CAES), Energy 32 (2007) 120–127

[19] Ibrahim, H., Ilinca, A.; Contribution of the Compressed Air Energy Storage in the Reduction of GHG - Case Study: Application on the Remote Area Power Supply Systems; in Air Pollution, editor InTech, 2012, to appear

[20] Ibrahim, H., Ilinca, A., and Perron, J.; Energy Storage Systems - Characteristics and Comparisons, Renewable and Sustainable Energy Reviews, v. 12, no. 5, pp. 1221-1250, 2008

[21] Basbous T, Younes R, Ilinca A, et al. ; Required time response of a variable valve actuator equipping a hybrid pneumatic–combustion engine; Int. J. Engine Res ; 2012; DOI: 10.1177/1468087412450812

[22] Basbous T, Younes R, Ilinca A, et al. Pneumatic hybridization of a diesel engine using compressed air storage for wind-diesel energy generation; Energy 2012; 38: 264–275.

[23] Basbous T, Younes R, Ilinca A, et al. ; Fuel consumption evaluation of an optimized new hybrid pneumatic–combustion vehicle engine on several driving cycles ; Int. J. Engine Res ; 2012; DOI: 10.1177/1468087411433250

[24] Basbous T, Younes R, Ilinca A, et al. ; A new hybrid pneumatic combustion engine to improve fuel consumption of Wind-Diesel power system for non-interconnected areas; Applied Energy; 2012; DOI: 10.1016/j.apenergy.2012.03.005

[25] Higelin, P., Charlet, A., Chamaillard, Y., Thermodynamic Simulation of a Hybrid Pneumatic-Combustion Engine Concept, Int.J. Applied Thermodynamics, Vol.5, (No.1), p.1-11; 2002

[26] Heywood, J.B., 1988, Internal Combustion Engine Fundamentals, New York, McGraw Hill.

[27] Stone, R., 1999, Introduction to internal combustion engines, Department of Engineering Science, University of Oxford

[28] Higelin, P., Vasile, I., Charlet, A., and Chamaillard, Y., Parametric optimization of a new hybrid pneumatic combustion engine concept, Int. J. Engine Res., Vol. 5; No. 2 205

[29] P. Higelin, A. Charlet, Y. Chamaillard, "Thermodynamic Simulation of a Hybrid Pneumatic Combustion Engine Concept International Journal of Applied Thermodynamics", Vol 5, No. 1, pp 1 – 11, ISSN 1301 9724; 2002

[30] Burton, T., Sharpe D., Jenkins, N., et al.; Wind Energy Handbook; John Wiley & Sons Ltd; ISBNs: 0-470-84606-2

Appendix

Complementary graphics:

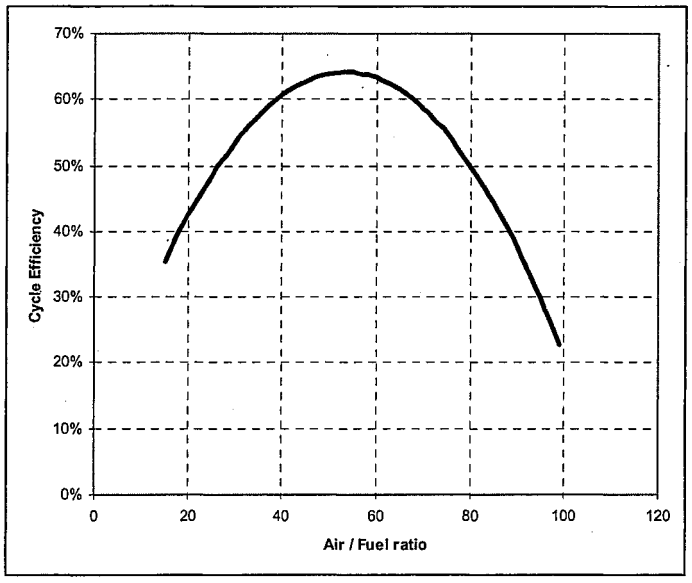

Figure A.1: Cycle efficiency as a function of AFR

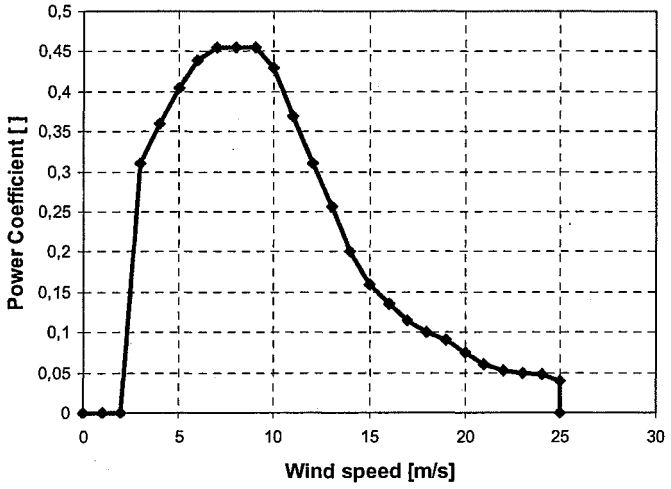

Figure A.2: Power Coefficient curve of the ENERCON 330kW wind turbine

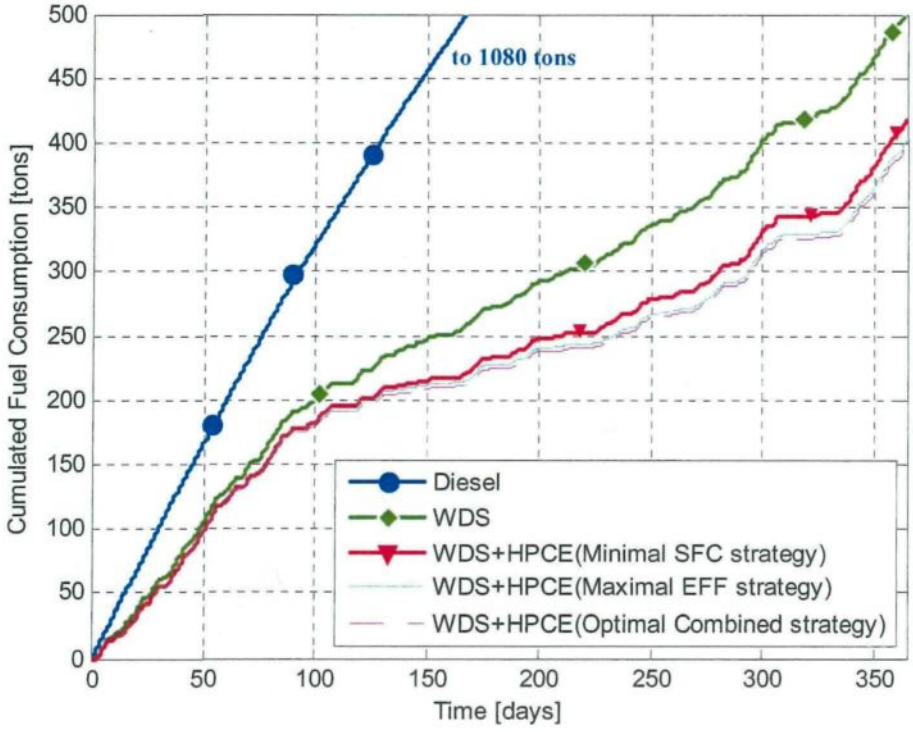

Figure A.3: Cumulated fuel consumption in Tuktoyaktuk for different case studies

CHAPITRE VII

Synthèse, conclusions et perspectives

VII.1. Synthèse des résultats obtenus au cours de notre étude

VII.1.1. Description du concept du Moteur Hybride Pneumatique-Diesel (MHPD)

Le concept que nous proposons est illustré dans la Figure VII.1.

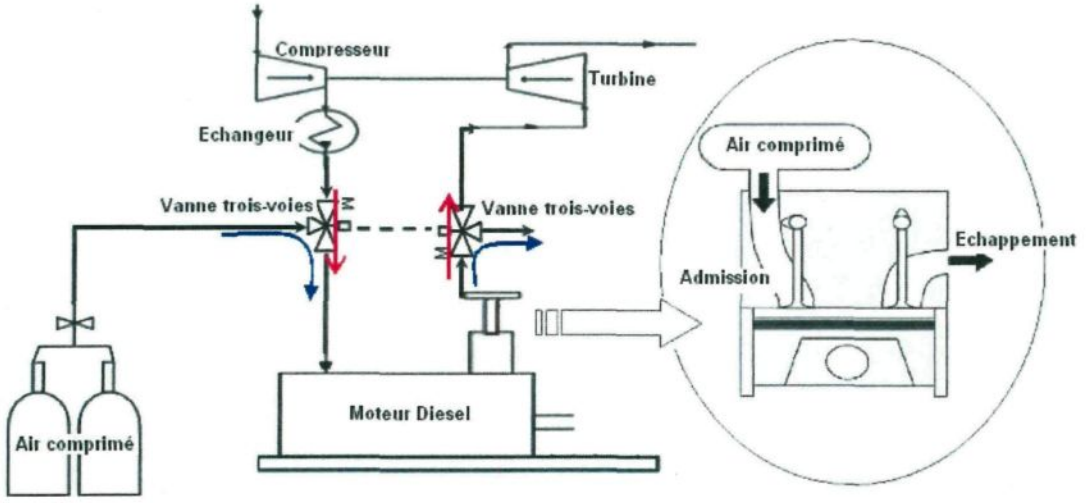

Figure VII. 1 : Schéma de principe du MHPD

Ce concept peut être obtenu à partir d'un moteur Diesel conventionnel en réalisant les modifications suivantes :

1) Le court-circuit du turbocompresseur à travers deux vannes trois voies. La première relie l'admission du moteur au réservoir d'air comprimé ou à la sortie du compresseur. La deuxième relie l'échappement du moteur à l'entrée de la turbine ou à l'air libre ;
2) L'ajout d'un Système de Distribution Variable (SDV) qui permet de prendre le contrôle total de chacune des soupapes d'admission et d'échappement du moteur ;
3) L'ajout d'un système de contrôle de l'injection de carburant.

Comme le montre la Figure VII.2, le concept MHPD est capable d'opérer selon les quatre modes suivants, et dont les cycles thermodynamiques idéaux sont illustrés dans les figures VII.3 à VII.6.

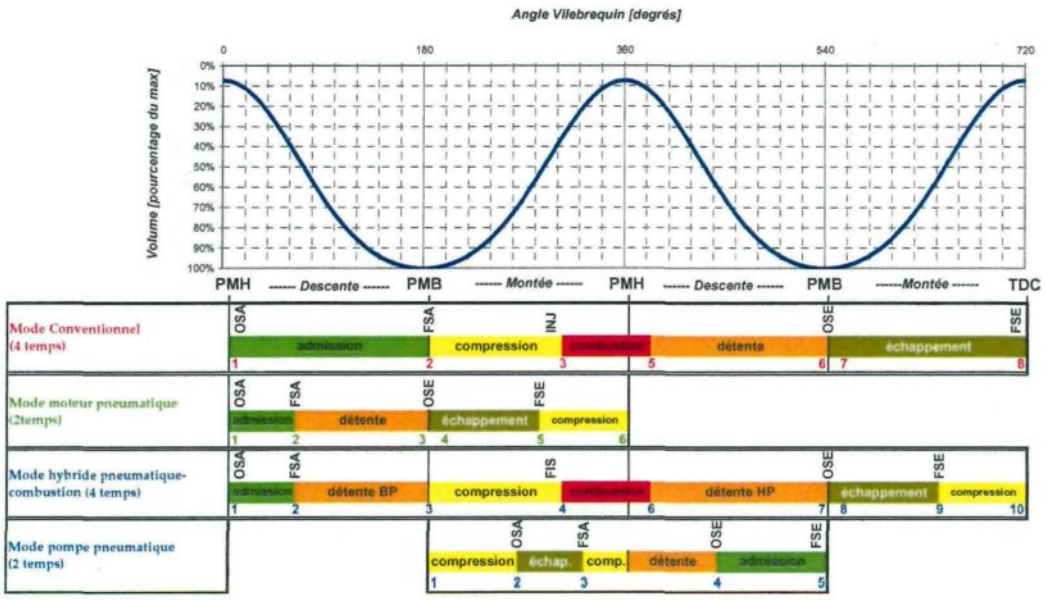

Figure VII. 2 : Principe de fonctionnement du MHPD

1) Mode conventionnel quatre-temps: les vannes trois-voies connectent l'admission et l'échappement du moteur à la sortie du compresseur et à l'entrée de la turbine respectivement. Les pressions d'admission et d'échappement sont établies par l'équilibre du turbocompresseur. Un cycle complet dure pendant deux tours du vilebrequin. La soupape d'admission est ouverte durant toute la période (1→2) de décente du piston du point mort haut (PMH) au point mort bas (PMB). Quand le piston arrive à son PMB, la phase de compression (2→3) commence et se termine bien avant l'arrivée du piston au PMH une deuxième fois, quand le carburant commence à être injecté (IC). Un peu plus tard la phase combustion (3→5) commence et se termine après le PMH. C'est à ce moment que la phase de détente (5→6) commence et dure jusqu'au PMB. C'est cette phase de détente qui permet de transformer l'énergie dégagée pendant la phase de combustion en travail mécanique. Quand le piston arrive au PMB, la soupape d'échappement s'ouvre et reste ouverte pendant toute la montée du piston vers le PMH autorisant ainsi la phase d'échappement (7→8).

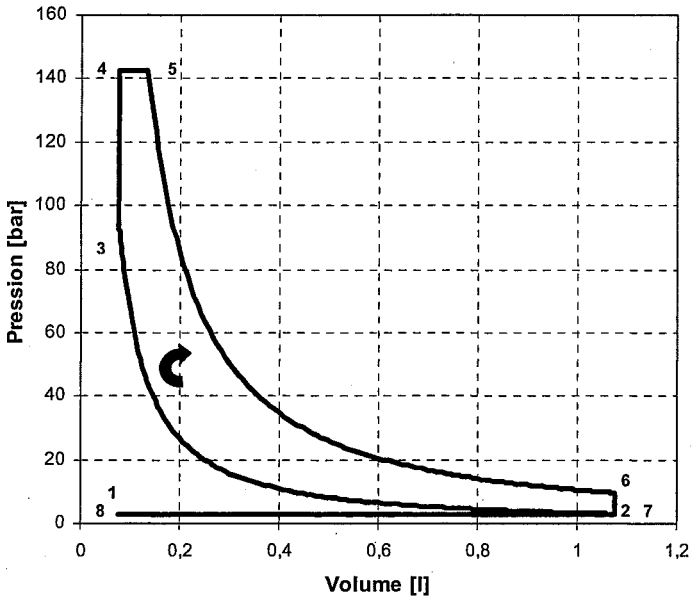

Figure VII. 3 : Cycle thermodynamique théorique décrivant le mode conventionnel

2) Mode moteur pneumatique deux-temps: les vannes trois-voies déconnectent le turbocompresseur et connectent l'admission et l'échappement du moteur au réservoir d'air comprimé et à l'air libre respectivement. La pression d'admission est égale à la pression de stockage d'air et la pression d'échappement est égale à la pression atmosphérique. Un cycle complet dure pendant un seul tour du vilebrequin. La soupape d'admission s'ouvre au PMH et reste ouverte jusqu'à un moment à définir entre le PMH et le PMB, c'est la phase d'admission (1→2). A la fin de cette phase, la soupape d'admission se ferme et la phase de détente (2→3) commence et dure jusqu'à l'arrivée du piston au PMB. Le travail de conversion de l'énergie potentielle stockée dans le réservoir en une énergie mécanique se réalise pendant les deux phases d'admission et de détente. Quand le piston arrive à son PMB, la soupape d'échappement s'ouvre autorisant ainsi la phase d'échappement (4→5). Il est possible, mais non obligatoire, que la soupape d'échappement se ferme avant le PMH afin de permettre une deuxième phase de compression (5→6) qui dure jusqu'au PMH. A l'ouverture de la soupape d'admission au PMH pour commencer le nouveau cycle, une phase d'admission isochore (6→) fait croître presque instantanément la pression dans la chambre.

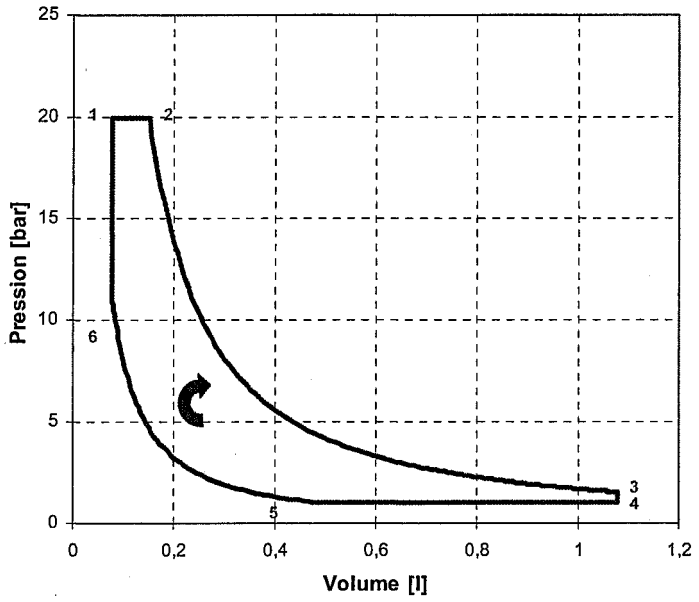

Figure VII. 4 : Cycle thermodynamique théorique décrivant le mode moteur pneumatique deux-temps

3) Mode moteur hybride pneumatique-combustion quatre-temps: ce mode est une combinaison des deux précédents modes. Les vannes trois-voies sont dans la même position qu'en mode moteur pneumatique. Le cycle dure pendant deux tours du vilebrequin. A peu de choses près, le premier tour est équivalent au cycle pneumatique deux temps et le deuxième tour est équivalent au demi-cycle haute pression du mode conventionnel. Le travail réalisé par le piston pendant le premier tour est un travail pneumatique issu de la conversion de l'énergie potentielle de l'air comprimé alors que le travail réalisé par le piston pendant le deuxième tour est issu de la conversion de l'énergie du combustible. On définit la Contribution de la Puissance Pneumatique (CPP) comme étant le ratio du travail pneumatique sur le travail total du cycle. Pour une même consigne de puissance mécanique, la CPP peut être modulée en retardant ou avançant la fermeture de la soupape d'admission et en corrigeant la quantité de carburant pour rencontrer la consigne.

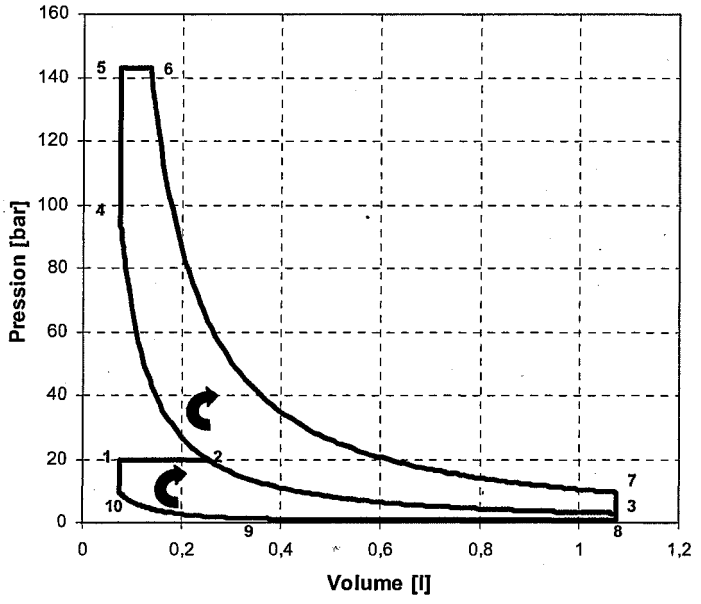

Figure VII. 5 : Cycle thermodynamique théorique décrivant le mode moteur hybride pneumatique-combustion quatre-temps

4) Mode pompe pneumatique deux-temps: A peu de choses près, ce mode est l'inverse du mode moteur pneumatique. Les vannes trois-voies sont dans la même position que dans ce mode mais l'admission de l'air à la pression atmosphérique se réalise via la soupape d'échappement et l'échappement de l'air comprimé se réalise via la soupape d'admission. Ceci est possible grâce à un contrôle des instants d'ouverture et de fermeture des soupapes. Ces instants sont optimisés de façon à permette de comprimer une quantité maximale d'air en consommant une énergie mécanique minimale. Le cycle dure pendant un tour du vilebrequin. Au PMB, la phase de compression (1→2) commence et la pression de l'air dans la chambre croît. Quand cette pression devient égale à la pression du réservoir, pression à laquelle la compression de l'air doit se faire, la soupape d'admission s'ouvre et autorise ainsi la phase d'échappement (2→3). Si la puissance mécanique disponible est suffisante, la phase d'échappement continue jusqu'au PMH, sinon la soupape d'admission se ferme avant le PMH. Après la fermeture de la soupape d'admission, une phase de compression suivie d'une phase de détente (3→4) a lieu jusqu'à ce que la pression dans la chambre devienne égale à la pression atmosphérique, ce qui arrive bien avant le PMB. A ce moment la soupape d'échappement s'ouvre autorisant ainsi la phase d'admission (4→5).

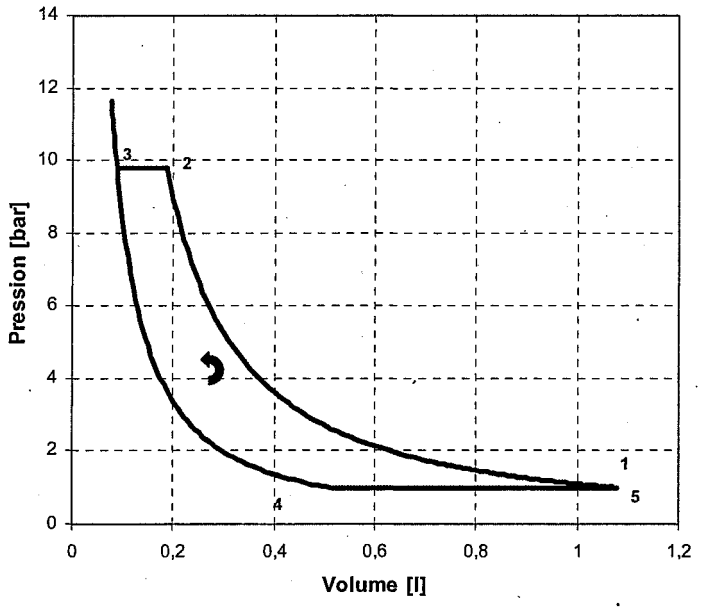

Figure VII. 6 : Cycle thermodynamique théorique décrivant le mode pompe pneumatique deux-temps

VII.1.2. Performance dynamique du Système de Distribution Variable (SDV) nécessaire pour permettre un fonctionnement correct du MHPD

Un Système de Distribution Variable (SDV) est nécessaire pour contrôler l'ouverture et la fermeture des soupapes d'admission et d'échappement du moteur, afin de piloter les différents modes opératoires. On définit le Temps de Réponse (TR) du SDV par le temps au bout duquel la soupape arrive à 95% de sa position finale, aussi bien en ouverture qu'en fermeture (Figure VII.7).

Suite à une étude paramétrique investiguant l'impact du TR sur la performance du Moteur Hybride Pneumatique Diesel (MHPD), il a été démontré que le TR requis pour opérer correctement le MHPD est inversement proportionnel au régime de rotation du moteur. Pour un moteur tournant à 750 tours par minute, un TR de 1 milliseconde est au minimum nécessaire pour un fonctionnement tel que décrit dans la section précédente. Toutefois, il est possible d'opérer le système avec un TR entre 1 et 5 millisecondes mais en se passant du mode pompe pneumatique. Un compresseur indépendant sera alors indispensable.

Il est toutefois important de mentionner que les SDV existant actuellement sur le marché, principalement pour l'application aux moteurs d'automobiles, ont des TR de l'ordre de 5 millisecondes.

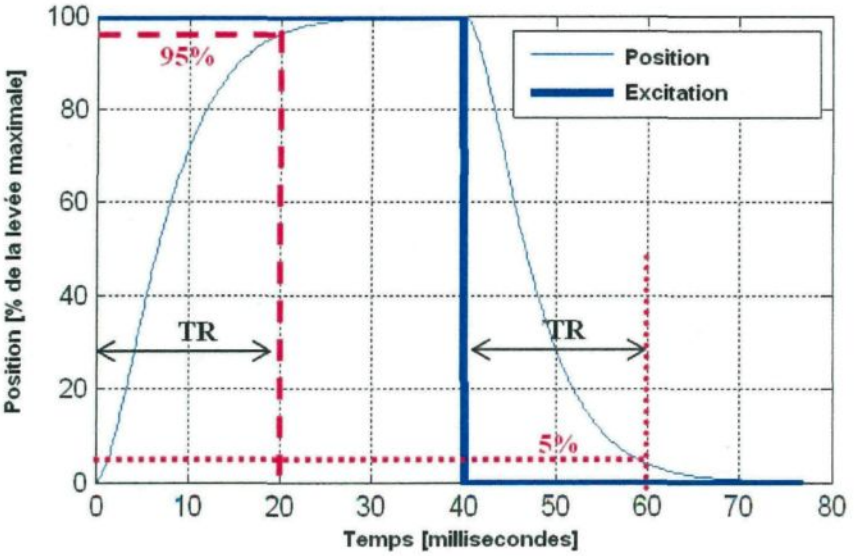

Figure VII. 7 : Définition du Temps de Réponse (TR) du SDV

VII.1.3. Volumes de stockage nécessaires pour réaliser des économies de carburant intéressantes avec le SHEDAC-MHPD

Le volume de stockage est un paramètre important pour la réalisation d'économies significatives de carburant. Suite à une étude paramétrique investiguant l'impact de ce volume, il a été démontré que plus le volume est important plus l'économie de carburant est intéressante. Cette variation est cependant asymptotique, autrement dit, il existe un volume « optimal » à partir duquel l'augmentation du volume n'a plus d'effet, voire elle a un effet négatif. Ce volume optimal est d'autant plus grand que le Taux de Pénétration en Puissance (TPP) éolienne est élevé et / ou que la vitesse moyenne du vent sur le site est élevée. A titre d'exemple, pour un site ayant une puissance moyenne de consommation de 500 kW et une vitesse moyenne du vent de 6.5 m/s et équipé avec un SHEDAC ayant un TPP de 1, le volume de stockage nécessaire pour obtenir la meilleure consommation annuelle de carburant est de 100,000 m^3. Toutefois, pour un volume de stockage de 25,000 m^3, 80% de

l'économie de carburant est réalisée et pour un volume de 50,000 m^3, 95% de l'économie de carburant est réalisée. Ce volume de stockage optimal varie proportionnellement avec le TPP et avec le cube de la vitesse moyenne sur le site.

VII.1.4. Stratégie de gestion optimale du stock d'air

Le concept MHPD est capable de fournir d'une infinité de façons une puissance demandée pour une pression disponible dans le réservoir. La variable d'ajustement est le taux de Contribution de la Puissance Pneumatique (CPP) dans la puissance totale fournie. Suite à une étude détaillée de ces possibilités, nous avons distingué trois stratégies :

1) Une stratégie qui minimise la consommation de carburant à chaque instant, en maximisant le CPP ;
2) Une stratégie qui maximise le rendement global à chaque instant en sélectionnant le CPP optimal ;
3) Une stratégie qui combine ces deux stratégies en privilégiant la première lors des périodes d'abondance du vent, et la seconde lors des périodes de déficit de vent ;

Nous avons démontré que la deuxième stratégie apporte globalement plus d'économies de carburant que la première, sur une année complète, même si, durant des courtes périodes, la première stratégie minimise, par conception, la consommation de carburant. L'écart de consommation de carburant entre ces deux premières stratégies pour un site ayant une puissance moyenne de consommation de 500 kW et une vitesse moyenne du vent de 6.5 m/s et équipé avec un SHEDAC ayant un TPP de 1 est de 15 tonnes par an environ, soit 3% ; et ceci quelque soit le volume de stockage entre 10,000 m^3 et 100,000 m^3. Ce résultat est à la fois innovant et important étant donné qu'il fait la preuve que notre concept MHPD est bien plus performant que certains concepts d'hybridation pneumatiques des moteurs Diesels qui ne proposent qu'un fonctionnement en mode moteur pneumatique.

Nous avons également démontré que la troisième stratégie est capable d'améliorer de 3 à 4 tonnes de carburant supplémentaires la consommation annuelle. Toutefois, elle nécessite de connaitre à l'avance la vitesse du vent et la consommation. Des logiciels de prédiction statistique existent et peuvent être utilisés pour atteindre cet objectif. Ce résultat est aussi très innovant étant donné qu'il prouve

qu'en commutant intelligemment entre deux stratégies, il est possible de réaliser un meilleur résultat que ceux réalisés avec chacune de ces deux stratégies.

VII.1.5. Économie de carburant réalisée grâce au SHEDAC-MHPD

La Figure VII.8 est une suite logique des Figures I.11 et I.12. Nous y avons ajouté les courbes de consommation réalisée par un système SHEDAC-MHPD en fonction du TPP et pour différentes valeurs moyennes de la vitesse du vent sur un site, dont la valeur moyenne de la puissance est 500 kW (cas de Tuktoyaktuk), et ceci pour une volume de stockage optimal tel que préconisé dans le paragraphe 1.3 et une stratégie d'utilisation de l'air comprimé optimale tel que décrite dans le chapitre 1.4.

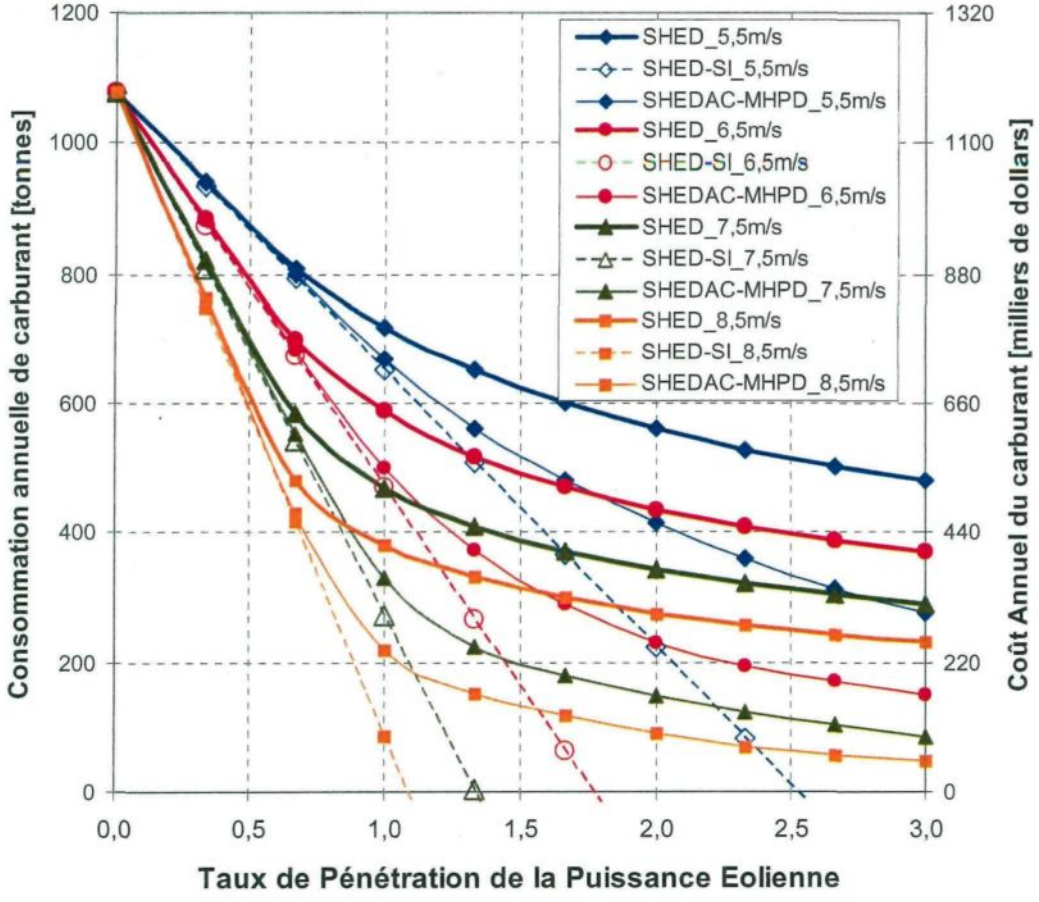

Figure VII. 8 : Consommation annuelle d'un SHED, d'un SHED-SI et d'un SHEDAC-MHPD, en fonction du TPP et de la vitesse moyenne du vent

Il est clair que le système SHEDAC-MHPD permet de réduire de façon significative la consommation de carburant. Dans le site de Tuktoyaktuk où la vitesse moyenne du vent est de 5.5 m/s, l'économie annuelle de carburant réalisée par rapport à un SHED à haute pénétration est de 47 tonnes pour un TPP de 1, de 146 tonnes pour un TPP de 2 et de 203 tonnes pour un TPP de 3. Si le site était plus venteux, avec une vitesse moyenne de 6.5 tonnes/an, l'économie annuelle de carburant qui aurait été réalisée par rapport à un SHED à haute pénétration est de 88 tonnes pour un TPP de 1, de 204 tonnes pour un TPP de 2 et de 219 tonnes pour un TPP de 3.

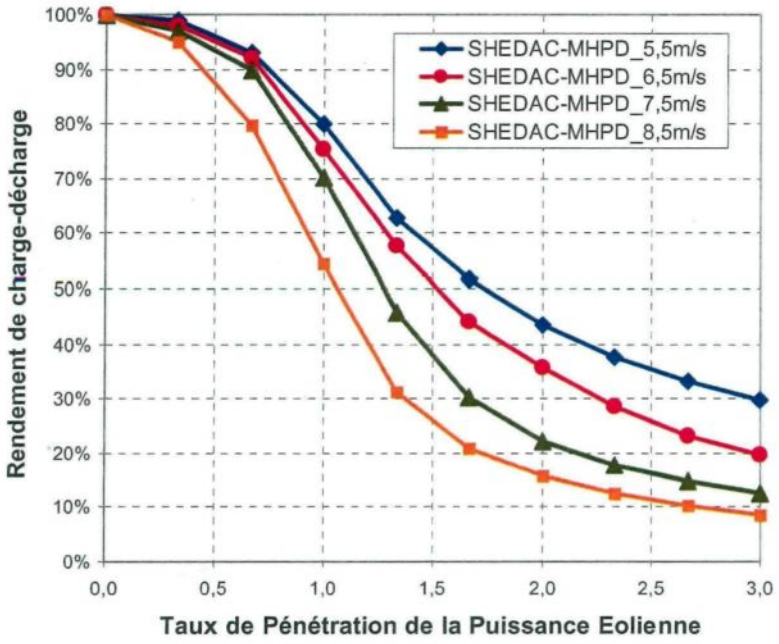

Figure VII. 9 : Rendement du cycle charge-décharge avec un SHEDAC-MHPD, en fonction du TPP et de la vitesse moyenne du vent

Quant à l'efficacité (EFF) de stockage-déstockage du SHEDAC-MHPD qui indique le taux de dissipation de l'énergie éolienne excédentaire, elle peut être évaluée en comparant la Consommation Annuelle de Carburant (CAC) du SHEDAC-MHPD avec celle du SHED-SI. Elle peut être calculée suivant la formule suivante :

$$EFF = \frac{CAC_{SHED} - CAC_{SHEDAC-MHPD}}{CAC_{SHED} - CAC_{SHED-SI}} \qquad \text{(VII.1)}$$

La figure VII.9 illustre cette efficacité pour tous les cas simulés. On observe que le SHEDAC-MHPD est plus efficace pour des faibles TPP et pour des faibles vitesses moyennes du vent. L'efficacité maximale se situe autour de 90% mais elle chute à moins que 10% pour les très forts TPP associés à une très forte vitesse moyenne du vent. La raison est que le MHPD, fonctionnant en mode pompe pneumatique, est limité en puissance récupérable. Les surplus de puissance éolienne excédant cette limite ne peuvent pas être convertis en air comprimé. Afin de retrouver une efficacité nominale de l'ordre de 90% du système pour des TPP très élevés, il est nécessaire d'ajouter des compresseurs indépendants et de se contenter à faire fonctionner le MHPD avec ses trois modes moteurs. Le système serait alors plus cher, mais il serait bien plus efficace.

VII.1.6. Autres applications possibles pour le concept MHPD

L'utilisation du concept MHPD ne se limite pas au SHED. En effet, toutes les applications pour lesquelles la puissance fluctue entre des valeurs positives (demande) et des valeurs négatives (offre) peuvent faire l'objet d'une amélioration de leur efficacité globale tout en utilisant ce concept. A titre d'exemple, pour les automobiles, la puissance mécanique à la roue est positive lors des accélérations et des roulages stabilisés, et négative lors des décélérations. Dans le cas d'un véhicule équipé d'moteur conventionnel, cette puissance négative est dissipée dans les freins, tout comme les charges de délestages utilisés pour dissiper l'excès de l'énergie éolienne dans un SHED. Ce même véhicule équipé par un MHPD est capable de stocker l'énergie disponible lors des décélérations du véhicule pour la restituer plus tard. Sa consommation de carburant est alors nettement améliorée. Nous avons démontré que l'économie de carburant réalisée sur un véhicule de 1500 kg, pour un volume de stockage d'air de 100 litres, est de 17% sur le cycle d'homologation Européen NEDC (Figure VII.10), 60% sur le cycle standard international ARTEMIS type urbain, et de 23% sur le cycle ARTEMIS type extra-urbain.

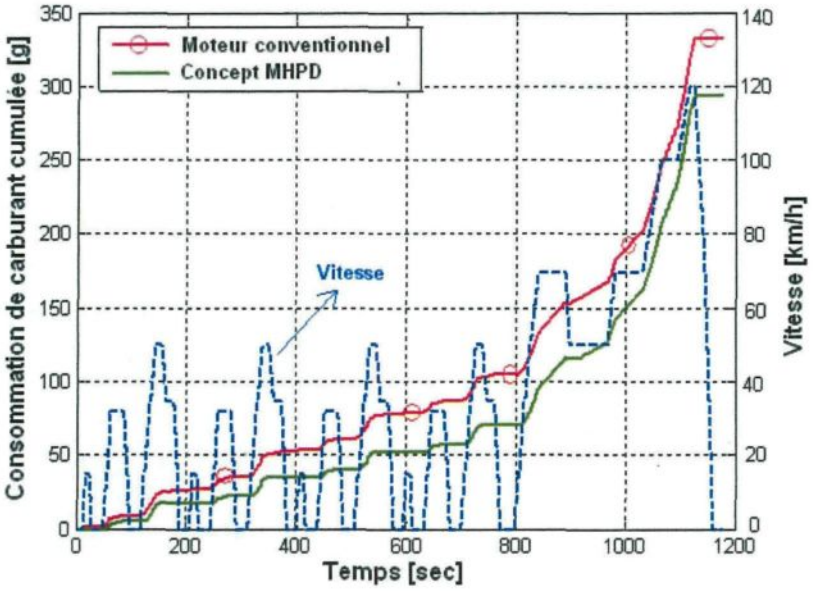

Figure VII. 10 : Consommation de carburant sur le cycle d'homologation Européen NEDC, d'un véhicule de 1500 kg équipé d'un moteur Diesel conventionnel ou d'un MHPD avec un réservoir d'air de 100 litres

VII.2. Conclusions et perspectives

VII.2.1. Conclusions

Cette thèse fait suite à une thèse précédente [64] dans laquelle il a été démontré, suite à une analyse multicritères, que le stockage d'énergie sous forme d'air comprimé (CAES) est le meilleur choix et le plus adaptable pour un Système Hybride Éolien-Diesel (SHED) destiné à alimenter en électricité des sites isolés. Nous avons conçu, optimisé et évalué une technique relativement simple à mettre en place, permettant de transformer un moteur Diesel, disponible dans la plupart de ces sites isolés, en un Moteur Hybride Pneumatique-Diesel (MHPD), capable de fonctionner à la fois comme un compresseur, un moteur à air comprimé, un moteur multi-énergie (air comprimé et carburant) aussi bien qu'un moteur Diesel conventionnel. Combiné à un système de stockage d'air bien dimensionné, le système multi-hybride SHED-MHPD est un concept innovant permettant de réduire significativement la consommation de carburant, et résoudre ainsi une problématique aussi bien économique et qu'écologique que génère la production d'électricité dans ces sites. En effet, le potentiel démontré de ce système permettrait d'éliminer la plupart des

barrières auxquelles fait face le déploiement de l'énergie éolienne dans les sites isolés. En effet, les SHED à haute pénétration éolienne ont été jugées peu rentables étant donné la dissipation d'énergie éolienne ; le SHED-MHPD permet de minimiser ce taux de dissipation et de mieux rentabiliser les investissements. A titre d'exemple, le village isolé nord-Canadien Tuktoyaktuk ayant une vitesse moyenne du vent relativement faible (5,5 m/s) est actuellement équipé d'une génératrice Diesel de puissance maximale 1 MW, qui consomme environ 1080 tonnes de carburant par année, soit environ 1,2 millions de dollars pour le prix du carburant seul, et qui monte à 2 millions de dollars en comptant tous les autres frais associés (transport et stockage du carburant, entretien du Diesel, main d'œuvre, etc.) . En considérant qu'un SHED à haute pénétration (TPP = 2) est mis en place dans ce village, en ajoutant donc un système d'éoliennes de 2 MW, la consommation de carburant baisse à 561 tonnes par an, soit une baisse de 48% seulement. Cependant, en ajoutant un système de stockage d'air comprimé de 100,000m^3 et en transformant le moteur Diesel en un MHPD, la consommation annuelle de carburant n'est que 415 tonnes, soit 13% de réduction supplémentaire.

VII.2.2. Perspectives

Cette thèse constitue une base théorique complète à partir de laquelle doit commencer une étude expérimentale pour valider les modèles théoriques et la stratégie de commande proposée. Cette validation expérimentale doit faire l'objet d'une nouvelle thèse qui doit commencer par la conception d'un nouveau banc de test permettant de mettre en œuvre toutes les modifications requises pour transformer un moteur Diesel conventionnel en un MHPD. Les actions préconisées à cet égard sont les suivantes :

1) La consultation de fournisseurs de vannes électromagnétiques ou autre afin de trouver ou de concevoir le Système de Distribution Variable SDV ayant les performances préconisées ;
2) La modification du circuit d'admission du moteur turbocompressé conventionnel en lui ajoutant les vannes trois voies permettant de court-circuiter à la demande le turbocompresseur et de connecter ou déconnecter un réservoir d'air comprimé à l'admission du moteur ;

3) La mise en place d'un système de contrôle de l'injection de carburant

4) La conception d'un système de commande de tous les actuateurs suivant les stratégies de pilotages décrites dans cette étude théorique ;

5) La mise en place d'une génératrice permettant de varier la puissance mécanique à l'arbre du moteur, entre des valeurs négatives (récupération d'énergie) et des valeurs positives (fourniture d'énergie) ;

6) L'instrumentation complète du banc d'essais avec des capteurs de température et de pression dans le circuit d'admission, le circuit d'échappement, le réservoir d'air et la chambre de combustion ; des capteurs de position de l'arbre du vilebrequin et des soupapes ; ainsi que des débitmètres d'air et de carburant.

Une fois ce banc d'essais mis en place, il est possible de valider ou éventuellement ajuster les stratégies de commande préconisées et de donner une évaluation robuste et confirmée de l'économie de carburant que pourrait apporter ce concept SHEDAC-MHPD.

RÉFÉRENCES (HORS ARTICLES)

[1] Sigma Engineering, Étude générale des questions énergétiques dans les collectivités éloignées du Canada. Préparé pour le programme de démonstration dans les collectivités éloignées. Énergie, Mines et Ressources Canada, Mars 1985.

[2] Liu W, Gu S, Qiu D, Techno-economic assessment for off-grid hybrid generation systems and the application prospects in China, http://www.worldenergy.org/wecgeis/publications.

[3] Adelaar & Ass., Communitech & Ass. « Community Specific Energy Supply in the Yukon and Northwest Territories », Gov. of Canada, Dep. of Indian & Northern Aff., Contract No. 81-117, 1981.

[4] B. Janz, D.G. Howell, A. Serna « Wind Energy in the Northwest Territories », prepared for The Science Advisory Board of the Northwest Territories, Yellowknife, Northwest Territories, 1982.

[5] Unies Consulting Eng. « Investigation of the Viability of a Remote Wind/Hydroelectric Power Supply in the Northwest Territories », Study No. 1, Energy Mines and Nat. Res. Canada, 1985

[6] M.S. Chappell « Wind Energy Research and Development at the National Research Council of Canada 1975-1985 », NRCC No. 27459, 1986.

[7] M. Lodge, J. Passmore « Wind-Diesel Systems for Remote Communities », report for Mushkegowuk Council, Ontario Energy Co., Ontario Hydro, CANMET, NRC, 1995.

[8] Arctic Energy Alliance « Review of Technical and Economic Viability of Wind Energy Systems in the NWT and Nunavut », NWT Power Corporation, Hay River, Northwest Territories, 2001.

[9] J.P. Pinard, T.M. Weis « Pre-Feasibility Analysis of Wind Energy for Inuvialuit Region in Northwest Territories », Aurora Research Institute, 2003.

[10] La stratégie énergétique du Québec 2006-2015, L'énergie pour construire le Québec de demain, http://www.mrnf.gouv.qc.ca/energie/eolien

[11] Kim Ah-You, Greg Leng, Énergies renouvelables dans les communautés éloignées du Canada, Programme des énergies renouvelables pour les communautés éloignées, Ressources Naturelles Canada.

[12] Philip Raphals, Søren Krohn, Martin Tampier, Technologies permettant de réduire l'utilisation du diesel dans les territoires des réseaux autonomes d'Hydro-Québec, Rapport Préparé pour Hydro-Québec, 15 mai 2006.

[13] NWT Energy Secretariat, (2003) "Towards an Energy Strategy for the NWT – A Discussion Paper", Government of the Northwest Territories, Department of Resources, Wildlife and Economic Development Energy Secretariat, Yellowknife, Canada.

[14] FORCIONE A., Système jumelé éolien-diesel aux Îles-de-la-Madeleine (Cap-aux-Meules) – Établissement de la VAN optimale, Institut de Recherche, Hydro-Québec, Février 2004.

[15] Hunter R, Elliot G. Wind-diesel systems – A guide to the technology and its implementation. Cambridge (UK): Cambridge University Press; 1994.

[16] J.F. Maisson « Wind Power Development in Sub-Arctic Conditions with Severe Rime Icing », Presented at the Circumpolar Climate Change Summit and Exposition, Whitehorse, Yukon, 2001

[17] World Wind Energy Association (WWEA), World Wind Energy Report 2012, décembre 2012.

[18] (24) Association canadienne de l'énergie éolienne, http://www.canwea.com, accès le 5 décembre 2012.

[19] http://www.mrnf.gouv.qc.ca/energie/eolien, accès le 10 mai 2012

[20] BOURILLON C., Wind Energy-Clean Power For Genertions, Renewable Energy 1999, vol. 16, pp. 948 – 953.

[21] www.nunavutpower.com, accès le 10 mai 2012.

[22] B. Reeves « Kotzebue Electric Association Wind Projects », Proceedings of NREL/AWEA 2002 Wind-Diesel Workshop, Anchorage, Alaska, USA, 2002

[23] E. Ian Baring-Gould, L. Flowers, P. Lundsager, Worlwide status of wind-diesel applications, Pre-Workshop Wind-Diesel 101, Anchorage, Alaska, 2004.

[24] Thèse doctorale de M. Hussein Ibrahim, Université du Québec à Chicoutimi, 2010

[25] Y. Jean, A. Nouaili, P. Viarouge, B. Saulnier, R. Reid, «Développement d'un système JEDHPSS représentatif d'un village typique des réseaux non reliés», rapport IREQ-94-169-C, 1994

[26] R. Gagnon, A. Nouaili, Y. Jean, P. Viarouge; «Mise à jour des outils de modélisation et de simulation du Jumelage Éolien-Diesel à Haute Pénétration Sans Stockage et rédaction du devis de fabrication de la charge de lissage», Rapport IREQ-97-124-C, 1997

[27] www.danvest.com, accès le 15 mai 2012

[28] Hussein Ibrahim, Adrian Ilinca, Jean Perron, Systèmes de stockage de l'énergie pour les éoliennes. Colloque international « Énergie éolienne et sites éloignés », Îles de la Madeleine, Québec, Canada, 19-21 octobre 2005.

[29] Hussein Ibrahim, Adrian Ilinca, Jean Perron, Solutions de stockage de l'énergie éolienne. Rapport interne, UQAR, UQAC, LREE–01, Janvier 2006. http://biblio.uqar.qc.ca/archives/24285067.pdf

[30] Hussein Ibrahim, Adrian Ilinca, Jean Perron ; Investigation on the Performances of Energy Storage Techniques. le 21ième congrès canadien de mécanique appliquée (CANCAM07-ETS-76), Toronto, Canada, 3-7 juin 2007, pp. 358-359.

[31] Hussein Ibrahim, Adrian Ilinca, Jean Perron, Energy Storage Systems - Characteristics and Comparisons; Renewable & Sustainable Energy Reviews, Volume 12, Issue 5, June 2008, Pages 1221-1250.

[32] Hussein Ibrahim, Adrian Ilinca, Jean Perron, Investigations des différentes alternatives renouvelables et hybrides pour l'électrification des sites isolés. Rapport interne, UQAR, UQAC, LREE–03, Septembre 2008, http://biblio.uqar.qc.ca/archives/30054690.pdf.

[33] Hussein Ibrahim, Systèmes de stockage de l'énergie pour les éoliennes. Séminaire de formation sur l'énergie éolienne à l'Université d'Alep, Syrie, 22-25 Octobre 2007.

[34] K. Khaitan and S. K. Khaitan; Modeling and simulation of compressed air storage in caverns: A case study of the Huntorf plant; Applied Energy 89 (2012) 474–481; 2012; DOI: 10.1016/j.apenergy.2011.08.019

[35] http://www.atlascopco.fr ; accès le 10/11/2012

[36] Schechter, M., New cycles for automobile engines, SAE 1999-01-0623, 1999

[37] Schechter, M., Regenerative Compression Braking – A Low Cost Alternative to Electric Hybrids, SAE 2000-01-1025

[38] Tai, C., Tsao, T., Levin, M., Barta, G., and Schechter, M., Using Camless Valvetrain for Air Hybrid Optimization, SAE 2003-01-0038

[39] Higelin, P., Charlet, A., Chamaillard, Y., Thermodynamic Simulation of a Hybrid Pneumatic-Combustion Engine Concept, Int.J. Applied Thermodynamics, Vol.5, (No.1), p.1-11; 2002

[40] Higelin, P., Vasile, I., Charlet, A., and Chamaillard, Y., Parametric optimization of a new hybrid pneumat ic±combustion engine concept, Int. J. Engine Res., Vol. 5; No. 2 205

[41] P. Higelin, A. Charlet, Y. Chamaillard, "Thermodynamic Simulation of a Hybrid Pneumatic Combustion Engine Concept International Journal of Applied Thermodynamics", Vol 5, No. 1, pp 1 – 11, ISSN 1301 9724; 2002

[42] Donitz, C., Vasile, I., Onder, C., and Guzzella, L., Realizing a Concept for High Efficiency and Excellent Driveability: The Downsized and Supercharged Hybrid Pneumatic Engine, SAE, 2009-01-1326; 2009

[43] Dönitz, C., Vasile, I.C., Onder, C.H., and Guzzella, H., Modelling and optimizing two- and four-stroke hybrid pneumatic engines, IMechE Part D - Journal of Automobile Engineering, Vol. 223, No. 2, pp. 255-280, 2009. xii, 27, 28, 30

[44] Hyungsuk K., H., Tai, C., Smith, E., Wang, X., Tsao, T., Stewart, J., and Blumberg, P., Demonstration of Air-Power-Assist (APA) Engine Technology for Clean Combustion and Direct Energy Recovery in Heavy Duty Application, SAE, 2008-01-1197; 2008

[45] Trajkovic, S., Tunestal, P., and Johansson, B, Introductory Study of Variable Valve Actuation for Pneumanic Hybridization, SAE, 2007-01-0288; 2007

[46] Trajkovic, S., Tunestal, P., and Johansson, B, Investigation of Different Valve Geometries and Valve Timing Strategies and their Effect on Regenerative Efficiency for a Pneumatic Hybrid with Variable Valve Actuation, SAE, 2008-01-1715; 2008

[47] Trajkovic, S., Tunestal, P., and Johansson, B, Simulation of a Pneumatic Hybrid Powertrain with VVT in GT-Power and Comparison with Experimental Data, SAE, 2009-01-1323; 2009

[48] Lee, CY., Zhao, H., and Ma, T., Pneumatic Regenerative Engine Braking Technology for Buses and Commercial Vehicles, SAE, 2011-01-2176

ANNEXE

Publications faites dans des congrès scientifiques

1) The 4th International Conference on Integrated Modeling and Analysis in Applied Control and Automation; part of the 7th International Mediterranean and Latin American Modelling Multiconference I3M2010; Fes, Maroc, octobre 13-15, 2010.

   PNEUMATIC HYBRIDIZATION OF DIESEL ENGINE IN A HYBRID WIND-DIESEL INSTALLATION WITH COMPRESSED AIR ENERGY STORAGE.

2) X^{ème} Colloque Interuniversitaire Franco-québécois sur la thermique des systèmes ; Chicoutimi, Québec, juin 20-22, 2011.

   HYBRIDATION PNEUMATIQUE D'UN MOTEUR DIESEL DANS UNE INSTALLATION HYBRIDE ÉOLIEN DIESEL AVEC STOCKAGE D'ÉNERGIE SOUS FORME D'AIR COMPRIMÉ.

3) IEEE International Conference on Renewable Energy for Developing Countries; Beyrouth, Liban, novembre 28-29, 2012.

   A NEW MULTI-HYBRID POWER SYSTEM FOR GRID DISCONNECTED AREAS.

PNEUMATIC HYBRIDIZATION OF DIESEL ENGINE IN A HYBRID WIND-DIESEL INSTALLATION WITH COMPRESSED AIR ENERGY STORAGE

Tammam Basbous [a], Rafic Younes [b], Adrian Ilinca [c], Jean Perron [d]

[a] Anti-icing Materials International Laboratory. Université du Québec à Chicoutimi, Canada
[b] Engineering Faculty, Lebanese University, Beirut, Lebanon
[c] Wind Energy Research Laboratory, Université du Québec à Rimouski, Canada
[d] Anti-icing Materials International Laboratory. Université du Québec à Chicoutimi, Canada

[a] tammam.basbous@uqac.ca, [b] ryounes@ul.edu.lb, [c] adrian_ilinca@uqar.qc.ca, [d] jean_perron@uqac.ca

ABSTRACT

In this paper, we are studying an innovative solution to reduce fuel consumption for electricity production in remote areas. Historically, in these areas electricity is provided by Diesel generators. The cost of energy is therefore very high not only because of inherent cost of technology but also because of transportation costs. On the other hand, use of fossil fuels for electricity generation is a significant source of Greenhouse Gas emissions. The use of hybrid systems that combine renewable sources and diesel generators, allows reducing fuel consumption, improves the operation cost and creates therefore environmental benefits. Adding a storage element to the hybrid system above increases fuel saving as it allows an increased penetration of the wind power in the overall system capacity. In a previous work, we demonstrated that Compressed Air Energy Storage (CAES) is a serious solution thanks to its low cost, high power density and reliability. Pneumatic Hybridization of the Diesel engine consists to introduce the CAES through the admission valve. We have proven that we can improve the combustion efficiency and therefore the fuel consumption by optimizing Air/Fuel ratio thanks to the CAES assistance. As a continuation of these previous analyses, we studied the effect of controlling the pressure at the inlet and the exhaust of the Diesel engine on the thermodynamic cycle and evaluated the potential on fuel consumption reduction.

Keywords: Pneumatic Hybridization, Wind Energy, Diesel Engine, Wind-Diesel Hybrid System, Compressed Air Energy Storage.

1. INTRODUCTION

Most of the remote and isolated communities or technical installations (communication relays, meteorological systems, tourist facilities, farms, etc.) that are disconnected from national electric distribution grids rely on diesel engines to generate electricity (Ibrahim 2007). Diesel generated electricity is more expensive in itself than large electric production plants (gas, hydro, nuclear, wind), even prior to taking into account the transport and environmental costs associated with this type of energy.

In Canada, approximately 200,000 people live in more than 300 remote communities (Yukon, Northwest Territories, Nunavut, etc.) that use diesel generated electricity, which is responsible for the emission of 1.2 million tons of greenhouse gases annually (Ibrahim 2007). In Quebec alone, there are over 14,000 subscribers scattered in about forty communities that disconnected from the main grid. Each community constitutes an autonomous network that uses diesel generators.

In Quebec, the total production of diesel power generating units is approximately 300 GWh per year. The operation of these diesel generators is extremely expensive due to the high oil price and transportation costs. Indeed, as the fuel has to be delivered to remote locations, some of them only reachable during the summer by boat, the cost of electricity in 2007 reached more than 50 cent/kWh in some communities, while in the rest of the province the electricity tariff was approximately 6 cent/kWh (Ibrahim 2007). The resulting deficit, which is shared among all Quebecers, is far from being negligible. In 2004, the autonomous networks accounted for 144 MW of installed power, and the consumption was established at 300 GWh. Hydro-Quebec, the provincial utility, estimated at approximately CAD $133 million the annual loss resulting from the difference between the diesel electricity production cost and the uniform electricity tariff (Ibrahim 2007).

Moreover, diesel electricity production is considered ineffective, presents significant environmental risks (spilling), pollutes local air and contributes to global warming. Overall, we estimate at 140,000 tons the annual GHG emission resulting from the use of diesel generators for the autonomous networks in Quebec. This is equivalent to the GHG emitted by 35,000 cars during one year.

While they require relatively little investment, diesel power generating units are generally expensive to operate and maintain, particularly when they function regularly with a partial load (Ibrahim 2007). The use of diesel power generators under weak operating factors

accelerates wear and increases fuel consumption (Ibrahim 2007).

The use of Hybrid Wind-Diesel Generators solves a part of the problems listed above, but its efficiency is limited by wind intermittency. Highly fluctuating wind energy requires the Diesel engine running on idle most of the time and dissipates a part of the wind power in order to control the balance between the energy production and the energy demand. Energy storage is the key to solve this issue, because it allows storing otherwise wasted energy and recover it later, when the Wind power is not sufficient to cover the demand. The use of storage allows an increased penetration of the wind power in the overall system capacity. The high penetration of wind energy means that the installed wind power exceeds the maximum load and, during periods of strong winds, diesel generators may be stopped while surplus of wind energy is stored. The overall energy provided by the Diesel generator is significantly decreased with beneficial economic and environmental results. In a previous work, we demonstrated that Compressed Air Storage (CAES) is a serious solution thanks to its low cost, high power density and reliability. Pneumatic Hybridization of the Diesel engine consists to introduce the CAES in the combustion chamber. We have proven that we can improve the combustion efficiency and therefore the fuel consumption through optimisation of Air/Fuel ratio. As a continuation of these previous analyses, we studied the effect of controlling the pressure at the inlet and the exhaust of the Diesel engine on the thermodynamic cycle and evaluated the potential on fuel consumption reduction

2. IMPROVING INDUSTRIAL DIESEL ENGINES EFFICIENCY

Due to their superior efficiency when compared to other thermal engines especially Spark Ignition engines, Diesel Engines are widely used for applications where high power concentration is required. For this reason, a great deal of research is conducted worldwide to reduce their pollutant emissions and to further improve their efficiency. Taking into account the green house effect that has been recognized the last years caused by increased CO2 emissions, it seems that they offer a reasonable solution for the minimization of this problem. The efficiency of the direct injection diesel engine has been considerably improved during the last decade mainly due to turbo-charging and downsizing technique.

Downsizing Diesel engines consists to reduce its displacement while providing the same maximum power. This is possible thanks to turbo-charging that increases the air filling and thus the specific power (i.e: maximum power per unit displacement) of the engine. Smaller engines have better efficiency than bigger engines, when working under the same load, thanks to better mechanical efficiency and reduced heat losses.

3. PNEUMATIC HYBRIDIZATION OF DIESEL ENGINES

Since the late 1990s, pneumatic hybridization of Internal Combustion Engines has been discussed, but mainly focusing for automotive application. The key idea is to use the engine also as a pump to recuperate the vehicle's kinetic energy during braking phases, and as an expansion motor for propulsion. This can be realized by connecting an air pressure tank to all cylinders via electronically controlled charge valves (Dönitz 2008) as shown in figure 1 – right (ibrabim 2010).

In addition to the recuperation capability, the idea offers the possibility of a rapid start/stop and permits to shift the engine's operating point to high efficiency zones. The latter can be achieved by operating half of the cylinders conventionally while the other half of the cylinders work in the *pump mode*. Previous concepts assumed two-stroke pump and pneumatic motor modes which is possible only if all valves of the cylinders can be variably actuated (Higelin 2002).

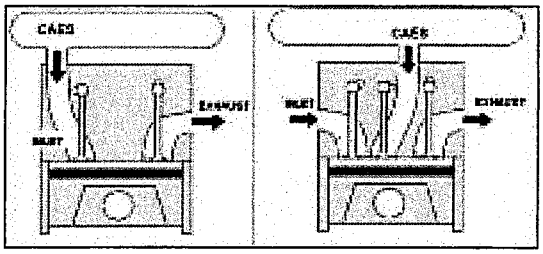

Figure 1: Pneumatic Hybrid ICE Engine through inlet valve (left), and through additional valve (right).

In our current study, we have focused on a more simple technique of Hybridizing Diesel engine. This technique consists in introducing the compressed air through the initial intake valve as shown in figure 1 – left (Ibrahim 2010). The main reason for this choice is to suggest a practical adaptation of existing Diesel power plants installations.

The compressed air is supposed to be previously generated by independent electric air compressor whose energy is provided by wind turbines, during periods of high Wind Power Penetration Rate (WPPR>1), as shown in figure 2 (Ibrahim 2010).

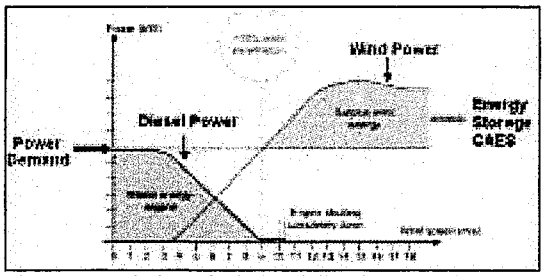

Figure 2: Variation of wind and diesel power with wind speed for a high-penetration Wind Diesel system

4. MATHEMATICAL MODEL

A zero dimensional mathematical model of the thermodynamic Diesel cycle has been developed to and used to conduct our parametric study. The mathematical models used are found in literature review (Heywood 1988; Lopes Correia da Silva 2007; Higelin 2002; Ibrahim 2007). We did not conduct any tests to calibrate and fit our model . We have used parameters that are found in literature review (Guibert 2002). The purpose actually of our study was to give orientations to our conception. In the future, a one dimensional modelling will be conducted to simulate the whole system in steady state mode and in transient mode.

Figure 3 shows the system considered to calculate the evolution of the thermodynamic characteristics (pressure, temperature, specific heat constant, etc...).

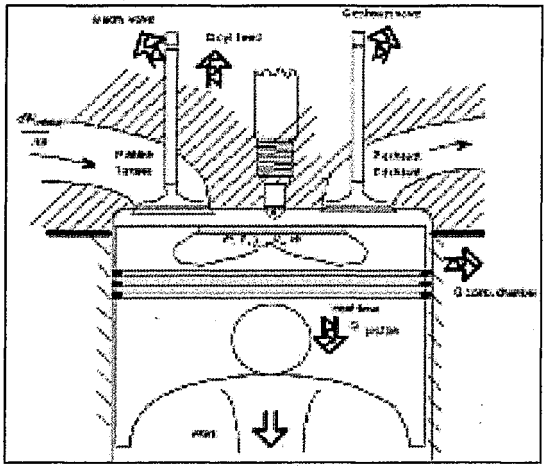

Figure 3: Direct injection Diesel engine simplified model

The hypotheses considered are the following:

1. The thermodynamic equilibrium is established for each step of calculation
2. The mass of gas is a homogeneous mixture of perfect gas. Its thermodynamic characteristics (enthalpy, intern energy, molar mass, etc...) are calculated by interpolation in JANAF thermo-chemical tables (third edition, 1985)
3. The mass transfers occur only through the admission and exhaust valves. The blow-by flow is neglected.
4. The admission back-flow is calculated and taken in consideration. The exhaust flow transferred back to the admission is readmitted in the cylinder at the exhaust temperature.
5. The fuel is injected in the combustion chamber at a constant temperature and it is immediately burned following Wiebe law.
6. The heat transfers occur through the five boundary limits (cylinder head, piston, cylinder wall, exhaust valve and admission valve) that are at a constant and uniform temperature.

4.1. Main equations

Main equations are issued from the mass and heat conservation equations as well as the ideal gas equations review (Heywood 1988).

$$\frac{dW}{dt} = \frac{dW_{intake}}{dt} + \frac{dW_{exhaust}}{dt} + \frac{dW_{inj}}{dt} \tag{1}$$

$$\frac{dW_{air}}{d\theta} = \frac{\frac{dW_{intake}}{d\theta}}{1+\frac{\lambda_{intake}}{\lambda_{st}}} + \frac{\frac{dW_{exhaust}}{d\theta}}{1+\frac{\lambda}{\lambda_{st}}} \tag{2}$$

$$\frac{d\lambda}{d\theta} = \frac{\frac{dW}{d\theta} - \left(1+\frac{\lambda}{\lambda_{st}}\right)\times\frac{dW_{air}}{d\theta}}{W_{air}} \times \lambda_{st} \tag{3}$$

$$\frac{dT}{d\theta} = \frac{A_1 - \frac{\frac{\partial u}{\partial P}}{A_2}\times\left(\frac{\frac{dW}{d\theta}}{W} + \frac{\frac{\partial r}{\partial \lambda}}{r}\times\frac{d\lambda}{d\theta} - \frac{\frac{dV}{d\theta}}{V}\right) - \frac{\partial u}{\partial \lambda}\times\frac{d\lambda}{d\theta}}{\frac{\partial u}{\partial T} + \frac{\partial u}{\partial P}\times\frac{A_2}{A_3}} \tag{4}$$

$$\frac{dP}{d\theta} = \frac{\frac{\frac{dW}{d\theta}}{W} + \frac{\frac{\partial r}{\partial \lambda}}{r}\times\frac{d\lambda}{d\theta} - \frac{\frac{dV}{d\theta}}{V} + A_3\times\frac{dT}{d\theta}}{A_2} \tag{5}$$

Where *A1*, *A2* and *A3* are calculated with equations 6, 7 and 8 (Heywood 1988)..

$$A_1 = \frac{\left(-P\times\frac{dV}{d\theta} + \frac{dQ}{d\theta} + h_{intake}\times\frac{dW_{intake}}{d\theta} + \cdots \right.}{W} \frac{\left. \cdots h_{ech}\times\frac{dW_{exhaust}}{d\theta} + h_{inj}\times\frac{dW_{inj}}{d\theta} - u\times\frac{dW}{d\theta}\right)}{} \tag{6}$$

$$A_2 = \frac{1}{P} - \frac{\frac{\partial r}{\partial P}}{r} \tag{7}$$

$$A_3 = \frac{1}{T} + \frac{\frac{\partial r}{\partial T}}{r} \tag{8}$$

4.2. Kinematic model

The volume delimited by the piston, the cylinder wall and the cylinder head can be calculated function of the angular position of the crankshaft θ as shown in equations 9 and 10.

$$V(\theta) = \frac{\pi D^2}{8}\times L\left(1+\frac{R}{L} - \cos\theta - \sqrt{\left(\frac{R}{L}\right)^2 - \sin^2\theta} + \frac{2}{\varepsilon - 1}\right) \tag{9}$$

$$\frac{dV(\theta)}{d\theta} = \frac{\pi D^2}{8} \times L \times \sin\theta \times \left(\frac{\cos\theta}{\sqrt{\left(\frac{R}{L}\right)^2 - \sin^2\theta}} + 1 \right) \quad (10)$$

The mean piston velocity is calculated as shown in equation 11.

$$VMP = 2 \times L \times \frac{N}{60} \quad (11)$$

4.3. Intake and exhaust flow models

The first principle of thermodynamics leads to the Baré Saint-Venant model of flow through the admission intake valve as shown in equation 12.

$$\frac{dW}{dt} = A_{intake} \times P_{intake} \times \ldots \sqrt{\frac{2.\gamma_{intake}}{(\gamma_{intake}-1) \times r_{intake} \times T_{intake}} \times \left[X^{\frac{2}{\gamma_{intake}}} - X^{\frac{\gamma_{intake}+1}{\gamma_{intake}}} \right]} \quad (12)$$

Where X is the maximum found between two values as shows equation 13.

$$X = max\left(\frac{P}{P_{intake}}; \left(\frac{2}{\gamma_{intake}+1} \right)^{\frac{\gamma_{intake}}{\gamma_{intake}-1}} \right) \quad (13)$$

4.4. Backflow model

Backflow is an undesirable phenomenon that reduces the amount of the amount of fresh air admitted in the engine. It occurs during the intake phase and during the exhaust phase.

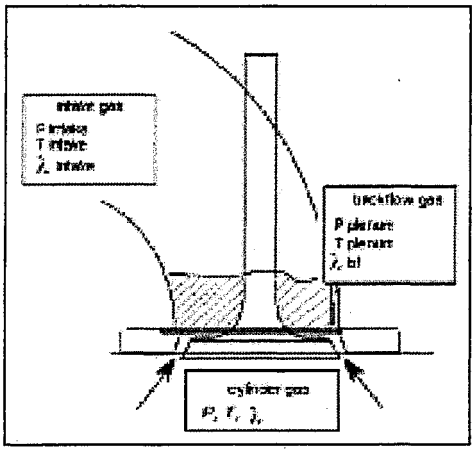

Figure 4: intake backflow phenomena illustration

As shown in figure 4 (case of admission backflow), the exhaust gas that backflow to the admission through intake valve are readmitted in the cylinder in the next cycle. The hypothesis taken for modelling the backflow are the following:

1. the exhaust gas is a homogeneous mixture
2. the temperature of the backflow gas is constant and is equal to the exhaust gas temperature
3. the pressure of the exhaust gas is equal to the intake pressure

The mass conservation laws applied to the admission can be written as shown in equation 14:

$$dW_{bfl} = -dW(\theta) \quad (14)$$

If $P>Pintake$, gas is backflow and $dW(\theta)$ is calculated with equation 12 after inverting in and out.

If $P<Pintake$, backflow gas are readmitted and $dW(\theta)$ is calculated with equation 12 in its standard form, until W_{bfl} equals to zero.

4.5. Combustion model

The accurate description of the combustion process in the Diesel engines requires the knowledge of different phenomena that occur starting with the fuel injection and ending with its transformation into combustion products. This knowledge needs the study of the aerodynamic motion in the combustion chamber, the penetration and the vaporization of the fuel as well as the self ignition delay and the combustion itself. Those phenomena cannot be modelled without a three dimensional study.

In our study, we have decided to simplify the modelling work in order to demonstrate a first order potential of our technical solution. A global approach of the combustion process has been modelled considering four phases:

1. The phase of the delay of self ignition: the injected fuel does not start burning before this delay ends
2. The phase of the pre-mixed combustion, where the fuel injected during the delay of self ignition is burned.
3. The phase of the diffusion combustion: while the injection is still ongoing and the combustion chamber is already hot, the combustion happens almost instantly and its speed is limited by the injection flow rate.
4. The final combustion phase: After the fuel injection ends, the remaining unburned fuel (relatively small quantity) burns slowly depending on the diffusion phenomena.

The global combustion model can be simplified by the combination of two Wiebe laws (Wiebe 1970). The first one describes the *pre-mixed combustion* and the second one describes the *diffusion combustion.* Each Wiebe law allowing the calculation of the burned fuel ratio is written as shown in equation 15.

$$xb = \frac{1 - exp\left(-w \times \left(\frac{\theta - \theta_{phase}}{\Delta\theta_{phase}}\right)^{m+1}\right)}{1 - exp(-w)} \quad (15)$$

Where m and w are constants verifying the equations 16 and 17.

$$w = \frac{m}{m+1} \times \frac{1}{\left(\frac{\theta_{HLC} - \theta_{phase}}{\Delta\theta_{HLC}}\right)^{m+1}} \quad (16)$$

$$HLC = \frac{m}{\left(\frac{\theta_{HLC} - \theta_{phase}}{\Delta\theta_{HLC}}\right)} \times \frac{\exp\left(-\frac{m}{m+1}\right)}{1 - \exp(-w)} \times \frac{1}{\Delta\theta_{phase}} \quad (17)$$

The contants above should be calibrated in order to fit with the studied engine performance. As mentioned previously, no test was conducted to fit those constants with a specific engine. All the parameters were taken from literature review (Guibert 2002).

4.6. Heat transfers model

Heat transfers through boundary limits are described with equation 18.

$$\frac{dQ}{d\theta} = \sum_{j=boundary} \varphi . A_j . (CT1 \cdot (Tj - Tsc) + CT2 \cdot (Tsc - T)) \quad (18)$$

Where the thermal exchange coefficient φ is calculated with Woschni (Woschni 1967) model illustrated in equation 19.

$$\varphi = 12.986 \times 10^{-3} \times D^{-0,2} \times P^{0.8} \times T^{-0,53} \times ... \\ ... \left(2.28 \times VMP + 0.00324 \times \frac{Vs \times T0}{V0 \times P0} \times (P - Psc)\right)^{0.8} \quad (19)$$

5. RESULTS AND DISCUSSIONS

5.1. Parametric study conducted

In order to demonstrate the potential of the pneumatic hybridization of the Diesel engine, we have conducted a parametric study varying simultaneously the intake and exhaust pressure. The intake temperature is considered constant and equals to 293 K.

Unfortunately, increasing intake pressure is constrained by stress levels in critical mechanical components. These maximum stress levels limit the maximum cylinder pressure which can be tolerated under continuous operation, though the thermal loading of critical components can become limiting too. As boost pressure is raised, unless engine design and operating conditions are changed, maximum pressures and thermal loadings will increase almost in proportion (Heywood 1988).

Reliability criteria of most common Diesel engines specify 200 bars and 1100 K as limits not to be exceeded. Those limits were taken in consideration in our parametric study.

5.2. Operating at low loads (BMEP = 5 bars)

Figure 5 shows the variation of the specific fuel consumption of the Diesel engine function of the intake and exhaust pressure for a fixed mechanical output equivalent to a BMEP of 5 bars. Natural aspirated engines have an inlet and exhaust pressure close to 1 bar, thus the specific consumption is about 250 g/kWh. Turbocharged Diesel engines has higher intake pressure but also higher exhaust pressure as well. At low loads, exhaust pressure are slightly higher than intake pressure because the exhaust gas enthalpy is relatively low. Previous work (Ibrahim 2007) has showed that intake pressure and exhaust pressure at BMEP of 5 bars for the same engine, are respectively 1.7 bar and 1.9 bar.

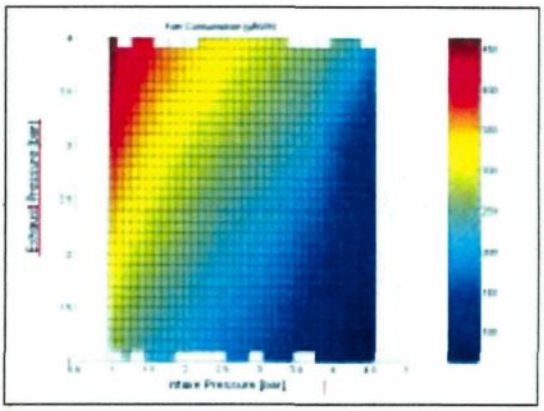

Figure 5: Fuel consumption at BMEP of 5 bars, function of intake and exhaust pressures

As we can see in figure 12, the maximum cylinder pressure increases directly and significantly with intake pressure and it is relatively independent from exhaust pressure. The maximum allowed pressure is reached at an intake pressure of 4.5 bars.

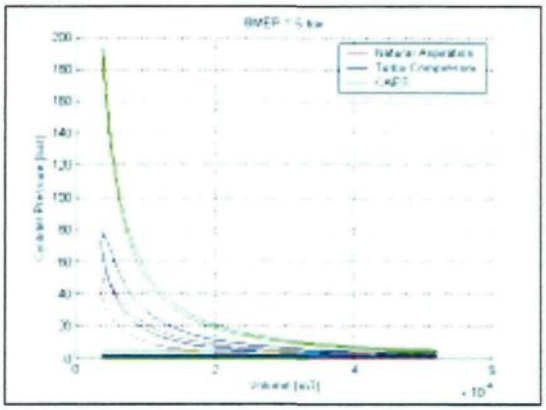

Figure 6: P-V Diagram of Thermodynamic Diesel cycle for Natural Aspirated engine (red), Turbocharged

engine (blue) and pneumatic hybrid engine (green), at BMEP of 5 bars

According to figure 5, the specific consumption for the turbocharged engine working will be close to 275 g/kWh. Now if the CAES is used to increase the inlet pressure until the peak cylinder pressure reaches its maximum allowed and the turbine is removed, the optimal operating point will be for an inlet pressure of 4.5 bars and an exhaust pressure of 1 bar. The specific consumption will be 75 g/kWh; witch is an improvement of about 70% comparing to natural aspirated engines and turbocharged engines. The reasons of this apparently huge improvement are explained as follows.

Figure 6 shows the thermodynamic Diesel cycle for the three operating types above. The three cycles develop the same area. We can observe that the more the intake pressure is, the higher is the peak pressure and the thinner is the shape high pressure cycle.

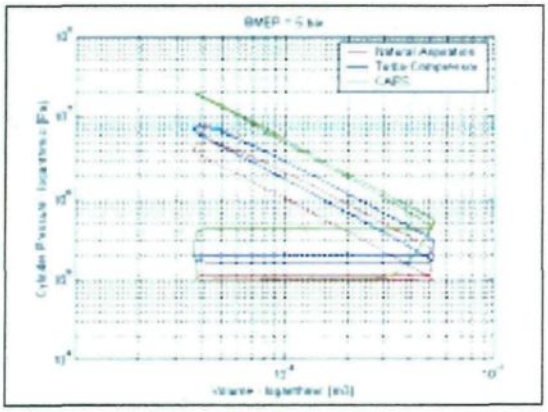

Figure 7: Log (P)-Log (V) Diagram of Thermodynamic Diesel cycle for Natural Aspirated engine (red), Turbocharged engine (blue) and pneumatic hybrid engine (green), at BMEP of 5 bars

Figure 7 is the same as figure 6 but drawn with a logarithmic scale. We can notice the difference in the low pressure cycle. For both Natural aspirated and Turbocharged operation, the low pressure cycle does not contribute significantly in the BMEP; at the opposite, for operation with CAES, the positive gap between inlet pressure and exhaust pressure generates work that contributes significantly in BMEP, as shown also in figure 9. This work is purely pneumatic and does not result from any combustion.

Figure 9 shows the contribution of the pneumatic *green* power in the total power generated by the engine. We can observe that for the highest allowed intake pressure and lowest exhaust pressure, the contribution is positive and can reach 40% witch means 40% of direct fuel saving. On the other hand, increasing intake pressure and reducing exhaust pressure make this contribution negative and thus increases the fuel consumption.

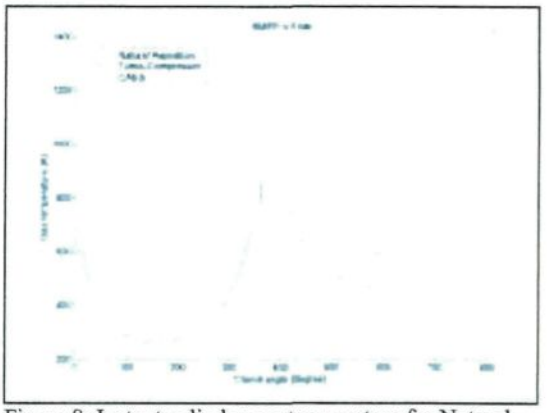

Figure 8: Instant cylinder gas temperature for Natural Aspirated engine (red), Turbocharged engine (blue) and pneumatic hybrid engine (green), at BMEP of 5 bars

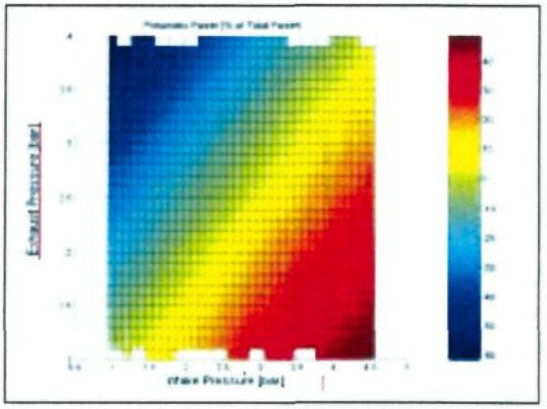

Figure 9: Contribution of the pneumatic power in the total power at BMEP of 5 bars, function of intake and exhaust pressure

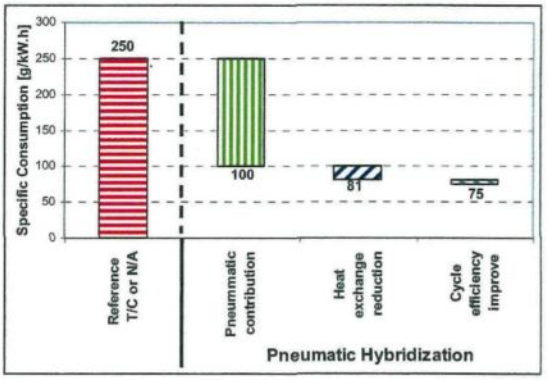

Figure 10: Fuel reduction contribution at BMEP of 5 bars, for Inlet pressure and exhaust pressure of 5 bars and 1 bar respectively

As shown in figure 10, the improvement in fuel consumption is not only the due to pneumatic power contribution, but also to two other phenomena:

1. The first phenomenon is the significant reduction of the heat exchange thanks to two reasons:
   (a) less fuel burned because less high pressure BMEP is needed to provide the target BMEP
   (b) higher air density and therefore high calorific capacity

   The heat exchange is responsible of about 25% according to figure 11 (Heywood 1988; Wanhua 2009) of the total loss in the engine. The gas temperature decrease from a Turbocharged engine to CAES assisted engine, reaches up to 300 K as shows figure 8. The thermal loss reduction is therefore around 30%.
2. The second phenomenon responsible of the remaining improvement is the increase of the combustion velocity thanks to the increase of air density and therefore the *cycle efficiency*.

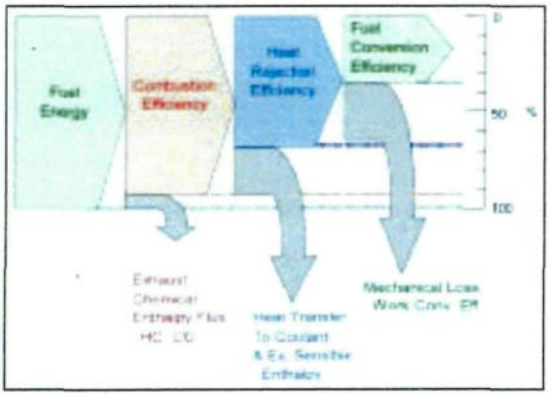

Figure 11: Typical fuel energy flow and efficiencies and losses in internal combustion engines (Heywood 1988; Wanhua 2009)

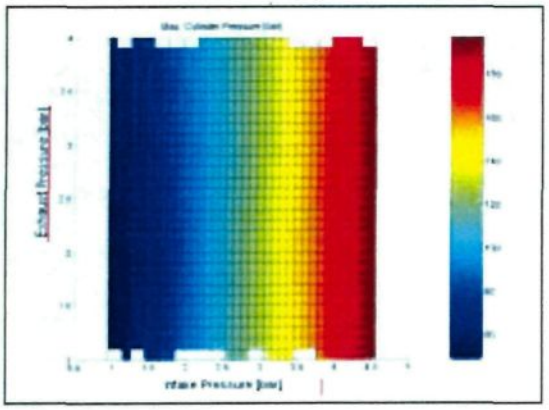

Figure 12: Peak cylinder pressure at BMEP of 5 bars, function of intake and exhaust pressures

The main limitation for fuel economy is the maximum allowed pressure in the combustion chamber. Increasing the admission pressure causes a much higher increase of the maximal pressure in the cylinder. For the Diesel engine specified above, 200 bars in the combustion chamber is reached when the admission pressure is about 5 bars at low engine load and 3.5 bars at high load.

5.3. Operating at medium loads (BMEP = 10 bars)

Operating at a BMEP of 10 bars is considered a medium load for turbocharged engine but is a full load for Natural Aspirated engine.

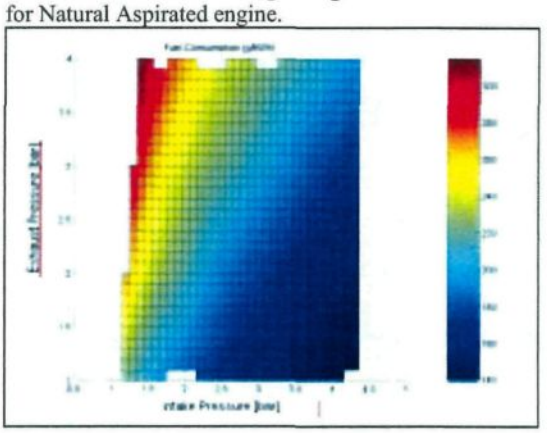

Figure 13: Fuel consumption at BMEP of 10 bars, function of intake and exhaust pressures

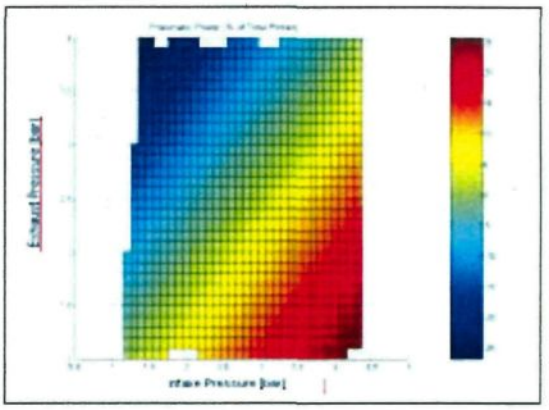

Figure 14: Contribution of the pneumatic power in the total power at BMEP of 10 bars, function of intake and exhaust pressure

For both turbocharged engine where the intake pressure and the exhaust pressure are both around 2.5 bars (Ibrahim 2007) and Natural aspirated engine where the intake pressure and the exhaust pressure are both around 1 bar, the fuel consumption is around 210 g/kWh, as shows figure 13.

Working under CAES assistance, at the limit of stress acceptance, intake pressure is 4.4 bars and exhaust pressure is 1 bar, therefore the fuel consumption is 140 g/kWh as shows figure 13, witch corresponds to an improvement of 33%. The pneumatic

power contribution in the total power reaches 20% as shown in figure 14.

As shown in figure 15, heat loss reduction improve contribute significantly in the global fuel economy, thanks to a great temperature drop of the gas in the cylinder chamber, that reaches up to 200 K.

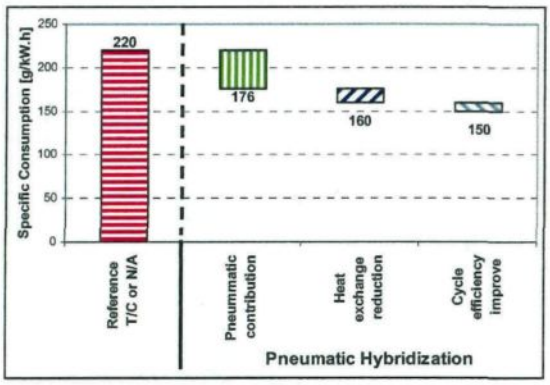

Figure 15: Fuel reduction contribution at BMEP of 10 bars, for Inlet pressure and exhaust pressure of 4 bars and 1 bar respectively

5.4. Operating at high loads (BMEP = 15 bars)

Natural Aspirated Engines cannot provide a torque equivalent to BMEP of 15 bars, while Turbocharged engines can do that. For turbocharged engine where the intake pressure and the exhaust pressure are both around 3 bars (Ibrahim 2007), the fuel consumption is around 250 g/kWh, as shows figure 16.

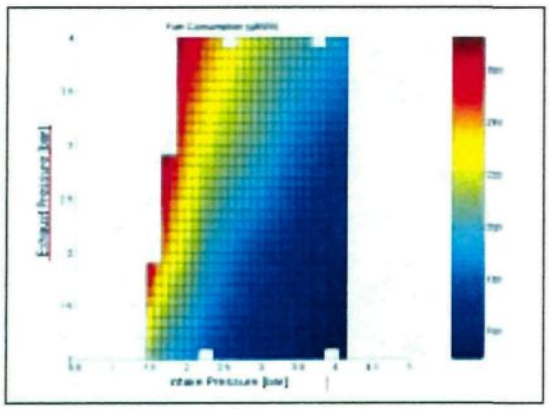

Figure 16: Fuel consumption at BMEP of 15 bars, function of intake and exhaust pressures

Working under CAES assistance, at the limit of stress acceptance, intake pressure is 4 bars and exhaust pressure is 1 bar, therefore the fuel consumption is 150 g/kWh as shows figure 15, witch corresponds to an improvement of 40%. The pneumatic power contribution in the total power reaches 15% as shown in figure 17.

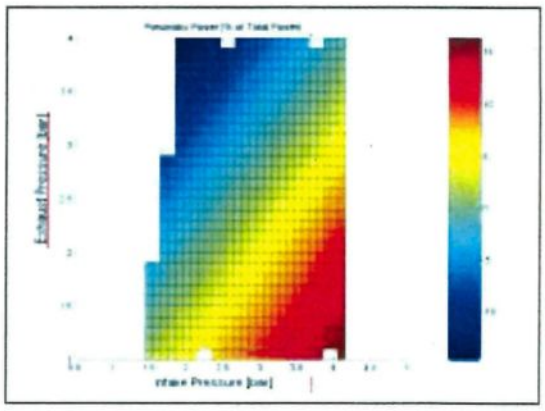

Figure 17: Contribution of the pneumatic power in the total power at BMEP of 15 bars, function of intake and exhaust pressure

Figure 18 shows the contribution of different phenomenon in fuel economy under CAES assistance at the maximum intake pressure allowed and the minimum exhaust pressure.

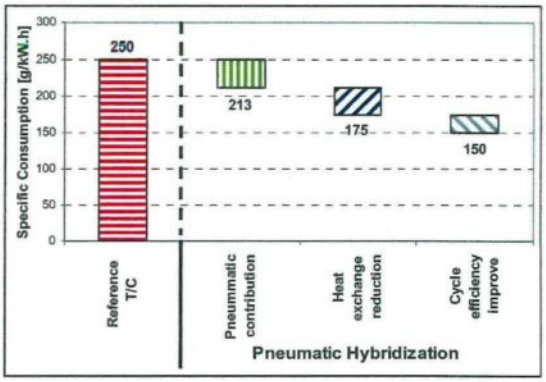

Figure 18: Fuel reduction contribution at BMEP of 15 bars, for Inlet pressure and exhaust pressure of 4 bars and 1 bar respectively

6. IMPACT OF PNEUMATIC HIBRIDIZATION ON POLLUTANT EMISSIONS

As mentioned in the previous paragraph, working under CAES assistance reduces significantly the temperature of gas in the combustion chamber. Previous work indicates that the lowered combustion temperature in diesel engines is capable of reducing soot and nitrogen oxides (NOx) simultaneously (Zheng 2006). CAES has therefore the same effect as Exhaust gas recirculation used in most Diesel applications in order to reduce NOx emissions. Figure 19 shows the impact of local temperature and equivalence ratio in the combustion chamber on the soot and NOx formation.

Operating with a high admission pressure and low exhaust pressure moves the local conditions in the combustion chamber to the right bottom side of Pischinger Diagram and therefore minimizes the

chances of NOx and soot formation and maximizes the chances of soot oxidation. Therefore the pneumatic hybridization of Diesel engines is expected to have a positive effect on pollutant emissions as well as greenhouse gas emissions.

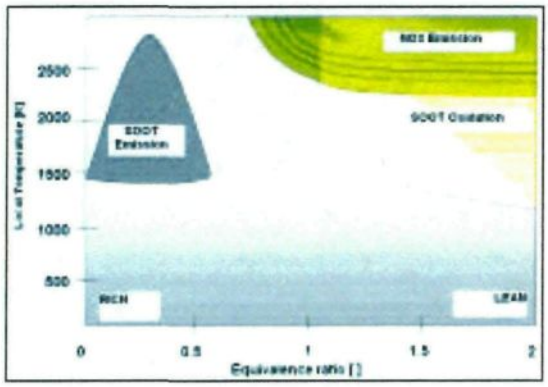

Figure 19: Pischinger Diagram (Pischinger 1988)

7. CONCLUSION

Increasing up to 4.5 bars the pressure at intake and decreasing down to 1 bar the pressure at exhaust of the Diesel engine results in increasing the power produced by the engine for the same fuel quantity and therefore improving the Diesel efficiency considering that the Compressed Air is free of charge. This improvement can reach up to 70% for the low loads (BMEP = 5 bar) and up to 40% for the high loads (BMEP = 15 bar), for a Diesel engine whose compression ratio is 14 and maximum allowed cylinder pressure is 200 bars.

This improvement is a combination of three phenomena:

1. The Low Pressure BMEP usually slightly negative for Turbo-Compressed engines and Natural Aspirated Engines becomes positive and therefore generates pure pneumatic power. The ratio of this pneumatic power to the total power can reach up to 40% for low loads and 10% for high loads.
2. The increase of intake air density reduces significantly the temperature in the cylinder and therefore reduces the thermal loss with the cylinder borders. This thermal loss is usually responsible of about 25% of the total loss in the engine. The gas temperature reduction due to increasing of air pressure can reach up to 200 K for low loads, and 350 K for high loads; the thermal loss reduction is therefore around 30% for low loads and 60% for high loads.
3. The increase of the combustion velocity thanks to the increase of air density and therefore the *cycle efficiency* is responsible of the remaining improvements.

In addition to its potential in fuel economy and greenhouse gas emission reduction, Diesel pneumatic hybridization is expected to have positive effect on pollutants emissions such as nitrogen oxides and soot.

NOMENCLATURE AND ABREVIATIONS

A	Effective area [m^2]
Aj	Boundary areas involved in heat transfer [m^2]
Cp	Specific heat capacity at constant pressure [J/kg/K]
$CT1$	Multiplicative coefficient
$CT2$	Multiplicative coefficient
Cv	Specific heat capacity at constant volume [J/kg/K]
D	Bore [m]
h	Enthalpy [J/kg]
HLC	Maximum heat release rate [1/deg]
L	Stroke [m]
N	Engine angular speed [RPM]
P	Pressure [Pa]
Psc	Gas pressure in the chamber if there was no combustion [Pa]
$P0$	Pressure of combustion chamber at the intake valve close [Pa]
Q	Heat transfer [j]
R	Manivelle radius [m]
T	Absolute temperature [K]
Tj	Mean temperatures of the boundary areas involved in heat transfer [K]
Tsc	Gas temperature in the chamber if there was no combustion [K]
$T0$	Temperature of combustion chamber at the intake valve close [K]
u	Internal specific energy [J/kg]
V	Volume [m^3]
VMP	Mean piston velocity [m/s]
Vs	Combustion chamber volume at Bottom Dead Centre [m3]
$V0$	Volume of combustion chamber at the intake valve close [Pa]
W	mass of gas [kg]
$WPPR$	Wind power penetration rate [%]
xb	Proportion of burned fuel [ ]
air	Refers to fresh air conditions
bfl	Refers to Backflow conditions
$exhaust$	Refers to exhaust conditions
inj	Refers to injected fuel conditions
$intake$	Refers to intake conditions
$phase$	Refers to the combustion phase start
$stoch$	Refers to stoichiometry conditions
ε	Compression ratio [ ]
Θ	Crankshaft angle [deg], where 360° refers to combustion phase Top Dead Center
Φ	Thermal exchange coefficient [J/m^2K]
λ	Equivalence ratio
r	Perfect gas constant [J/kg/K]
γ	Specific or molar volume [ ]

REFERENCES

Dönitz, C., Vasile, I.C., Onder, C.H., and Guzzella, H., 2009, Modelling and optimizing two- and four-stroke hybrid pneumatic engines, *IMechE.*

Guibert, P., 2002, *Etude des cycles thermodynamiques des moteurs thermiques et modélisation*, Rueil Malmaison, Ecole Nationale Supérieure du Pétrole et des Moteurs.

Heywood, J.B., 1988, *Internal Combustion Engine Fundamentals*, New York, McGraw Hill.

Higelin, P., Charlet, A., Chamaillard, Y., 2002, Thermodynamic Simulation of a Hybrid Pneumatic-Combustion Engine Concept, Int.J. *Applied Thermodynamics*, Vol.5, (No.1), p.1-11,

Ibrahim H., Ilinca A., Younes R., Basbous T., 2007, Study of a Hybrid Wind-Diesel System with Compressed Air Energy Storage, *IEEE Canada,*

Ibrahim H., Ilinca A., Younes R., Basbous T., 2007, Study of a Hybrid Wind-Diesel System with Compressed Air Energy Storage, *Renewable and Alternative Energy Ressources.*

Ibrahim H., 2010, *Etude et conception d'un générateur hybride d'électricité de type Eolien-Diesel avec élément de stockage d'air comprimé*, PHD, Université du Québec à Chicoutimi.

Lopes Correia da Silva, L., 2007, Simulation of the Thermodynamic Processes in Diesel Cycle Internal Combustion Engines, *SAE*, 931899.

Pischinger, F., Schulte, H., and Hansen J., 1988, *Grundlagen und Entwicklungslinien des dieselmotorischen Brennverfahren*, Düsseldorf, VDI-Berichte, p. 61-93.

Wiebe, I., 1970, Brennverlauf und Kreisprozess von Verbrennungsmotoren. Berlin, Verlag Technik, p. 286.

Wanhua, S., Yingying, L., Wenbin, Y., Changqing W., and Yiqiang, P., 2009, Density-Low Temperature Combustion in Diesel Engine Based on Technologies of Variable Boost Pressure and Intake Valve Timing, *SAE*, 2009-01-1911.

Woschni, G., 1967, A universally applicable equation for the instantaneous heat transfer coefficient in the internal combustion engine, *SAE*, 670 931.

Zheng, M., and Reader, G.T. Reader, Adaptive Control to Improve Low Temperature Diesel Engine Combustion, *12th Diesel Engine-Efficiency and Emission Reduction Conference*, 2006

X[ème] Colloque Interuniversitaire Franco-Québécois
sur la Thermique des Systèmes
20-22 juin 2011, Saguenay

CIFQ2011 / ÉnergSyst03

HYBRIDATION PNEUMATIQUE D'UN MOTEUR DIESEL DANS UNE INSTALLATION HYBRIDE ÉOLIEN DIESEL AVEC STOCKAGE D'ÉNERGIE SOUS FORME D'AIR COMPRIMÉ

Tammam **BASBOUS** [a,*], Adrian **ILINCA** [b], Rafic **YOUNES** [c], Jean **PERRON** [a]

[a] *Laboratoire International des Matériaux Antigivre, Université du Québec à Chicoutimi, Chicoutimi, Québec, Canada*
[b] *Laboratoire de Recherche en Energie Eolienne, Université du Québec àRimouski, Rimouski, Québec, Canada*
[c] *Faculté de Génie, Université Libanaise, Beyrouth, Liban*

RÉSUMÉ

Cette étude a été réalisée dans le cadre d'un projet de recherche consistant à analyser la faisabilité technique et économique d'un système Hybride Eolien Diesel avec Stockage d'Energie sous forme d'Air Comprimé (HEDSEAC). L'hybridation pneumatique d'un moteur Diesel consiste à introduire de l'air comprimé à son admission afin d'améliorer ses performances ou sa consommation. L'introduction peut être via la soupape d'admission ou via une soupape supplémentaire. Dans un travail précédent, nous avons démontré qu'une économie importante de carburant peut être attendue d'une hybridation pneumatique d'un moteur Diesel si on contrôle le rapport air/carburant à l'admission, de façon à garantir un fonctionnement permanent à un régime optimal. Comme complément à ces études, nous avons analysé l'impact de contrôler la pression et la température à l'admission sur le cycle thermodynamique et sur la consommation de carburant. Ce contrôle est possible grâce à l'air comprimé stocké préalablement en utilisant l'énergie éolienne en excès lors des périodes de fort taux de pénétration. Les résultats obtenus montrent que des gains très intéressants peuvent être attendus, surtout aux faibles charges du moteur.

Mots Clés : *Air comprimé, hybridation pneumatique, moteur Diesel, stockage d'énergie, éolien-diesel*

NOMENCLATURE

Symboles :

W	masse de gaz, kg
HLC	hauteur de la loi de dégagement d'énergie, deg^{-1}
H	enthalpie massique, $J.kg^{-1}$
D	diamètre du piston, m
Vmp	vitesse moyenne du piston, m/s
A	surface efficace, m^2
Aj	surface efficace de la surface participant aux échanges, m^2
Tj	température moyenne des surfaces, K
T	température des gaz du cylindre, K
Tsc	température des gaz du cylindre hors combustion, K
Psc	pression des gaz hors combustion, Pa
CT1	coefficient multiplicatif pour la phase de compression
CT2	coefficient multiplicatif pour la phase de combustion détente
Cp	chaleur spécifique à pression constante, $J.kg^{-1}.K^{-1}$
Cv	chaleur spécifique à volume constant, $J.kg^{-1}.K^{-1}$
L	course du piston, m
Vs	volume de la chambre de combustion au point mort bas, m^3
T0	tempérarture des gaz à la fermeture de la soupape d'admission, K
P0	pression des gaz à la fermeture de la soupape d'admission, Pa
V0	volume des gaz à la fermeture de la soupape d'admission m^3
P	pression des gaz dans le cylindre, Pa
T	température des gaz dans le cylindre, K
N	vitesse de rotation, $tr.min^{-1}$
Q	quantité d'énergie échangée, J
R	rayon de la manivelle, m
u	energie interne, $J.kg^{-1}$
xb	proportion de gaz brûlés
r	constante des gaz parfaits, $J.kg^{-1}.K^{-1}$

Indices / Exposants :

ph	phase du cycle thermodynamique
HLC	angle de dégagement maximal d'énergie
air	air frais
bfl	back-flow
ech	échappement
inj	carburant injecté
stc	stochéométrie
tot	total injecté

Lettres grecques :

θ	angle du vilebrequin, deg
Δθ	variation de l'angle vilebrequin, deg
ε	taux de compression
Φ	coefficient d'échange thermique, $J.m^{-2}.K^{-1}$
φ	Richesse du mélange
λ	rapport air sur carburant
γ	volume molaire

* auteur correspondant
Adresse électronique : tammam.basbous@uqac.ca

1. INTRODUCTION

Engagé dans la réduction des gaz à effet de serre (GES) par la signature du protocole de Kyoto, le Canada doit multiplier ses actions en ce sens dans le secteur de la production d'énergie. L'énergie éolienne représente le meilleur compromis entre le coût de production, qui assure la viabilité économique et les impacts sur l'émission des GES. Ceci explique le très fort taux de croissance de cette filière énergétique partout dans le monde. Cependant, l'énergie éolienne est intermittente et doit être utilisée en parallèle avec d'autres sources d'énergie. Le plus commun est de relier des parcs éoliens au réseau de distribution haute tension. Une autre utilisation, spécifique au grand territoire Canadien, est pour les sites isolés ou les réseaux autonomes (Yukon, Téritoires du Nord-Ouest, Nunavut, Îles) pour lesquels le déploiement de l'énergie éolienne présente un impact significatif, environnemental et économique, en remplaçant une partie de la production électrique par du Diesel [1-7].

Au Canada, plus de 200,000 personnes vivent dans plus de 300 communautés isolées qui ne sont pas connectés aux réseaux provinciaux ou nationaux de transport d'électricité. La plupart de ces communautés utilisent des Diesels pour générer de l'électricité, une méthode relativement inefficace et très dispendieuse, responsable de l'émission de 1.2 millions de tonnes de GES annuellement.

Le «Jumelage Éolien-Diesel» (JED) représente une technique de génération d'énergie électrique en utilisant en parallèle une ou plusieurs éoliennes avec un ou plusieurs groupes Diesel. Cette approche est utilisée actuellement dans des communautés nordiques au Yukon [8], Nunavut [9] et en Alaska [10]. Le taux de pénétration en puissance (TPP) est défini comme le rapport entre la puissance éolienne installée et la puissance maximum de la charge tandis que le taux de pénétration en énergie (TPE) est défini comme le rapport entre l'énergie éolienne annuelle produite et l'énergie consommée par la charge. Le «Jumelage Éolien-Diesel à Haute Pénétration» (JEDHP), caractérisé par des valeurs de TPP supérieures à 1, permet l'arrêt complet des groupes Diesel pendant que la production éolienne est supérieure à la demande. Elle permet la réduction la plus importante de la consommation de carburant et des émissions de GES mais elle est sujet à des problèmes techniques complexes dont les solutions sont très coûteuses [11-14] ce qui fait qu'un seul projet de ce type, sans aucun stockage, est actuellement opérationnel en Alaska [10]. L'utilisation des moyens de stockage permet de réduire ces difficultés [15] et maximiser le pourcentage d'énergie éolienne dans l'énergie annuelle totale (le TPE). Les moyens de stockage de l'énergie éolienne excédentaire envisagés présentement sont sous forme thermique (eau chaude), ou par des bancs de batteries. Ces dernières sont dispendieuses, difficiles à recycler, une source de pollution (plomb-acides) et limitées en puissance et en durée de vie. Les piles à combustible représentent une alternative viable mais la complexité technique, le prix prohibitif et le faible rendement retardent l'acceptation par le marché.

Nous tentons dans ce projet de trouver un moyen pour stocker le surplus d'énergie d'une manière fiable, relativement peu coûteuse et utilisable directement pour la réduction de la consommation de carburant, réduisant ainsi le coût d'un kWh produit, notamment pour les sites isolés auxquels le transport de carburant devient très coûteux. Nous proposons d'utiliser le Jumelage Eolien - Diesel, avec Stockage d'Energie sous forme d'Air Comprimé (JEDSEAC) illustré dans la figure 1 et qui, combiné avec une Hybridation Pneumatique du moteur Diesel, aura comme effet La réduction de la consommation de celui-ci.

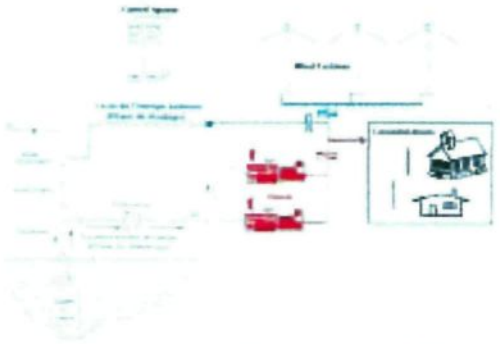

Figure 1 : Schéma du Jumelage Eolien – Diesel avec Stockage d'Energie sous forme d'Air Comprimé

L'hybridation pneumatique d'un moteur Diesel consiste à introduire l'air comprimé à son admission afin d'améliorer ses performances ou sa consommation. L'introduction peut être via la soupape d'admission ou via une soupape supplémentaire, comme le montre la figure 2.

2. HYBRIDATION PNEUMATIQUE DES MOTEURS DIESELS

Depuis les années 90, l'hybridation pneumatique des moteurs à combustion interne est discutée, mais principalement dans le cadre d'application à l'automobile. L'idée est d'utiliser le moteur comme un compresseur d'air fonctionnant avec l'énergie mécanique récupérée lors des décélérations du véhicule, fonctionnalité appelée habituellement « freinage récupératif » et comme un moteur à air comprimé lors des accélérations. Ceci est possible en connectant un réservoir d'air à l'admission du moteur via une soupape supplémentaire appelée soupape de charge [17], comme le montre la figure 2 (droite). Contrairement à cette approche, nous avons choisi dans notre étude d'utiliser

une technique d'hybridation plus simple qui consiste à introduire l'air comprimé via la soupape d'admission initiale de chaque cylindre du moteur, comme le montre la figure 2 (gauche).

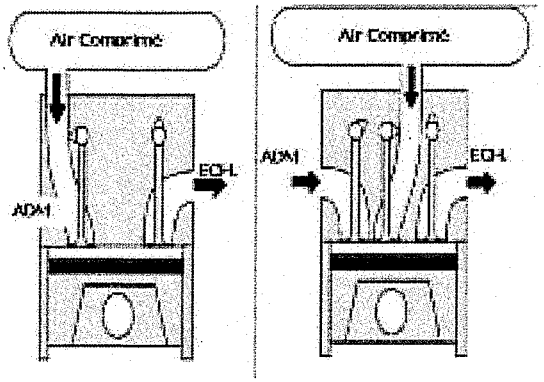

Figure 2 : Schéma de principe de l'hybridation pneumatique d'un moteur à combustion interne via la soupape d'admission (gauche) ou une soupape supplémentaire (droite)

La raison principale pour ce choix est de proposer une solution facilement adaptable aux installations Hybrides Eolien Diesel existantes. L'air comprimé est supposé produit par un compresseur électrique indépendant fonctionnant avec l'énergie électrique éolienne pendant les périodes de fortes pénétrations comme le montre la figure 3 [18].

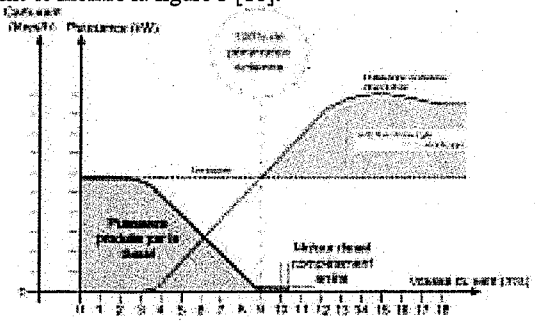

Figure 3 : Variation de la puissance éolienne et Diesel en fonction de la vitesse du vent, dans un système Hybride Eolien Diesel à haut taux de pénétration

3. MODELE MATHEMATIQUE

Nous avons pour cette étude devéloppé un modèle zéro dimensionnel du cycle thermodynamique Diesel. Aucune nouveauté par rapport à ce qui existe dans la littérature n'a été introduite dans cette modélisation. Les différents sous-modèles ainsi que leurs paramétrages ont donc été choisis dans différentes revues et livres scientifiques confirmés [20-24]. La figure 4 montre le système considéré pour calculer les évolutions des différentes variables d'état thermodynamique.

Les hypothèses qui sous-tendent ce modèle formel sont les suivantes, à tout instant:

- la masse de gaz est en équilibre thermodynamique;
- elle a des propriétés (pression, température, richesse, composition) homogènes en tout point du cylindre;
- elle est composée d'air et de produits de combustion;
- elle est considérée comme un mélange de gaz parfaits. Ses propriétés thermodynamiques (enthalpie, énergie interne, chaleurs massiques, masse molaire, ...) sont calculées suivant les lois de mélange et par interpolation de tables thermodynamiques [19];
- les transferts de masse se réalisent au travers des seules soupapes d'admission et d'échappement. Le "blow-by" est négligé;
- la pression, la température et la composition du mélange admis sont constantes;
- la pression du collecteur d'échappement est constante;

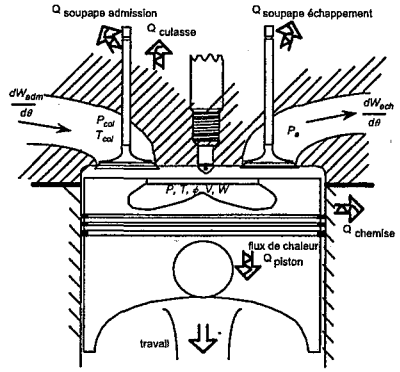

Figure 4 : Shéma du modèle du moteur Diesel à injection directe

- le "back-flow" à l'admission, circulation des gaz du cylindre vers le collecteur d'admission, est pris en considération. La masse qui "remonte" dans le collecteur est totalisée. Elle est ensuite réadmise aux conditions de température du cylindre;
- les gaz du collecteur d'échappement réadmis dans le cylindre ont la température des gaz du cylindre. Leur composition est celle des gaz du cylindre en début de phase d'échappement;
- le carburant est injecté à température constante. Il est immédiatement brûlé et transformé en produits de combustion;
- la masse de gaz du cylindre échange de la chaleur avec cinq parois de la chambre (la culasse, le piston, la chemise, les soupapes d'admission et

d'échappement) qui ont une température constante et uniforme.

3.1. *Equations de base*

Elles sont dérivées des lois de conservation de la masse et de l'énergie, ainsi que de l'équation d'état des gaz parfaits :

$$\frac{dW}{dt} = \frac{dW_{adm}}{dt} + \frac{dW_{ech}}{dt} + \frac{dW_{inj}}{dt} \quad (1)$$

$$\frac{dW_{air}}{d\theta} = \frac{\frac{dW_{adm}}{d\theta}}{1+\frac{\varphi_{adm}}{\varphi_{stc}}} + \frac{\frac{dW_{ech}}{d\theta}}{1+\frac{\varphi}{\varphi_{stc}}} \quad (2)$$

$$\frac{d\varphi}{d\theta} = \frac{\frac{dW}{d\theta} - \left(1+\frac{\varphi}{\varphi_{stc}}\right)\cdot\frac{dW_{air}}{d\theta}}{W_{air}} \cdot \varphi_{stc} \quad (3)$$

$$\frac{dT}{d\theta} = \frac{A_1 - \frac{\frac{\partial u}{\partial P}}{A_2}\cdot\left(\frac{\frac{dW}{d\theta}}{W} + \frac{\frac{\partial r}{\partial \varphi}}{r}\cdot\frac{d\varphi}{d\theta} - \frac{\frac{dV}{d\theta}}{V}\right) - \frac{\partial u}{\partial \varphi}\cdot\frac{d\varphi}{d\theta}}{\frac{\partial u}{\partial T} + \frac{\partial u}{\partial P}\frac{A_2}{A_3}} \quad (4)$$

$$\frac{dP}{d\theta} = \frac{\frac{\frac{dW}{d\theta}}{W} + \frac{\frac{\partial r}{\partial \varphi}}{r}\cdot\frac{d\varphi}{d\theta} - \frac{\frac{dV}{d\theta}}{V} + A_3\cdot\frac{dT}{d\theta}}{A_2} \quad (5)$$

avec:

$$A_1 = \frac{1}{W}\times\left(\begin{array}{l} -P\cdot\frac{dV}{d\theta} + \frac{dQ}{d\theta} + h_{adm}\cdot\frac{dW_{adm}}{d\theta} \\ +h_{ech}\cdot\frac{dW_{ech}}{d\theta} + h_{inj}\cdot\frac{dW_{inj}}{d\theta} - u\cdot\frac{dW}{d\theta}\end{array}\right);$$

$$A_2 = \frac{1}{P} - \frac{\frac{\partial r}{\partial P}}{r} \; ; \; A_3 = \frac{1}{T} + \frac{\frac{\partial r}{\partial T}}{r}$$

3.2. *Modèle cinématique*

Le volume délimité par le piston, les parois du cylindre et la culasse est instantanément calculé par les équations suivantes:

$$V(\theta) = \frac{\pi\times D^2}{8}\times L\left(1+\frac{R}{L}-\cos\theta-\sqrt{\left(\frac{R}{L}\right)^2-\sin^2\theta}+\frac{2}{\varepsilon-1}\right) \quad (6)$$

$$\frac{dV(\theta)}{d\theta} = \frac{\pi\times D^2}{8}\times L\times\sin\theta\times\left(\frac{\cos\theta}{\sqrt{\left(\frac{R}{L}\right)^2-\sin^2\theta}}+1\right) \quad (7)$$

La vitesse moyenne du piston est calculée par l'équation suivante:

$$Vmp = 2\times L\times\frac{N}{60} \quad (8)$$

3.3. *La loi de vitesse de dégagement d'énergie*

La description détaillée de la combustion dans les moteurs Diesel nécessite une connaissance des phénomènes qui se produisent depuis l'injection du combustible jusqu'à sa transformation en produits de combustion. Ces phénomènes impliquent l'étude de l'aérodynamique interne à la chambre de combustion, l'étude de la pénétration et de la vaporisation du carburant, l'étude du délai d'auto-inflammation et l'étude de la combustion proprement dite. En plus, cette description devrait tenir compte des gradients de température et de concentrations des espèces dans la chambre de combustion. De telles modèles ne peuvent être envisagés que dans le cadre des études en 2 ou 3D. Aussi a-t-il été choisi de représenter les phénomènes liés à la combustion par une loi globale de dégagement apparent d'énergie. Or, l'analyse de la combustion des moteurs diesel montre que la combustion peut être divisée en quatre phases:

- *la phase du délai d'auto-inflammation.* Le carburant introduit ne brûle pas tant que le délai d'auto-inflammantion ne s'est pas écoulé;
- *la phase de combustion en prémélange.* Cette phase correspond à la combustion en masse du carburant qui a été injecté durant le délai d'auto-inflammation. Cette combustion est particulièrement rapide puisque le carburant est mélangé à l'air;
- *la phase de combustion contrôlée par l'introduction du carburant.* Une fois la combustion en prémélange achevée, le carburant est introduit dans un milieu déjà chaud. Il brûle donc quasiment immédiatement. La combustion est donc gouvernée par la loi de débit de l'injecteur;
- *la phase de combustion finale.* L'injection étant terminée, le carburant encore non brûlé est brassé par les mouvements des gaz. La vitesse de combustion qui est alors très faible dépend des phénomènes de diffusion.

Pour représenter ces différentes phases, en supposant que le carburant injecté brûle immédiatement, la loi de dégagement apparent d'énergie est identique à la loi de débit apparent de carburant injecté. La loi de dégagement apparent d'énergie peut être modélisée par l'addition de deux lois de Wiebe [25]: la première correspond à la combustion en prémélange, la seconde à une combustion gouvernée par l'injection du carburant et sa diffusion. La loi de Wiebe permettant le calcul de la masse apparente injectée par une des phases s'écrit:

$$W_{inj} = W_{tot}\cdot\frac{1-exp\left(-w.\left(\frac{\theta_{HLC}-\theta_{ph}}{\Delta\theta_{HLC}}\right)^{m+1}\right)}{1-exp(-w)} \quad (9)$$

avec :

$$w = \frac{m}{m+1}\cdot\frac{1}{y_{HLC}^{\;m+1}}$$

$$HLC = \frac{m}{\left(\frac{\theta_{HLC} - \theta_{ph}}{\Delta\theta_{HLC}}\right)} \cdot \frac{exp\left(-\frac{m}{m+1}\right)}{1-exp(-w)} \cdot \frac{1}{\Delta\theta_{ph}} \quad (10)$$

3.4. Les transferts thermiques aux parois

Les transferts thermiques sont modélisés avec le modèle de Woshni [26]

$$\frac{dQ}{d\theta} = \sum_{j=\begin{cases}\text{soupapes d'admission}\\ \text{soupapes d'échappement}\\ \text{piston}\\ \text{culasse}\\ \text{chemise}\end{cases}} \Phi.Aj.\begin{pmatrix} CT1\cdot(Tj-Tsc) \\ +CT2\cdot(Tsc-T)\end{pmatrix} \quad (11)$$

Φ étant le coefficient d'échange thermique instantané calculé à l'aide de la relation suivante qui est le modèle dit de **Woschni** [26] :

$$\Phi = \frac{12986.10^{-6}\cdot P^{0.8}}{D^{0.2}\cdot T^{0.53}} \cdot \begin{pmatrix} 2.28\cdot V_{mp} \times \frac{N}{60} + \\ 0.00324\cdot\frac{V_s T_0}{V_0 P_0}\cdot(P-Psc)\end{pmatrix}^{0,8} \quad (12)$$

3.5. Les phases de "back-flow"

Ce phénomène se produit, à l'admission ou à l'échappement, lorsque la pression dans le cylindre est supérieure à celle du collecteur. Comme le montre la figure 3 (cas de l'admission), les gaz qui sortent ainsi du cylindre vont constituer une masse qui va être réadmise lorsque la pression dans le cylindre sera de nouveau inférieure à la pression du collecteur. Ce phénomène se produit essentiellement durant les premiers degrés de l'ouverture de la soupape d'admission. Les gaz concernés sont essentiellement des produits de combustion. Leur réadmission va concourir à diminuer la quantité d'air admise dans le moteur.

Dans le cas de l'admission, les hypothèses prises sont les suivantes:

- les gaz de back-flow ont une température, une pression et une composition homogène;
- la pression des gaz de back-flow est celle du collecteur d'admission;
- la température de ces gaz est égale à la température des gaz dans le cylindre. Cette hypothèse simple à mettre en œuvre est critiquable: un calcul plus rigoureux demande en effet de modéliser les transferts thermiques dans le collecteur d'admission.

Le schéma illustré par la figure 5 montre le modèle considéré pour prendre en compte le back-flow à l'admission. Les lois de conservation de la masse conduisent aux relations suivantes:

- si $P>Pcol$ (constitution de la masse de back-flow):

$$\varphi_{bfl} = \frac{W_{bfl} - W_{air\,bfl}}{W_{air\,bfl}} \cdot \varphi_{stc} \quad (13)$$

$$\frac{dW_{bfl}}{d\theta} = -\frac{dW_{adm}}{d\theta} = -\frac{dW_x}{d\theta}(P,T,r,\gamma,P_{col}) \quad (14)$$

$$\frac{dW_{air\,bfl}}{d\theta} = \frac{\frac{dW_{bfl}}{d\theta}}{1+\frac{\varphi_{bfl}}{\varphi_{stc}}} \quad (15)$$

$$h_{adm} = h_{\substack{gaz\\ brûlés}}(T,P,\varphi) \quad (16)$$

- si $P<Pcol$ (admission de gaz):
  - cas où $W_{bfl} > 0$:

    les gaz issus d'un « back-flow » précédemment constitué sont introduits dans le cylindre:

$$\frac{dW_{bfl}}{d\theta} = -\frac{dW_{adm}}{d\theta} = -\frac{dW_x}{d\theta}(P_{col},T,r_{bfl},\gamma_{bfl},P) \quad (17)$$

$$\frac{dW_{bfl}}{d\theta} = -\frac{dW_{adm}}{d\theta} = -\frac{dW_x}{d\theta}(P_{col},T,r_{bfl},\gamma_{bfl},P) \quad (18)$$

$$\frac{dW_{airbfl}}{d\theta} = \frac{\frac{dW_{bfl}}{d\theta}}{1+\frac{\varphi_{bfl}}{\varphi_{stc}}} \quad (19)$$

$$h_{adm} = h_{\substack{gaz\\ brûlés}}(T,P_{col},\varphi_{bfl}) \quad (20)$$

  - cas où $W_{bfl} = 0$:

    des gaz d'admission (air, carburant) sont admis:

$$W_{bfl} = W_{air\,bfl} = 0 \quad (21)$$

$$\frac{dW_{adm}}{d\theta} = -\frac{dW_x}{d\theta}(P_{col},T_{col},r_{col},\gamma_{col},P) \quad (22)$$

$$h_{adm} = h_{\substack{gaz\\ brûlés}}(T_{col},P_{col},\varphi_{col}) \quad (23)$$

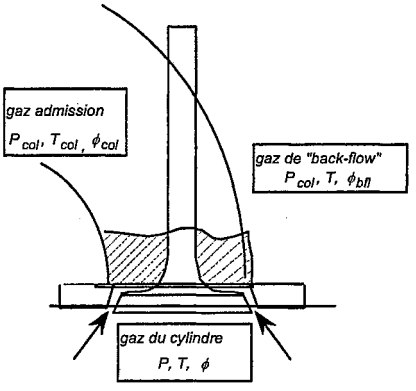

Figure 5 : Shéma du modèle du backflow admission

Dans le cas de l'échappement, le modèle est plus simple que pour l'admission dans la mesure où l'on considère que les gaz qui sont réintroduits ont une température qui est celle du cylindre, une pression égale à la pression d'échappement *Pe* et une composition massique en air, gaz brûlés et carburant identique à celle

des gaz en fin de combustion. Avec de telles hypothèses, on obtient les équations suivantes:

- si $P<Pe$ (réadmission de gaz d'échappement):
$$h_{ech} = h_{\substack{gaz \\ brûlés}}(T, P_e, \varphi) \quad (24)$$
- si $P>Pe$ (échappement des gaz du cylindre):
$$h_{ech} = h_{\substack{gaz \\ brûlés}}(T, P, \varphi) \quad (25)$$

4. RESULTATS ET DISCUSSION

4.1. Etude paramétrique réalisée

Nous avons réalisé une étude paramétrique de la pression d'admission, la pression d'échappement et la température d'admission pour différentes charges du moteur. Nous nous sommes contraints dans cette variation des paramètres de respecter les limites thermomécaniques que peut supporter le moteur. Il s'agit de la pression maximale des gaz dans le cylindre (200-220 bars) et la température maximale des gaz à la sortie d'échappement (1100 K).

4.2. Résultats obtenus à 10 bars de PMI

A un point de fonctionnement du moteur correspondant à une PMI de 10 bars, la consommation de carburant obtenue pour différentes valeurs de pression d'admission et d'échappement pour une température d'admission constante à 25°C est illustrée par la figure 6.

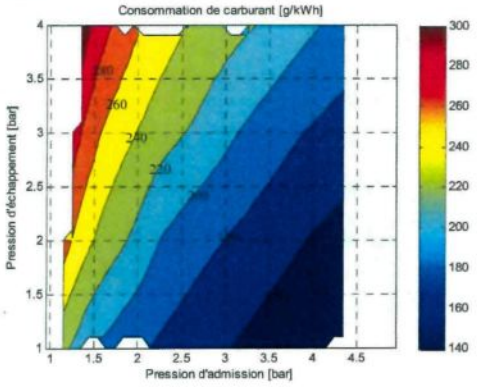

Figure 6 : Consommation de carburant en fonction des pressions d'admission et d'échappemement, à une température d'admission de 25°C, pour PMI=10 bars

Nous observons que la consommation de carburant est minimale pour une pression d'admission maximale et une pression d'échappement minimale. Les limites thermomécaniques fixés sont atteintes pour une pression d'admission de 4.3 bar. Pour un moteur suralimenté par turbocompresseur adapté, la pression d'admission et la pression d'échappement sont tous les deux aux environs de 2.2 bars [23], la consommation spécifique de carburant est alors de 220 g/kWh environs. En supprimant le turbo compresseur la pression d'échappement devient environ 1 bar et la pression d'admission peut être mise à 4.3 bars grâce à la présence d'un réservoir de stockage d'énergie sous forme d'air comprimé, la consommation peut baisser jusqu'à 140 g/kWh, soit 36% d'économie.

La détente de l'air comprimé stocké à une trentaine de bars pour atteindre 4.3 bars entraine une baisse conséquente de sa température. Nous avons ainsi la possibilité de conserver cet état froid de l'ai comprimé ou de le réchauffer avant de l'introduire dans le moteur. La deuxième étude paramétrique est faite dans le but d'orienter ce choix. La figure 7 montre la consommation de carburant en fonction de la pression et la température d'échappement pour une pression d'échappement égale à 1 bar.

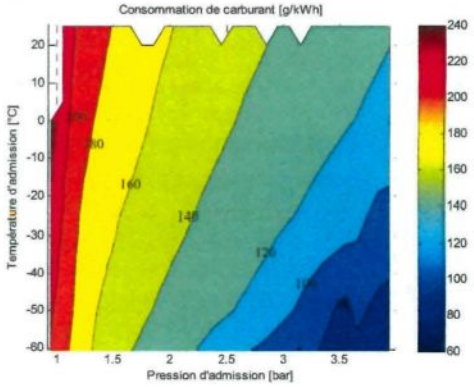

Figure 7 : Consommation de carburant en fonction de la pression et de la température à l'admission, à une pression d'échappement de 1 bar, pour PMI=10 bars

Nous constatons qu'il est bénéfique d'introduire de l'air le plus froid possible à l'admission du moteur. Pour une température de -50°C et une pression de 4.3 bar, la consommation de carburant peut atteindre 110 g/kWh, soit une économie de carburant de 50% par rapport à la consommation du moteur suralimenté par turbocompresseur.

Afin de comprendre les raisons de ces gains importants de la consommation de carburant, nous avons tracé différentes courbes d'analyse de cycle thermodynamique à une même PMI de 10 bar, pour les différentes conditions de suralimentations suivantes :

- **TC 25°C** : suralimentation classique par un turbocompresseur avec une Pression d'admission et une pression d'échappement égales à 2.2 bars et une température d'admission égale à 25°C.
- **AC 25°C** : suralimentation par air comprimé à une pression d'admission de 4.2 bars, une pression d'échappement égale à 1 bars et une température d'admission égale à 25°C.
- **AC 0°C** : suralimentation par air comprimé à une pression d'admission de 4.2 bars, une pression

d'échappement égale à 1 bars et une température d'admission égale à 0°C.

- **AC -25°C** : suralimentation par air comprimé à une pression d'admission de 4.2 bars, une pression d'échappement égale à 1 bars et une température d'admission égale à -25°C.

La figure 8 montre le diagramme pression-volume à l'échelle logarithmique des quatre cas précédents. On observe que pour les trois cas de suralimentation par air comprimé, le travail de la boucle basse pression (ou balayage) est moteur et participe à la production du travail total. On observe aussi que la montée en pression est plus franche avec la baisse de la température d'admission.

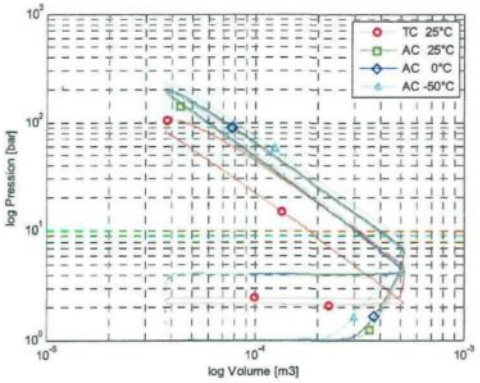

Figure 8 : Cycles logP-logV pour différentes techniques de suralimentation, à une PMI=10 bars

La figure 9 illustre pour ces même cycles thermodynamiques, l'évolution de la température en fonction de l'angle du vilebrequin. On observe d'abord que passer d'un *TC 25°C* à un mode *AC 25°C*, entraîne une baisse importante de la température sur le cycle, malgré le fait que la température d'admission est identique. Cette baisse est due à deux phénomènes :

1. l'augmentation du débit d'air admis dû à la pression d'admission accrue ce qui entraîne l'augmenrtation de l'énergie nécessaire pour élever de 1°C la température du mélange ;
2. la baisse de la pression échappement qui entraine une réduction des gaz brûlés résiduels chauds.

Plus la température de l'admission baisse, plus la température des gaz dans le cylindre baisse aussi. La baisse de température des gaz a pour intérêt de réduire les échanges thermiques entre les gaz et et les parois de la chambre de combustion. En effet, comme l'indique l'équation 11, ces échanges thermiques sont proportionnelles à la différence de température entre les gaz et ces surfaces de contact.

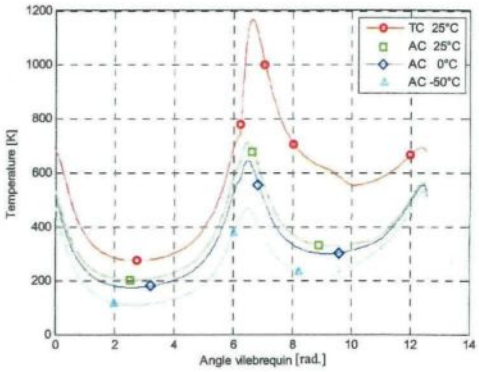

Figure 9 : Cycles θ-T pour différentes techniques de suralimentation, à une PMI=10 bars

Le détail du gain entre les configurations TC 25°C, AC 25°C et AC -50°C est illustré par la figure 10.

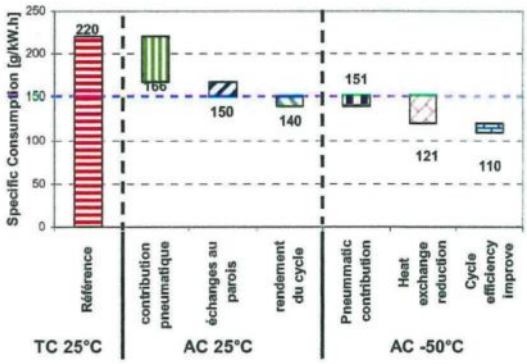

Figure 10 : explication des économies de carburant entre TC 25°C et AC -50°C en passant par AC 25°C

L'économie de carburant est donc réalisée grace à trois phénomènes :

1. la contribution pneumatique : c'est la part du travail qui a été produit par la boucle basse pression et auquel le carburant n'a pas participé.
2. la réduction des échanges au parois grace à la basse de la température des gaz
3. l'amélioration du rendement du cycle grâce à une quantité d'air plus importante accélèrant donc la vitesse de combustion.

Afin d'évaluer l'économie de carburant envisageable pour différents points de fonctionnement du moteur, nous avons fait la même étude précédente pour plusieurs valeurs de la Pression Moyenne Indiquée (PMI) et nous avons retenu les points de gain maximal, c'est-à-dire à la pression d'admission maximale permettant de respecter les contraintes thermomécaniques du système.

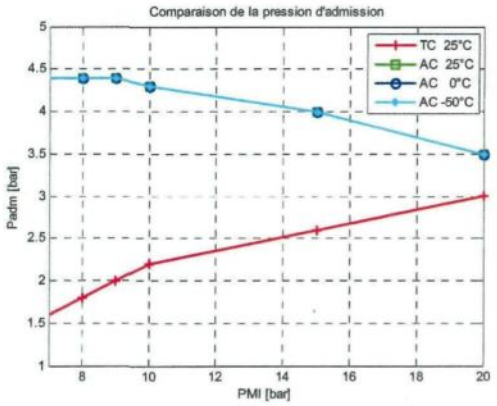

Figure 11 : Pression d'admission maximale en suralimentation par air comprimé comparée à la pression d'admission en suralimentation par turbocompresseur

La figure 11 montre cette valeur de pression d'admission retenue pour les différentes températures d'admission, comparée à la pression d'admission du moteur suralimenté par turbocompresseur. Nous observons donc que plus le moteur fonctionne à des PMI élevées, moins la pression d'admission maximale qu'il supporte est élevée. La figure 12 illustre la consommation de carburant pour les différents cas simulés.

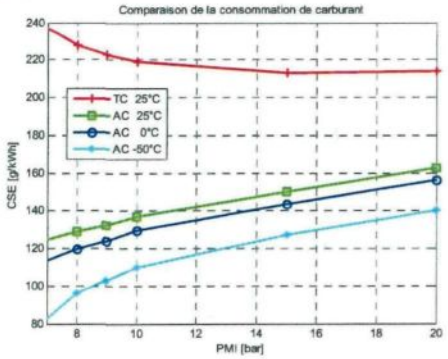

Figure 12 : Consommation de carburant en fonction de la technique de suralimentation et de la PMI

Nous observons que l'économie de carburant est plus faible sur les fortes charges. Cette réduction est principalement due à la baisse de la part du travail pneumatique qui elle-même est due à la baisse de la pression d'admission maximale. La figure 13 illustre la part du travail pneumatique dans le travail total du cycle pour les différents cas simulés.

Nous nous intéressons enfin à la consommation d'air comprimé compte tenu de l'importance de cet item dans le dimensionnement du réservoir de stockage. Le critère que nous avons retenu est le gain de carburant réalisé pour une consommation d'un kilogramme d'air. Ce critère permettra ultérieurement de concevoir une stratégie d'optimisation de l'utilisation de l'air comprimé sur une année complète. Il est donc primordial d'utiliser l'air disponible de façon à réaliser la meilleure économie globale de carburant.

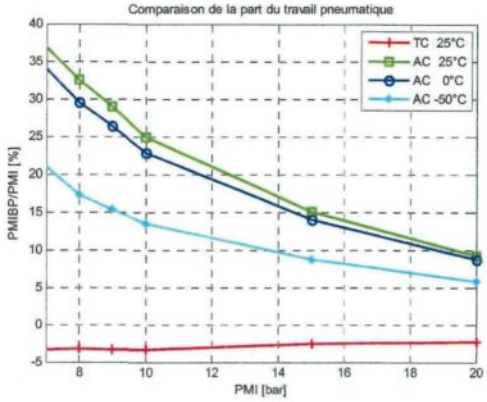

Figure 13 : Part du travail pneumatique dans le travail total en fonction de la technique de suralimentation et de la PMI

La figure 14 illustre l'économie de carburant par rapport à la consommation de référence qui est celle du moteur suralimenté par turbocompresseur.

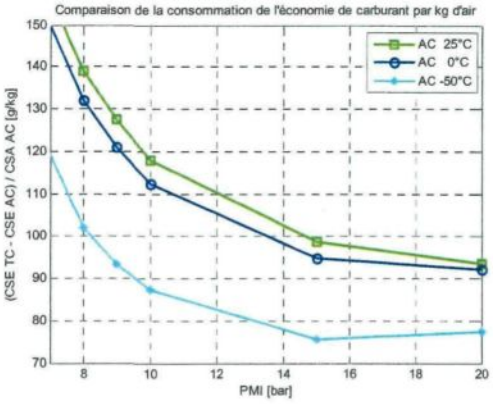

Figure 14 : Gain de consommation de carburant par kg d'air consommé, en fonction de la température de suralimentation et de la PMI

Nous observons que malgré le gain en consommation réalisé en réduisant la température de l'air à l'admission, l'augmentation de la consommation d'air due à l'augmentation de la densité de celui-ci en diminuant sa température est plus importante que l'économie de carburant réalisée. Nous observons aussi que l'économie de carburant rapportée à la consommation d'air est plus importante aux faibles couples ou PMI du moteur.

5. CONCLUSION

Cette analyse fait partie d'une étude globale de faisabilité technico-économique d'un système Hybride Eolien Diesel avec Stockage d'Energie sous forme d'Air Comprimé (HEDSEAC). Nous avons étudié le potentiel de l'économie de carburant réalisée en contrôlant la pression et la température à l'admission du moteur. Ce contrôle est possible grâce à l'air comprimé stocké préalablement en utilisant l'énergie éolienne en excès lors des périodes de fort taux de pénétration. Les résultats obtenus montrent que des gains très intéressants peuvent être attendus, surtout aux faibles charges du moteur en baissant au maximum la température à l'admission. Cette baisse se fait naturellement lors de la détente de l'air comprimé de sa pression de stockage à la pression d'admission. Cependant, rapportée à la consommation d'air qui est une contrainte à optimiser, l'économie de carburant est plus intéressante pour les températures d'admission les plus élevées. Il serait donc plus rentable de réchauffer l'air comprimé avant son introduction dans le moteur lorsque la quantité d'air comprimé stocké devient critique.

RÉFÉRENCES

[1] **DURAND**, J.P., et **DUPONT**, J.J., Titre de l'article ou de l'ouvrage, *Journal ou Congrès (Editeur)*, Ville, Pays, pp. xx-xx, (1999).

[1] **ADELAAR** & Ass., et **COMMUNITECH** & Ass, Contract No. 81-117, *Community Specific Energy Supply in the Yukon and Northwest Territories*, Gov. of Canada, Dep. of Indian & Northern Aff., (1981).

[2] **JANZ**, B., **HOWELL**, D.G., et **SERNA**, A., Wind Energy in the Northwest Territories, *prepared for The Science Advisory Board of the Northwest Territories*, Yellowknife, Northwest Territories, (1982).

[3] **UNIES CONSULTING ENG.**, Investigation of the Viability of a Remote Wind/Hydroelectric Power Supply in the Northwest Territories, Study No. 1, Energy Mines and Nat. Res. Canada, (1985).

[4] **CHAPPELL**, M.S., Wind Energy Research and Development at the National Research Council of Canada 1975-1985, *NRCC No. 27459*, (1986).

[5] **LODGE**, M., et **PASSMORE**, J., Wind-Diesel Systems for Remote Communities, *report for Mushkegowuk Council*, Ontario Energy Co., Ontario Hydro, CANMET, NRC, (1995).

[6] **ARCTIC ENERGY ALLIANCE**, Review of Technical and Economic Viability of Wind Energy Systems in the NWT and Nunavut, *NWT Power Corporation,* Hay River, Northwest Territories, (2001).

[7] **PINARD**, J.P., et **WEIS**, T.M., Pre-Feasibility Analysis of Wind Energy for Inuvialuit Region in Northwest Territories, *Aurora Research Institute*, (2003).

[8] **MAISSON**, J.F., Wind Power Development in Sub-Arctic Conditions with Severe Rime Icing, *Presented at the Circumpolar Climate Change Summit and Exposition*, Whitehorse, Yukon, (2001).

[9] Site internet www.nunavutpower.com

[10] **REEVES**, B., Kotzebue Electric Association Wind Projects, *Proceedings of NREL/AWEA 2002 Wind-Diesel Workshop*, Anchorage, Alaska, USA, (2002).

[11] **JEAN**, Y., **VIAROUGE**, P., **CHAMPAGNE**, D., **REID**, R., et **SAULNIER**, B., Perfectionnement des outils pour l'implantation des éoliennes à Hydro-Québec, *rapport IREQ-92-065*, (1992).

[12] **JEAN**, Y., **VIAROUGE**, P., **CHAMPAGNE**, D., **REID**, R., et **SAULNIER**, B., Analyse des essais 1992, validation du modèle dynamique, *rapport IREQ-93-103-C*, (1993).

[13] **JEAN**, Y., **VIAROUGE**, P., **CHAMPAGNE**, D., **REID**, R., et **SAULNIER**, B., Développement d'un système JEDHPSS représentatif d'un village typique des réseaux non reliés, *rapport IREQ-94-169-C*, (1994).

[14] **GAGNON**, R., **NOUAILI**, A., **JEAN**, Y., et **VIAROUGE**, P., Mise à jour des outils de modélisation et de simulation du Jumelage Éolien-Diesel à Haute Pénétration Sans Stockage et rédaction du devis de fabrication de la charge de lissage, *Rapport IREQ-97-124-C*, (1997).

[15] **ILINCA**, A., et **CHAUMEL**, J.L., Implantation d'une centrale éolienne comme source d'énergie d'appoint pour des stations de télécommunications, *Colloque international sur l'énergie éolienne et les sites isolées*, Îles de la Madeleine, (2005).

[16] **BASBOUS**, T., **ILINCA**, A., **YOUNES**, R., et **PERRON**, J., Pneumatic Hybridization of Diesel Engine in a Hybrid Wind-Diesel installation with Compressed Air Energy Storage, *The 4th International Conference on Integrated Modeling and Analysis in Applied Control and Automation*, (2010)

[17] **DONITZ**, C., **VASILE**, I.C., **ONDER**, C.H., et **GUZZELLA**, H., Modelling and optimizing two- and four-stroke hybrid pneumatic engines, *ImechE*, (2009).

[18] **IBRAHIM**, H., Etude et conception d'un générateur hybride d'électricité de type Eolien-Diesel avec élément de stockage d'air comprimé, PHD, *Université du Québec à Chicoutimi*, (2010).

[19] **JANAF** Thermochemical Tables, third edition, (1985)

[20] **HEYWOOD**, J.B., Internal Combustion Engine Fundamentals, New York, *McGraw Hill*, (1988).

[21] **LOPES CORREIA DA SILVA**, L., Simulation of the Thermodynamic Processes in Diesel Cycle Internal Combustion Engines, *SAE 931899*, (2007).

[22] **HIGELIN**, P., **CHARLET**, A., et **CHAMAILLARD**, Y., Thermodynamic Simulation of a Hybrid Pneumatic-Combustion Engine Concept, *Int.J. Applied Thermodynamics*, Vol.5, (No.1), p.1-11, (2002).

[23] **IBRAHIM**, H., **ILINCA**, A., **YOUNES**, R., et **BASBOUS**, T., Study of a Hybrid Wind-Diesel System with Compressed Air Energy Storage, *IEEE Canada*, (2007).

[24] **GUIBERT**, P., Etude des cycles thermodynamiques des moteurs thermiques et modélisation, Rueil Malmaison, *Ecole Nationale Supérieure du Pétrole et des Moteurs*, (2002).

[25] **WIEBE**, I., Brennverlauf und Kreisprozess von Verbrennungsmotoren. Berlin, *Verlag Technik*, p. 286, (1970).

[26] **WOSCHNI**, G., A universally applicable equation for the instantaneous heat transfer coefficient in the internal combustion engine, *SAE 670 931*, (1967).

International Conference on Renewable Energy for Developing Countries

A new multi-hybrid power system for grid-disconnected areas

Wind – Diesel - Compressed Air Energy Storage

BASBOUS Tammam
Université du Québec à Chicoutimi
Chicoutimi, Québec, Canada
tammam.basbous@uqac.ca

ILINCA Adrian
Université du Québec à Rimouski
Rimouski, Québec, Canada
adrian_ilinca@uqar.qc.ca

YOUNES Rafic
Université Libanaise
Faculté de génie
Beyrouth, Liban
ryounes@ul.edu.lb

PERRON Jean
Université du Québec à Chicoutimi
Chicoutimi, Québec, Canada
Jean_Perron@uqac.ca

Abstract— **The power generation for remote areas is historically ensured with Diesel engines generators. The economical cost of energy is therefore very high not only due to inherent cost of fuel but also due to transportation and maintenance costs. The environmental cost of energy is also high as the use of fossil fuels for electricity generation is a significant source of greenhouse gas emissions. The use of hybrid systems that combine renewable sources, especially wind, and Diesel generators, reduces fuel consumption, operational cost and pollution. Adding a storage element to the hybrid system increases the penetration level of the renewable sources, which is the percentage of renewable energy in the overall production, and further improves fuel savings. Compressed Air Energy Storage (CAES) has several advantages for hybrid Wind-Diesel Systems (WDS) due to its low cost, high power density and reliability. To store and restore the CAES, we suggest doing few modifications on the Diesel engine to turn it into a Hybrid Pneumatic-Diesel Engine (HPDE) able to operate with two-stroke pneumatic motor mode, two-stroke pneumatic pump mode and four-stroke hybrid mode. We evaluate in this paper the annual fuel economy generated by this concept, function of the air storage volume and the wind power penetration rate, on a typical remote area.**

Keywords-Pneumatic Hybridization; Diesel Engine; Wind-Diesel System; Compressed Air Energy Storage

I. INTRODUCTION

Most of the remote and isolated communities or technical installations (communication relays, meteorological systems, tourist facilities, farms, etc.) which are not connected to national electric distribution grids rely on Diesel engines to generate electricity [1]. Diesel-generated electricity is more expensive in itself than large electric production plants (gas, hydro, nuclear, wind) and, on top of that, should be added the transport and environmental cost associated with this type of energy.

In Canada, approximately 200,000 people live in more than 300 remote communities (Yukon, TNO, Nunavut, islands) and are using Diesel-generated electricity, responsible for the emission of 1.2 million tons of greenhouse gases (GHG) annually [2]. In Quebec province, there are over 14,000 subscribers distributed in about forty communities not connected to the main grid. Each community constitutes an autonomous network that uses Diesel generators. The total production of Diesel power generating units in Quebec is approximately 300 GWh per year. In the mean time, the exploitation of the Diesel generators is extremely expensive due to the oil price increase and transportation costs. Indeed, as the fuel should be delivered to remote locations, some of them reachable only during summer periods by barge, the cost of electricity produced by Diesel generators reached in 2007 more than 50 ¢/kWh in some communities, while the price for selling the electricity is established, as in the rest of Quebec, at approximately 6 ¢/kWh [3]. The deficit is spread among all Quebec population as the total consumption of the autonomous grids is far from being negligible. In 2004, the autonomous networks represented 144 MW of installed power, and the consumption was established at 300 GWh. Hydro-Quebec, the provincial utility, estimated at approximately 133 millions CAD$ the annual loss, resulting from the difference between the Diesel electricity production cost and the uniform selling price of electricity [3]. Moreover, the electricity production by the Diesel is ineffective, presents significant environmental risks (spilling), contaminates the local air and largely contributes to GHG emission. In all, we estimate at 140000 tons annual GHG emission resulting from the use of Diesel generators for the subscribers of the autonomous networks in Quebec. This is equivalent to GHG emitted by 35,000 cars during one year.

II. HYBRID WIND-DIESEL SYSTEMS FOR REMOTE AREAS

The Diesel power generating units, while requiring relatively little investment, are generally expensive to exploit and maintain, particularly when are functioning regularly at partial load [4]. The use of Diesel power generators under weak operating factors accelerates wear and increases fuel consumption [5]. Therefore, the use of hybrid systems, which combine renewable sources and Diesel generators, allows reducing the total Diesel consumption, improving the operation cost and environmental benefits.

Among all renewable energies, the wind energy experiences the fastest growing rate, at more than 30% annually for the last 5 years [7,8]. Presently, wind energy offers cost effective solutions for isolated grids when coupled with

Diesel generators. The Wind- Diesel System (WDS) represents a technique of generation of electrical energy by using in parallel one or several wind turbines with one or several Diesel groups. This approach is at present used in Nordic communities in Yukon [9], Nunavut [10] and in Alaska [11].The "penetration rate" is used in reference to the rated capacity of the installed wind turbines compared to the maximum and minimum loads. A strict definition of a "low-penetration" system is one when the maximum rated capacity of the wind component of the system does not exceed the minimum load of the community. In practical terms however, a low-penetration system is one where the wind turbines are sized so as not to interfere with the Diesel generators' ability to set the voltage and frequency on the grid. In effect, the wind-generated electricity is "seen" by the Diesel plant as a negative load to the overall system. It is important to note however that, because such a system needs to be designed for the peak capacity of the wind generator, it will typically operate with an average annual output of 20-35% of its rated power, such that while low-penetration systems will have noticeable fuel and emissions savings they will be fairly minor [12,2]. In many cases it is likely that similar savings could be achieved through energy efficiency upgrades for similar capital costs. A "high-penetration" system without storage [13] is one where the output from the wind generators frequently exceeds the maximum load for extended periods of time (10 min to several hours), such that the Diesel generators can be shut off completely when there is significant wind. The Diesel generators therefore are required only during periods of low winds and/or to meet peak demands. The advantage of such systems are that very significant fuel savings can be achieved reducing import and storage costs, but also will extend the life and servicing frequency of the Diesel generators as they will log less hours. Such systems can also benefit from economies of scale for construction and maintenance, but require much more significant and expensive control systems [14,15] to regulate the grid frequency and voltage while the Diesel generators are turned off. A "dump" load is required during periods when the power from the wind turbines exceeds the demand in order to maintain system frequency and voltage [11].

A medium-penetration system refers to a system in between the low- and high-penetration configurations. A medium-penetration system will have periods of time when the wind-generated electricity dominates the Diesel-generated electricity and may also be able to meet the system load for brief periods of time (30 sec/ min). When wind speeds are high and/or the community demand is very low, the Diesel generators may not be required at all, but are not shut off, rather they are left to idle to be able to respond quickly to load demands. A medium-penetration system is potentially subjected to both the benefits and the drawbacks of low- and high penetration configurations. Beyond a certain penetration, the obligation to maintain idle the Diesel at any time, generally around 25-30% of its nominal output power, forces the system to function at a very inefficient regime. Indeed, for low- and medium-penetration systems, the Diesel consumes, even without load, approximately 50% of the fuel at nominal power output. These systems are easier to implant but their economic and environmental benefits are marginal [12].

The use of high-penetration systems allows the stop of the thermal groups, ideally as soon as the wind power equals the instantaneous charge, to maximize the fuel savings. However, considering the Diesel starting time as well as the instantaneous charge and wind speed fluctuations, the thermal production must be available (Diesel group to minimal regime) from the moment when the over-production passes under a threshold, named power reserve, considered as security to answer to the instantaneous requested power. The value of this reserve should be chosen so that it insures the reliability of the system and has a direct effect on the fuel consumption and the exploitation and maintenance costs of the Diesel generators. In other words, the Diesels must still idle to compensate for a sudden wind power decrease under the level of the charge. A greater value of the power reserve leads to longer periods of time during which the Diesels are functioning at inefficient regimes. During time intervals when the excess of wind energy over the charge is considerable, the Diesel engine must still be maintained on standby so that it can quickly respond to a wind speed reduction (reduce the time of starting up and consequent heating of the engine). This is an important source of over consumption because the engine could turn during hours without supplying any useful energy.

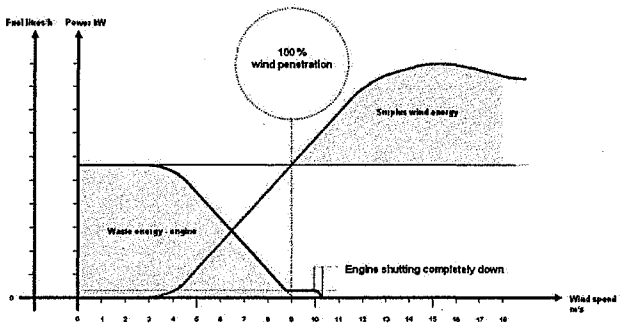

Figure 1. example of power contribution and fuel consumption of a high penetration Wind-Diesel generator [16]

Figure 1 [16] illustrates an example of power contribution of a high Wind Power Penetration Ratio (WPPR) in a remote area's Wind Diesel System (WDS), for a 450 kW consumer load. As long as the wind speed is higher than 4 m/s, a Fuel saving can be obtained. When wind speed reaches 9 m/s, the wind power is high enough to cover consumers demand without the need of Diesel engine's contribution. The engine could be stopped, however, only when a margin of 30% is reached between consumers' demand and the available wind power. The surplus wind power is lost.

III. COMPRESSED AIR ENERGY STORAGE (CAES) FOR HIGH WIND PENETRATION SYSTEM

The idea is to store the excess of wind energy that frequently occurs in WDS and is otherwise dissipated, then to restore it later when needed. The request for fuel energy is therefore reduced. Assuming optimum exploitation conditions [17,2] the use of energy storage with WDS can lead to better economic and environmental results, allows reduction of the overall cost of energy supply and increase the wind energy

penetration rate (i.e., the proportion of wind energy as the total energy consumption on an annual basis) [2].

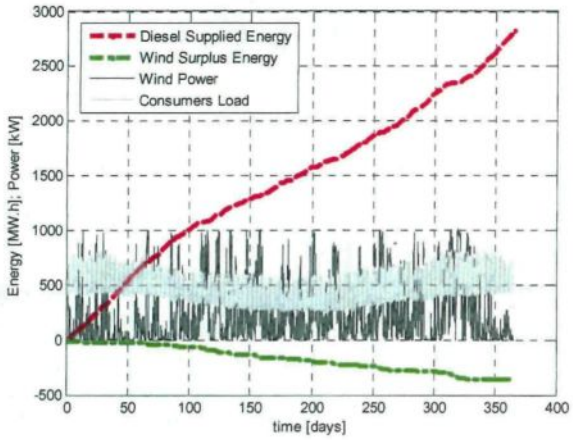

Figure 2. Recoverable energy compared to positive energy of a WDS having a WPPR of one, at Tuktoyaktuk site during year 2007

Among all the techniques permitting the storage of intermittent renewable energy, such as Pumped hydroelectric storage, batteries, superconducting magnets, flywheels, regenerative fuel cells and Compressed Air Energy Storage (CAES), the last one has an overwhelming advantage considering its low cost, low environmental impact and high reliability [18].

CAES relies on relatively mature technology with several high-power projects in place [24]. A power plant with a standard gas turbine uses nearly two-thirds of the available power to compress the combustion air. It therefore seems possible, by separating the processes in time, to use electrical power during off-peak hours (storage hours) in order to compress the air, and then to produce, during peak hours (retrieval hours), three times the power for the same fuel consumption by expanding the air in a combustion chamber before feeding it into the turbines. Residual heat from the fuel gas is recovered and used to heat the air.

CAES is achieved at high pressures (40–70 bars), at near-ambient temperatures [23] which means less volume and a smaller storage reservoir. Large caverns made of high-quality rock deep in the ground, ancient salt mines, or underground natural gas storage caves are the best options for compressed air storage, as they benefit from geostatic pressure, which facilitates the containment of the air mass (Figure 4). A large number of studies [20] have shown that the air could be compressed and stored in underground high-pressure piping (20–100 bars). This method would eliminate the geological constraints and make the system easier to operate (Figure 3). The energy density for this type of system is approximately 12kWh/m3 [31], while the estimated efficiency is around 70% [21]. The first storage station using an underground compressed air reservoir has been in operation since November 1978 in Huntorf, near Bremen, Germany [19]. In 1991, an American installation in Macintosh, Alabama, began to deliver 100MW of power for 226 h. The ambient air is compressed and stored at a pressure between 40 and 70 bars in a 2,555.10^3 m3 cavern, 700m deep in the ground [22]. During summer, the system generates energy 10 h per day on weekdays. The company using this application partially recharges the cavern weekday nights and full recharge is done on weekends. The system is in use 1770 hours per year [22].

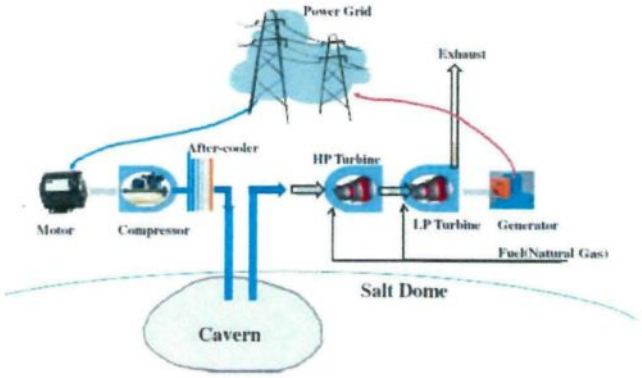

Figure 3. Example of an existing Compressed Air Energy Storage for power generation

IV. Pneumatic Hybridization of the Diesel Engine

To make a WDS combined to CAES economically competitive, it is important not to suggest a multiplication of the Engines by adding independent air motors and compressors. That is why Pneumatic Hybridization of the existing Diesel engine is being investigated in this article. This technique consists in enabling the Diesel engine to work under pneumatic mode, conventional combustion mode or mix pneumatic–combustion mode. Diesel engine can therefore be used as a pneumatic pump during energy excess to store this energy as compressed air in the tank. The stored energy can be discharged later through a pneumatic motor operation or through a hybrid pneumatic combustion operation.

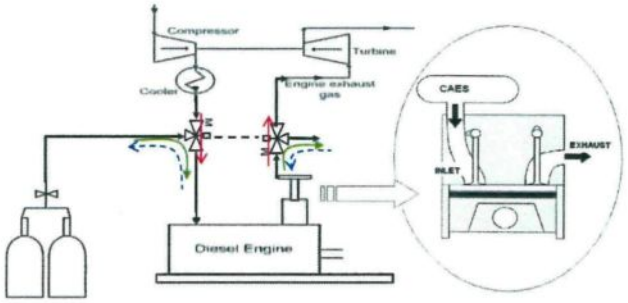

Figure 4. Suggested hybrid pneumatic-combustion engine

We suggest a new technique for pneumatic hybridization of Diesel engine based on bypassing the turbocharger and connecting the air tank to the intake valve using two three-way valves as shown in Figure 4. The first three-way valve connects the ICE's inlet to either the air tank or the compressor's outlet while the second three-way valve connects the ICE's exhaust to either the turbine's inlet or to the atmosphere. It also requires a full control of the intake valves, the exhaust valves and the

fuel injectors. It is assumed that the volume of the CAES tank is much higher than the displacement of the engine. The concept is able to operate with the four modes illustrated in Figure 5.

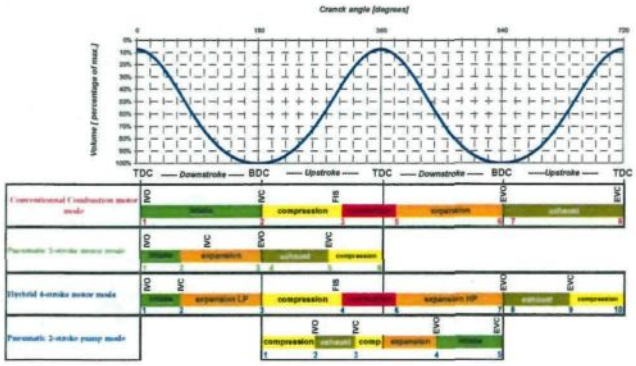

Figure 5. Operating principles of the suggested hybrid pneumatic-combustion engine

Mode 1: Four-stroke conventional Combustion motor mode: The three-way valves connect the turbocharger to the inlet and the exhaust of the engine. The cycle lasts during two rounds of the piston. The intake valve is open during the whole piston's way down (1→2) of the fist stroke. When the piston reaches the Bottom Dead Center (BDC), the compression phase (2→3) starts. A few degrees before the TDC, the fuel starts to be injected (FIS). Combustion phase (3→5) starts a few degrees later and finishes a few degrees after the TDC. After the combustion, expansion phase (5→6) occurs during the piston's way down until it reaches the BDC. At BDC, the exhaust valve opens and exhaust phase (6→8) occurs during the piston's way up. At TDC, exhaust valve closes. The intake and exhaust pressure are set by the turbocharger.

Mode 2: Two-stroke pneumatic motor mode: the three-way valves disconnect the turbocharger and connect the intake of the engine to the air tank and the exhaust to the atmosphere. The intake pressure is equal to the air storage pressure while exhaust pressure is equal to the atmospheric pressure. The fuel injection is disabled. The cycle lasts only one piston round. At TDC, intake valve opens and closes shortly after enabling therefore admission phase (1→2). Then an expansion phase (2→3) starts and lasts until piston reaches the BDC. Then exhaust valve opens and enables exhaust phase (3→5) during the piston's way up. Somewhere between BDC and TDC, exhaust valve closes and a compression phase starts (5→6) until piston reaches the TDC.

Mode 3: Four-stroke hybrid Pneumatic-Combustion motor mode: the three-way valves disconnect the turbocharger and connect the intake of the engine to the air tank. The intake pressure is equal to the air storage pressure. The intake valve is open during a part of piston's way down of the fist stroke, enabling the intake phase (1→2). Somewhere between TDC and BDC, the intake valve closes and an expansion phase (2→3) starts. When the piston gets to the BDC, operation continues exactly as the conventional mode.This mode operates normally even with Diesel engines because fuel injection can start anytime during piston compression between points 3 and 4, in order to ensure that the fuel burn starts when needed for getting the best cycle efficiency.

Mode 4: Two-stroke pneumatic pump mode: this mode is the reverse of the two-stroke pneumatic motor mode. The three-way valve is in the same position and the engine runs in the same way. However, by changing the intake and exhaust valve timings, low-pressure air is admitted through exhaust valve and high-pressure air is rejected through intake valve. Compressed air can therefore be stored in the tank. In this mode, fuel injection is disabled. Compression phase (1→2) starts at BDC and lasts until intake valve opens, somewhere between BDC and TDC enabling therefore exhaust phase (2→3). Intake valve closes a few degrees after it opens. the IVC angle will have to be dynamically adjusted for maximum braking energy recovery. If the available torque is high enough, IVC occurs at TDC in order to compress the maximum possible air quantity. If the available torque is relatively low, IVC occurs before TDC, reducing therefore the compressed air quantity as well as the work needed for the compression. After IVC, an expansion phase (3→4) occurs during piston's way down in the first case (IVC at TDC) and a compression phase followed by an expansion phase occur during the piston's way up then down in the second case (IVC before TDC). Somewhere between TDC and BDC, cylinder air pressure becomes exactly equal to atmospheric pressure. At that moment, exhaust valve opens and enables intake phase (4→5). Fresh air fills therefore the cylinder until the piston gets the BDC when exhaust valve closes.

V. ANNUAL FUEL CONSUMTION EVALUATION

A. Mathematical modeling of the thermodynamic cycle

The mathematical model used for simulating the ideal thermodynamic cycle of the Hybrid Pneumatic-Combustion Engine operation was exposed in a previous paper [32]. The same model is used in the present work. All the equations are simply the application of the first thermodynamic law to the different phases of the thermodynamic cycle.

We apply the equation (1) to all phases except intake and exhaust:

$$dU = dW + dQ \quad (1)$$

We apply the equation (2) for intake and exhaust phases:

$$dH = dU + PdV + VdP \quad (2)$$

Where U, H, W and Q respectively designate the internal energy, the enthalpy, the work and the heat loss. They can be calculated using equations 3 to 6:

$$dU = m * cv * dT + dm * cv * T \quad (3)$$

$$dH = m * cp * dT + dm * cp * T \quad (4)$$

$$dW = -PdV \quad (5)$$

$$dQ=dm\_f * pci \quad (6)$$

Where m is the mass, m_f is the mass of fuel, cv is the Specific heat at constant volume, cp is Specific heat at constant pressure and T is the temperature.

It is worth noting that the model used is an ideal one omitting all the losses in the engine. All the results are to be used to bind the benefits of the system.

B. Characterization of the HPCE

Figures 6 to 8 illustrate the Specific Air Consumption (SAC) of each mode of the HPCE and Figure 9 illustrates the Specific Fuel Consumption (SFC) for mode 3, as a result from the modeling above. The mode 3 is used when the mode 1 is not able to provide sufficient power. The mode 4 is used for negative torque which means energy storage request.

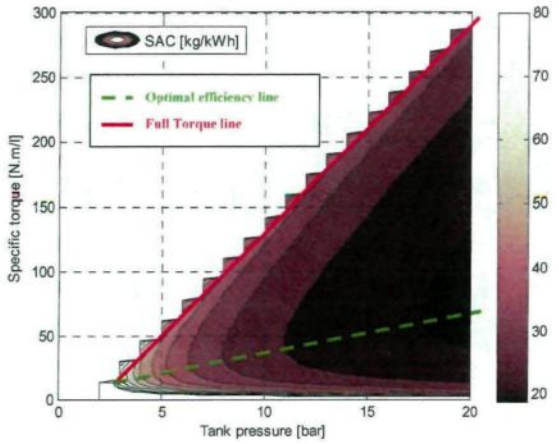

Figure 6. Specific Air Consumption of mode 2, as a function of the tank pressure and the specific torque

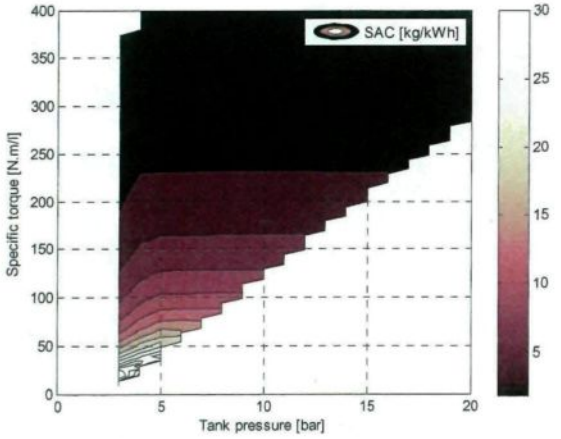

Figure 7. Specific air consumption of mode 3 as a function of the tank pressure and the specific torque

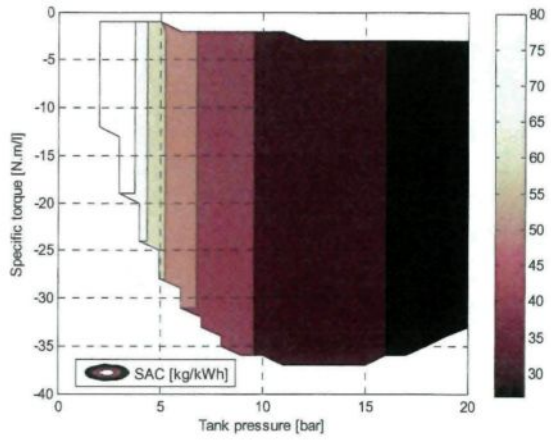

Figure 8. Specific Air Consumption of mode 4, as a function of the tank pressure and the specific torque

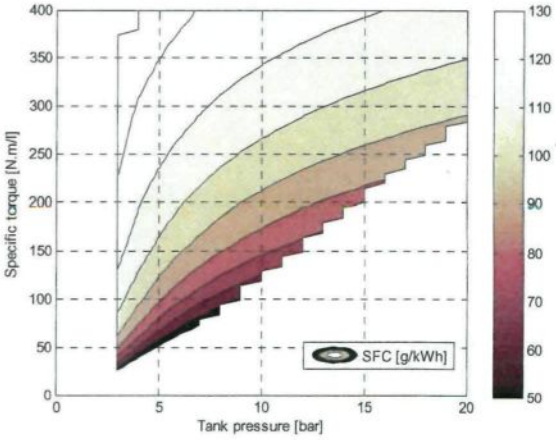

Figure 9. Optimal specific fuel consumption as a function of the tank pressure and the specific torque of a hybrid 4-stroke operation

C. Mathematical model of the multi-hybrid power system

A simplified mathematical model is developed to evaluate the fuel economy of the multi-hybrid power system WDS-CAES. Figure 10 illustrates the structure of the model.

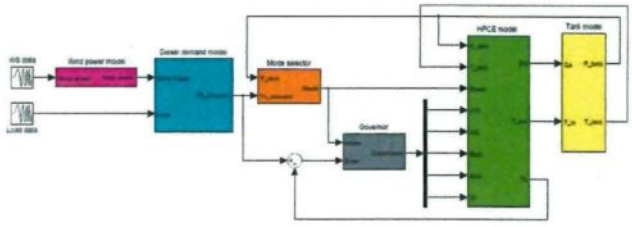

Figure 10. Structure of the mathematical model

Following are the details of the main sub-models.

- **Wind power model**

The model considers the available wind power, P_Wind, as a product of the Bet's limit, P_Betz, with the Power factor of the turbine, P_factor .

$$P\_Wind = P\_Betz * P\_factor \quad (7)$$

Where

$$P\_Betz = ½ * \rho * A * (S\_wind)^3 \quad (8)$$

And P_factor is given by the Turbine's manufacturer as a function of the wind speed, as shown in the Figure 11.

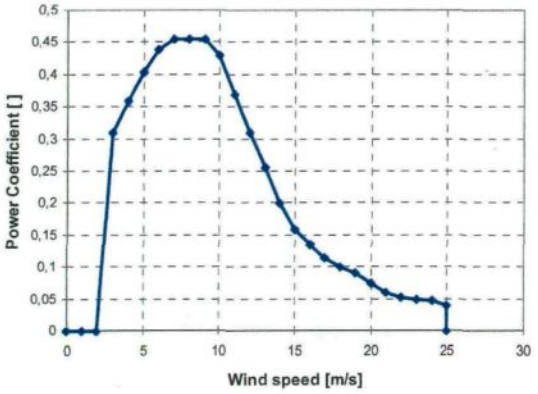

Figure 11. Power Coefficient curve of the ENERCON 330kW wind turbine

- **Diesel demand model**

The Diesel power (P_Diesel) demand model is simply the difference between the load (P_Load) and the available wind power (P_Wind):

$$P\_Diesel = P\_Load - P\_Wind \quad (9)$$

The torque applied to the Diesel engine (T_Diesel) is calculated as follows:

$$T\_Diesel = (P\_Diesel * 30) / (D\_Diesel * w\_Diesel * \pi) \quad (10)$$

Where D_Diesel is the displacement and w_Diesel is the engine rotational speed. We note that the T_Diesel could have a positive or a negative value.

- **Mode selector model**

The mode selector model is a two-dimensional map that decides the mode to apply depending on the instantaneous tank pressure and the instantaneous torque applied to the Diesel engine, as shown in Figure 12.

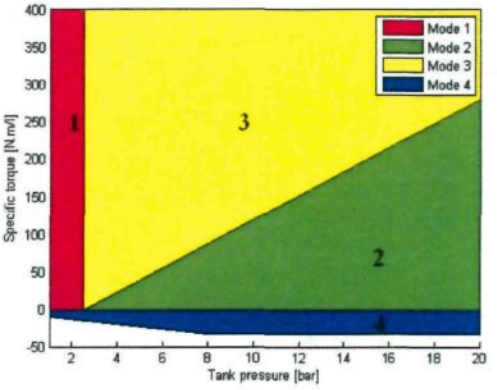

Figure 12. Mode selector strategy

- **HPCE model**

The HPCE model is explained in section A.

- **Governor**

The governor is a PI corrector that aims at meeting the torque request by changing one of the parameters:

- Fuel injection in mode 1
- Intake valve close timing in mode 2
- Intake valve close timing and fuel injection in mode 3
- Exhaust valve close timing in mode 4

- **Tank model:**

We simply apply the first thermodynamic system to the open system. The equation is the same as the one used in the HPCE model (Equation 2).

D. Annual fuel consumption

The combined effect of tank volume and WPPR on annual fuel consumption is investigated. The result is shown in Figure 13. The variation of WPPR from 0 to 2 is obtained by increasing from 0 to 6 the number of wind turbines. The values of fuel consumption obtained for tank volume equals to zero correspond to those of the Wind Diesel System (WDS) without pneumatic hybridization.

As observed in Figure 13, when WPPR increases, fuel consumption of WDS decreases. The improvement can reach for WPPR of 2, up to 50 % comparing to a Diesel-only power generation (WPPR=0). When WPPR increases, pneumatic hybridization permits more absolute and relative fuel economy. Finally, when tank volume increases, pneumatic hybridization permits as well more absolute and relative fuel economy. For the example, considering the case studied in the previous paragraph, where WPPR is 1, the fuel economy obtained using a 10000m^3 tank is only 3%, but it can reach 10% if the tank volume is 100000m^3.

For low and medium WPPR (lower than 1), the HPCE concept has no real interest in reducing fuel consumption, whereas for

high WPPR (higher than 1), fuel economy generated by HPCE concept is significant and increases with volume available for air storage. For a WPPR of 2, fuel economy generated by HPCE reaches 26% for a 108 m3 tan, which represents around 200 tons per year; and for a more classical high WPPR of 1, fuel economy generated by HPCE reaches 10% for a 100000 m^3 tank, which represents around 80 tons per year.

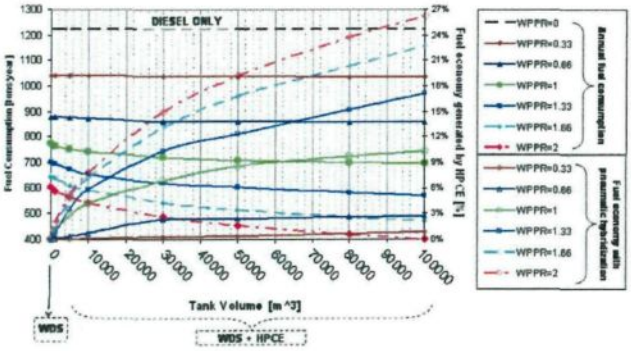

Figure 13. Annual fuel consumption and economy generated by hybrid concept, as a function of tank volume and WPPR

VI. CONCLUSION AND PRESPECTIVES

This article presented a fuel saving evaluation of a new concept of Hybrid Pneumatic-Combustion Engine (HPCE) that can be obtained by slightly modifying a conventional Internal Combustion Engine (ICE). The evaluation of the HPCE concept was based on ideal thermodynamic cycle modeling. The fuel economy is calculated for the village of Tuktoyaktuk in the north of Canada, during the whole year of 2007. A parametric study of the impact of the air storage volume and the Wind Power Penetration Ratio (WPPR) on the fuel economy generated by the HPCE concept has been conducted.

For low and medium WPPR (lower than 1), the HPCE concept has no real interest in reducing fuel consumption, whereas for high WPPR (higher than 1), fuel economy generated by HPCE concept is significant and increases with volume available for air storage. For a WPPR of 2, fuel economy generated by HPCE reaches 26% for a 108 m3 tan, which represents around 200 tons per year; and for a more classical high WPPR of 1, fuel economy generated by HPCE reaches 10% for a 108 m3 tank, which represents around 80 tons per year.

However, in the present paper, only an evaluation based on ideal cycle modeling has been conducted. Real cycle has to be studied to take in consideration several phenomena that might influence the fuel saving estimation, such as flow supersonic limitations through valves, valves response time for opening and closing, fuel injection shape, fuel burn process and heat exchanges through boundary. The next phase of this study will focus on evaluating the HPCE concept using real cycle modeling, then on performing engine bench tests to validate the models and make sure of the concept's interest.

REFERENCES

[1] Liu W, Gu S, Qiu D. Techno-economic assessment for off-grid hybrid generation systems and the application prospects in China. http://www.worldenergy.org/wecgeis/publications/.

[2] Weis TM, Ilinca A. The utility of energy storage to improve the economics of wind-Diesel power plants in Canada. Renewable Energy 2008; 33(7):1544-57.

[3] La stratégie énergétique du Québec 2006-2015. L'énergie pour construire le Québec de demain. http://www.mrnf.gouv.qc.ca/energie/eolien.

[4] Hunter R, Elliot G. WindeDiesel systems - a guide to the technology and its implementation. Cambridge (UK): Cambridge University Press; 1994.

[5] Forcione A. Système jumelé éolien-Diesel aux Îles-de-la-Madeleine (Cap-aux-Meules) - Établissement de la VAN optimale. Institut de Recherche, Hydro-Québec, Février; 2004.

[6] HOMER v2.0 - the optimisation model for distributed power. NREL. www.nrel.org.

[7] Ibrahim H, Ilinca A, Perron J. Solutions actuelles pour une meilleure gestion et intégration de la ressource éolienne. CSME/SCGM Forum 2008 at Ottawa. The Canadian Society for Mechanical Engineering, 5-8 June 2008.

[8] ACÉÉ. Association canadienne de l'énergie éolienne. http://www.canwea.com; access on June 2011

[9] Maisson JF. Wind power development in sub-arctic conditions with severe rime icing. In: Presented at the circumpolar climate change summit and exposition, Whitehorse, Yukon; 2001.

[10] www.nunavutpower.com; ; access on May 2012

[11] Reeves B. Kotzebue electric association wind projects. In: Proceedings of NREL/AWEA 2002 wind-Diesel workshop, Anchorage, Alaska, USA, 2002.

[12] Singh V. Blending wind and solar into the Diesel generator market. Renewable Energy Policy Project (REPP) research report, Winter 2001, No. 12, Washington, DC.

[13] Reid R. Application de l'éolien en réseaux non reliés. Liaison Énergie-Francophonie, N°35/2e Trimestre; 1997.

[14] Jean Y, Nouaili A, Viarouge P, Saulnier B, Reid R. Développement d'un système JEDHPSS représentatif d'un village typique des réseaux non relies. Rapport IREQ-94-169-C; 1994.

[15] Gagnon R, Nouaili A, Jean Y, Viarouge P. Mise à jour des outils de modélisation et de simulation du Jumelage Éolien-Diesel à Haute Pénétration Sans Stockage et rédaction du devis de fabrication de la charge de lissage. Rapport IREQ-97- 124-C; 1997.

[16] www.danvest.com. ; access on September 2012

[17] Ilinca A, Chaumel JL. Implantation d'une centrale éolienne comme source d'énergie d'appoint pour des stations de télécommunications. Colloque international sur l'énergie éolienne et les sites isolées, Îles de la Madeleine; 2005.

[18] Ibrahim H, Ilinca A, Perron J. Energy storage systems e characteristics and comparisons. Renewable & Sustainable Energy Reviews 2008;12(5):1221-50.

[19] Ibrahim H, Ilinca A, Perron J. Comparison and analysis of different energy storage techniques based on their performance index. IEEE Canada, Electrical Power Conference 2007, "Renewable and alternative energy resources", EPC2007, Montreal, Canada, October 25-26, 2007.

[20] Belhamed M, Moussa S, Kaabeche A. Production d'électricité au moyen d'un système hybride éolien-photovoltaïque-Diesel. Revue Énergies Renouvelables: Zones Arides; 2002:49-54.

[21] Kaldellis JK, Vlachos GTh, Kavadias KA. Optimum sizing basic-principles of a combined photovoltaic wind-Diesel hybrid system for isolated consumers. In: Proceedings of EuroSun 2002 international conference, Paper W141, Bologna, Italy; 2002.

[22] Bowen AJ, Cowie M, Zakay N. The performance of a remote wind-Diesel power system. Renewable Energy 2001;22(4):429-45.

[23] Broderick, J. K., Combined internal combustion and compressed air engine, US Patent 1013528, Jan 1912

[24] Ochel, W., Beyermann, O., and Gehrmann, F., Multicylinder 4-stroke cycle Diesel engine and compressor, US Patent 2676752; April 1954

[25] Brown, R., Compressed air engine, US Patent 3765180; October 1973

[26] Ueno, T., Convertible engine-air compressor apparatus for driving a vehicle, US Patent 3963379; June 1976

[27] Donitz, C., Vasile, I., Onder, C., and Guzzella, L., Realizing a Concept for High Efficiency and Excellent Driveability: The Downsized and Supercharged Hybrid Pneumatic Engine, SAE, 2009-01-1326; 2009

[28] Dönitz, C., Vasile, I.C., Onder, C.H., and Guzzella, H., Modeling and optimizing two- and four-stroke hybrid pneumatic engines, IMechE; 2009

[29] Lopes Correia da Silva, L., Simulation of the Thermodynamic Processes in Diesel Cycle Internal Combustion Engines, SAE, 931899; 2007

[30] Higelin, P., Charlet, A., Chamaillard, Y., Thermodynamic Simulation of a Hybrid Pneumatic-Combustion Engine Concept, Int.J. Applied Thermodynamics, Vol.5, (No.1), p.1-11; 2002

[31] Higelin, P., Vasile, I., Charlet, A., and Chamaillard, Y., Parametric optimization of a new hybrid pneumatic-combustion engine concept, Int. J. Engine Res., Vol. 5; No. 2 205

[32] Basbous, T., Younes, R., Ilinca, A., and Perron, J.; A new hybrid pneumatic combustion engine to improve fuel consumption of wind–Diesel power system for non-interconnected areas, Applied Energy, Volume 96, August 2012, Pages 459-476.

NOMENCLATURE

m	mass [kg]
cp	specific heat at constant pressure [J/kg/K]
cv	specific heat at constant volume [J/kg/K]
T	temperature [K]
U	internal energy [J]
W	work [J]
Q	heat [J]
V	volume [m^3]
P	pressure [Pa]
H	enthalpy [J]
m_f	mass of fuel [kg]
d	derivative of
P_Wind	wind power [kW]
P_Betz	Betz limit [kW]
P_factor	Power factor [ ]
ρ	density [kg/m^3]
A	Area [m^2]
S_wind	area of wind turbine [m^3]
P_Diesel	Diesel engine power [kW]
P_Load	load power [kW]

ABBREVIATIONS

HPCE	Hybrid Pneumatic Combustion Engine
HPDE	Hybrid Pneumatic Diesel Engine
WPPR	Wind Power Penetration Ratio
ICE	Internal combustion Engine
WDS	Wind Diesel System
CAES	Compressed Air Energy Storage